MASTERARBEIT / MASTER'S THESIS

Titel der Masterarbeit / Title of the Master's Thesis

„Intersecting Brane Worlds - a Path to the Standard Model and Beyond"

verfasst von / submitted by

Elias Niederwieser, BSc

angestrebter akademischer Grad / in partial fulfilment of the requirements for the degree of

Master of Science (MSc)

Wien, 2024 / Vienna, 2024

Studienkennzahl lt. Studienblatt / degree programme code as it appears on the student record sheet:	A 066 876
Studienrichtung lt. Studienblatt / degree programme as it appears on the student record sheet:	Masterstudium Physik
Betreut von / Supervisor:	Univ.-Prof. Dipl.-Phys. Dr. Stefan Fredenhagen

Abstract

Intersecting brane world scenarios offer a promising path to the implementation of the standard model of particle physics into the framework of string theory. In this thesis, we shed light on the foundations of such realisations of semi-realistic standard models using typ IIA superstring theory on a compactified Calabi-Yau space. By providing a geometrical and pedagogical introduction, we will highlight the key features of such models. We will illuminate that the gauge sector of the standard model emerges from open strings attached to a stack of coincident D-branes. In addition, we will discover that D-branes wrap 3-cycles on the compact space and that strings stretched near the multiple intersections of two D-branes give rise to three generations of chiral massless fermions furnishing the matter content of the standard model. Moreover, a tower of massive copies - baptised as light stringy states - appears near these intersections. The mass of these states depends on the relative angles of the branes and the same angles will provide us with a criterion to preserve supersymmetry. Since the resulting effective field theory endows potential anomalies, we will resolve them by a generalised Green-Schwarz mechanism. From the plythora of possibilities, we will pick out a non-supersymmetric configuration with a toroidal orientifold background to derive the content of the standard model. On top of that, we discuss a supersymmetric extension leading to a Pati-Salam model. Such intersecting brane models allow a string scale at the order of the TeV scale - opening up a playground for phenomenology. In that context, we will investigate a Yukawa interaction involving a scalar light stringy state, which corresponds to an excited Higgs particle. From the decay rate of this state, we will derive its lifetime. Finally, we find that such a massive weakly interacting scalar has an almost stable lifetime, if we fine-tune the angles of the corresponding branes. Such a particle represents a tempting candidate for dark matter.

Zusammenfassung

Intersecting Brane World Szenarien bieten einen vielversprechenden Weg zur Implementierung des Standardmodells der Teilchenphysik in die Stringtheorie. In dieser Arbeit beleuchten wir die Grundlagen solcher Realisierungen von semi-realistischen Standardmodellen unter Verwendung der Typ IIA Superstringtheorie auf einer kompaktifizierten Calabi-Yau-Mannigfaltigkeit. Mittels einer geometrischen und pädagogischen Einführung werden wir die wichtigsten Merkmale solcher Modelle herausarbeiten. Wir werden zeigen, dass die Eichgruppe des Standardmodells aus offenen Strings hervorgeht, die an einem Stapel von koinzidenten D-Branes verlaufen. Darüber hinaus werden wir darlegen, dass D-Branes 3-Zyklen auf dem kompakten Raum wickeln und dass Strings, die nahe der multiplen Schnittpunkte zweier D-Brane lokalisiert sind, drei Generationen von chiralen masselosen Fermionen hervorbringen, die den Materiegehalt des Standardmodells liefern. Darüber hinaus erscheinen in diesen Schnittpunkte massereiche Kopien, die als light stringy states bekannt sind. Die Masse dieser Zustände hängt von den relativen Winkeln der Branes ab. Dieselben Winkel liefern ein Kriterium für die Erhaltung der Supersymmetrie. Da die resultierende effektive Feldtheorie potentielle Anomalien birgt, werden wir sie durch einen verallgemeinerten Green-Schwarz-Mechanismus beheben. Um den Inhalt des Standardmodells abzuleiten, werden wir eine nicht-supersymmetrische Konfigration mit einem toroidalen Orientifold auswählen. Weiters diskutieren wir eine supersymmetrische Erweiterung, die zu einem Pati-Salam-Modell führt. Solche D-Brane Modelle erlauben eine String-Skala in der Größenordnung der TeV-Skala und ermöglichen damit phänomenologische Betrachtungen. In diesem Kontext werden wir eine Yukawa-Wechselwirkung untersuchen, an der ein skalarer light stringy state beteiligt ist, der einem angeregten Higgs-Teilchen entspricht. Aus der Zerfallsrate dieses Zustands werden wir seine Lebensdauer ableiten. Wir werden feststellen, dass ein solch massives, schwach wechselwirkendes Skalar eine nahezu stabile Lebensdauer hat, wenn wir die Winkel der entsprechenden Branes fein abstimmen. Ein solches Teilchen stellt einen verlockenden Kandidat für dunkle Materie.

“ *The most beautiful thing we can experience is the mysterious. It is the source of all true art and science.* ”

Albert Einstein, *The World As I See It*, 1932.

“ *Sometimes science is more art than science, Morty. Lot of people don't get that.* ”

Rick Sanchez, *Rick And Morty*, Season 1, Episode 6.

Contents

Chapter 1

Introduction

1.1 The Roots and Fruits of Superstring Theory

If something is in no way inferior to the fascination and richness of string theory, it is its genesis, the still developing history, and its extraordinary creators.

A priori, the birth of string theory was in a certain sense accidental, beginning around 1968 with the Italian physicist Gabriele Veneziano, who was driven to explain the strong interaction. While trying to construct the S-matrix for a scattering of mesons, in summer of 1968, he found a solution linked to a result which at that time had already been known for almost two hundred years and has been lying dormant in mathematical textbooks to finally find its true purpose: The *Euler beta function* [1]. Veneziano went on a vacation after his publication [2], not knowing that this result and mathematical peculiarity, today known as the *Veneziano amplitude*, had already attracted inquisitive young physicists upon his return [3].

One of these ingenious minds, who dealt with Veneziano's original model, was the young theoretical physicist Leonard Susskind. Bored by his unsuccessful work with hadrons, he wanted to step away from his own work in this field, until he coincidentally came across Veneziano's result to his delight [4]. It was immediately clear to him that Veneziano's result had the inherent properties of a harmonic oscillator. After the previously inconclusive work, he soon found himself playing with the "forbidden fruit" [4]. He spent months alone in his attic, consumed by giving Veneziano's result a physical interpretation. At the end of his almost delusional state, he finally had his "Eureka" moment. He realised that Veneziano's amplitude describes "rubber bands" colliding with each other [5, 6]. To Susskind's amazement, he was not the only one to come to this glorious result of a "rubber band theory" or "elastic string theory". Despite this success to describe the nuclear force with the help of one-dimensional vibrating strings, the theory was rather smiled at than discussed by the scientific community [4, 7].

To the regret of the fathers of string theory, this theory also gave results that were contradicted by experimental data [8]. The death blow was the introduction of the *Parton model* and *quantum chromodynamic* (QCD) in 1974, which agreed with the empirical data [9, 10]. These can be considered anni mirabiles in the history of particle physics. Students ran through the corridors and halls of universities, loudly announcing which new particles had been discovered. It solidified into popular understanding that the most fundamental components of the universe were point-like and had nothing to do with the one-dimensional ideas of the late 1960s. Finally, there was also an answer to what binds the world's innermost together. The fundamental interactions were themselves described by messenger particles. This was the birth of the *standard model of particle physics* (SM) which unifies the weak, strong, and electromagnetic interactions in a consistent theory by using the same language – the language of *quantum field theory* (QFT).

Despite this severe setback, there were still some physicists who wrestled with this theory of strings [7]. One of them was John H. Schwarz, who dealt with several problems of the theory. The theory predicted the existence of a massless particle which did not agree with any experiment. However, it was this very particle that led to the paradigm shift of string theory to something more fundamental than originally assumed. Even by failing to describe hadronic physics in its beginnings, it contained a much deeper insight. It turned out that this mysterious particle could be identified with the graviton and that the theory could provide a prescription to explain gravity on a quantum level [11, 12].

By adding this missing piece to the puzzle, string theory, as a quantum theory of one-dimensional objects, became the manifestation of a single theory with the claim and potential to describe the universe in its most fundamental aspects.

According to string theory, the mass and inherent properties of the particles are just determined by the vibration of the fundamental strings. Analogous to how the fretting of violin strings results in specific tones and thus describing the universe at its most fundamental aspect as a giant symphony orchestra. Moreover, it lived up to Einstein's wildest dream by describing all four fundamental interactions and being a candidate for their unification or *theory of everything* (TOE). Being such a theory, in its limits it must reproduce general relativity (GR) on the one hand and the standard model on the other, which describe the world with incredible accuracy. The length of a string is the only free parameter of the theory which at the same time determines the scale of the theory which is in the regime of the Planck scale. Beyond this scale, string theory describes gravity and the standard model as an effective field theory (EFT) by considering only the lightest oscillations of the strings [13].

Nevertheless, Schwarz and Michael Green were confronted with a huge problem at the beginning of the 1980s. The string theory formulated until then contained quantum anomalies, which had the appearance to end the history of the string theory at this point. During a storm [14], which according to Green was sent by God and supposed to prevent them from finding the "holy grail", they managed to construct a consistent supersymmetric string theory in ten dimensions using the so-called *Green-Schwarz mechanism*, which eliminated all anomalies [15]. This triggered the first string revolution and hundreds of physicists were inspired by it and dedicated themselves to this field. After this success, the so-called heterotic superstring theories [1] were discovered, which are equipped with either a $SO(32)$ or a $E_8 \times E_8$ gauge group [16]. Especially the latter string theory caused excitement, because it included both, gravity, and a gauge group large enough to contain the gauge group of the standard model as a subgroup.

The first attempt to obtain the standard model was performed on $E_8 \times E_8$ heterotic string compactifications. The gauge group of the standard model was embedded in one of the E_8 factors, while the second one was kept as a *hidden* gauge group and could only be reached via gravity [17]. To satisfy $\mathcal{N} = 1$ supersymmetry (SUSY), it was found that the six extra dimensions had to be compacted on a Calabi-Yau threefold CY_3 [18]. In such a theory, realistic models could indeed be constructed, such that they introduced families of chiral fermions.

At that time, a total of five different but consistent superstring theories have been established. Type I, type IIA, type IIB [19], and the two heterotic ones. While physicists worked on the respective superstring theories, there was one in particular who could not stop asking himself why there were five different string theories. It was in 1995 at a conference at the University of Southern California where Edward Witten gave a lecture and announced to the scientific community which of the five string theories was the correct one - namely all of them [4]. Witten claimed that the respective string theories are connected by *dualities* and can be transformed into each other, which is illustrated in Fig. 1.1. Thus, the string theories are per se different ways of

[1] String theory in its first formulation was a pure bosonic theory and had the problem of a tachyonic ground state. However, by adding supersymmetry, this could be resolved.

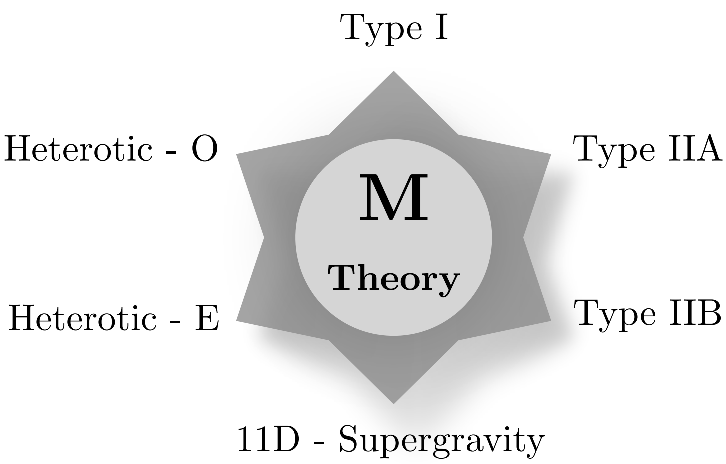

Figure 1.1: The M-theory promises and offers to combine all five different superstring theories in a superordinate framework in eleven dimensions. In this theory, the individual superstring theories are individual limits of M-theory, which are represented as corners in the figure. These known vertices can be transformed into each other via dualities. Another limit of the M-theory is the 11-dimensional supergravity.

looking at the same phenomenon and all of them give the same result, but under a different point of view. Furthermore, Witten stated that the theories are limiting cases of a higher fundamental theory: the mother of all string theories or the *M-theory* [2] [20, 21].

This M-theory, whose exact nature is still rather obscure, and which is formulated in eleven instead of ten dimensions, triggered the second string revolution by explaining that the fundamental objects in such a theory are higher-dimensional membranes or branes and by changing the perturbative framework to a framework of non-perturbative nature.

So-called D-branes played a particularly central role. The introduction of such non-perturbative objects turned the focus to the type I and type II string theories, since these D-branes lead to the gauge groups of the standard model without endowing string theories with gauge groups. It even became possible to construct non-supersymmetric models which were not possible before. This was the historical origin of the *intersecting brane world scenarios* with the quest to build the standard model.

1.2 A Path to the Standard Model with Intersecting Worlds

In order for string theory to live up to its claim of being a unified theory of *quantum gravity* (QG), it must, as we have seen, be able to reproduce within its limits, Einsteins Theory of Gravity, and the standard model with its quantum field theory. In this thesis, we will largely ignore the aspect of gravity and focus on realisations of the standard model. To construct such a model from intersecting brane worlds, there are basically two different methods. The *top-down* and the *bottom-up* approach. While the first approach uses mathematical consistencies of string theory to derive realisations of the standard model and is historically older and related

[2] There are wild speculations what the "M" in M-Theory actually stands for. Witten himself said he did not want a final name for a theory that has not yet revealed itself in its entirety. In this case, the letter stands for mysterious, magical, mother, monster or simply membrane or matrix. Others claim that it represents an inverted "W", whereby Witten wanted to immortalise himself in the name. Another possibility is, that it is to be understood much more symbolically, because the symbol "M" connects five points harmoniously with each other.

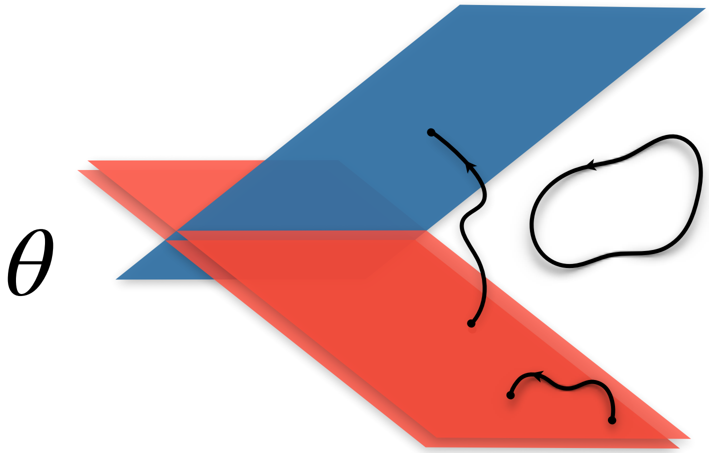

Figure 1.2: D-branes furnish a geometric illustration of the standard model's origin. Open strings that are confined to the hyperplanes of a stack of coincident D-branes provide natural gauge symmetries. Furthermore, open strings stretched near the intersection between two different stacks of D-branes and an angle θ explain charged chiral fermions. Gravity, on the other hand, is described by closed strings which can propagate freely in all dimensions of the string theory.

to the heterotic string models, the bottom-up approach is of phenomenological nature and tries to provide the correct particle content starting from experimental observations and only subsequently introducing adjustments in form of constraints. In this work, we will use the latter strategy.

Furthermore, we agree on four key properties of the standard model on the basis of which we construct and test these so-called semi-realistic models.

- First of all, we want to obtain a **gauge group** corresponding to the one of the standard model. This is given by $SU(3)_C \times SU(2)_L \times U(1)_Y$.
- In order to get the matter content of the standard model, we have to make sure that it has the right **chiral spectrum**.
- The third key feature is given by the fact that the quarks and leptons of the standard model occur in **three generations**.
- Finally, the fourth key feature is that we want a standard model with $\mathcal{N} = 1$ **supersymmetry**.

A semi-realistic effective field theory arising from such a string theory should provide these key features. In addition, it should explain the origin of the standard model and give possible extension of it. It should also make phenomenological predictions and ultimately clarify problems of the standard model, like the incorporation of gravity, dark matter, neutrino masses and the origin of the three generations or families.

The intersecting brane world scenarios within the type IIA superstring theory, which we encountered in the previous historical overview, have the thrilling property of deriving the desired four-dimensional theories with the help of a very geometric framework. The basic idea is fairly simple. The gauge symmetries originate from open strings attached within overlapping D-branes, while charged chiral fermions are described by open strings living in the intersections between such branes. This is indicated in Fig. 1.2.

The first such models were constructed in type I string theory using magnetised D-branes [22–24], which are related by duality [25] with the geometrically more intuitive intersecting D-branes. The first intersecting D-brane models were discussed in [26, 27]. The first non-chiral orientifold models with intersecting D-branes were presented in [28–33]. The first chiral intersecting D-branes at an angle were discussed in [34–37], where in the last two the background space consisted of a factorisable $\mathbb{T}^6$ torus with an $\Omega_{\mathcal{P}}\mathcal{R}(-)^{\mathcal{F}_L}$ orientifold. The first chiral and supersymmetric models were presented in [38, 39]. For further reviews of constructed intersection D-brane models, we recommend [40].

1.3 Outline of this Thesis

The outline of this thesis is essentially divided into two parts. In the first part, we will discuss and review the main mathematical and technical concepts necessary to build such semi-realistic models. We will take a bottom-up approach in the framework of type IIA superstring theory, which has the advantage that it provides a largely geometric and therefore descriptive explanation. In the second part of this thesis, we will shift the focus to applications and concrete realisation of the standard model using D-brane configurations. Furthermore, we will do phenomenology within this developed framework and turn to a possible application, which is at the same time a current research topic.

This thesis also carries the hope of the author to provide a pedagogical introduction to this very complex and often opaque or daunting, but incredibly exciting field. Nevertheless, this work will also discuss details and take a closer look at essential steps and conceptual ideas.

In chapter 2, we will derive the origin of the gauge sector, which is related to the D-brane world-volume. For this purpose, we will discuss Dp-branes in detail and show how open superstrings - attached to a higher dimensional single Dp-brane - yield an abelian $U(1)$ gauge theory. We will generalise this result by considering stacks of N coincident Dp-branes incorporating non-abelian $U(N)$ gauge theories.

In chapter 3, we will consider the foundations for the origin of the chiral matter sector. For this purpose, we will use D6-branes which intersect at non-trivial angles relatively to each other. Near these intersections, open strings are localised which are stretched from one brane to the other. We will find that at lowest energy open strings in these intersections give rise to massless four-dimensional spacetime fermions in a *bi-fundamental* representation. Furthermore, we will find a whole tower of more massive excitations whose mass depends on the intersection angle, known as *light stringy states.* Finally, we will derive how the exact choice of the relative angle makes a statement about the supersymmetry of the model.

In chapter 4, we will compactify six of the ten dimensions. We will choose a factorisable $\mathbb{T}^6$ torus as the simplest Calabi-Yau space. We will find that D6-branes can thus be viewed as homological 3-cycles which intersect in the compact space. This intersection number will give us a measure of how often the branes intersect. Consequently, open strings living near the intersections of two D6-branes appear in a multiplicity based on this mere topological *intersection number.*

This compactifications with just D6-branes will not be sufficient to provoke an $\mathcal{N}=1$ supersymmetry. To make this possible, we will introduce the concept of *orientifolds.* We will conclude this chapter with a detailed investigation of *global consistency conditions.* We will explicitly derive how all quantum anomalies can be resolved using the generalised Green-Schwarz mechanism.

In chapter 5, we will start to construct semi-realistic standard models using the techniques and concepts discussed in the first part of this thesis. At the beginning, we will investigate how we get from unitary gauge groups introduced by the D-branes to the special unitary groups of the standard model at the cost of additional $U(1)$'s. To avoid extra exotic chiral fermions, we will introduce the concept of orientifold projection, which serves as one possible method in this thesis to avoid extra fermions. Moreover, we will apply the generalised Green-Schwarz mechanism, which endows the $U(1)$'s with a *Stückelberg* mass and decouples them from the theory in the low-energy limit but preserves them as a global symmetry. At the end of this chapter, all considerations will lead to two numerical examples.

In chapter 6, we will investigate a supersymmetric D-brane model which realises a *minimal supersymmetric standard model* (MSSM). To ensure $\mathcal{N} = 1$ supersymmetry in that case, we will use a $\mathbb{Z}_2 \times \mathbb{Z}_2$ orbifold in addition to the orientifold projection. Furthermore, we will explore that by brane recombination of this model configuration, a *Pati-Salam model* emerges, which is a possible model for a *grand unified theory* (GUT).

In chapter 7, we will turn to a phenomenological aspect. Intersecting brane world scenarios make it possible to lower the string scale to a few TeV. This chapter will be based on a recent publication [41] by Pascal Anastasopoulos and the author of this thesis, my humble self. We will investigate the lifetime of a light stringy state which is a possible candidate for *dark matter*.

Part I

General Overview and Theoretical Background

Chapter 2

D-branes and Gauge Field Theories

In this chapter, we will develop the relationship between stacks of N Dp-branes and $U(N)$ gauge field theories. For this purpose, we will review how Dp-branes are introduced in string theory and emphasise that these objects constitute a class of their own with a dynamic which is independent of the string.

Subsequently, we will analyse the resulting spectrum of open strings attached to a single Dp-brane. The spectrum of an open superstring with fixed endpoints in the transversal directions of the world-volume of the Dp-brane will provide us with Goldstone bosons (resp. Goldstinos) - as these hyperplanes break the translation invariance of the Poincaré symmetry (resp. the associated supersymmetry) - and a Maxwell field, which lays out a connection between open strings, Dp-branes, and abelian $U(1)$ gauge fields.

Further, we will discover that these considerations can be generalised through the implementation of so-called stacks of N parallel Dp-branes. These stacks of branes, which are coincident but still distinguishable, provide us with the concept of stretched strings between different Dp-branes and make it possible to incorporate non-abelian $U(N)$ gauge theories in a modern, intuitive, and geometrical way. These results will finally yield gauge bosons, which correspond to the force carriers that mediate the strong, weak, and electromagnetic fundamental interactions in the standard model.

Finally, we will present the effective D-brane action. This establishes a remarkable connection since the effective $(p+1)$ dimensional world-volume action for the massless open string modes describes the dynamic of the Dp-brane.

In order to introduce Dp-branes, we will briefly review how the dynamics of open strings in bosonic string theory are described by the Brink-DiVecchia-Howe (BDH) action, better known as the so-called Polyakov action. The action in conformal gauge is defined as [42, 43]

$$\mathcal{S}_{\text{BDH}} = -\frac{T}{2}\int_\Sigma d^2\xi \; \eta^{ab}\, \partial_a X^\mu(\xi)\, \partial_b X^\nu(\xi)\, \eta_{\mu\nu} \; . \tag{2.1}$$

The string tension T is characterised in terms of the so-called Regge slope α' or the string (mass) scale M_s according to [44]

$$T = \frac{1}{2\pi\alpha'} = \frac{M_s^2}{2\pi} \; . \tag{2.2}$$

The spacetime indices on the string coordinates X^μ are contracted with the Minkowski metric $\eta_{\mu\nu}$, while η^{ab} denotes the world-sheet metric. Further, X^μ constitutes a spacetime vector, but is a scalar from the point of view of the world-sheet Σ. The indices a and b run over two values of

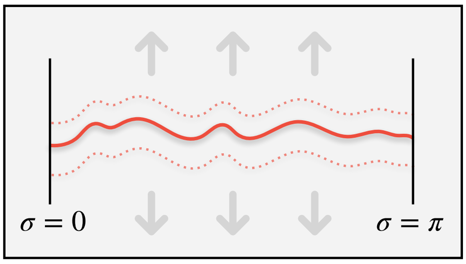

(a) NN boundary conditions. The derivatives vanish at the boundaries. The strings can move freely along the boundaries.

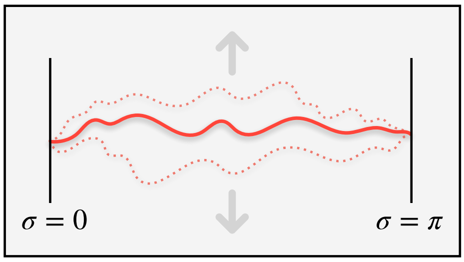

(b) DD boundary conditions. Strings are fixed at the boundaries but can oscillate in the transverse directions.

Figure 2.1: Illustration of an open string with NN and DD boundary conditions.

the corresponding world-sheet coordinates τ and σ. Further, we use the common and compact convention [45] in the definition of Eq. (2.1)

$$\xi^a = \left(\xi^1, \xi^2\right) = (\tau, \sigma) \quad \text{and} \quad \partial_a = \frac{\partial}{\partial \xi^a} \, . \tag{2.3}$$

To find the equations of motion, we extremise the action in Eq. (2.1) as usual and use partial integration [46]

$$\begin{aligned} \delta \mathcal{S}_{\text{BDH}} &= -\frac{T}{2} \int_{\tau_1}^{\tau_2} d\tau \int_0^\pi d\sigma \; 2\,\eta^{ab}\, \partial_a X^\mu \, \delta(\partial_a X_\mu) \\ &= T \int_{\tau_1}^{\tau_2} d\tau \int_0^\pi d\sigma \;\, \partial_a \left(\eta^{ab} \partial_b \, X^\mu\right) \delta X_\mu + \text{a total derivative} \, . \end{aligned} \tag{2.4}$$

The total derivative in Eq. (2.4) can be split into two different boundary terms, the τ-boundary term and the σ-boundary term. Together these terms read

$$T \left[\int_0^\pi d\sigma \; \partial_\tau X^\mu \delta X_\mu \right]_{\tau=\tau_1}^{\tau=\tau_2} \quad \text{and} \quad T \left[\int_{\tau_1}^{\tau_2} d\tau \; \partial_\sigma X^\mu \delta X_\mu \right]_{\sigma=0}^{\sigma=\pi} \, . \tag{2.5}$$

As always, the first term vanishes by assumption, if we demand that $\delta X^\mu = 0$ at $\tau = \tau_1$ and $\tau = \tau_2$. However, the second term is more subtle. The second term has also to vanish to give us a two-dimensional wave equation $\partial_a \partial^a X^\mu = \Box X^\mu = 0$ [46]. Involving a non-local boundary condition would further not give a local two-dimensional worlds-heet theory. In order to fulfil this requirement, we demand

$$\partial_\sigma X^\mu \delta X_\mu = 0 \qquad \text{at} \qquad \sigma = 0,\, \pi. \tag{2.6}$$

This can be achieved in the following ways for open strings [44, 46]:

- $\partial_\sigma X^\mu|_{\sigma=0} = \partial_\sigma X^\mu|_{\sigma=\pi} = 0$, which corresponds to the so-called Neumann boundary condition. There is no restriction on δX^μ, thus the string is free to move in all directions. This case is also known as an open string with so-called NN boundary conditions because both endpoints of the strings satisfy Neumann boundary conditions.
- $\delta X^\mu|_{\sigma=0} = \delta X^\mu|_{\sigma=\pi} = 0$, which corresponds to the so-called Dirichlet boundary condition. Intuitively, this means that the endpoints of the string coordinates are fixed at a constant position $X^\mu = \widetilde{x}^\mu$. In this case, one speaks of an open string with DD boundary conditions
- In general, mixed boundary conditions are also allowed. These are called ND (DN) boundary conditions. These are especially relevant when open strings are stretched between Dp-branes and Dq-branes (where $p \neq q$).

An illustration of an open string with NN and DD boundary conditions is depicted in Fig. 2.1a and Fig. 2.1b.

At first, especially Dirichlet boundary conditions might raise the question why the strings should not be able to move freely in some directions while they are completely free in others. These hyperplanes on which open strings can end and which restrict their motion were given the suggestive name D-branes, where the D stands for Dirichlet. It was Joseph Polchinski in 1996, who gave these D-branes a more *objective reality* [47]. This paradigm shift represents the second revolution within string theory, as D-branes became non-trivial objects with their own dynamics.

Without going into great detail, Dp-branes are stable[1] extended objects with p spatial dimensions spanning a $(p+1)$ dimensional world-volume. For example, a D1-brane would be a string-like object or a D0-brane, somehow particle-like in covariant quantisation. If the string is completely free to move in all spatial dimensions and thus fulfils NN boundary conditions everywhere, this can also be interpreted as if there was a D$(d-1)$ brane in all spatial directions. This special D-brane is a so-called space filling D-brane. These special types of branes are further dynamical (described by their own action) and non-perturbative objects. Further, they are charged under so-called *RR p-forms* [40, 47, 49].

The world-volume of a Dp-brane is not static but undergoes quantum fluctuations. Figuratively speaking, the brane is fluctuating in the normal or transverse direction, which can be interpreted as light open string excitations.

At this point, it is advisable to make a brief but rather important digression. Strings are the fundamental building blocks in string theory, so one could now ask the legitimate question to what extent D-branes play a role in this theory, since they represent objects in their own right. Are these objects more or less fundamental than strings or are they just additionally needed for reasons of consistency? This question is strongly related to the epistemological field of *reductionism* in physics or philosophical science [50]. Let us think, for example, of particle physics where attempts are being made to reduce the standard model to a few elementary building blocks. Reductionism inherits the hope to simplify the entire theory. Despite this attempt by reductionism, the theory fails to be simplified. Indefinite parameters, discrepancies between experiment and theory and the non-existent incorporation of gravity leave the theory incomplete. String theory takes a slightly different approach here. To quote Leonard Susskind [51]:

> “ *String theory and other developments in modern physics mark the end of reductionism.* ”
>
> Leonard Susskind, *Stanford Lectures*, Fall 2010.

For a better understanding, we will explain it with a more pictorial example. Originally, we introduced Dp-branes for mathematical reasons, knowing that they are a class of non-trivial objects. Let us think of D1-branes. These branes somehow akin to strings and are therefore also called D-strings. Despite their similarities, D-strings are heavier than the fundamental strings (F-strings), measured in units of length. Let us assume in the following that there is a coupling constant g, which corresponds to whether a string breaks into two or not. A schematic depiction of this example can be found in Fig. 2.2.

For $g << 1$, we have typical thin and light F-strings and heavy and complex D-strings. If we

[1] In the way, as we have defined Dp-branes, there are always Neumann boundary conditions along the X^0 coordinate. One could of course also allow Dirichlet conditions along this direction, which would physically mean that the brane is fixed at a certain point in (space-)time. Such a brane is called a D(-1)-brane and corresponds to a so-called D-instanton or Euclidean instanton. [48]

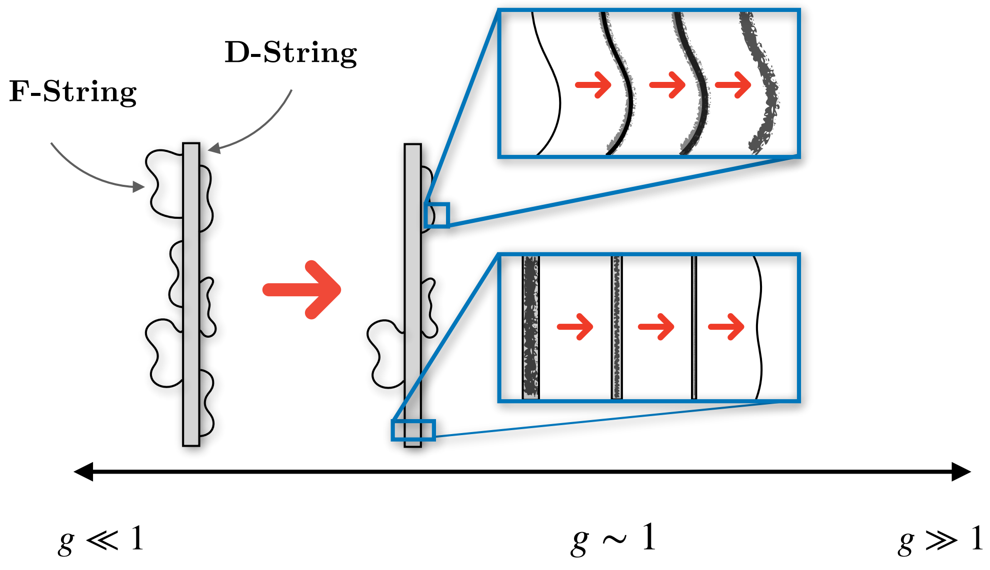

Figure 2.2: A pictorial illustration of the relation between F-strings and D-strings.

increase the parameter g, the F-strings will break apart and their pieces will form an "atmosphere" around the original location of the string. The higher g becomes, the more complex will be this atmosphere. At the same time, the D-string is getting thinner and thinner and stops therefore producing more F-strings. Around $g \sim 1$, we can no longer distinguish between a F-string or a D-string.

For $g >> 1$, the reverse process happens, and the original F-string becomes a D-string and the D-string becomes a F-string. This phenomenon is sometimes referred to as the so-called S-duality in string theory [52]. The parameter g indicates which object can be regarded as more fundamental, but it is not as simple as one thinks, since $g = g(x^\mu)$ is a field and can vary its value in space. Thus, the answer to the question which object is more fundamental is nothing but tossing a coin. [51, 53].

2.1 Open Superstrings on a Single Dp-brane

In this section, we desire to derive the spectrum of an open string, whose endpoints are attached to a single Dp-brane. In standard literature, this is mostly done in the context of bosonic string theory. Here, we deliberately choose a slightly different route and discuss the spectrum within the framework of *RNS* formalism already. We will not discuss the entire quantisation in detail here, as this can be found in standard introductory books such as [45] and [40]. Furthermore, the *non-supersymmetrical bosonic* case is discussed in detail in these two books.

The introduction of D-branes has an enormous influence on the symmetries of the superstring theory. First and foremost, the Lorentz group $\mathcal{L}$ is *spontaneously* broken into

$$SO(1, d-1) \to \underbrace{SO(1, p)}_{\mathcal{L}\text{ in the world-volume of the Dp-brane}} \times \underbrace{SO(d-1-p)}_{\text{rotation group in the } d-1-p \text{ directions}} . \tag{2.7}$$

Secondly, half of the supersymmetry of spacetime is broken on the Dp-brane [54]. The spacetime

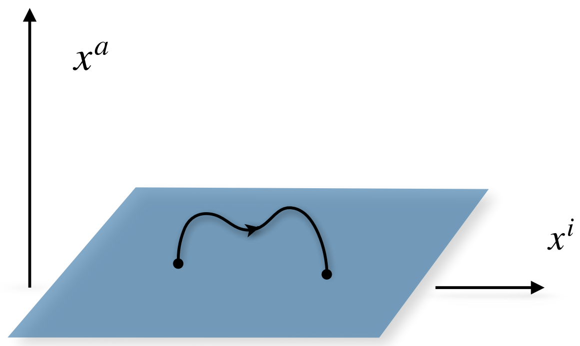

Figure 2.3: An oriented string whose endpoints lie on a D-brane. These endpoints satisfy NN boundary conditions, since the string can move along the x^i coordinates as long as the endpoints are confined to the hypersurface of the D-brane. From the point of view of the x^a coordinates, the endpoints are fixed and satisfy thus DD boundary conditions.

coordinates x^μ can thus be divided into two groups. The first group consists of the coordinates $\{x^0, \ldots, x^p\}$, which are longitudinal to the Dp-brane world-volume and thus satisfy NN boundary conditions. The second group of coordinates $\{x^{p+1}, \ldots, x^{d-1}\}$ consists of those who are normal to the world-volume of the Dp-brane, which satisfy DD boundary conditions. The Dp-brane itself is fixed by coordinates $x^a = \tilde{x}^a$ for $a = p+1, \ldots, d-1$. By further introducing *light cone coordinates*, for which a spatial tangential coordinate is used with the temporal coordinate in order to deliver $X^\pm = \frac{1}{\sqrt{2}}(X^0 \pm X^p)$, we obtain the following distinction for the string coordinates [45]

$$\begin{aligned}
&\text{NN}: \quad X^+, X^-, \left\{X^i\right\} \qquad \text{with} \quad i = 1, , \ldots, p-1, \\
&\text{DD}: \qquad\qquad\quad\; \left\{X^a\right\} \qquad \text{with} \quad a = p+1, \ldots, d-1 \;.
\end{aligned} \tag{2.8}$$

Figure 2.3 illustrates this scenario. Imposing the boundary conditions on the mode expansion for an open string yields [45]

$$\begin{aligned}
X^i(\tau, \sigma) &= \tilde{x}^i + \frac{p^i}{p^+}\tau + i\sqrt{2\alpha'} \sum_{n \neq 0} \frac{\alpha_n^i}{n} e^{-in\tau} \cos n\sigma \;, \\
X^a(\tau, \sigma) &= \tilde{x}^a + \sqrt{2\alpha'} \sum_{n \neq 0} \frac{\alpha_n^a}{n} e^{-in\tau} \sin n\sigma \;.
\end{aligned} \tag{2.9}$$

We note that in the second line of Eq. (2.9) no terms appear linearly in τ. This is due to the DD boundary conditions and means that the string does not have a net time-average momentum in these x^a directions. This is of course intuitively reasonable since the string is attached to the brane and the endpoints are fixed there. Through *canonical quantisation* in light cone coordinates, the modes become creation and annihilation operators satisfying the commutators [45]

$$[\alpha_m^i, \alpha_n^j] = m\, \delta^{ij}\, \delta_{m+n,0} \quad , \quad [\alpha_m^a, \alpha_n^b] = m\, \delta^{ab}\, \delta_{m+n,0} \;. \tag{2.10}$$

In superstring theory, of course, we must also consider the fermionic oscillation degrees of freedom. Analogous to the bosonic case, this leads us to *Grassmann-valued* modes, which obey the following anti-commutators after quantisation [40]

$$\left\{\psi_{n+r}^i, \psi_{-(m+r)}^j\right\} = \delta_{nm}\delta^{ij} \,, \left\{\psi_{n+r}^a, \psi_{-(m+r)}^b\right\} = \delta_{nm}\delta^{ab} \quad \text{with} \quad r = \left\{ \begin{array}{ll} r = 0, & \text{R} \\ r = \frac{1}{2}, & \text{NS}, \end{array} \right. \tag{2.11}$$

where R stands for the *Ramond* sector and NS for the *Neveu-Schwarz* sector. Finally, we give the spacetime mass squared formula [55]

$$\alpha' M^2 = N_\mathrm{B} + N_\mathrm{F} + a_{\mathrm{NS/R}} \quad \text{with} \quad a_{\mathrm{NS/R}} = -\frac{r(d-2)}{8} \ . \tag{2.12}$$

with the bosonic (B) and fermionic (F) number operators in light-cone gauge

$$N_B = \sum_{m\in\mathbb{N}} \left[\sum_{i=1}^{p-1} \alpha^i_{-m}\alpha^i_m + \sum_{a=p+1}^{d-1} \alpha^a_{-m}\alpha^a_m \right] \quad \text{and} \quad N_F = \sum_{n\in\mathbb{N}} \left[\sum_{i,a} (n+r)\ \psi_{-(n+r)}\psi_{n+r} \right] \tag{2.13}$$

Accompanied by these ingredients, we can build the Fock space in the NS and R sector and discuss the spectrum of an open string on a single Dp-brane. Before we begin, we want to briefly mention how the states in the string spectrum are classified.

From *Wigner's Classification* [56] we understand that particles (or string excitations) can be classified into irreducible, projective, and unitary representations of the stabiliser (or little group) [57]. The stabiliser forms a subgroup of the Lorentz Group $SO(d-1,1)$ that leaves the momentum invariant. Light-cone coordinates manifestly break the $SO(d-1,1)$ symmetry to the subgroups $SO(d-2) \subset SO(d-1,1)$. The spectrum of the string can be organised a priori into representations of $SO(d-2)$, which must be re-organised into representations with respect to the little group [40].

2.1.1 The NS Sector on a Single Dp-brane

A generic state in the NS sector Fock space takes the form of

$$\left\{ \prod_{m=1}^{\infty}\prod_{i=1}^{p-1} \left(\alpha^i_{-m}\right)^{\lambda_{m,i}} \prod_{n=1}^{\infty}\prod_{a=p+1}^{d-1} \left(\alpha^a_{-n}\right)^{\lambda_{n,a}} \prod_{i=1}^{p-1}\prod_{r} \left(\psi^i_{-r}\right)^{\rho_{r,i}} \prod_{a=p+1}^{d-1}\prod_{s} \left(\psi^a_{-s}\right)^{\rho_{s,a}} \right\} |0;\boldsymbol{p}\rangle_{\mathrm{NS}} \tag{2.14}$$

with $r,s \in \mathbb{Z}+\frac{1}{2}$ and $\rho \in \{0,1\}$. For the sake of clarity and compactness, we will use the following $|\mathrm{B}\rangle \otimes |\mathrm{NS}\rangle \equiv |0;\boldsymbol{p}\rangle_{\mathrm{NS}}$. The state $|\mathrm{B}\rangle$ denotes the usual bosonic vacuum $|0;\boldsymbol{p}\rangle$ with $\boldsymbol{p} = p^i$, while $|\mathrm{NS}\rangle \equiv |0\rangle_{\mathrm{NS}}$ constitutes the unique ground state of the NS-sector.

The Ground State in the NS Sector

The ground state $|\mathrm{GS}\rangle$ is the vacuum, which is defined as $\alpha^i_m\,|0;\boldsymbol{p}\rangle = 0$ for $\forall m > 0$ and $\psi^i_r\,|\mathrm{NS}\rangle = 0$ for $\forall r > 0$. This insinuates that $N_\perp\,|0;\boldsymbol{p}\rangle = 0$, which yields for the mass squared operator

$$M^2|0;\boldsymbol{p}\rangle_{\mathrm{NS}} = \frac{a_{\mathrm{NS}}}{\alpha'}|0;\boldsymbol{p}\rangle_{\mathrm{NS}} = -\frac{1}{2\alpha'}|0;\boldsymbol{p}\rangle_{\mathrm{NS}} \ . \tag{2.15}$$

Where we used the fact, that the critical dimension of superstring theory is $d = 10$. Thus, the ground state is given as

$$|\mathrm{GS}\rangle \equiv |0;\boldsymbol{p}\rangle_{\mathrm{NS}} \quad \text{with} \quad M^2 = -\frac{1}{2\alpha'} \ . \tag{2.16}$$

This is clearly a pure Neumann state, whose field corresponds to a tachyon field [2], but because of the momentum $\boldsymbol{p}$ it is confined in the NN directions along the Dp-brane. It is a scalar or, in terms of Young tabelaux, a $\bullet$ of the little group $SO(d-1)$. Hence, the field transforms as a Lorentz scalar on the Dp-brane [58] [40].

[2] In contrast to the tachyonic ground state in the closed string sector, the open string tachyon can be interpreted as an instability of the Dp-brane. The Dp-brane will decay by disintegrating into closed string modes. This vacuum is therefore not as sensitive as within the closed string sector, but for bosonic string theory it means, that the Dp-branes are consequently not stable objects. We will see that this is different in superstring theory.

First Excitations in the NS sector

To get the first excited states, we must act with the lowest possible creation operators in Eq. (2.14) on the ground state. As a consequence, the first excited state can be written as a linear combination

$$|L1\rangle = \left(\sum_{i=1}^{p-1} A_i \, \psi^i_{-\frac{1}{2}} + \sum_{a=p+1}^{d-1} \phi_a \, \psi^a_{-\frac{1}{2}} \right) |0; \boldsymbol{p}\rangle_{\mathrm{NS}} \ . \tag{2.17}$$

Here, we must distinguish between two different cases, because the Dp-brane breaks the $SO(d-2)$ into $SO(p-1) \times SO(d-1-p)$.

1. **Parallel or longitudinal excitations**

   The longitudinal, massless, and linearly independent excitations in Eq. (2.17) are created by

   $$\sum_{i=1}^{p-1} A_i \, \psi^i_{-\frac{1}{2}} \, |0; \boldsymbol{p}\rangle_{\mathrm{NS}} \quad \text{with} \quad M_A^2 = 0. \tag{2.18}$$

   The index i lies within the Dp-brane and from that point of view the excitation propagates along the Dp-brane. Thus, the state transforms according to the *vector* or *fundamental representation* $\square$ of $SO(p-1)$. Especially for the case of a space filling $D(d-1)$-brane, and thus only NN boundary conditions, the a-priori representation would be $\square$ of $SO(d-1-1)$ and conventionally for $d = 10$, a $\mathbf{8}_v$ with respect to $SO(8)$. The stabiliser for a massless state is $SO(d-2)$ and therefor it is legitimate to associate a massless spin 1 particle to this state. As a general statement of QFT, every massless vector boson corresponds to a gauge potential [40]. Thus, we have found that there is a *Maxwell gauge field* living on the world-volume of the Dp-brane.

   Generally speaking, we can therefore say that a single Dp-brane hosts a $U(1)$ gauge theory.

2. **Normal or transversal excitations**

   The normal excitations in Eq. (2.17) are created as follows, by acting on the ground state

   $$\sum_{a=p+1}^{d-1} \phi_a \, \psi^a_{-\frac{1}{2}} \, |0; \boldsymbol{p}\rangle_{\mathrm{NS}} \quad \text{with} \quad M_\phi^2 = 0. \tag{2.19}$$

   From the perspective of the D-brane, these states correspond to a set of $(d-1-p)$ massless scalar fields living on the D-brane, since there is no index i. We denote them again as $\bullet$, since they transform as $(d-1-p)$ scalars of $SO(p-1)$ [3]. These fields can be interpreted as *Goldstone* modes, arising from the spontaneous symmetry breaking of the translational invariance due to the Dp-brane. This also confirms our initial statement that Dp-branes are dynamic objects, as these excitations can be understood as fluctuations of the brane.

   Generally speaking, we can say that for each normal direction a Dp-brane gives a massless Goldstone boson.

We will not discuss higher and consequently massive excitations, but the considerations are analogous to the previous cases, except that all light-cone states, which form tensors under $SO(d-2)$ must be recombined into tensors of $SO(d-1)$ - the little group for massive states in d dimensions.

[3] Although they transform as scalar fields under the $SO(p-1)$, they still transform as a vector under $SO(d-1-p)$ transverse to the brane. This is a global symmetry on the brane world-volume. [46]

2.1.2 The R Sector on a Single Dp-brane

A generic state in the R sector Fock space is given by

$$\left\{ \prod_{m=1}^{\infty} \prod_{i=1}^{p-1} \left(\alpha^i_{-m}\right)^{\lambda_{m,i}} \prod_{n=1}^{\infty} \prod_{a=p+1}^{d-1} \left(\alpha^a_{-n}\right)^{\lambda_{n,a}} \prod_{i=1}^{p-1} \prod_{r} \left(\psi^i_{-r}\right)^{\rho_{r,i}} \prod_{a=p+1}^{d-1} \prod_{s} \left(\psi^a_{-s}\right)^{\rho_{s,a}} \right\} |0;\boldsymbol{p}\rangle_{\mathrm{R}} \tag{2.20}$$

where $r, s \in \mathbb{Z}$. Here we will again use the usual convention that $|\mathrm{B}\rangle \otimes |\mathrm{R}\rangle \equiv |0;\boldsymbol{p}\rangle_{\mathrm{R}}$, where $|\mathrm{R}\rangle \equiv |0\rangle_{\mathrm{R}}$ denotes the degenerated (spinorial) ground state of the R sector.

The ground state in the R sector

The ground state for the R sector is defined by $\alpha^i_m |0;\boldsymbol{p}\rangle_{\mathrm{R}} = \psi^i_r |0;\boldsymbol{p}\rangle_{\mathrm{R}} = 0$ for $\forall m, r > 0$. Unlike the NS sector, this vacuum is not uniquely defined because of the appearance of zero modes ψ^i_0 in the R sector, which are commuting with the mass operator. This means that $\psi^i_0 |0;\boldsymbol{p}\rangle_{\mathrm{R}}$ and $|0;\boldsymbol{p}\rangle_{\mathrm{R}}$ have the same mass [54]. In this context, the R vacuum is called *degenerated*.

A special characteristic inherent in the R sector is that these zero modes - with the redefinition $\psi^\mu_0 = \frac{1}{\sqrt{2}}\Gamma^\mu$ and suppressing spinor indices - satisfy a *Clifford algebra* $\{\Gamma^\mu, \Gamma^\nu\} = 2\eta^{\mu\nu}$ in d dimensions, where Γ^μ are the usual *gamma matrices* in d dimensions. Thus, the Ramond ground state transforms in a spinor representation and can be collected into a representation of $SO(1, d-1)$ [4]. That means that the R ground state is a priori a d-dimensional Dirac spinor with $2^{\frac{d}{2}}$ complex components creating spacetime fermions. For superstring theory, where $d = 10$, the vacuum constitutes a 32-fold degenerated vacuum. To take advantage of this representation in ten dimensions, we introduce the following new basis [59–62]

$$d_0^{\pm} = \frac{1}{\sqrt{2}}\left(\psi^1_0 \mp \psi^0_0\right), \quad d_i^{\pm} = \frac{1}{\sqrt{2}}\left(\psi^{2i}_0 \pm i\psi^{2i+1}_0\right) \qquad i = 1, \ldots, 4\,. \tag{2.21}$$

In this new basis, the Clifford algebra is defined by $\left\{d_i^+, d_j^-\right\} = \delta_{ij}$. These redefined creation and annihilation operators give rise to 32 Ramond ground states, which we denote as

$$|\boldsymbol{s}\rangle \equiv |s_0, s_1, s_2, s_3, s_4\rangle \quad \text{with} \quad s_i = \pm\frac{1}{2},\ \forall i = 0, \ldots, 4. \tag{2.22}$$

The creation operators d_i^+ are raising s_i from $-\frac{1}{2}$ to $\frac{1}{2}$, while $d_i^- \left|-\frac{1}{2}, -\frac{1}{2}, -\frac{1}{2}, -\frac{1}{2}, -\frac{1}{2}\right\rangle = 0$.

In dimensions with $d = 2$ mod 8 we can impose further constraints. The 32 complex degrees of freedom reduce to 32 real degrees of freedom due to the reality or "Majorana" condition (possible for $d = 0, 1, 2, 3, 4$ mod 8). Further, we can decompose it into a 16 component Weyl spinor (possible for even dimensions) with positive and negative (denoted by a prime) chirality.

$$[\mathbf{32}]_{\mathrm{Dirac}} = [\mathbf{16}]_{\mathrm{Weyl}} \oplus [\mathbf{16'}]_{\mathrm{Weyl}}\ . \tag{2.23}$$

The world-sheet fermions are thus real, chiral, and represented as so called Majorana-Weyl spinors.

Since we are making use of light cone gauge, we encounter through the manifestly spacetime symmetry breaking the subgroups $SO(d-2) \subset SO(d-1, 1)$. For $d = 10$, this yields $SO(8)$ as the subgroup of $SO(1, 9)$. Choosing the light cone gauge, the Weyl spinors decompose according to [59–62]

$$\mathbf{16} \to \left(\frac{1}{2}, \mathbf{8}\right) \oplus \left(-\frac{1}{2}, \mathbf{8'}\right) \quad \text{and} \quad \mathbf{16'} \to \left(\frac{1}{2}, \mathbf{8'}\right) \oplus \left(-\frac{1}{2}, \mathbf{8}\right)\ . \tag{2.24}$$

[4] Unfortunately, this is an abuse of notation that has been established in most of the literature. Of course we mean $\mathrm{Spin}(1, d-1)$, which is the double cover of $SO(1, d-1)$.

Sector	$\alpha' m^2$	Representation		Group	GSO
NS	$-\frac{1}{2\alpha'}$	$\|0\rangle$: $\bullet$		$SO(9)$	✗
NS	0	$\psi^a_{-1/2}\|0\rangle$: $\bullet$	$\psi^i_{-1/2}\|0\rangle$: $\square$	$SO(p-1)$	✓
R	0	$\|a\rangle$:	$(\mathbf{8})_s$	$SO(p-1)$	✗
R	0	$\|\dot{a}\rangle$:	$(\mathbf{8})_c$	$SO(p-1)$	✓

Table 2.1: The two lowest mass levels of the open string in the NS- and R sector for $d = 10$

That indicates that we are able to pack the 16 states into two sets of 8 states with distinguishable chirality. By denoting $\pm\frac{1}{2} \equiv \pm$ for the sake of clarity, we get

$$\underbrace{\underbrace{\begin{matrix} |+----\rangle & |++--+\rangle \\ |+++++\rangle & |+-++-\rangle \\ |+-+-+\rangle & |+--++\rangle \\ |++-+-\rangle & |+++--\rangle \end{matrix}}_{\left(\frac{1}{2},\mathbf{8}\right)} \quad \underbrace{\begin{matrix} |----+\rangle & |-+---\rangle \\ |-+++-\rangle & |--+++\rangle \\ |--+--\rangle & |---+-\rangle \\ |-+-++\rangle & |-++-+\rangle \end{matrix}}_{\left(-\frac{1}{2},\mathbf{8}\right)}}_{\mathbf{16}}$$

$$\underbrace{\underbrace{\begin{matrix} |+---+\rangle & |++---\rangle \\ |++++-\rangle & |+-+++\rangle \\ |+-+--\rangle & |+--+-\rangle \\ |++-++\rangle & |+++-+\rangle \end{matrix}}_{\left(\frac{1}{2},\mathbf{8'}\right)} \quad \underbrace{\begin{matrix} |-----\rangle & |-+--+\rangle \\ |-++++\rangle & |--++-\rangle \\ |--+-+\rangle & |---++\rangle \\ |-+-+-\rangle & |-++--\rangle \end{matrix}}_{\left(-\frac{1}{2},\mathbf{8}\right)}}_{\mathbf{16'}} \tag{2.25}$$

Since we expect the fermions to propagate through spacetime, we must impose the Dirac equation on $|\boldsymbol{s}\rangle$. By implying this on-shell condition only the states with $s_0 = \frac{1}{2}$ survive. All together, we can finally give the Ramond ground state [59–62].

$$|0\rangle_{\mathrm{R}} = \left(\frac{1}{2}, \mathbf{8}\right) \oplus \left(\frac{1}{2}, \mathbf{8'}\right) \equiv |a\rangle \oplus |\dot{a}\rangle \ , \tag{2.26}$$

where a is a spinor index of $SO(8)$. The Ramond ground state constitutes therefor two spinor representations $\mathbf{8}_s$ and $\mathbf{8}_c$ of the $SO(8)$, where the former and latter representations have an opposite chirality [63]. [5].

Since the corresponding fields live in the $(p+1)$-dimensional world-volume of the Dp-brane, we get $(p+1)$ dimensional fermions. The exact number of fermions can be computed by a decomposing of $\mathbf{8}_c$ of $SO(8)$ under $SO(p-1)$. Together with the results from the NS sector, we can now record all the found states - excluding the massive states - into table 2.1 [40, 55].

To get a consistent model in superstring theory, we use the GSO (Gliozzi-Scherk-Olive) projection, which projects out states regarding their fermion number $(-1)^F$. Thus, the tachyonic ground

[5] Having a deeper background in group theory, this result is not very unexpected but somehow still peculiar. The group $SO(8)$ or more precisely its universal cover Spin(8) is a special simple Lie group with an unique maximally symmetric *Dynkin* diagram

$D_4 \doteq$ 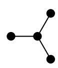 . (2.27)

Thus Spin(8) inherence a three-fold symmetry, which goes under the name *triality*. The group Spin(8) has three inequivalent eight-dimensional representations - two spinorial representations and a vector representation.

state disappears in the NS Sector and only the massless states survive, while in the R sector only one of the two chiral massless states survives. This ensures a tachyon free and spacetime supersymmetric spectrum for the open string [40].

Finally, we have found that the set of massless particles on a Dp-brane world-volume in ten dimensions is given by

- A $(p+1)$ dimensional $U(1)$ gauge boson from the NS sector.
- $9-p$ real Goldstone bosons propagating in the $(p+1)$ dimensional world-volume of the Dp-brane, which arise by breaking the translational symmetry or supersymmetry respectively, by the presence of a Dp-brane.
- Superpartners in form of $(p+1)$ dimensional spacetime fermions from the R sector in a representation by decomposing $\mathbf{8}_c$ of $SO(8)$ under $SO(p-1)$ [63].

2.2 Open Strings between a Stack of Parallel Dp-branes

In this section, we will generalise the previous results for strings stretched between N parallel Dp-branes. The position of a Dp-brane is determined by the coordinate $\tilde{x}$. For a stack of parallel Dp-branes, it applies that these branes are coincident if $\tilde{x}_1 = \tilde{x}_2 = \ldots = \tilde{x}_N$. Even though these Dp-branes are *coincident*, they are still *distinguishable* [6].

In contrast to the previous case, this setup opens up 4 different sectors:

- Open string starting at the a^{th} Dp-brane and ending at the a^{th} Dp-brane.
- Open string starting at the b^{th} Dp-brane and ending at the b^{th} Dp-brane.
- Open string starting at the a^{th} Dp-brane and ending at the b^{th} Dp-brane.
- Open string starting at the b^{th} Dp-brane and ending at the a^{th} Dp-brane.

From this, it can be concluded that the previous case of a single Dp-brane is a special case for parallel Dp-branes. Furthermore, we get two sectors in which the string is stretched between two different Dp-branes which differ only in the orientation of the string. In order to examine these two sectors in more detail, we will only consider the NS sector, since all considerations can be transferred to the R sector without complications. The setup is depicted in Fig. 2.4.

2.2.1 The Ground State in the NS Sector between Parallel Dp-branes

Before building the new ground state in the NS sector, we face a new problem. In addition to the oscillation numbers of the Fock states $|n\rangle$ and the momentum vector $\boldsymbol{p}$ lying in the NN dimensions, a new label is required to distinguish the different sectors: the so-called Chan-Paton labels or matrices $\boldsymbol{\lambda}$. Thus, with this label that encodes the different sectors, a general state can be written as [49, 54, 63]

$$|n, \boldsymbol{p}, \boldsymbol{\lambda}\rangle = \sum_{r=1}^{N} \sum_{s=1}^{N} \lambda^{q}_{rs} \, |n; \boldsymbol{p}; r, s\rangle \, . \tag{2.28}$$

with $r, s = 1, \ldots, N$. The first index r denotes the brane on which the string begins at $\sigma = 0$ and the second index s denotes the brane on which the string ends at $\sigma = \pi$. It is advisable to

[6] Of course it is also possible to consider parallel D-branes which are not coincident, but separated in the transverse directions by a separation distance $\Delta\tilde{x} \neq 0$. In that case, the original non-abelian theory is broken into its abelian subgroup $U(N) \rightsquigarrow U(1) \times \ldots \times U(1) = U(1)^N$. This is known as moving along the Coulomb or Higgs branch of the moduli space of gauge theories. For the case with moved apart D-branes, the mass-squared formula in Eq. 2.12 receives an additional positive contribution $\alpha' M^2 = \frac{\Delta\tilde{x}^2}{4\pi^2\alpha'} + N_{\mathrm{B}} + N_{\mathrm{F}} + a_{\mathrm{NS/R}}$. Since some originally massless gauge fields acquire a VEV and become massive, this is sometimes sloppily referred to as "higgsing". In fact, this is one possible interpretation of the *Higgs mechanism* in the context of D-branes [45, 49, 64, 65]

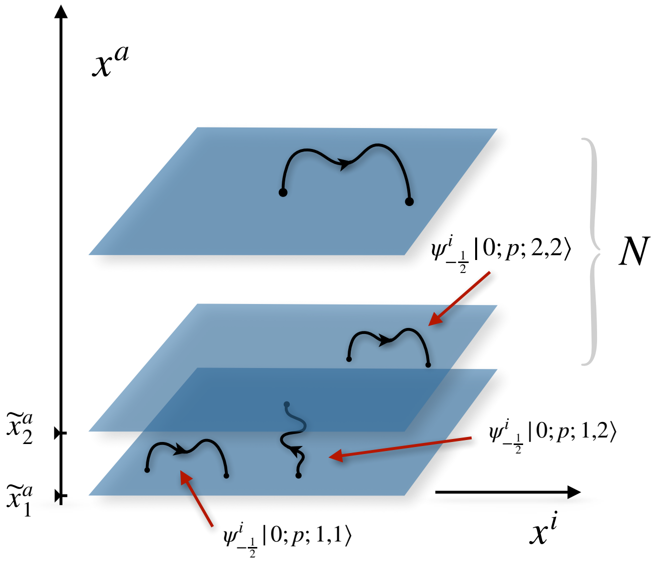

Figure 2.4: With a stack of N coincident D-branes, a $U(N)$ gauge symmetry arises. The strings have more freedom here, as they can have their endpoints on the same D-brane as well as leave a brane to reach another D-brane from the same stack. This is hold for account in the Chan-Paton labels. The term *leaving* the brane is to be used with caution, as these branes do not enjoy any spatial distance from each other. A better way to visualise it is to imagine a brane with different charges which are indexed by the Chan-Paton labels.

choose these $N \times N$ matrices in such a way that they are hermitian. Therefore, we choose a basis, such that $\lambda^q = (\lambda^q)^\dagger$ for $q = 1, \ldots, N^2$. Since the Chan-Paton labels commute with the modes, we still find that $N_\perp\, |0; \boldsymbol{p}; \boldsymbol{\lambda}\rangle = 0$, which yields for the mass squared operator

$$M^2 |0; \boldsymbol{p}; \boldsymbol{\lambda}\rangle_{\mathrm{NS}} = \frac{a_{\mathrm{NS}}}{\alpha'} |0; \boldsymbol{p}, \boldsymbol{\lambda}\rangle_{\mathrm{NS}} = -\frac{1}{2\alpha'} |0; \boldsymbol{p}, \boldsymbol{\lambda}\rangle_{\mathrm{NS}} \; . \tag{2.29}$$

Thus, the ground state is given as

$$|GS\rangle \equiv \sum_{r,s}^{N} \lambda^q_{rs}\, |0; \boldsymbol{p}, rs\rangle_{\mathrm{NS}} \quad \text{with} \quad M^2 = -\frac{1}{2\alpha'}. \tag{2.30}$$

Apart from the distinction between the different sectors, this ground state does not differ from the result of the vacuum for a single brane.

2.2.2 The First Excitations in the NS Sector between Parallel Dp-branes

The first excited state can again be written as a linear combination

$$|L1\rangle = \sum_{r=1}^{N} \sum_{s=1}^{N} \left(\sum_{i=1}^{p-1} \boldsymbol{A}_i^{rs}\, \psi^i_{-\frac{1}{2}} + \sum_{a=p+1}^{d-1} \boldsymbol{\phi}_a^{rs}\, \psi^a_{-\frac{1}{2}} \right) |0; \boldsymbol{p}; r, s\rangle_{\mathrm{NS}} \; . \tag{2.31}$$

As done previously, we can distinguish two different types of excitations:

1. **Parallel excitations**

   In this case, following the same reasoning as for a single brane, we get N^2 massless vectors

$$\sum_{r=1}^{N}\sum_{s=1}^{N}\left(\sum_{i=1}^{p-1}\boldsymbol{A}_i^{rs}\,\psi^i_{-\frac{1}{2}}\right)|0;\boldsymbol{p};r,s\rangle_{\mathrm{NS}}\quad \text{with}\quad M_A^2=0. \tag{2.32}$$

   The N^2 massless vector bosons with a momentum transversal to the world-volume of the Dp-brane indicate an extension of our original abelian gauge symmetry $U(1)$ to a non-abelian gauge symmetry $U(N)$. This justifies our specific choice of hermitian Chan-Paton matrices λ^q, because they span the Lie algebra of $U(N)$. The N^2 indicates that the massless vectors transform in the adjoint representation of $U(N)$. To put it in other words:

   N coincident Dp-branes define a $U(N)$ Yang-Mills theory on their $(p+1)$-dimensional world-volume.

2. **Normal excitations**

   Analogous to the single brane, we get a massless scalar field for each orthogonal direction. As a consequence of having N coincident Dp-branes, this yields $N^2\times(D-1-p)$ scalars. These N^2 sets of Goldstone bosons transform under the *adjoint* of $U(N)$.

$$\sum_{r=1}^{N}\sum_{s=1}^{N}\left(\sum_{i=1}^{p-1}\boldsymbol{\phi}_i^{rs}\,\psi^i_{-\frac{1}{2}}\right)|0;\boldsymbol{p};rs\rangle_{\mathrm{NS}}\quad \text{with}\quad M_\phi^2=0. \tag{2.33}$$

If we were to select a vacuum in the Ramond sector again and truncate the basic tachyonic state using GSO projection by following the standard RNS formalism, we would finally get the following spectrum for the case of an open super string between Dp-branes within a stack of N Dp-branes.

- N^2 $(p+1)$ dimensional and massless $U(N)$ gauge bosons.
- N^2 sets of $(9-p)$ massless scalars in an adjoint representation of $U(N)$.
- N^2 sets of $(p+1)$ dimensional fermions in a representation by decomposing $\mathbf{8}_c$ of $SO(8)$ under $SO(p-1)$ [60, 66].

This result is remarkable, because on the one hand, Dp-branes offer a new intuitive way of thinking about non-abelian gauge theories. Instead of the usual differential geometric approach, it can be done using dynamic Dp-branes.

On the other hand, we will realise later that these bosons can be related to the gauge bosons of a $U(N)$ Yang-Mills theory and thus be a key component to build semi-realistic standard models. The N coincident Dp-branes define on their world-volume a $U(N)$ Yang-Mills theory.

2.3 The Dp-brane Effective Action

Dp-branes, as we have already mentioned, are dynamic objects and therefore obey an action. The effective action $\mathcal{S}_{\mathrm{eff}}$ at leading order in derivatives and string coupling describes the dynamics of massless open string oscillations in the $(p+1)$ dimensional world-volume $\mathcal{W}_{p+1}$. It consists of two parts. The *Dirac-Born-Infeld* (DBI) action and the *Wess-Zumino* (WZ) action. The latter one is purely topological and thus metric independent and sometimes also referred to as *Chern-Simons* (CS) action. The action describing the relevant world-volume is given as [40, 63, 67, 68]

$$\mathcal{S}_{\mathrm{D-brane}}\supset\mathcal{S}_{\mathrm{eff}}=\mathcal{S}_{\mathrm{DBI}}+\mathcal{S}_{\mathrm{WZ}}\ . \tag{2.34}$$

Let's begin to describe the first part of this effective action in more detail. In a way, the DBI action [7] [8] is a mixture of the Born-Infeld (BI) action, which describes the dynamic of gauge fields on Dp-branes, and the Dirac (D) [82] action, which describes the fluctuations of the brane itself [46]. The BI action is a non-linear alternative of the Maxwell action, where the leading order term coincides with the Maxwell action for small field strengths F_{ab} [83–86]. The DBI action describes low energy dynamics of Dp-branes in a generic background, created by massless closed string excitations $G_{\mu\nu}, B_{\mu\nu}, \Phi$.

$$\mathcal{S}_{\mathrm{DBI}}[G,B,\Phi] = -T_p \int_{\mathcal{W}_{p+1}} d^{p+1}\xi \; e^{-\Phi} \sqrt{-\det\left(\gamma_{ab} + B_{ab} + 2\pi\alpha' F_{ab}\right)} \; . \tag{2.35}$$

where the ξ^a, with $a = 0, \ldots, p$, are world-volume coordinates of the Dp-brane. The pull-back metric γ_{ab} of the bulk spacetime onto the world-volume $\mathcal{W}_{p+1}$ and the pull-back function B_{ab} are defined via the background metric $G_{\mu\nu}$ and space-time 2-form or *Kalb-Ramond* field $B_{\mu\nu}$, respectively.

$$\gamma_{ab} = \frac{\partial X^\mu}{\partial \xi^a}\frac{\partial X^\nu}{\partial \xi^b} G_{\mu\nu}(X(\xi)) \quad \text{and} \quad B_{ab} = \frac{\partial X^\mu}{\partial \xi^a}\frac{\partial X^\nu}{\partial \xi^b} B_{\mu\nu}(X(\xi)) \; , \tag{2.36}$$

where the X^μ embed the world-volume into ten dimensional spacetime. The field Φ corresponds to the usual *dilaton*. In contrast, the $U(1)$ field strength F_{ab} is not a pulled-back form, but rather a field restricted to the world-volume. The string tension in Eq. (2.35) depends now on p and is given as [40]

$$T_p = \mu_p = \frac{2\pi}{(4\pi^2\alpha')^{\frac{p+1}{2}}} = 2\pi\ell_s^{-p+1} \; . \tag{2.37}$$

The second term in the effective open string action in Eq. (2.34) is the Wess-Zumino action. This action plays a very special role as it contributes to the tadpole cancellation and the generalised Green-Schwarz mechanics and is crucial for SUSY. Without deducing - what can be found in [87–91] - the action formally reads

$$S_{\mathrm{WZ}}[C_p] = \pm\, T_p \int_{\mathcal{W}_{p+1}} d^{p+1}\xi \; \mathrm{Ch}_{\mathrm{R}}(2\pi\alpha'\mathcal{F}) \wedge \sqrt{\frac{\hat{A}\left(\mathcal{R}_T\right)}{\hat{A}\left(\mathcal{R}_N\right)}} \wedge \bigoplus_q \varphi^* C_q \Bigg|_{p+1} \; . \tag{2.38}$$

The first term of the wedge product in Eq. (2.38) denotes the Chern character of the curvature 2-form $\mathcal{F} = F + (2\pi\alpha')^{-1}B$, containing the NSNS 2-form B. This part characterises the gauge bundle of $\mathcal{W}_{p+1}$. The second term describes the curvature induced on the Dp-brane. $\hat{A}$ denotes the *A-roof* or *Dirac genus*, which characterises the tangent bundle of $\mathcal{W}_{p+1}$ and can be expressed in terms of *Pontryagin* classes. $\mathcal{R}_T$ and $\mathcal{R}_N$ are curvature forms of the tangent and normal bundle of $\mathcal{W}_{p+1}$, respectively. The last term consists of the formal sum of pull-backs of the bulk potential to $\mathcal{W}_{p+1}$, which are referred to as RR 2-form potentials C_p.

Much more could be said, especially for WZ action. However, we are not interested in the exact form in the further course since we will work with approximations. Thus, we end our discussion at this point and relegate to the literature already referred to. The curious reader can find some briefly explained topological "tools" in the appendix A.

In the end, it can be stated that the DBI action heuristically describes the coupling of the open string gauge fields to the NSNS fields. The WZ action describes the coupling of the RR forms with the gauge field F. This action is of topological nature and, if interpreted intuitively, describes or "measures" the charge of the Dp-Brane [40].

[7] It is also possible to find a supersymmetrised formulation of the DBI action. For example, this is done in [69–72], by using superfield formulation.

[8] There is no generalisation for a DBI action in the case for coincident and thus non-Abelian Dp-branes. Some widely accepted proposal can be found in [73–77] and problems resulting from it in [78–81].

Chapter 3

Intersecting D-branes at Angles

In this chapter, we will consider open and oriented superstrings in Type IIA string theory, which are stretched between intersecting D6-branes, with a relative angle to each other. For this purpose, we will describe this system classically and determine the non-trivial, so-called, twisted boundary conditions. We will find that these twisted boundary conditions shift the modding of the oscillator modes and lead to a non-integer mode expansion.

In a brief interlude, we will discuss some conditions and restrictions to the angles of the branes, which are given by supersymmetry.

After finding the classical mode expansion for the open strings, we will quantise the system, determine the twisted vacuum of the theory and construct the vertex operators corresponding to the physical states. With these ingredients we will finally examine the spectrum of the open superstrings living at the intersection of D6-branes.

At lowest energy, we will find a spacetime boson, whose mass depends on the relative angles of the branes and a massless four dimensional spacetime fermion in the bi-fundamental (or it's conjugate) representation $(N_a, \overline{N_b})$ of $U(N_a) \times U(N_b)$. By the specific requirement that the angles between the mutually rotated D-branes are in sum zero, we obtain a $\mathcal{N} = 1$ chiral supermultiplet. This will show the origin of charged matter in string theory.

3.1 Twisted Boundary Conditions

By studying open strings for the first time in the framework of bosonic string theory, the coordinates satisfy Neumann boundary conditions, moving on the world-volume of a space-filling D25-brane. Details can be found in nearly every introduction to string theory, e.g., in [45]. In general, however, it is possible to think up more complicated scenarios. In this chapter, we will deal with a generalisation of such special conditions - specifically D6-branes that are rotated relative to each other.

For this purpose, we consider pairs of D6-branes in Type IIA superstring theory, which are coincident along the coordinates $\mathcal{M}_4 = \{x^0, x^1, x^2, x^3\}$ and rotated by relative angles in the remaining directions $\mathcal{I}_6 = \{x^i\}$ with $i = 4, \ldots, 9$. The $\mathcal{M}_4$ spans the flat and non-compact Minkowski space, since its underlying structure corresponds to a *Lorentzian manifold*. Hence, we will refer to this space as our physical spacetime, while we refer to the other remaining dimensions as so-called internal dimensions or internal space. This is shown schematically in Fig. 3.1. The boundary conditions for the open string coordinates along $\mathcal{M}_4$ are obviously still Neumann-Neumann boundary conditions, which preserves Lorentz symmetry. [63]. To get the correct boundary conditions for the internal directions, where the D6-branes form non-trivial

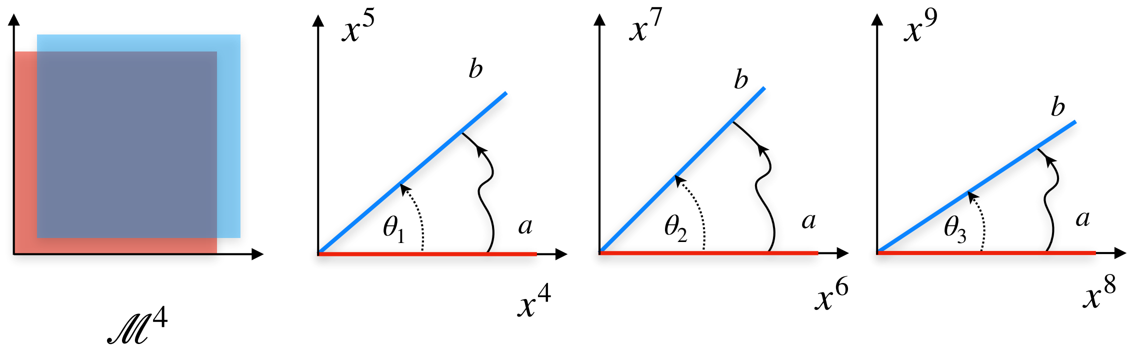

Figure 3.1: A pair of D6-branes intersecting at non-trivial angles θ_1, θ_2 and θ_3 in $\mathcal{I}_6$. The red line corresponds to a D6$_b$-brane, while the blue line represents a D6$_a$-brane. The two branes cover the non-compact dimensions of $\mathcal{M}_4$.

angles, we consider two stacks of D6-branes in the (x^{2k+2}, x^{2k+3}) - plane, where $k = 1, 2, 3$. The first stack of N_a D6-branes[1], which we will denote as D6$_a$-brane, are horizontally aligned with the x^{2k+2} coordinate, while the second stack of N_b D6$_b$-branes are rotated by an angle θ_k in a mathematically positive sense, as depicted in Fig. 3.2. Further, we assume that the stretched string is oriented and starts on the horizontal D6$_a$-brane and ends on the twisted D6$_b$-brane. At $\sigma = 0$ the string coordinate X^{2k+3} vanishes, which corresponds to a Dirichlet boundary condition. On the other hand, the endpoint of the string is free to move along x^{2k+2}, thus the string coordinates satisfy a Neumann boundary condition [63, 92]. This results in

$$\partial_\sigma X^{2k+2}(\tau, \sigma)|_{\sigma=0} = X^{2k+3}(\tau, \sigma)|_{\sigma=0} = 0 \,. \tag{3.1}$$

The endpoint of the string at $\sigma = \pi$ is attached to the brane obtained from the horizontal one by a counter clockwise rotation. For this purpose, we use a new coordinate system (x'^{2k+2}, x'^{2k+3}), so that x'^{2k+3} aligns with the rotated brane. The coordinate x'^{2k+2} is therefore orthogonal to the rotated brane. From Fig. (3.2), we can determine the transformation behaviour

$$\begin{pmatrix} x'^{2k+2} \\ x'^{2k+3} \end{pmatrix} = \begin{pmatrix} \cos\theta_k & \sin\theta_k \\ -\sin\theta_k & \cos\theta_k \end{pmatrix} \begin{pmatrix} x^{2k+2} \\ x^{2k+3} \end{pmatrix} = \begin{pmatrix} x^{2k+2}\cos\theta_k + x^{2k+3}\sin\theta_k \\ -x^{2k+2}\sin\theta_k + x^{2k+3}\cos\theta_k \end{pmatrix} \,. \tag{3.2}$$

The endpoint of the string at $\sigma = \pi$ is free to move along the x'^{2k+3} coordinate, thus the string coordinate satisfies a Neumann boundary condition

$$\partial_\sigma X^{2k+2}(\tau, \sigma)|_{\sigma=\pi} \cos\theta_k + \partial_\sigma X^{2k+3}(\tau, \sigma)|_{\sigma=\pi} \sin\theta_k = 0 \,. \tag{3.3}$$

Furthermore, at $\sigma = \pi$ the string satisfies the Dirichlet boundary condition $x'^{2k+3} = 0$, which yields

$$- X^{2k+2}(\tau, \sigma)|_{\sigma=\pi} \sin\theta_k + X^{2k+3}(\tau, \sigma)|_{\sigma=\pi} \cos\theta_k \,. \tag{3.4}$$

To make some calculations simpler, we introduce complex target space coordinates for our internal space $\mathcal{I}_6^{\mathbb{C}} \equiv \mathcal{I}_3$, which leads to [93]

$$Z^k = \frac{1}{\sqrt{2}} \left(X^{2k+2} + iX^{2k+3} \right) \qquad \text{for } k = 1, 2, 3. \tag{3.5}$$

$$\bar{Z}^k = \frac{1}{\sqrt{2}} \left(X^{2k+2} - iX^{2k+3} \right) \qquad \text{for } k = 1, 2, 3. \tag{3.6}$$

[1] For the sake of compactness, we will omit the notation of the N_a and N_b stacks in this chapter, as it is not essential for the further analysis.

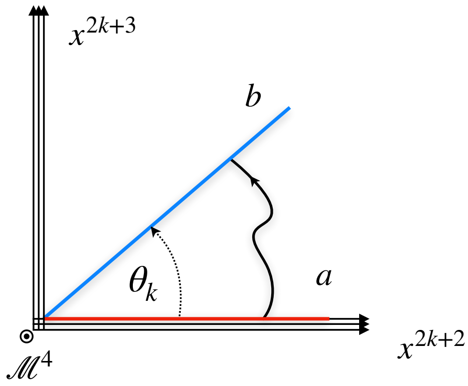

Figure 3.2: Two intersecting D6-branes in the (x^{2k+2}, x^{2k+3})-plane. The angles θ_k are measured according to the indication in the figure. The angles run counterclockwise form the D6$_a$-brane to the D6$_b$-brane. This convention yields positive angles.

The complex coordinates Z_k and $\bar{Z}_k$ are now rotated according to [63]:

$$Z^k \to R^k_l Z^l \quad \text{with } R \in U(3) \ , \tag{3.7}$$

where R can be represented as

$$R = \mathrm{diag}(e^{i\theta_1}, e^{i\theta_2}, e^{i\theta_3}). \tag{3.8}$$

In terms of these new coordinates, the boundary conditions can be re-expressed as [92, 94]

$$\begin{aligned} \partial_\sigma \,\mathrm{Re}\left[Z^k(\tau,\sigma)\right]\Big|_{\sigma=0} &= 0; \qquad \mathrm{Im}\left[Z^k(\tau,\sigma)\right]\Big|_{\sigma=0} = 0; \\ \partial_\sigma \,\mathrm{Re}\left[e^{i\theta_k} Z^k(\tau,\sigma)\right]\Big|_{\sigma=\pi} &= 0; \quad \mathrm{Im}\left[e^{i\theta_k} Z^k(\tau,\sigma)\right]\Big|_{\sigma=\pi} = 0 \ . \end{aligned} \tag{3.9}$$

3.2 Classical Mode Expansion

To find the mode expansion for the still classical fields Z and $\bar{Z}$, we make the usual oscillator modes expansion. In contrast to the case of parallel D-branes, the centre of mass is located at the point of intersection, which corresponds to the origin of the complex plane in Fig. 3.2 [40, 54]. Roughly speaking, one can say that the strings in the internal space are stuck in the corresponding intersections. As an ansatz we therefore write

$$Z^k(\tau,\sigma) = i\sqrt{\frac{\alpha'}{2}} \sum_{n\in\mathbb{Z}} \left[\frac{1}{n}\alpha^k_n e^{-in(\tau-\sigma)} + \frac{1}{n}\tilde{\alpha}^k_n e^{-in(\tau+\sigma)}\right] \ , \tag{3.10}$$

$$\overline{Z}^k(\tau,\sigma) = i\sqrt{\frac{\alpha'}{2}} \sum_{n\in\mathbb{Z}} \left[\frac{1}{n}\bar{\alpha}^k_n e^{-in(\tau-\sigma)} + \frac{1}{n}\tilde{\bar{\alpha}}^k_n e^{-in(\tau+\sigma)}\right] \ , \tag{3.11}$$

where we used

$$\alpha^k_n = \frac{1}{\sqrt{2}}\left(\alpha^{X^{2k+2}}_n + i\alpha^{X^{2k+3}}_n\right) \quad \text{and} \quad \bar{\alpha}^k_n = \frac{1}{\sqrt{2}}\left(\alpha^{X^{2k+2}}_n - i\alpha^{X^{2k+3}}_n\right) \ . \tag{3.12}$$

Following this, we demand that the ansatz fulfils the boundary conditions. The first pair of conditions in (3.9) for $\sigma = 0$ leads to a condition so that $\bar{\alpha}_n = \tilde{\alpha}_n$ and $\bar{\tilde{\alpha}}_n = \alpha_n$. The ansatz also fulfils the remaining conditions in (3.9) if the modes become a function of the angle, i.e., $\tilde{\alpha}_{n-\epsilon_k}$ and $\alpha_{n+\epsilon_k}$, with $\epsilon_k = \frac{\theta_k}{\pi}$. Combining these results, the mode expansion for a complex bosonic field is

$$Z^k(\tau,\sigma) = i\sqrt{\frac{\alpha'}{2}} \sum_{m\in\mathbb{Z}} \left[\frac{1}{m+\epsilon_k} \alpha^k_{m+\epsilon_k} e^{-i(m+\epsilon_k)(\tau-\sigma)} + \frac{1}{m-\epsilon_k} \tilde{\alpha}^k_{m-\epsilon_k} e^{-i(m-\epsilon_k)(\tau+\sigma)} \right] \tag{3.13}$$

and similarly for $\bar{Z}^k(\tau,\sigma)$ [54]. Therefore, we can conclude that $Z^k \mapsto \bar{Z}^k$ if we substitute $\epsilon_k \mapsto -\epsilon_k$.

By inserting the angle $\epsilon_k = 0$, we get the solutions for a string stretched between parallel branes, while for $\epsilon_k = \frac{1}{2}$ one gets a string between two orthogonal D6-branes. These special cases are well known and can be found in standard literature, as in [45].

For superstring theory, of course, we must also consider the fermionic part. Our previous considerations can be repeated and are the same for the world-sheet fermions, where we again use complex target coordinates given by [92]

$$\Psi^k = \frac{1}{\sqrt{2}} \left(\psi^{2k+2} + i\psi^{2k+3}\right) \qquad \text{for } k = 1,2,3. \tag{3.14}$$

$$\bar{\Psi}^k = \frac{1}{\sqrt{2}} \left(\psi^{2k+2} - i\psi^{2k+3}\right) \qquad \text{for } k = 1,2,3. \tag{3.15}$$

The modes are again shifted by the angle ϵ_k and we will denote them conventionally as

$$\psi^k_{r+\epsilon_k},\ \tilde{\psi}^k_{r-\epsilon_k} \quad \text{with} \quad \begin{cases} r \in \mathbb{Z} & \text{R.} \\ r \in \mathbb{Z} + \frac{1}{2} & \text{NS .} \end{cases} \tag{3.16}$$

3.3 Supersymmetry Preserving D-Branes

Supersymmetry is a spacetime symmetry between bosons and fermions, which - since we do not observe it in nature - must be broken at low energies. Consequently, it requires that for every boson there is a corresponding fermion and for every boson a corresponding fermion [95]. These predicted supersymmetric particles are generally called *superpartners*. There are several SUSY theories and in this thesis, we will concentrate on the simplest four dimensional $\mathcal{N} = 1$ supersymmetry, where $\mathcal{N}$ indicates how many SUSY generators the theory provides [96, 97].

There are several ways to describe D-branes and their role in supersymmetry breaking. One possibility is given by the fact, that D-branes are so-called BPS states, which are characterized by being invariant under a subalgebra of the full SUSY algebra. Another particularly clever choice is offered by T-duality. Since this is beyond the scope of this thesis, we therefore refer to literature such as [98], Chapter 13.4, and [54], Chapter 10.4. and Chapter 9.5.

A relatively intuitive possibility which is compatible with the already discussed material is nevertheless given and shall demonstrate the essential idea behind it. By introducing Dp-branese, Poincaré invariance is broken in the normal directions [49]. Now it is a fact that Poincaré symmetry and supersymmetry are related. This can already be seen from the point of view of the anti-commutator relation [96]

$$\{Q, \bar{Q}\} \simeq \gamma P \ , \tag{3.17}$$

with Q denoting the supercharge generator and P being the momentum four vector. This already tells us that SUSY must be broken to a certain degree. In the following, we consider a concrete case with two D6-branes at angles in type IIA string theory. Furthermore, we assume that we have a configuration like the one shown in Fig. (3.1). Therefore, we have two different D6-branes, which are coincident along the four directions x^0, x^1, x^2, x^3 and twisted in the remaining directions by a rotation R, which is parametrised by the three angles θ_k.

It is now well founded [98] that an arbitrary stack of D6-branes preserves supercharge according to

$$\hat{Q}_\alpha = Q_\alpha + P\tilde{Q}_\alpha \quad \text{with} \quad P = \prod_{i \text{ normal to } D6} P^i \ . \tag{3.18}$$

P is a parity operator in the space normal to the D6-brane and should not be confused with the four momenta in Eq. (3.17). This also provides the necessary condition for SUSY that Q_a and $P\tilde{Q}_a$ have the same chirality resulting in type IIA (IIB) string theory having Dp-branes with p even (p odd) as SUSY-preserving branes.

The D6_a-brane of our configuration thus preserves

$$D6_a: \quad \hat{Q}^a_\alpha = Q_\alpha + P_1\tilde{Q}_\alpha \quad \text{with} \quad P_1 = P^5P^7P^9 \ . \tag{3.19}$$

The D6_b-brane preserves

$$D6_b: \quad \hat{Q}^b_\alpha = Q_\alpha + P_2\tilde{Q}_\alpha = Q_\alpha + (R^{-1}P_1R)\tilde{Q}_\alpha \ , \tag{3.20}$$

where R corresponds to the above-mentioned rotation. Comparing Eq. (3.19) to Eq. (3.20) yields the spinor equation

$$P_1\varepsilon = R^{-1}P_1R\varepsilon \ . \tag{3.21}$$

A simple calculation yields

$$\varepsilon = P_1^{-1}R^{-1}P_1R\varepsilon = P_1^{-1}P_1RR\varepsilon = R^2\varepsilon \ , \tag{3.22}$$

where we took advantage of the fact that the parity operation flips the rotation angle, i.e.

$$R^{-1}P_1 = P_1R \tag{3.23}$$

Choosing the ten-dimensional spinor $|\mathbf{s}\rangle = |s_0, s_1, s_2, s_3, s_4\rangle$, which we have already introduced in Section 2.1.2, we perform the following double rotation [99]

$$R^2 |s\rangle = e^{2i\sum_{k=0}^{4} s_k\theta_k} |s\rangle = e^{2i(s_1\theta_1+s_2\theta_2+s_3\theta_3)} |s\rangle \stackrel{!}{=} |s\rangle \ , \quad \text{with} \quad s_k = \pm\frac{1}{2} \ . \tag{3.24}$$

Supersymmetry therefore requires that

$$\theta_1 \pm \theta_2 \pm \theta_3 = 0 \pmod{2\pi} \ . \tag{3.25}$$

By redefining $\theta_k \to -\theta_k$, we can focus without loss of generality on solutions to $R^2|s\rangle = |s\rangle$ with all $s_k > 0$ or $s_k < 0$. Thus, we have seen that the total amount of supersymmetry depends directly on the sum of the three angles θ_k. We can therefore distinguish four different cases [54, 99]:

- The angles θ_k are generic which, direct consequence is that all supersymmetry is broken.
- The angles satisfy $\theta_1 + \theta_2 + \theta_3 = 0 \pmod{2\pi}$ but can be otherwise arbitrary. This choice preserves $\frac{1}{4}$ of 16 supersymmetries of the D6_a-brane. On that score, we expect four real supercharges. Thus, it follows a $\mathcal{N} = 1$ supersymmetry in four dimensional spacetime providing a *chiral supermultiplet*.
- Two angles satisfy $\theta_1 + \theta_2 = 0 \pmod{2\pi}$, while $\theta_3 = 0$. It follows a $\mathcal{N} = 2$ supersymmetry in four dimensional spacetime with eight real supercharges and *hypermultiplets*.
- The special case $\theta_1 = \theta_2 = \theta_3 = 0$ allows a $4d$ $\mathcal{N} = 4$ system of parallel D-branes with a *vector supermultiplet*.

3.4 Quantisation of the Open String Sector in the Internal Space

The quantisation procedure for the spacetime dimensions is similar to the known one for more trivial boundary conditions. The textbook [45] is recommended as a good and comprehensive source for the quantisation procedure in the presence of orthogonal or parallel D-branes. In this thesis, we will only restrict ourselves to the quantisation of the open string sector D6$_a$ - D6$_b$ in the internal space. We have seen that boundary conditions shift the oscillator modes by $\pm\epsilon_k$. Thus, we will quantise the system that up to now has been treated in a classical way, with the focus being on the internal dimensions. By doing so, we will use some key techniques of conformal field theory (CFT).

First, we will reconstitute our fields differently. Our mode expansion $Z(z,\bar{z})$ is not a (quasi-) primary field, thus we will use [2] $\partial Z^k(z)$, which indeed is a primary field. It is well known from CFT, that the world-sheet of a free propagating open string can be parameterised as a strip with a length $0<\sigma<\pi$ and $-\infty<\tau<\infty$. By performing a Wick rotation and substituting $w=\tau+i\sigma$, we can do the usual mapping to the upper half plane $\mathbb{H}_+$, which is specified by

$$z = e^{iw}. \tag{3.26}$$

Via this map we get the following mode expansion

$$\begin{aligned} \partial Z^k(z) &= -i\sqrt{\tfrac{\alpha'}{2}}\textstyle\sum_n \alpha^k_{n-\epsilon_k} z^{-n+\epsilon_k-1}\ ; \qquad & \partial\bar{Z}^k(z) &= -i\sqrt{\tfrac{\alpha'}{2}}\textstyle\sum_n \alpha^k_{n+\epsilon_k} z^{-n-\epsilon_k-1}\ ; \\ \Psi^k(z) &= \sqrt{\tfrac{\alpha'}{2}}\textstyle\sum_{r\in Z+\nu} \psi^k_{r-\epsilon_k} z^{-r-\frac{1}{2}+\epsilon_k}\ ; \qquad & \bar{\Psi}^k(z) &= \sqrt{\tfrac{\alpha'}{2}}\textstyle\sum_{r\in Z+\nu} \psi^k_{r+\epsilon_k} z^{-n-\frac{1}{2}-\epsilon_k}\ . \end{aligned} \tag{3.27}$$

Inverting the mode expansion for the world-sheet bosons in Eq. (3.27) gives an equation for the modes in terms of a contour integral

$$\alpha^k_{n\pm\epsilon_k} = i\sqrt{\frac{2}{\alpha'}}\oint\frac{dz}{2\pi i} z^{n\pm\epsilon_k}\partial Z^k(z)\ . \tag{3.28}$$

With this integral representation of the bosonic modes, we can calculate the commutator $\left[\alpha^I_{m\pm\epsilon_k},\tilde{\alpha}^J_{n\mp\epsilon_k}\right]$. Since the result of that commutator is mentioned in a lot of publications, but the way to it is not obvious, it will be shown in more detail in the appendix B.

Following the appendix B, we find

$$\left[\alpha^I_{m\pm\epsilon_k},\tilde{\alpha}^J_{n\mp\epsilon_k}\right] = (m\pm\epsilon_k)\ \delta_{m+n,0}\ \delta^{I,J}\ . \tag{3.29}$$

The same can be done for the world-sheet fermions, which leads to the only non-zero anti-commutator [100]

$$\left\{\psi^I_{r+\varepsilon_k},\widetilde{\psi}^J_{s-\varepsilon_k}\right\} = \delta_{r+s,0}\ \delta^{I,J}\ . \tag{3.30}$$

A pivotal moment in the process of quantisation is the construction of the vacuum of theory. Hence, we next construct the vacuum of the internal space. For the internal dimensions we have a new type of vacuum, which satisfies and incorporates the previously investigated twisted boundary conditions. From now on, we will refer to these new vacua $|\Theta\rangle_{\mathrm{B\otimes NS}} \equiv |\{\theta_k\}\rangle_{\mathrm{B\otimes NS}}$ and $|\Theta\rangle_{\mathrm{B\otimes R}} \equiv |\{\theta_k\}\rangle_{\mathrm{B\otimes R}}$ as the twisted NS vacuum and the twisted R vacuum, respectively. In the next section we will see that so-called conformal twisted fields are associated with the twisted vacuum, which create the twisted vacuum out from the untwisted one. We will explicitly derive how the twisted vacuum can be built by acting with conformal twist fields on the untwisted and $SL(2,\mathbb{R})$ invariant vacua, which will be denoted as $|0\rangle^u_{\mathrm{B\otimes NS}}$ and $|0\rangle^u_{\mathrm{B\otimes R}}$ [92, 100].

[2] we focus on chiral fields $Z^I(z)$, because all calculations are analogous for the anti-chiral fields $Z^I(\bar{z})$.

Further, we must make a case distinction with regard to the choice of the angle ϵ_k. If we choose the angle to be $0 < \epsilon_k < 1$, the vacuum appears to be

$$\begin{aligned}
&\alpha^k_{m-\epsilon_k}\left|\Theta\right\rangle = 0, \quad \forall\, m \geqslant 1, \qquad \psi^k_{r-\epsilon_k}\left|\Theta\right\rangle = 0, \quad \forall\, r \geqslant \left\{ \begin{array}{ll} 1, & \text{R} \\ \frac{1}{2}, & \text{NS} \end{array} \right. , \\
&\alpha^k_{m+\epsilon_k}\left|\Theta\right\rangle = 0, \quad \forall\, m \geqslant 0, \qquad \psi^k_{r+\epsilon_k}\left|\Theta\right\rangle = 0, \quad \forall\, r \geqslant \left\{ \begin{array}{ll} 0, & \text{R} \\ \frac{1}{2}, & \text{NS} \end{array} \right. .
\end{aligned} \tag{3.31}$$

The mass-squared operator M^2 for the whole theory - including both the ordinary spacetime and the internal dimensions - is given by the following formula [68]

$$\alpha' M^2 = N^Z + N^\Psi + a_0 \tag{3.32}$$

with the so-called number operators, which measure the numbers of oscillators in accordance with

$$N^Z \equiv \sum_{\mu=1}^{2} \sum_{n \in \mathbb{Z}} a^\mu_{-n} a^\mu_n + \sum_{k=1}^{3} \sum_{m \in \mathbb{Z}} a^k_{-m+\epsilon_k} a^k_{m-\epsilon_k} \ , \tag{3.33}$$

$$N^\Psi \equiv \sum_{\mu=1}^{2} \sum_{r \in Z+\nu} r \psi^\mu_{-r} \psi^\mu_r + \sum_{k=1}^{3} \sum_{r \in Z+\nu} \left(r - \epsilon_k\right) \psi^k_{-r+\epsilon_k} \psi^k_{r-\epsilon_k} \tag{3.34}$$

and the normal ordering number

$$a_0 = 2\nu \left(-\frac{1}{2} + \frac{1}{2} \sum_{I=1}^{3} \epsilon_k \right) \ , \tag{3.35}$$

which arises from the normal ordering with respect to the twisted vacuum. This corresponds to the zero-point energy of our theory with intersecting D6-branes. A detailed derivation of the formula and the determination of the vacuum energy is carried out in the Appendix C.

For negative angles $-1 < \epsilon_k < 0$, we define the vacuum as [92]

$$\begin{aligned}
&\alpha^k_{m-\epsilon_k}|\Theta\rangle = 0, \quad m \geqslant 0, \qquad \psi^k_{r-\epsilon_k}|\Theta\rangle = 0, \quad r \geqslant \left\{ \begin{array}{ll} 0, & \text{R} \\ \frac{1}{2}, & \text{NS} \end{array} \right. , \\
&\alpha^k_{m+\epsilon_k}|\Theta\rangle = 0, \quad m \geqslant 1, \qquad \psi^k_{r+\epsilon_k}|\Theta\rangle = 0, \quad r \geqslant \left\{ \begin{array}{ll} 1, & \text{R} \\ \frac{1}{2}, & \text{NS} \end{array} \right. .
\end{aligned} \tag{3.36}$$

which leads to a zero-point energy given (remember $\epsilon_k < 0$) by

$$a_0 = 2\nu \left(-\frac{1}{2} - \frac{1}{2} \sum_{k=1}^{3} \epsilon_k \right) \ . \tag{3.37}$$

3.5 Vertex Operators and the Spectrum

In this section, we will derive the relationship between the twisted and the untwisted vacuum, both in the NS sector and in the R sector. In order to accomplish that, we will introduce twisted conformal fields. The advantage of these new sort of conformal fields will enable us to create a collection of operation product expansions, which will serve as a “dictionary” and allow us to write down the vertex operators (VO’s). We will further take a closer look at the spectrum of this theory at the lowest energy state and use the so-called BRST invariance to build physical states. Finally, these will provide us with a key feature of the standard model. For the sake of concreteness, we choose a supersymmetric setup with $\theta^1_{ab} \geq 0$, $\theta^2_{ab} \geq 0$ and $\theta^3_{ab} \leq 0$.

3.5.1 Vertex Operators in the NS Sector

Intending to get the vertex operators, we will focus on how the conformal fields $\bar{\Psi}, \Psi, \partial Z$ and $\partial\bar{Z}$ operate on the twisted ground-state $|\Theta\rangle_{\mathrm{B}\otimes\mathrm{NS}}$. This inspection will serve as a collection or a "dictionary", which will be useful to construct the vertex operators in the further course. For the sake of clarity, we will use just one angle $\epsilon \in \Theta$ as a representative for the three different ones. The generalisation is straight forward. Once again - assuming that the angle is positive - we start with the bosonic conformal fields, which act in the following particular way on the ground-state [101]

$$\begin{aligned} \lim_{z\to 0} \partial Z(z)|\theta\rangle_{\mathrm{B}} &= \sum_{n\in\mathbb{Z}} \lim_{z\to 0} \alpha_{n-\epsilon} z^{-n+\epsilon-1}|\theta\rangle_{\mathrm{B}} \to z^{\epsilon-1}\alpha_{-\epsilon}|\theta\rangle_{\mathrm{B}} = z^{\epsilon-1}\sigma_\theta^+(0)\tau_\theta^+(0)|0\rangle_B^u \ , \\ \lim_{z\to 0} \partial \bar{Z}(z)|\theta\rangle_{\mathrm{B}} &= \sum_{n\in\mathbb{Z}} \lim_{z\to 0} \alpha_{n+\epsilon} z^{-n-\epsilon-1}|\theta\rangle_{\mathrm{B}} \to z^{-\epsilon}\alpha_{-1+\epsilon}|\theta\rangle_{\mathrm{B}} = z^{-\epsilon}\sigma_\theta^+(0)\tilde{\tau}_\theta^+(0)|0\rangle_{\mathrm{B}}^u \ , \end{aligned} \tag{3.38}$$

where we used the so-called state-operator correspondence [54] with respect to Eq. (3.31). The field $\sigma_\theta^+(0)$ denotes the conformal bosonic twist field, which follows from $|\theta\rangle_{\mathrm{B}} = \lim_{z\to 0}\sigma_\theta^+(z)|0\rangle_{\mathrm{B}}^u$. Loosely speaking, acting with that twist field on the untwisted vacuum will turn it into a twisted vacuum, according to $\sigma_\theta^+(0)\,|0\rangle_{\mathrm{B}} = |\theta\rangle_{\mathrm{B}}$.

Consequently, the fields τ_ϵ^+ and $\tilde{\tau}_\epsilon^+$ are excited twist fields with conformal dimensions $h_{\tau_\epsilon^+} = \frac{1}{2}\epsilon(3-\epsilon)$ and $h_{\tilde{\tau}_\epsilon^+} = \frac{1}{2}(1-\epsilon)(2+\epsilon)$, respectively [101]. The "hierarchy" of excitation of the twisted fields is shown schematically in Fig. 3.3 to make it less abstract. The second line in Eq. (3.38) for instance helps to identify $\tilde{\tau}$ with the state $\alpha_{-1+\epsilon}|\theta\rangle_{\mathrm{B}}$. This reproduces the following OPE [102]

$$\partial\bar{Z}(z)\ {\sigma_\theta}^+(w) \sim (z-w)^{-\epsilon}\ \tilde{\tau}_\theta^+(w)\ . \tag{3.39}$$

Subsequently, we could also build higher excitations. In particular, we can show that by acting with ∂Z on $\alpha_{-1+\epsilon}|\theta\rangle_{\mathrm{B}} \sim \tilde{\tau}(0)$, we obtain

$$\lim_{z\to 0}\ \partial Z(z)\ \alpha_{-1+\epsilon}|\theta\rangle_{\mathrm{B}} = \sum_n \alpha_{n-\epsilon} z^{-n+\epsilon-1}\alpha_{-1+\epsilon}\ |\theta\rangle_{\mathrm{B}} \sim (1-\epsilon)\ z^{-2+\epsilon}|\theta\rangle_{\mathrm{B}}\ , \tag{3.40}$$

where we used the commutation relation from Eq. (3.29) in the penultimate step. Thus, the OPE reads

$$\partial Z(z)\tilde{\tau}_\theta(w) \sim (1-\epsilon)(z-w)^{-2+\epsilon}\ \sigma_\theta(w)\ . \tag{3.41}$$

Equivalently, we could derive all other OPE's containing bosonic twist fields. The same can again be done analogously with Ψ and $\bar{\Psi}$ acting on the twisted vacuum $|\theta\rangle_{\mathrm{NS}}$, where we obtain

$$\begin{aligned} \lim_{z\to 0}\Psi(z)|\theta\rangle_{\mathrm{NS}} &= \sum_{r\in\mathbb{Z}+\frac{1}{2}} z^{-r-\frac{1}{2}+\epsilon}\psi_{r-\epsilon}|\theta\rangle_{\mathrm{NS}} \to z^\epsilon\psi_{-\frac{1}{2}-\epsilon}|\theta\rangle_{\mathrm{NS}} = z^\epsilon\tilde{t}_\theta^+(0)s_\theta^+(0)|0\rangle_{\mathrm{NS}}^u\ , \\ \lim_{z\to 0}\bar{\Psi}(z)|\theta\rangle_{\mathrm{NS}} &= \sum_{r\in\mathbb{Z}+\frac{1}{2}} z^{-r-\frac{1}{2}-\epsilon}\psi_{r+\epsilon}|\theta\rangle_{\mathrm{NS}} \to z^{-\epsilon}\psi_{-\frac{1}{2}+\epsilon}|\theta\rangle_{\mathrm{NS}} = z^{-\epsilon}t_\theta^+(0)s_\theta^+(0)|0\rangle_{\mathrm{NS}}^u\ , \end{aligned} \tag{3.42}$$

where $\tilde{t}_\theta^+$ and t_θ^+ represent excited fermionic twist fields with conformal dimension $h_{\tilde{t}_\theta^+} = \frac{1}{2}(1+\epsilon)^2$ and $h_{t_\theta^+} = \frac{1}{2}(1-\epsilon)^2$, respectively [101]. The field $s_\theta^+(0)$ denotes the conformal fermionic twist field, which builds the twisted vacuum $|\theta\rangle_{\mathrm{NS}}$ in the NS sector.

In the previous Section 3.4 we already revealed some details about the construction of this new twisted vacuum, on which the internal creation and annihilation operators act. In the NS sector the twisted vacuum is finally related to the untwisted vacuum via

$$|\Theta\rangle_{\mathrm{B}\otimes\mathrm{NS}} = \lim_{z\to 0}\prod_{k=1}^{3}\sigma_{\theta_k}^+(z)s_{\theta_k}^+(z)|0\rangle_{\mathrm{B}\otimes\mathrm{NS}}^u\ . \tag{3.43}$$

It is a special and beneficial feature of 2-dimensional CFT that the fermionic RNS theory can be formulated fully in terms of bosons, which goes under the name of *bosonisation.* This identification is due to the fact that the OPEs match each other [98]. We have the following identifications for the NS sector

$$\Psi(z) \equiv e^{iH(z)},\ \bar{\Psi}(z) \equiv e^{-iH(z)}$$
$$s_\theta^+(z) \equiv e^{i\epsilon H(z)},\ t_\theta^+(z) \equiv e^{i(\epsilon+1)H(z)},\ \tilde{t}_\theta^+(z) \equiv e^{i(\epsilon-1)H(z)}\ , \tag{3.44}$$

where H(z) is a bosonic conformal field now [98, 101]. Note that we have the following identifications among twist- and anti-twist fields [3]

$$\sigma_\theta^-(z) = \sigma_{1+\theta}^+(z)\ , \quad \tau_\theta^-(z) = \tau_{1+\theta}^+(z)\ , \quad \tilde{\tau}_\theta^-(z) = \tilde{\tau}_{1+\theta}^+(z)\ , \tag{3.45}$$

which of course is also valid for higher excited twist fields. The corespondence of state and vertex operator for a couple of states and different convention for the angles can be found in Table 3.1 [101].

Positive angle		Negative angle	
State	Vertex operator	State	Vertex operator
$\vert\,\theta\,\rangle_{\mathrm{NS}}$	$e^{i\epsilon H(z)}\sigma_\theta^+(z)$	$\vert\,\theta\,\rangle_{\mathrm{NS}}$	$e^{i\epsilon H(z)}\sigma_\theta^-(z)$
$\alpha_{-\epsilon}\vert\,\theta\,\rangle_{\mathrm{NS}}$	$e^{i\epsilon H_(z)}\tau_\theta^+(z)$	$\alpha_\epsilon\vert\,\theta\,\rangle_{\mathrm{NS}}$	$e^{i\epsilon H(z)}\tilde{\tau}_\theta^-(z)$
$(\alpha_{-\epsilon})^2\,\vert\,\theta\,\rangle_{\mathrm{NS}}$	$e^{i\epsilon H(z)}\omega_\theta^+(z)$	$(\alpha_\epsilon)^2\,\vert\,\theta\,\rangle_{\mathrm{NS}}$	$e^{i\epsilon H(z)}\widetilde{\omega}_\theta^-(z)$
$\psi_{-\frac{1}{2}+\epsilon}\vert\,\theta\,\rangle_{\mathrm{NS}}$	$e^{i(\epsilon-1)H(z)}\sigma_\theta^+(z)$	$\psi_{-\frac{1}{2}-\epsilon}\vert\,\theta\,\rangle_{\mathrm{NS}}$	$e^{i(\epsilon+1)H(z)}\sigma_\theta^-(z)$
$\alpha_{-\epsilon}\,\psi_{-\frac{1}{2}+\epsilon}\vert\,\theta\,\rangle_{\mathrm{NS}}$	$e^{i(\epsilon-1)H(z)}\tau_\theta^+(z)$	$\alpha_\epsilon\,\psi_{-\frac{1}{2}-\epsilon}\vert\,\theta\,\rangle_{\mathrm{NS}}$	$e^{i(\epsilon+1)H(z)}\tilde{\tau}_\theta^-(z)$
$(\alpha_{-\epsilon})^2\,\psi_{-\frac{1}{2}+\epsilon}\vert\,\theta\,\rangle_{\mathrm{NS}}$	$e^{i(\epsilon-1)H(z)}\omega_\theta^+(z)$	$(\alpha_\epsilon)^2\,\psi_{-\frac{1}{2}-\epsilon}\vert\,\theta\,\rangle_{\mathrm{NS}}$	$e^{i(\epsilon+1)H(z)}\widetilde{\omega}_\theta^-(z)$
$\alpha_{-1+\epsilon}\vert\,\theta\,\rangle_{\mathrm{NS}}$	$e^{i\epsilon H(z)}\tilde{\tau}_\theta^+(z)$	$\alpha_{-1-\epsilon}\vert\,\theta\,\rangle_{\mathrm{NS}}$	$e^{i\epsilon H(z)}\tau_\theta^-(z)$
$\alpha_{-1+\epsilon}\psi_{-\frac{1}{2}+\epsilon}\vert\,\theta\,\rangle_{\mathrm{NS}}$	$e^{i(\epsilon-1)H(z)}\tilde{\tau}_\theta^+(z)$	$\alpha_{-1-\epsilon}\psi_{-\frac{1}{2}-\epsilon}\vert\,\theta\,\rangle_{\mathrm{NS}}$	$e^{i(\epsilon+1)H(z)}\tau_\theta^-(z)$

Table 3.1: Vertex operators for different corresponding excitations in the NS sector.

3.5.2 Vertex Operators in the R Sector

If we consider the R sector, we observe that the bosonic part is obviously the same as for the NS sector. Thus, we will immediately turn to the fermionic part. The vacuum follows again from the definition in Eq. (3.31). Acting with Ψ and $\bar{\Psi}$ (the sum is now over integers) on the twisted vacuum $|\theta\rangle_{\mathrm{R}}$, we obtain [101]

$$\lim_{z\to 0}\Psi(z)|\theta\rangle_{\mathrm{R}} = \sum_{n\in\mathbb{Z}}\lim_{z\to 0}\psi_{n-\epsilon}z^{-\epsilon-\frac{1}{2}+\epsilon}|\theta\rangle_{\mathrm{R}} \quad\longrightarrow\quad z^{-\frac{1}{2}+\epsilon}\,T_\theta^+(0)\,S_\theta^+(0)|0\rangle_{\mathrm{R}}^u$$
$$\lim_{z\to 0}\bar{\Psi}(z)|\theta\rangle_{\mathrm{R}} = \sum_{n\in\mathbb{Z}}\lim_{z\to 0}\psi_{n+\epsilon}z^{-n-\frac{1}{2}-\epsilon}|\theta\rangle_{\mathrm{R}} \quad\longrightarrow\quad z^{\frac{1}{2}-\epsilon}\,\widetilde{T}_\theta^+(0)\,S_\theta^+(0)|0\rangle_{\mathrm{R}}^u\ . \tag{3.46}$$

Similarly to the NS sector, we have a corresponding relation between the untwisted vacuum and the twisted vacuum in the R sector

$$|\Theta\rangle_{\mathrm{B}\otimes\mathrm{R}} = \lim_{z\to 0}\prod_{k=1}^{3}\sigma_{\theta_k}(z)S_{\theta_k}(z)|0\rangle_{\mathrm{B}\otimes\mathrm{R}}^u\ . \tag{3.47}$$

[3]Negative angles θ get replaced by $1+\theta$.

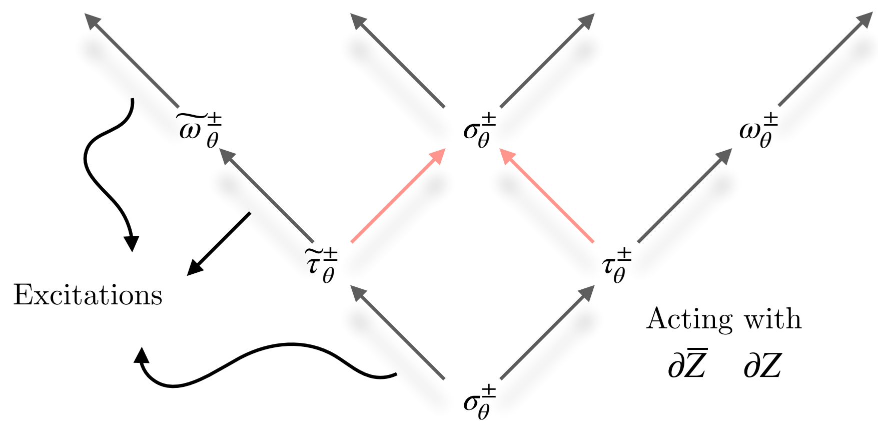

Figure 3.3: Schematic depiction of the action of ∂Z and $\partial\bar{Z}$ on the twisted and anti-twisted conformal fields. The same can be generalised for the Ramond sector by exchanging the appropriate fields. [93]

Positive angle		Negative angle	
State	Vertex operator	State	Vertex operator
$\vert\theta\rangle_{\mathrm{R}}$	$e^{i\left(\theta-\frac{1}{2}\right)H(z)}\sigma^{+}_{\theta}(z)$	$\vert\theta\rangle_{\mathrm{R}}$	$e^{i\left(\frac{1}{2}+\theta\right)H(z)}\sigma^{-}_{\theta}(z)$
$\alpha_{-\theta}\vert\theta\rangle_{\mathrm{R}}$	$e^{i\left(\theta-\frac{1}{2}\right)H(z)}\tau^{+}_{\theta}(z)$	$\alpha_{\theta}\vert\theta\rangle_{\mathrm{R}}$	$e^{i\left(\frac{1}{2}+\theta\right)H(z)}\widetilde{\tau}^{-}_{\theta}(z)$
$\psi_{-\theta}\vert\theta\rangle_{\mathrm{R}}$	$e^{i\left(\theta+\frac{1}{2}\right)H(z)}\sigma^{+}_{\theta}(z)$	$\psi_{\theta}\vert\theta\rangle_{\mathrm{R}}$	$e^{i\left(\theta-\frac{1}{2}\right)H(z)}\sigma^{-}_{\theta}(z)$
$\alpha_{-\theta}\psi_{-\theta}\vert\theta\rangle_{\mathrm{R}}$	$e^{i\left(\theta+\frac{1}{2}\right)H(z)}\tau^{+}_{\theta}(z)$	$\alpha_{\theta}\psi_{\theta}\vert\theta\rangle_{\mathrm{R}}$	$e^{i\left(\theta-\frac{1}{2}\right)H(z)}\widetilde{\tau}^{-}_{\theta}(z)$
$\psi_{-1+\theta}\vert\theta\rangle_{\mathrm{R}}$	$e^{i\left(\theta-\frac{3}{2}\right)H(z)}\sigma^{+}_{\theta}(z)$	$\psi_{-1-\theta}\vert\theta\rangle_{\mathrm{R}}$	$e^{i\left(\theta+\frac{3}{2}\right)H(z)}\sigma^{-}_{\theta}(z)$
$\alpha_{-\theta}\psi_{-1+\theta}\vert\theta\rangle_{\mathrm{R}}$	$e^{i\left(\theta-\frac{3}{2}\right)H(z)}\tau^{+}_{\theta}(z)$	$\alpha_{\theta}\psi_{-1-\theta}\vert\theta\rangle_{\mathrm{R}}$	$e^{i\left(\left(\theta+\frac{3}{2}\right)H(z)\right.}\widetilde{\tau}^{-}_{\theta}(z)$

Table 3.2: Vertex operators for different corresponding excitations in the R sector.

Here T^{+}_{θ} and $\widetilde{T}^{+}_{\theta}$ symbolize excited twist fields in the R sector that can be again bosonised

$$S^{+}_{\theta}(z)=e^{i\left(\epsilon-\frac{1}{2}\right)H(z)}\;,\quad T^{+}_{\theta}(z)=e^{i\left(\epsilon+\frac{1}{2}\right)H(z)}\;,\quad \widetilde{T}^{+}_{\theta}(z)=e^{i\left(\epsilon-\frac{3}{2}\right)H(z)}\;. \tag{3.48}$$

Analogously to the previous section, we can derive the vertex operator corresponding to any excitation. We summarize the results in table 3.2 below.

3.5.3 Lowest Energy States in the NS sector - A Light Stringy Scalar Boson

We can now look at the resulting Fock space in more detail. The contributing state in the NS sector, which will turn out to be massless for a supersymetric configuration, is

$$\Phi(k):\;\psi_{-\frac{1}{2}-\theta^{3}_{ab}}\left|\theta^{1}_{ab},\theta^{2}_{ab},\theta^{3}_{ab}\right\rangle_{\mathrm{NS}} \tag{3.49}$$

The mass squared operator in that case is given by Eq. (3.32) and reduces to[4]

$$M^2=-\frac{1}{2}+\frac{1}{2}\theta^{1}_{ab}+\frac{1}{2}\theta^{2}_{ab}-\frac{1}{2}\theta^{3}_{ab}+\frac{1}{2}+\theta^{3}_{ab}=\frac{1}{2}\left(\theta^{1}_{ab}+\theta^{2}_{ab}+\theta^{3}_{ab}\right)M_s^2\overset{\mathcal{N}=1}{=}0 \tag{3.50}$$

[4]States like e.g. $\psi_{-\frac{1}{2}-\theta^{2}_{ab}}$ yield a massive state under the condition for $\mathcal{N}=1$ with $M^2=(\theta^{2}_{ab}+\theta^{2}_{ab})M_s^2$. Thus, (3.49) is the *only* massless state.

By using the Table 3.1, we can construct the corresponding vertex operator in the canonical -1 super-ghost picture for that state. We further replace the negative angle θ with $1+\theta$, where θ is now defined as a multiple of π. We receive

$$\psi_{-\frac{1}{2}-\theta^3_{ab}} \left|\theta^1_{ab}, \theta^2_{ab}, \theta^3_{ab}\right\rangle_{\text{NS}} : \quad V_\phi^{(-1)} = g_\phi [\Lambda_{ab}]^{\alpha_1}_{\beta_1}\, \phi\, e^{-\varphi} \prod_{I=1}^{2} \sigma^+_{\theta^I_{ab}} e^{i\theta^I_{ab} H^I} \sigma^+_{1+\theta^3_{ab}} e^{i\left(1+\theta^3_{ab}\right)H^3} e^{ikX} \ , \tag{3.51}$$

where for the internal space we get contributions from the bosonic twist fields and the bosonised fermionic twist fields. The additional e^{ikX} comes from the four-dimensional spacetime structure, where the string can move freely. The so-called Chan-Paton factors $[\Lambda_{ab}]^{\alpha_1}_{\beta_1}$ indicate that string is stretched between the two D-brane stacks a and b. On each D-brane stack there lives a gauge group, thus the indices α_1 and β_1 run from one to the dimension of the fundamental representation of that gauge group. The string vertex coupling[5] is denoted by g_ϕ [103].

According to our convention, the string stretches from the stack a to the stack b of the corresponding D6 branes. Reverting the orientation of the string – from brane b to brane a – the complex conjugate state ϕ^* arises. This corresponds to the vertex operator in Eq. (3.51) with opposite orientation of the angles. Consequently, a string with a reverse orientation corresponds to an antiparticle [92] [68].

Given by the BRST symmetry, each Vertex operator has to obey the physical state condition

$$[Q_{BRST}, V] = 0 \ , \tag{3.52}$$

where the BRST Charge is given by [41]

$$\begin{aligned} Q_{BRST} = \oint \frac{dz}{2\pi i} \Bigg\{ & e^{\varphi} \eta \frac{1}{\sqrt{2\alpha'}} \left(i\partial X^\mu \psi_\mu + \sum_{I=1}^{3} \partial Z^I e^{-iH_I} + \sum_{I=1}^{3} \partial \bar{Z}^I e^{iH_I} \right) \\ & + c \left(\frac{1}{\alpha'} i\partial X^\mu i\partial X_\mu - \frac{1}{2}\psi^\mu \partial \psi_\mu + \sum_{I=1}^{3} \left(\frac{1}{\alpha'} \partial Z^I \partial \bar{Z}_I - \frac{1}{2} e^{-iH_I} \partial e^{iH_I} \right) \right) \Bigg\} + \dots \ , \end{aligned} \tag{3.53}$$

where we only consider the matter part, while the ellipsis stands for pure ghost terms [101, 104].

Using this physical state condition and the known OPE's, we typically get a simple and a double pole. This tells us a lot about the states. The simple pole corresponds to the equations of motion, while the double pole gives us information about the energy-momentum equation.

Now we can check if $V_\phi^{(-1)}$ is BRST invariant. The calculation is carried out in Mathematica© [6]. The physical condition $\left[Q_{BRST}, V_\phi^{(-1)}\right] = 0$ gives:

1. A simple pole, which corresponds to the equations of motion, vanishes identically for this case.
2. A double pole, which corresponds to the energy-momentum equation, vanishes if we require that $k^2 = 0$. This mass-shell condition is always fulfilled for massless bosonic or fermionic vertex operators.

At this point, we should mention an alternative route to find the mass formula by studying the conformal dimension of the VO, which is a primary field of dimension $h = 1$. The conformal

[5] The string vertex coupling g_ϕ can be derived by calculating the three-point amplitude [102]

[6] The Mathematica© code, with which the condition in Eq. (3.52) was checked, is based on an OPE library provided by Pascal Anastasopolous.

weights of all fields appearing in the vertex operators in Eq. (3.51) are [103]

$$[e^{\alpha\varphi}] = \frac{-\alpha\,(\alpha+2)}{2}\ , \quad \left[e^{iaH^I}\right] = \frac{a^2}{2}\ , \quad [\sigma_\theta] = \frac{\theta\,(1-\theta)}{2}\ , \quad \left[e^{ikX}\right] = \frac{\alpha' k^2}{2}\ . \tag{3.54}$$

Using these results, we get

$$\begin{aligned}\left[V_\phi^{-1}\right] &= \frac{1}{2} + \sum_{I=1}^{2}\left(\frac{\theta_I\,(1-\theta_I)}{2} + \frac{1}{2}\theta_I^2\right) + \frac{(\theta_3+1)\,(-\theta_3)}{2} + \frac{(\theta_3+1)^2}{2} + \frac{\alpha' k^2}{2} \\ &= \frac{1}{2} + \frac{1}{2}\sum_{I=1}^{3}\theta_I + \frac{1}{2} + \frac{\alpha' k^2}{2}\ .\end{aligned} \tag{3.55}$$

To achieve that $[V_\phi^{-1}] = 1$ we must set $\alpha' M^2 = \sum_{I=1}^3 \theta_{ab}^I$. Thus, we have found a physical "light" scalar. Depending on the choice of the angles, this scalar can be massive ($\sum_i^3 \theta_i > 0$), tachyonic ($\sum_i^3 \theta_i < 0$) or – if the intersections preserve supersymmetry ($\sum_i^3 \theta_i = 0$) – massless.

3.5.4 Lowest Energy State in the R Sector - A Massless Chiral Fermion

The same can now be done for the R sector, where we have the zero-state given by

$$\Psi^\alpha(k): \ \left|\theta_{ab}^1, \theta_{ab}^2, \theta_{ab}^3\right\rangle_{\mathrm{R}} \tag{3.56}$$

with a vanishing mass squared operator $M^2 = 0$, independent of the choice of angles. We now use the table (3.2) to build the vertex operator in the canonical $-1/2$ super ghost picture. Doing so, we obtain

$$|\theta\rangle_{\mathrm{R}}^{ab} : V_\psi^{(-1/2)} = g_\psi\,[\Lambda_{ab}]_{\beta_1}^{\alpha_1}\, e^{-\varphi/2} v^\alpha S_\alpha \prod_{I=1}^{2} \sigma^+_{\theta_{ab}^I}\, e^{i\left(\theta_{ab}^I - \frac{1}{2}\right)H_I} \sigma^+_{1+\theta_{ab}^3}\, e^{i\left(\theta_{ab}^3 + \frac{1}{2}\right)H_3} e^{ikX} \tag{3.57}$$

Now, this vertex operator carries a spinor index. To the spinor wave function v^α, we have an additional new type of field S_α in this VO, which denotes a $SO(1,3)$ spin field. The spin field is determined by the GSO projection.

The physical state condition $\left[Q_{BRST}, V_\psi^{(-1/2)}\right] = 0$ yields:

1. The simple pole vanishes if we require the equation of motion for a massless Weyl fermion.

$$k^\mu \bar{\sigma}_\mu^{\dot{\alpha}\alpha} v_\alpha(k) = 0\ . \tag{3.58}$$

2. The double pole vanishes again for $k^2 = 0$.

Analogously to the bosonic case, we can crosscheck the conformal weight of the Vertex operator. The only additional weight to the previously presented ones in Eq. (3.54) is [103].

$$[S^\alpha] = \left[e^{i\left(\pm\frac{1}{2}H_1 \pm \frac{1}{2}H_2\right)}\right] = 2\frac{\left(\pm\frac{1}{2}\right)^2}{2} = \frac{1}{4} \tag{3.59}$$

For the vertex operator we get

$$\left[V_{-\frac{1}{2}}\right] = \frac{3}{8} + \frac{1}{4} + 3\frac{1}{8} + \frac{\alpha' k^2}{2}\ . \tag{3.60}$$

Demanding that $[V_{-\frac{1}{2}}] = 1$ yields $\alpha' M^2 = 0$.

Therefore, this is a physical massless four-dimensional spacetime fermion. In sequence, that could be chiral fermion in the SM massless spectrum.

In summary, we have found a massless Weyl fermion in four dimensions at the lowest energy level - no matter how the D6 branes intersect. This fermion is in the bi-fundamental $(N_a, \bar{N}_b)$ representation (or its conjugate representation) of $U(N_a) \times U(N_b)$. The convention we choose here is that a string starting at a brane a gets a positive charge $+1$ under the corresponding U(N_a), while a string ending at a brane gets the opposite charge, i.e. -1. In the next section, we will explicitly see how chirality is naturally established by the intersection of such D6-branes.

Additionally, we get a further complex spacetime scalar boson, whose mass depends entirely on the angles. Choosing a supersymmetric set-up, where the sum of the angles is a subset of $SU(3)$ rotations, we get a boson with $M^2 = 0$ in the same representation as the fermion. Thus, at each intersection we have a $\mathcal{N} = 1$ chiral supermultiplet $(\phi,\ \psi)^T$ in bi-fundamental representation, which gives us a key feature of the standard model. This is the origin of charged matter in string theory.

3.5.5 Tower of Massive Copies

At each intersection we further find a tower of massive copies. In literature, these excitations are referred to as so-called "light stringy states" [93]. The logic to build such higher excitations is the same as shown in the previous sections. The "dictionary" provides a simple way to construct vertex operators and by using BRST invariance, further states can be identified with the already mentioned code.

With these results it is possible to work out couplings between the light stringy states and standard model states or even to elaborate an effective action to study phenomenology [93, 101, 102, 105]. In chapter 7, we will develop such light stringy states for phenomenological purposes.

Chapter 4

String Compactifications with D-Branes

In this chapter, we will compactify the unobserved dimensions in order to ensure a consistent four-dimensional effective spacetime theory. The approach of toroidal compactification is a simple but yet vivid possibility to get rid of the extra dimensions. The D6-branes can thus be viewed as homological 3-cycles which intersect in the compact space. This intersection number will give us a measure of how often the branes intersect. Consequently, open strings living near the intersections of two D6-branes appear in a multiplicity based on a mere topological setting. For the special case of a triple intersection and thus a threefold copy of the spectrum, it gives a replication of the matter content allocated at a single intersection. This yields a powerful geometrical explanation for the family replications and the three generations of the standard model.

In contrast to a more general compactification of so-called Calabi-Yau manifolds, the toroidal compactification serves us as a satisfactory simplified model. However, the toroidal compactification with just D6-branes does not provide $\mathcal{N} = 1$ *supersymmetry. For this reason, we will introduce the concept of orientifolds, which provides us with a realisation that is still comprehendible to analyse and lays out the foundation of a semi-realistic standard model.*

Checking global consistencies plays a crucial role in such compactified theories. We will find that quantum anomalies occur in the effective four-dimensional theory, which can, however, be resolved by making use of so-called tadpole conditions on the one hand and by introducing a generalised Green-Schwarz mechanism on the other hand. The latter will provide the $U(1)$ *gauge bosons with a so-called Stückelberg mass and add further conditions to the theory. To fulfil these conditions, we will once again find that we have to introduce orientifolds and the corresponding O6-planes.*

We have already established that for reasons of consistency superstring theory requires the critical dimensionality of ten. Since only four-dimensions are physically observable, an explanation must be provided of how these “additional” dimensions are manifested so that an effective four-dimensional spacetime theory results. In the history of string theory, several different possibilities for such a realisation have been introduced. In order to make it manageable, we will assume that these additional unobservable dimensions are wrapped up on themselves. This goes under the name of *compactification*.

The original idea goes back to Theodor Kaluza, who in 1921 tried to combine gravity and electromagnetism (based on ideas of Gunnar Nordström) by adopting an additional fifth dimension [106–109]. As is well known, this original attempt of unification failed but provided generations of mathematicians and physicist with inspiration for theories, which go far beyond the *Kaluza-Klein theory* (KK).

For the purpose of compactification within superstring theory, the ten-dimensional spacetime is split up into an external non-compact maximally symmetric spacetime, which can be identified with spacetimes such as de Sitter (dS), Anti-de Sitter (AdS) or the conventional Minkowski space ($\mathbb{R}^{3,1}$), and an internal compact space. Formally expressed, we write [110]

$$\mathcal{M}^{9,1} = \mathbb{R}^{3,1} \times \mathcal{X}_6 \ . \tag{4.1}$$

For all sorts of different reasons, such as leaving the original supersymetry unbroken or to ensure that conformal field theory is viable, there are certain conditions, which must be fulfilled by this compact space. Therefore, most of the time we generically demand from $\mathcal{X}_6$ to be a Calabi-Yau 3-fold CY_3 [54, 63, 110–112]. The general framework is attempted to be artistically interpreted in Fig. 4.1.

The downside of working with string theory compactification on Calabi-Yau manifolds is that these spaces are highly complicated, and hence we will look at a more simplified case. On that account, we will go the route of *toroidal compactification*, which we will later expand to so-called toroidal orientifold and orbifold compactification, which lies between the comprehensible toroidal case and the more exotic Calabi-Yau diegesis. Furthermore, this choice of toroidal compactification provides generally a compliant example of *mirror symmetry* [63, 113–115], which generalises *T-duality* [54, 63, 116, 117] and therefore makes it possible to translate Type IIA into Type IIB and vice versa.

4.1 Toroidal Compactification

For the tractable case of toroidal compactification, we choose the internal compact space $\mathcal{X}_6$ to be a 6-torus $\mathbb{T}^6$, which is factorisable into three 2-tori of the form $\mathbb{T}^6 = \mathbb{T}^2 \times \mathbb{T}^2 \times \mathbb{T}^2$. According to this definition, the spacetime can be split into

$$\mathcal{M}^{9,1} = \mathbb{R}^{3,1} \times \mathbb{T}^6 = \mathbb{R}^{3,1} \times \mathbb{T}^2 \times \mathbb{T}^2 \times \mathbb{T}^2 \ . \tag{4.2}$$

Choosing this particular compactification enables two important advantages of great avail. Firstly, we can visualise *holonomy classes* more easily, and secondly, we can use conformal field theory description, which enables and justifies the use of the vertex operator formalism, which we used in section 3.5.

Returning to the Dp-brane discourse, we choose these branes so that the $\mathbb{R}^{3,1}$ is filled out [1], while the remaining $(p-3)$ dimensions of the Dp-brane form submanifolds in the compact space. Generally, one speaks of so-called $(p-3)$-cycles. In order to better understand terms such as p-cycles and related concepts such as homology, there is a small introduction in the appendix D, which serves the reader as a primer. For example, we assume that we have n stacks of D6-branes, where each stack a contains N_a coincident parallel D6$_a$-branes. These D6$_a$-branes are thus spanning the four-dimensional spacetime and are further wrapped on 3-cycles on $\mathbb{T}^6$, which are from now on denoted as $\Pi_a^3 \subset \mathbb{T}^6$. For the case that $n = 3$, a schematic depiction can be found in Fig. 4.2 [17].

A generic feature of the compactification is that the 3-cycles will generate intersections at multiple points in the six-dimensional compact space. The remaining aim of this section will be to determine this *intersection number*. The intersection number I_{ab} is a purely topological quantity and thus independent of metric-related problems. Therefore, further analysis will be based on topological considerations, which is why it makes sense to introduce the 3-homology

[1] This is necessary to provide Poincare symmetry in $\mathbb{R}^{3,1}$.

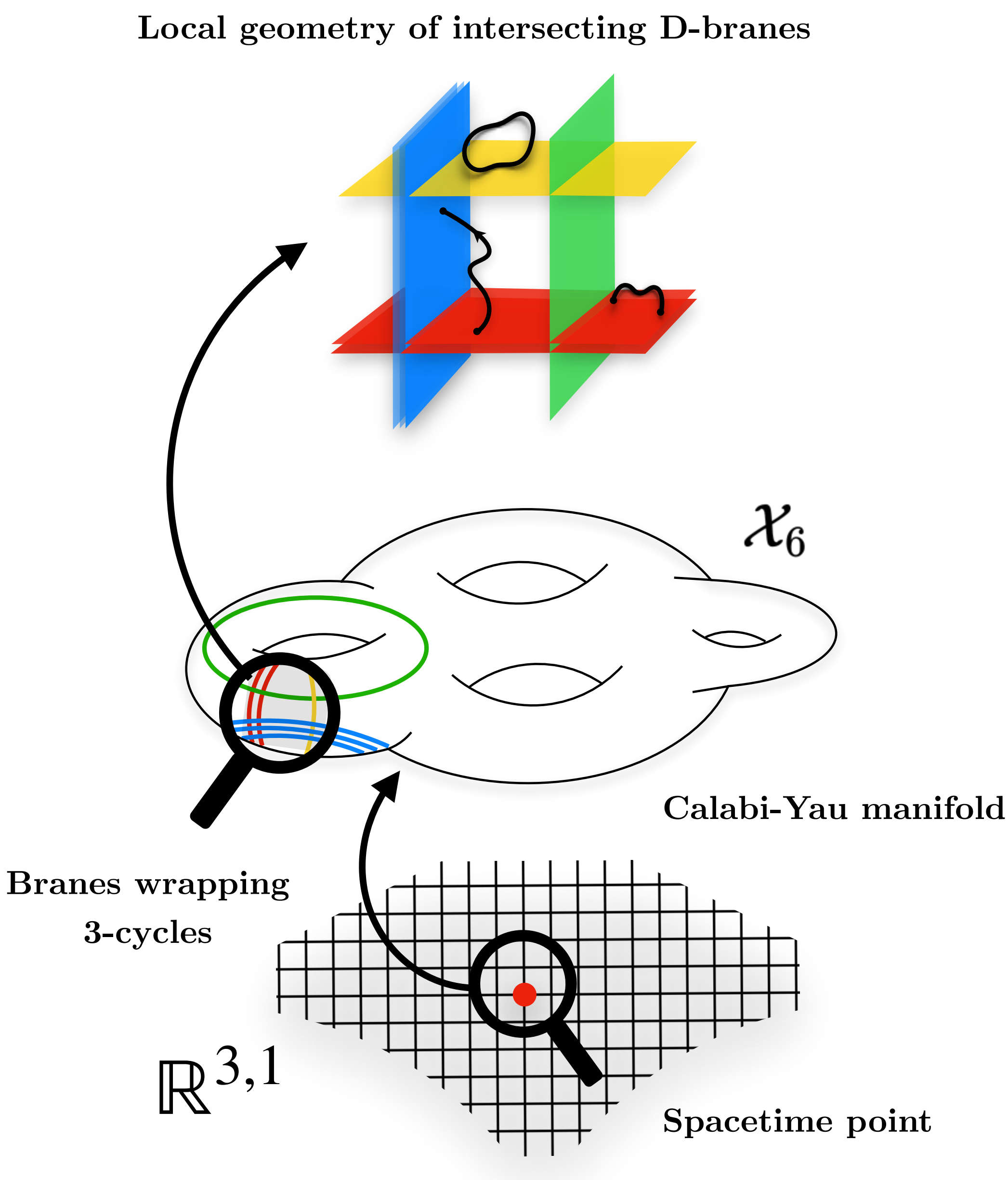

Figure 4.1: String theory tries to solve the puzzle why only four of the ten-dimensions are perceived in our physical reality by using the concept of compactification. According to this, a tiny compact six-dimensional space sits at every point of the four-dimensional spacetime, which escapes our perception. This internal space must have many special properties, which are fulfilled by so-called Calabi-Yau manifolds. D-branes wrap on such compact spaces 3-cycles that frequently intersect. Locally, we can always consider these configurations as in chapter 3 where we used conventional flat $\mathbb{R}^6$ instead of tori.

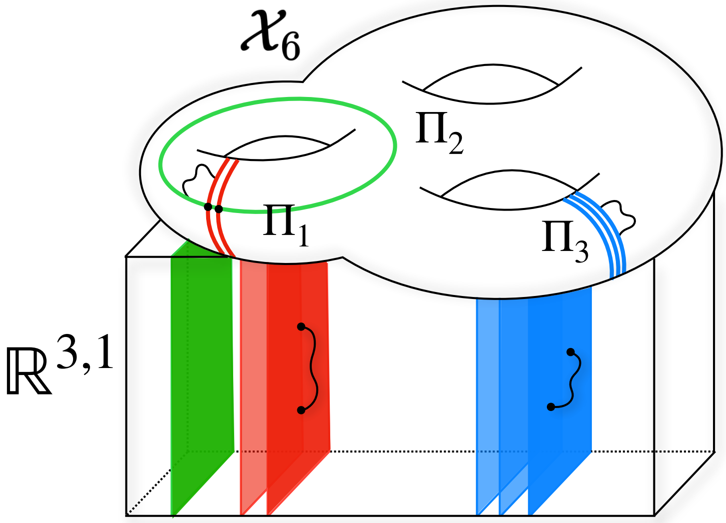

Figure 4.2: The depicted spacetime has the form $\mathbb{R}^{3,1} \times \mathcal{X}_6$. Where $\mathbb{R}^{3,1}$ describes the four-dimensional spacetime and $\mathcal{X}_6$ denotes the compact space. The D6-branes fill the Minkowski space and wrap 3-cycles $\Pi_a^3 \subset \mathcal{X}_6$ in the remaining six-dimensions. Such 3-cycles intersect in a six-dimensional compact space and the D6-branes thereby intersect at the $\mathbb{R}^{3,1}$ subspace. Through compactification the ten-dimensional gravitational interaction and the seven dimensional gauge interactions can be reduced to a four-dimensional effective theory. Furthermore, the 3-cycles can intersect several times in the internal space, which leads to a reproduction of the spectrum in the respective sectors.

class $[\Pi_a^3] \in H_3(\mathbb{T}^6, \mathbb{Z})$ of the 3-cycle Π_a^3, where $H_3(\mathbb{T}^6, \mathbb{Z})$ is the 3^{th} homology group of $\mathbb{T}^6$ [17]. As already indicated, the 6-torus can be factorised into three plane 2-tori. Accordingly, the 3-cycles Π_a^3 can be expressed as a product of three 1-cycles Π_a. For illustrative purposes, we now use the fact that a 2-torus can be described as the quotient of the unit xy-plane under the boundary identification

$$x \sim x + 1 \quad \text{and} \quad y \sim y + 1 \; . \tag{4.3}$$

A 1-cycle in the i^{th} 2-torus can be represented as a line segment which runs from $(0^{(i)}, 0^{(i)})$ to $(n^{(i)}, m^{(i)}) \sim (0^{(i)}, 0^{(i)})$. Thus, $n^{(i)}$ and $m^{(i)}$ are coprime integers and therefore their greatest common divisor corresponds to $\gcd(n^{(i)}, m^{(i)}) = 1$ [45, 63]. If $(n^{(i)}, m^{(i)})$ is not relatively prime, $\gcd(n^{(i)}, m^{(i)})$ indicates how often the line is wrapped around the i^{th} torus. An example is given in Fig. 4.4. Accordingly, these tuples are called *wrapping numbers* [45, 63]. With this tool, we are able to describe a 1-cycle in a very intuitive way. It is advisable to represent the 1-cycle in a so-called integral basis (whose coefficients are the wrapping numbers) with a canonical 1-cycle $a_{(i)}$ and the associated dual one $b_{(i)}$ [103]. The canonical 1-cycles are chosen as those segments, respectively defined by $y = 0$ and $x = 0$. This is graphically shown in Fig. 4.3 for better understanding. In the following, we obtain

$$H_1(\mathbb{T}^2, \mathbb{Z}) \ni [\Pi_a^{(i)}] = n_a^{(i)}[a_{(i)}] + m_a^{(i)}[b_{(i)}] \; , \quad \forall i \; . \tag{4.4}$$

Further, topology allows us to define a product between cycles. From Fig. 4.3 it is very easy to deduce, that 1-cycles $a_{(i)}$ and $b_{(i)}$ never intersect, unless they are on the same torus. Further, the product is skew-symmetric since we have an orientation. In the context of holonomy, the product is defined according to

$$[a_i] \circ [b_j] = \delta_{ij} \quad \text{and} \quad [b_i] \circ [a_j] = -\delta_{ij} \; . \tag{4.5}$$

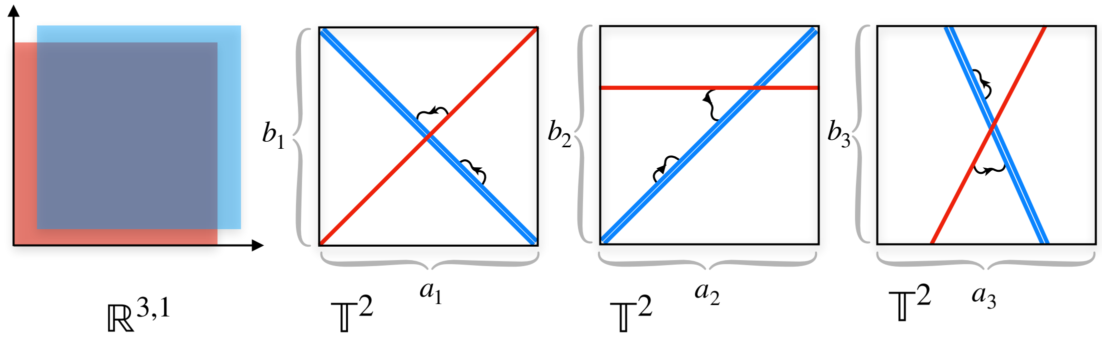

Figure 4.3: Schematic representation of two D6-branes described on a factorised $\mathbb{T}^6 = \mathbb{T}^2 \times \mathbb{T}^2 \times \mathbb{T}^2$ via 3-cycles. This pair of D6-branes fills the four-dimensional spacetime, making the intersection points four-dimensional. By the factorisation the 3-cycles can be expressed by 1-cycles. A natural basis can be chosen along the horizontal and vertical orientation of the three planar 2-tori.

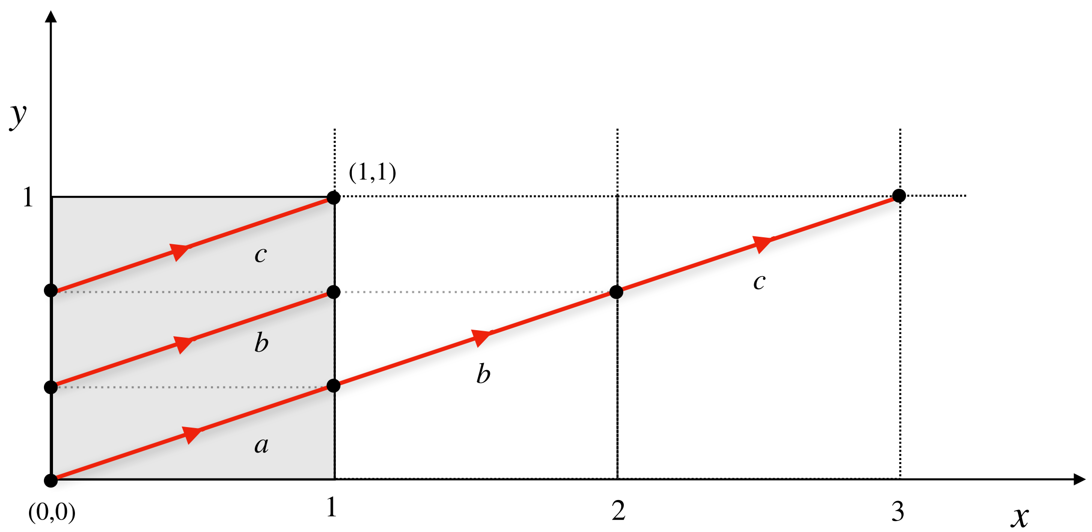

Figure 4.4: In this figure, the fundamental domain of a 2-torus is shown. The drawn 1-cycle is given by $\Pi = 3a + 1b$. This is to be understood in such a way that this cycle runs between the points $(0,0)$ and $(3,1)$. If we supplement this fundamental domain with three copies, we can draw this segment as a continuous line. By toroidal identification, these points in the copies correspond to points in the original fundamental domain. This gives the 1-cycle in the fundamental domain, which is denoted by the segments a, b and c. This 1-cycle is repeatedly wrapped on the 2-torus [45].

Following the argument that the 3-cycle is factorisable on the 6-torus and given the fact that we have three 2-tori, we can decompose the original 3-cycle as a direct product of the three 1-cycles. The 3-homology class is given by [2]

$$[\Pi_a^3] = \bigotimes_{i=1}^{3} [\Pi_a^{(i)}] = \bigotimes_{i=1}^{3} \left(n_a^{(i)} [a_{(i)}] + m_a^{(i)} [b_{(i)}] \right) \ . \tag{4.6}$$

Having found a suitable parameterisation for our 3-cycle, we can now determine the homological intersection number at $[\Pi_a] \cap [\Pi_b]$. The intersection number $I_{ab}^{(i)}$ for 1-homology classes is a skew-symmetrical bilinear map $H_1(\mathcal{X}, \mathbb{Z}) \times H_1(\mathcal{X}, \mathbb{Z}) \to \mathbb{Z}$. Given the definition of the product in Eq. (4.5), we compute

$$\begin{aligned} I_{ab} \equiv \bigotimes_{i=1}^{3} I_{ab}^{(i)} = [\Pi_a] \circ [\Pi_b] &= \bigotimes_{i,j=1}^{3} \left(n_a^{(i)} [a_{(i)}] + m_a^{(i)} [b_{(i)}] \right) \circ \left(n_b^{(j)} [a_{(j)}] + m_b^{(j)} [b_{(j)}] \right) \\ &= \bigotimes_{i,j=1}^{3} \left\{ n_a^{(i)} m_b^{(j)} [a_{(i)}] \circ [b_{(j)}] + m_a^{(i)} n_b^{(j)} [b_{(i)}] \circ [a_{(j)}] \right\} = \bigotimes_{i=1}^{3} \left(n_a^{(i)} m_b^{(i)} - m_a^{(i)} n_b^{(i)} \right) \ . \end{aligned} \tag{4.7}$$

This intersection number now reveals two important facts for the case of toroidal compactifications.

The first special feature of the intersection number is that it is weighted with a global sign. According to our convention a string with the orientation $a \to b$ and a positive intersection number corresponds to left-handed fermions, whereas a negative intersection is identified with right-handed fermion with the orientation $a \to b$. From $I_{ab} = -I_{ba}$ it follows, that the sector $\mathrm{D6}_b\mathrm{D6}_a$ includes the antiparticles from the $\mathrm{D6}_a\mathrm{D6}_b$ sector.

The second property is that the absolute value $|I_{ab}|$ counts the number of intersections and thus the replication of the chiral fermions in the bi-fundamental representation $(N_a, \overline{N}_b)$. This is usually notated as [17]

$$|I_{ab}| = \#([\Pi_a] \cap [\Pi_b]) \ . \tag{4.8}$$

This yields the remarkable result that intersecting D6-branes give rise to four-dimensional chiral fermions from open strings localised near each intersection, where $|I_{ab}|$ indicates how many replicas are given in this intersection. This gives a clear way to explain the family replications of the standard model.

Until now, we have highly praised toroidal compactification because, unlike Calabi-Yau manifolds, it gives us a clear geometric picture and simplifies concrete calculations. Consider our results from chapter 3. We have seen that the intersections of D6-branes in flat ten-dimensions give rise to four-dimensional spacetime fermions and bosons which we can combine into a chiral supermultiplet if the choice of the relative angles of the D6-branes is chosen appropriately. This corresponds to a $\mathcal{N} = 1$ supersymmetry which we need to construct possible extensions of the standard model. However, since we are forced to describe the reality with our theoretical models, we have compactified these extra dimensions of chapter 3 which *locally* corresponded to an $\mathbb{R}^6$ [3]. The mere use of toroidal compactifications destroys the original supersymmetry. This is in fact a general feature of the compactification of a $\mathcal{N} = 1$ supersymmetry to a smaller number of dimensions. In the case of toroidal compactification to four-dimensions, we end up with an $\mathcal{N} = 4$ supersymmetry [119]. Nevertheless, constraining this system can still be reduced $\mathcal{N} = 4$ to $\mathcal{N} = 1$, which comes in with the introduction of so-called orientifolds. We will discuss this in the following section.

[2] In the following we will omit the label for the 3-cycles, which is given by the symbol 3 and only use it if it is not clear from the context whether we mean a 3-cycle or 1-cycle.

[3] For the toroidal case the background metric and the induced metric on the worldvolumes of the associated D6-branes is flat. Therefore, we are allowed to describe locally intersecting branes on a compact space as intersection on a non-compact flat space. [118]

The spectrum contains [63]:

- Four-dimensional[4] gauge bosons (and potential superpartners) from the D6$_a$-D6$_a$ sector, according to the gauge group:
$$\bigotimes_a U(N_a) \ . \tag{4.9}$$

- Generations of chiral fermions (and potential superpartners) from the D6$_a$D6$_b$ (resp. D6$_b$D6$_a$) sector:
$$\sum_{a<b} I_{ab} \left(N_a, \overline{N}_b\right) \ . \tag{4.10}$$

At the end, we point out that the angles θ_k are now a derived quantity [63]. From a simple geometrical consideration, we determine that the angles are given by

$$\tan\theta_{(i)} = \frac{m^{(i)}R_2^{(i)}}{n^{(i)}R_1^{(i)}} = \frac{m^{(i)}}{n^{(i)}}\,\mathrm{Re}\,U^{(i)} \ , \tag{4.11}$$

where $R_1^{(i)}, R_2^{(i)}$ are the radii of the i$^{\text{th}}$ 2-torus along the horizontal and vertical directions. $U^{(i)}$ denotes the *complex structure modulus* of the 2-torus.

4.2 Global Consistency and Tadpole Cancellation

Type IIA string theory equipped with Dp-branes contains *quantum anomalies* [40, 63, 67], which are fatal in the ultra-violet regime of a quantum field theory [120]. For reasons of consistency, these anomalies, which manifest themselves in so-called RR tadpole diagrams [54], have to be cancelled. In this section, we examine our previous theory for such *global consistencies.* As we have already stated, Dp-branes are sources of charge for RR $(p+1)$ forms. The Gauss law demands that the total net charge must disappear in a compact space. This can be easily illustrated by using the more conventional picture of electrodynamics. Let us assume that we have a non-compact space with a charged particle located there (see Fig. 4.5a). The flux lines of the charged particle can disappear into infinity and therefore the total charge does not have to disappear. If, on the other hand, the space is compact, such as the 2-sphere S^2, we can again position a probe charge on the surface[5]. Here, however, the flux lines cannot escape into infinity and the problem can only be resolved by adding a second particle with the opposite charge (see Fig. 4.5b) [17].

In the toroidal case with D6-branes wrapping 3-cycle in the compact space $\mathbb{T}^6$ it is necessary to impose a vanishing RR charge in order to insure tadpole cancellation. In order to investigate this issue, we first have to find an effective action for the RR 7-form [67].

As we have already established in section 2.3, the WZ action is part of the effective Dp-brane action responsible for the coupling of the RR forms. In order to work with this rather abstract action in Eq. (2.38), we have to expand it to make it more explicit. The appendix A contains

[4]The former seven-dimensional gauge bosons reduce to four-dimensional gauge bosons from the point of view of the non-compactified four-dimensional spacetime $\mathbb{R}^{3,1}$, as we can "subtract" the compactified 3-cycles.

[5]This can be shown quickly as a one-liner from the Maxwell equations. Consider $\nabla \cdot \vec{E} = \rho$. Integrating both over a compact space S without boundaries ($\partial S = 0$) yields

$$Q = \int_S \rho = \int_S \nabla \cdot \mathbf{E}\, dV = \int_{\partial S} \mathbf{E} \cdot d\mathbf{A} = 0 \tag{4.12}$$

Thus, by using the divergence theorem, we have shown that the total charge must vanish.

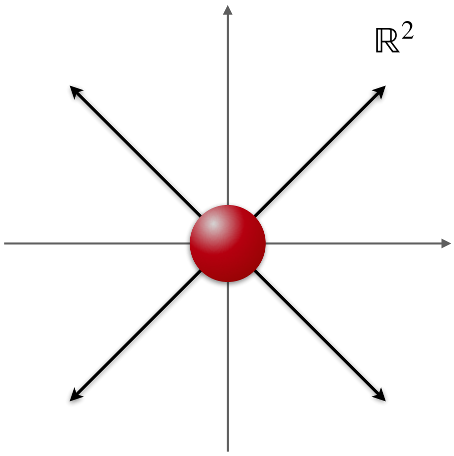

(a) Flux-lines in a non-compact space can escape to infinity, which is here illustrated for the $\mathbb{R}^2$.

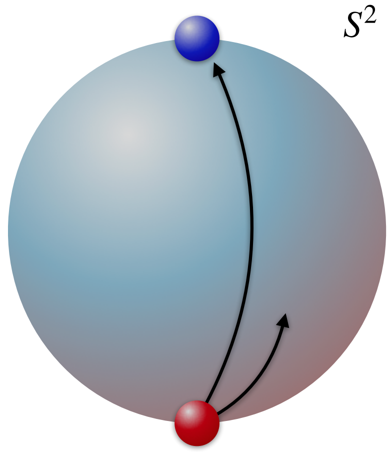

(b) Flux-lines in a compact space cannot escape into infinity. Thus, the net charge on such a space must vanish.

Figure 4.5: The RR tadpole cancellation can be interpreted as a Gaus Law. According to this law, the net charge on a compact space must vanish.

further steps in this regard and with its guide, the WZ-action reads

$$\begin{aligned}\mathcal{S}_{\mathrm{WZ}}[C_p] = T_p \int_{\mathcal{W}_{p+1}} \Big(& N\, C_{p+1} + 2\pi\alpha' C_{p-1} \wedge \mathrm{tr} F \\ & + \frac{1}{2} (2\pi\alpha')^2\, C_{p-3} \wedge \Big[\mathrm{tr}\, F \wedge F + \frac{N}{48} (\mathrm{tr}\, \mathcal{R}_T \wedge \mathcal{R}_T - \mathrm{tr}\, \mathcal{R}_N \wedge \mathcal{R}_N) \Big] + \ldots \Big) \,. \end{aligned} \tag{4.13}$$

The B field is set to zero for comprehensibility and F is again the field strength, which takes values in the fundamental representation of $U(N)$. [54, 63]. Using the toroidal model with D6-branes and the leading order term in the expansion, Eq. (4.13) leads to the simplified effective action

$$\mathcal{S}_{\mathrm{WZ}}[C_6] = T_6 \sum_a N_a \int_{\mathbb{R}^{3,1}\times\Pi_a} C_7 + \mathcal{O}(\alpha') \,. \tag{4.14}$$

To ensure the 7-form to propagate, we add a kinetic term to the action, which arises from the effective open string action, which is also known as the *supergravity* (SUGRA) action [46, 54, 121]. Together, we find

$$\begin{aligned}\mathcal{S}_{\mathrm{eff}}^{C_7} &= -\frac{1}{2\kappa^2} \int_{\mathbb{R}^{3,1}\times\mathbb{T}^6} H_8 \wedge \star H_8 + T_6 \sum_a N_a \int_{\mathbb{R}^{3,1}\times\Pi_a} C_7 \\ &= -\frac{1}{2\kappa^2} \int_{\mathbb{R}^{3,1}\times\mathbb{T}^6} dC_7 \wedge \star dC_7 + T_6 \sum_a N_a \int_{\mathbb{R}^{3,1}\times\mathbb{T}^6} C_7 \wedge \delta_3(\Pi_a) \,. \end{aligned} \tag{4.15}$$

The 8-form $H_8 = dC_7$ is the field strength of the RR 7-form and $\kappa^2 = \frac{1}{2}(2\pi)^7(\alpha')^4$ denotes the ten-dimensional gravitational coupling [68, 103]. In the last step[6], the integral on the 3-cycles is extended over the entire compact space $\mathbb{T}^6$.

[6]Without introducing concepts like *de Rahm duality* and *cohomology*, we state that the so-called Poincaré dual forms permit to extend integrals on p-cycles to integrals on the manifold $\mathcal{M}$, according to the isomorphism

$$\int_{\pi_p} \alpha_p = \int_{\mathcal{M}} \alpha_p \wedge \delta(\pi_p) \quad \forall \alpha_p \in \Omega^p(\mathcal{M}) \,. \tag{4.16}$$

In a nutshell, every non-trivial p-cycle α_p is assigned to a non-trivial $d-p$ cohomology class. The paradigmatic example of such an element of the cohomology class is the so-called "bump" form $\delta(\pi_p)$, living in the $d-p$ transverse directions to the cycle. The coefficients of the form are specified by a Dirac delta "function" with support on π_p [63, 111, 122].

To find the equation of motion for the C_7, we vary the action according to

$$
\begin{aligned}
0 = \delta\mathcal{S}^{C_7}_{\text{eff}} &= -\frac{1}{\kappa^2}\int_{\mathcal{M}_{9,1}} d\delta C_7 \wedge \star dC_7 + T_6 \sum_a N_a \int_{\mathcal{M}_{9,1}} \delta C_7 \wedge \delta_3(\Pi_a) \\
&= -\frac{1}{\kappa^2}\int_{\mathcal{M}_{9,1}} d(\delta C_7 \wedge \star dC_7) - \frac{1}{\kappa^2}\int_{\mathcal{M}_{9,1}} \delta C_7 \wedge d\star dC_7 + T_6 \sum_a N_a \int_{\mathcal{M}_{9,1}} \delta C_7 \wedge \delta_3(\Pi_a) \\
&= -\frac{1}{\kappa^2}\int_{\partial\mathcal{M}_{9,1}} \delta C_7 \wedge \star dC_7 - \frac{1}{\kappa^2}\int_{\mathcal{M}_{9,1}} \delta C_7 \wedge d\star dC_7 + T_6 \sum_a N_a \int_{\mathcal{M}_{9,1}} \delta C_7 \wedge \delta_3(\Pi_a) \\
&= -\frac{1}{\kappa^2}\int_{\mathcal{M}_{9,1}} \delta C_7 \wedge d\star dC_7 + T_6 \sum_a N_a \int_{\mathcal{M}_{9,1}} \delta C_7 \wedge \delta_3(\Pi_a)\ .
\end{aligned}
\tag{4.17}
$$

In the first line in Eq. (4.17), we used the Hodge operator rule $\alpha \wedge \star\beta = \beta \wedge \star\alpha$ for p-forms $\alpha, \beta \in \Omega^p(\mathcal{M})$. In the second line, we used the product rule $d(\delta C_7 \wedge \star dC_7) = d\delta C_7 \wedge \star dC_7 - \delta C_7 \wedge d\star dC_7$ to split the integral. In the third line, we converted the first integral to a surface integral, according to Stokes theorem. This integral does not contribute as the variation δC_7 on the surface vanishes [123].

For all variations δC_7, the equation of motion is

$$
\frac{1}{\kappa^2} d\star dC_7 = \underbrace{d\,(dC_2)}_{dH_2} = T_6 \sum_a N_a \delta_3\,(\Pi_a)\ \ , \tag{4.18}
$$

where H_2 is the Hodge dual of the field strength $\star dH_8 = dH_2$. Thus, the left handside of Eq. (4.18) is an exact form. It can also be rewritten into $\int_{\mathcal{M}} dH_2 = \int_{\partial\mathcal{M}} H_2$, which is nothing more than the Stokes theorem [111]. Using Gauss law, the expression in Eq. (4.18) yields zero, which formulates mathematically that the total charge in the internal space is zero

$$
\sum_a N_a \delta_3\,(\Pi_a) = 0\ , \tag{4.19}
$$

Further, by using Poincaré duality it allows to rewrite the last equation as an equation in homology

$$
[\Pi_{\text{tot}}] \equiv \sum_a N_a\,[\Pi_a] = 0. \tag{4.20}
$$

Imposing the decomposition into wrapping numbers $[\Pi_a] = \bigotimes_{i=1}^3 (n_a^{(i)}[a_{(i)}] + m_a^{(i)}[b_{(i)}])$ for the 3-homology class given by Eq. (4.6), we can write the RR tadpole conditions in a very explicit form:

$$
\begin{aligned}
&\sum_a N_a n_a^{(1)} n_a^{(2)} n_a^{(3)} = 0\,, \quad \sum_a N_a m_a^{(1)} m_a^{(2)} m_a^{(3)} = 0 \\
&\underbrace{\sum_a N_a n_a^{(1)} n_a^{(2)} m_a^{(3)} = 0\,,}_{+\ 2\ \text{two permutations}} \quad \underbrace{\sum_a N_a n_a^{(1)} m_a^{(2)} m_a^{(3)} = 0}_{+\ 2\ \text{permutations}}
\end{aligned}
\tag{4.21}
$$

Therefore, in order to have a net charge of zero, there are two possible realisations for D6-branes. The first implementation is rendered possible by the introduction of *antibranes* with a negative charge, which explicitly breaks supersymmetry and brings potential instabilities, or the second option, namely not having branes at all. Therefore, an additional object is needed for a supersymmetrical D6-brane set up to circumvent this problem [63].

4.3 Orientifold Planes

Since we are interested in phenomenological aspects and the related SM or MSSM, we demand a reduction to $\mathcal{N} = 1$ supersymmetry. As we have already indicated in the previous section, Dp-branes are charged under antisymmetric RR fields and the net charge on compact spaces has to vanish. This can be achieved through the introduction of an orientifold projection and the associated orientifold planes with negative tension or charge, respectively [67].

In summary, it is indeed possible to obtain the desired four-dimensional $\mathcal{N} = 1$ supersymmetry, if we additionally require that there is an orientifold projection on the compactified CY_3. However, in chapter 6 we will also see that the toroidal orientifold model will not be sufficient to guarantee a four-dimensional $\mathcal{N} = 1$ supersymmetry. It is thus necessary to constrain the toroidal compactification even further by using a a toroidal compactification on an *orbifold* with an orientifold projection. This idea of using orbifolds goes back to the proposal of Dixon, Harvey, Vafa and Witten [124, 125].

To realise such an orientifold compactification in type IIA string theory, the initial internal Calabi-Yau manifold $\mathcal{X}_6$ gets modded out by a discrete symmetry $\mathcal{G}$, which is referred to as an orientifold projection. This is shown schematically in Fig. 4.6. This *orientifold projection* gets introduced by the following actions of the form [126–129]:

- $\Omega_{\mathcal{P}}$, which is basically the world-sheet parity action.
- $\mathcal{R}$ is a $\mathbb{Z}_2$ geometric symmetry of $\mathcal{X}_6$, which acts as an involution on the Calabi-Yau manifold.
- $(-)^{\mathcal{F}_L}$ acting on the world-sheet fermions.

The operator $\Omega_{\mathcal{P}}$ changes the orientation of the strings according to $\sigma \mapsto \pi - \sigma$. Further, it also reverses left moving states to right moving states [130]. The full world-sheet parity action is given by

$$\begin{aligned} \text{Open :} \qquad & \Omega_{\mathcal{P}} : (\tau, \sigma) \mapsto (\tau, \pi - \sigma) \ , \\ \text{Closed :} \qquad & \Omega_{\mathcal{P}} : (\sigma_1, \sigma_2) \mapsto (2\pi - \sigma_1, \sigma_2) \ . \end{aligned} \tag{4.22}$$

This operator is accompanied by another action, which we introduced as $(-)^{\mathcal{F}_L}$. $\mathcal{F}_L$ indicates the left-moving spacetime fermion number and yields -1 for RNS and RR sectors. Furthermore, this particular action is needed so that the orientifold action squares to the identity. The full action on the world-sheet fermions reads

$$(-)^{\mathcal{F}_L} = \begin{cases} +1 & \text{on states in the left-moving NS sector.} \\ -1 & \text{on states in the left-moving R sector.} \end{cases} \tag{4.23}$$

Another required action that is not solely related to the world-sheet symmetry is the geometric action $\mathcal{R}$ that is analogous to a $\mathbb{Z}_2$ involution. In order to preserve $\mathcal{N} = 1$ supersymmetry, this action needs to be an isometric and anti-holomorphic involution of the Calabi-Yau manifold [131].

For the sake of completeness, it should be mentioned how this projection applies to the general case of a CY_3 in type IIA. In this case, a nontrivial transformation behaviour of the so-called Kähler form J and the holomorphic 3-cycle Ω_3 (not to be confused with the parity operator $\Omega_{\mathcal{P}}$) of the CY–manifold occurs under the action of the pull-back of the involution $\mathcal{R}$ to be

$$\mathcal{R}^* J = -J \quad \text{and} \quad \mathcal{R}^* \, \Omega_3 = e^{2i\theta} \, \overline{\Omega}_3 \ , \tag{4.24}$$

where $e^{2i\theta}$ is a constant phase. The full orientifold projection is thus given by

$$\text{Type IIA :} \qquad \mathcal{G} = \Omega_{\mathcal{P}} \, \mathcal{R} \, (-)^{\mathcal{F}_L} \ . \tag{4.25}$$

Since we are interested in more concrete realisations and their phenomenological aspect, we will not jump into the more general case of CY_3 here, and refer to literature, such as [63, 132, 133].

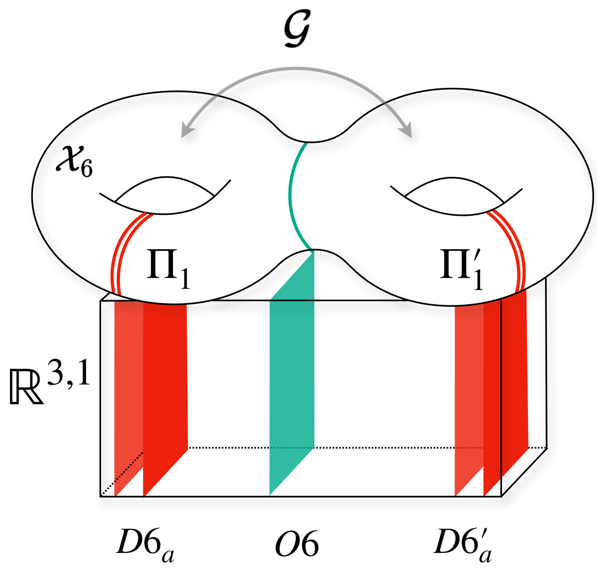

Figure 4.6: The depicted spacetime has the form $\mathbb{R}^{3,1} \times \mathcal{X}_6$. $\mathbb{R}^{3,1}$ describes once again the four-dimensional spacetime and $\mathcal{X}_6$ denotes the compact space. The D6-branes fill the Minkowski space and wrap 3-cycles $\Pi_a^3 \subset \mathcal{X}_6$ in the remaining six-dimensions. Through the introduction of the orientifold projection, fixed point loci are created, which are invariant under the orientifold projection. These invariant points are the orientifold planes or simply O6-planes. Moreover, the projection creates a mirrored image at these O6-planes. Thus, the O6-planes produce image D6′-branes.

Toroidal Orientifold Compactifications

Returning to the toroidal compactification model, we can now apply the orientifold projection to a more concrete case. Once again, we will describe the factorised 6-torus by means of three rectangular 2-tori $\mathbb{T}^6 = \mathbb{T}^2 \times \mathbb{T}^2 \times \mathbb{T}^2$. In terms of complexified coordinates, the torus is parametrised by $z^i = x^{2i+2} + ix^{2i+3}$, with the usual identifications $z^i \simeq z^i + R_1^i$ and $z^i \simeq z^i + iR_2^i$. The type II orientifold background can be formally written as

$$\mathcal{M}^{9,1} = \frac{\mathbb{R}^{3,1} \times \mathbb{T}^6}{\mathcal{G}} \; . \tag{4.26}$$

To investigate the impact of the orientifold projection on this specific model, we first consider $\mathcal{R} = \mathcal{R}_{(1)}\mathcal{R}_{(2)}\mathcal{R}_{(3)}$ in detail [17]. We have seen that in order to preserve $\mathcal{N} = 1$ symmetry in type IIA string theory, $\mathcal{R}$ acts as an anti-holomorphic and isometric involution of the internal space. For this configuration we thus obtain the following transformation

$$\mathcal{R}_{(i)} : z^i \to \bar{z}^i \, , \quad \text{with} \quad i = 1, 2, 3 \; . \tag{4.27}$$

This provides a very illustrative transformation behaviour, since Eq. (4.27) can be interpreted just as complex conjugation or a reflection on R_1^i. This can also be seen in Fig. 4.7. This conclusion leads to two important observations. First, the projection gives rise to so-called mirror images. Cycles thus have a mirrored version of themselves, which ensures that the theory is invariant under the orientifold group. For each Dp_a-brane we introduce in our model, the configuration is extended by a “mirror” brane through the orientifold projection $\mathcal{G}$. These mirror image of Dp-branes will be denoted by

$$\mathrm{D}p_{\mathcal{G}a}\text{– brane} \;\equiv \mathrm{D}p_{a'}\text{– brane} \quad . \tag{4.28}$$

Second, loci of fixed point are created. These fixed points, which in our case coincide with the

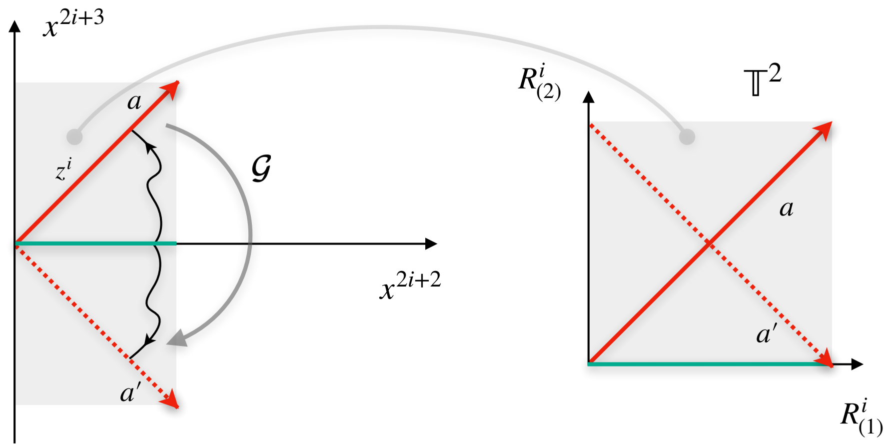

Figure 4.7: The i$^{\text{th}}$ 2-torus can be parameterised in $\mathbb{C}$. Points in the fundamental domain of the i$^{\text{th}}$ torus are complex conjugated by the orientifold projection, which corresponds to a reflection along the x^{2i+2} axis. This axis represents the O6-plane.

horizontal axis along R^i_1 in the Fig. 4.7, form a new class of objects which span a hyperplane in p-spatial dimensions. In contrast to the Dp-branes, these orientifold planes or just Op-planes are not dynamical objects, but still carry a charge and a tension. These objects are classified according to this charge or tension. In the further course, we will always have to do with Op-planes which have a negative tension and a negative charge. Therefore, when we write Op-plane, we implicitly assume that we mean $O_p^{(\epsilon_1,\epsilon_2)}$-plane, with $\epsilon_1 = \epsilon_2 = -1$, where the ϵ indicate whether the tension or charge is positive or negative, respectively [134].

The RR charge of an Op-plane is negative as already mentioned and can be expressed in units of RR charge of the Dp brane as follows

$$Q_{\text{Op}} = -2 \cdot 2^{p-5}\, Q_{\text{Dp}} \,. \tag{4.29}$$

The fixed points of the orientifold projections for the toroidal model are illustrated in Fig. 4.8 and are described by [130]

$$\mathbb{R}^{3,1} \times \text{Fix}(\mathcal{R}) = \mathbb{R}^{3,1} \times \left\{ \text{Im}(z^i) = 0,\ \frac{1}{2} R^i_1, \quad \text{for } i = 1,2,3. \right\} \,. \tag{4.30}$$

Fix($\mathcal{R}$) is a 3-cycle on $\mathbb{T}^6$ and without going into more detail, such 3-cycles on compact spaces $\mathcal{X}_6$ go under the name of *special Lagrangians* (SLag) [17,63,135,136]. In addition, for the presence of O6-planes, the analysis performed in section 4.2 can be refined and extended accordingly. For this purpose, we consider the effective action in Eq. (4.15). This is supplemented in the orientifold model by the contribution of the orientifold planes and the resulting mirror images. The adjusted effective action in the presence of an orientifold plane reads

$$\begin{aligned} \mathcal{S}^{C_7}_{\text{eff}} = &- \frac{1}{2\kappa^2} \int_{\mathbb{R}^{3,1}\times\mathbb{T}^6} H_8 \wedge \star H_8 + T_6 \sum_a N_a \int_{\mathbb{R}^{3,1}\times\Pi_a} C_7 \\ &+ T_6 \sum_a N_a \int_{\mathbb{R}^{3,1}\times\Pi'_a} C_7 - 4\,T_6 \sum_a N_a \int_{\mathbb{R}^{3,1}\times\Pi_{\text{O6}}} C_7 \,. \end{aligned} \tag{4.31}$$

Analogous to Eq. (4.17), we obtain by variation

$$d \star dC_7 = -\ell_s \left(\sum_a N_a \left[\delta_3\left(\Pi_a\right) + \delta_3\left(\Pi'_a\right) \right] - 4\delta_3\left(\Pi_{\text{O6}}\right) \right) \,. \tag{4.32}$$

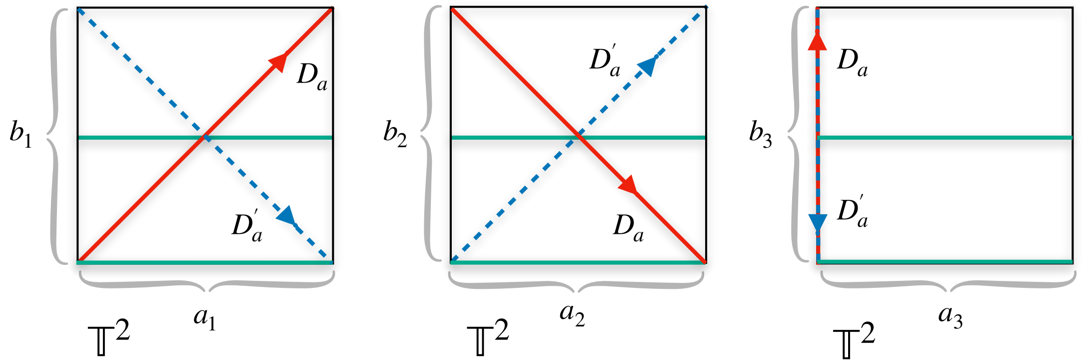

Figure 4.8: An example of a factorisable 6-torus. the respective orientifold planes in the i$^{\text{th}}$ torus are drawn in teal. Shown are also 1-cycles (red) corresponding to D6-branes and their reflection and resulting D6' branes (blue).

This in turn gives us a new tadpole condition and thus a global condition that is modified by image D6$_a$-branes and O6-planes.

$$\sum_a N_a\left([\Pi_a]+[\Pi_{a'}]\right)=4\,[\Pi_{O6}]\ . \tag{4.33}$$

Equation (4.33) already spoils that the net charge vanishes in this configuration. This can be seen as the tadpole condition reveals how the charges are distributed in the orientifold model. Here, the charge contribution of the orientifold plane is just cancelled by that of the D6-brane and its mirror image. The next question one can ask is how these tadpole conditions manifest themselves concretely by expressing them explicitly in terms of wrapping numbers. The 3-cycles can again be represented in an integral basis as a product of 1-cycles.

$$[\Pi_a]=\bigotimes_{i=1}^{3}\left(n_i^a[a^i]+m_i^a[b^i]\right)\ . \tag{4.34}$$

If D6-branes are given again as such, we can derive the representation of the mirror images D6$_{a'}$. In the case of rectangular 2-tori this is particularly intuitive. If we look at Fig. 4.7, it is obvious that the base is chosen in such a way that a^i is placed along the horizontal axis x^{2i+2} and b^i is placed vertically along x^{2i+3}. From this it is obvious that by the involution only the part which corresponds to b^i transforms and gets a negative sign. The part corresponding to a^i is invariant. This yields the transformation behaviour $\mathcal{R}_{(i)}:(n^a_{(i)}.m^a_{(i)})\mapsto(n^a_{(i)},-m^a_{(i)})$ for the wrapping numbers and for the mirror branes we therefore get

$$[\Pi_a']=\bigotimes_{i=1}^{3}\left(n_i^a[a^i]-m_i^a[b^i]\right)\ . \tag{4.35}$$

Finally, we need to represent the 3-cycle that belongs to the O6-plane. These O6-planes are located at the fix points $x^{2i+3}=\{0,{}^1\!/_2\,R_i\}$ and their wrapping number is $(n_i^a,m_i^a)=(1,0)$. As evident in Fig. 4.8, it should be noted that there are exactly two fixed point loci per 2-torus, which is of course related to the fact that the 3-cycle, which lies at $x^{2i+3}={}^1\!/_2$, gets mirrored at the O6-plane at $x^{2i+3}=0$ [63]. However, this particular 3-cycle merges into itself, because of the identified ends of the plain rectangular representation of the compact space.

$$[\Pi_{\mathrm{O6}}]=\bigotimes_{i=1}^{3}[a^i]\ . \tag{4.36}$$

We have now all ingredients to translate Eq. (4.33) into a equation in terms of wrapping numbers. For that purpose, we obtain

$$\sum_a N_a \left\{ \bigotimes_{i=1}^{3} \left(n_i^a [a^i] + m_i^a [b^i] \right) + \bigotimes_{j=1}^{3} \left(n_j^a [a^j] - m_j^a [b^j] \right) \right\} = 4 \bigotimes_{i=1}^{3} [a_i] \ . \tag{4.37}$$

Now all possible cases must be considered individually. The first case corresponds to $[a_1] \otimes [a_2] \otimes [a_3]$. This results in the contribution 8 $[a_1] \otimes [a_2] \otimes [a_3]$ for the orientifold part in Eq. (4.33). The prefactor arises from the fact that there are 2 fix point loci per torus which multiply to 8 for the case of three 2-tori. Next, we turn to the contribution of the D6-branes to this possible case. Simply by reading off, we obtain $\sum_a N_a n_1^a \, n_2^a \, n_3^a \, [a_1] \otimes [a_2] \otimes [a_3]$. It occurs that we get the exact term from the mirror image D6-brane. Thus, the last expression counts twice. A next possible term we can investigate is given by $[a_1] \otimes [b_2] \otimes [b_3]$. In this basis, and of course all other basis directions, there is no contribution from the O_p-plane term. Thus, this part disappears for all further cases. For the D6-brane and the corresponding mirror image we again get the same contribution which is given by $2 \sum_a N_a n_1^a \, m_2^a \, m_3^a \, [a_1] \otimes [b_2] \otimes [b_3]$. The same applies to the two permutations where $1 \to 2$ and $1 \to 3$. This is also the end of this discussion, as all other possibilities disappear. This can be simply shown by the example for the case $[b_1] \otimes [b_2] \otimes [b_3]$. The D6-brane yields $\sum_a N_a m_1 \, m_2 \, m_3 \, [b_1] \otimes [b_2] \otimes [b_3]$, while the O6-plane gives $- \sum_a N_a n_1 \, n_2 \, n_3 \, [b_1] \otimes [b_2] \otimes [b_3]$. This cancels these possibilities. All in all, we find four types of conditions

$$\begin{aligned} \sum_a N_a n_1^a n_2^a n_3^a &= 16 \, , \quad & \sum_a N_a n_1^a m_2^a m_3^a &= 0 \\ \sum_a N_a m_1^a n_2^a m_3^a &= 0 \, , \quad & \sum_a N_a m_1^a m_2^a n_3^a &= 0 \ . \end{aligned} \tag{4.38}$$

Modified Massless Spectrum

Now that we are acquainted with the very basics of orientifolds and their impact on our theory, we will examine how this modifies the spectrum of open strings. The introduction of O_6-planes results in various new geometric configurations. With this wealth of new possibilities, we focus only on those configurations in which D6-branes do not coincide with their image D6′-branes. A more general and non-torus dependent analysis can be found in [63]. We focus again on the local description of the internal space. D6-branes again represent submanifolds running along 3-cycles but in this case, we must conclude the involution of the compact space. Encountering new intersections, we thus expect new chiral matter to appear. All that remains is to determine in which representation this massless matter appears.

In theories containing orientifolds, the open string spectrum is obtained by simply projecting onto invariant states. Here, of course, it must also be taken into account that the orientation of open strings gets reverted by the action of $\Omega_{\mathcal{P}}$. Labelling different stacks of D6-branes again by a and b, we get the following different sectors with $\mathcal{G}$ acting as [63,127,134,137,138]

$$\Omega_{\mathcal{P}} \mathcal{R} \, (-)^{\mathcal{F}_L} : \begin{pmatrix} aa & a'a & ba & b'a \\ aa' & a'a' & ba' & b'a' \end{pmatrix} \mapsto \begin{pmatrix} a'a' & a'a & a'b' & a'b \\ aa' & aa & ab' & ab \end{pmatrix} . \tag{4.39}$$

One possible and already known scenario in this extended configuration are open strings that are located between D6$_a$-branes and D6$_b$-branes. Under the action of $\mathcal{G}$, the open string is identified with an open string that is located between the image branes D6$'_a$ and D6$'_b$. This is illustrated in Fig. 4.9. Before this orientifold identification we thus have a gauge group $U(N_a) \times U(N_b) \times U(N'_a) \times U(N'_b)$ with four-dimensional chiral fermions in the representation $(\Box_a, \overline{\Box}_b)_{(+1,-1)}$ and $(\Box_{b'}, \overline{\Box}_{a'})_{(+1,-1)}$. However, after the identification the gauge group reduces

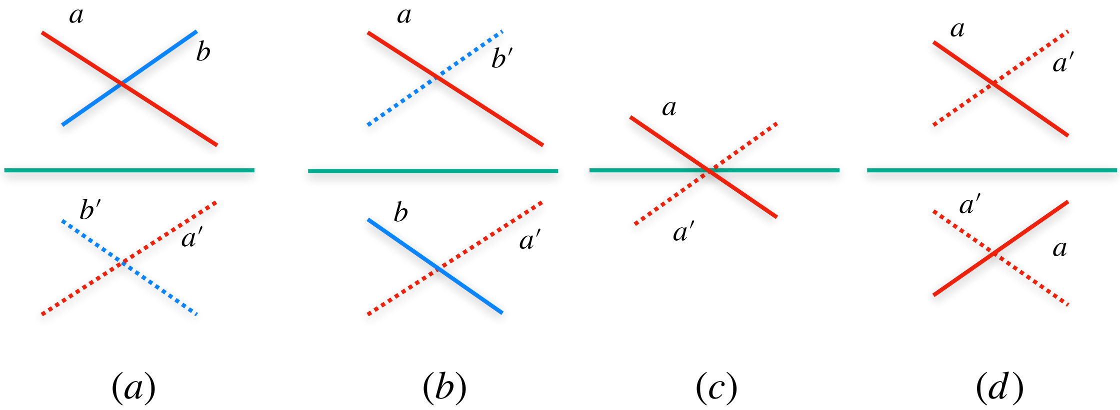

Figure 4.9: A pair of intersecting D6 branes in the presence of an orientifold plane. In (a), the a-brane intersects with the b-brane, but the intersection point is not on the O6-plane. (b) shows the intersection of an a-brane with the image of the b-brane. Again, the intersection point is away from the fixed points. In (c), an a-brane intersects with its image brane. The intersection point is on the O6 plane. In (d) the intersection of an a-brane with its image brane is shown, but this time the intersection point is not a fix-point.

to $U(N_a) \times U(N_b)$ and we get four-dimensional chiral fermions which transform into the bi-fundamental representation $(\square_a, \overline{\square}_b)_{(+1,-1)}$. This can be explained geometrically by the re-orientation of the string orientation by the action of $\Omega_{\mathcal{P}}$. The open strings that start from the stack of the D6_a or terminates on the same are identified with those open strings, that end or raise at the D$6'_a$ stack. Therefore, the group $U(N)_a$ is associated with its image $U(N)'_a$. Consequently, the fundamental representation $\square_a$ of the $U(N)_a$ gets identified with anti-fundamental representation $\overline{\square}'_a$ of $U(N)'_a$ [63]. Further, that means that we are left with states, which are invariant under the orientifold projection.

For the case of open strings running between branes in the same stack a, we obtain gauge bosons in the adjoint representation of $U(N)_a$. The first novelty not present in the plain toroidal case is given by the configuration of an open string stretched between a D6_a-brane and an image D6_b-brane. This case is again depicted in Fig. 4.9. The gauge group for this case is furnished by $U(N_a) \times U(N'_b) \times U(N'_a) \times U(N_b)$. The four-dimensional chiral fermions transform in the corresponding bi-fundamental representations $(\square_a, \overline{\square}_{b'})_{(+1,-1)}$ and $(\square_b, \overline{\square}_{a'})_{(+1,-1)}$. After the orientifold truncation we obtain the fermions in the $(\square_a, \square_b)_{(+1,+1)}$ representation with a multiplicity given by $[\Pi_a] \circ [\mathcal{R}\Pi_b] = [\Pi_a] \circ [\Pi'_b]$. The interpretation is that strings in the bi-fundamental representation $(\square_a, \overline{\square}_b)$ are associated with oriented strings. Strings in the bi-fundamental representation $(\square_a, \square_b)$, on the other hand, reverse their orientation induced by the O6-planes [63].

The last case to be discussed is that of D6_a-branes coincident to orientifold planes. More precisely, D6_a-branes and their image D$6'_a$-brane. Through the invariance under the orientifold action, a gauge symmetry of $SO(2N_a)$ or $Sp(2N_a)$ results [139].

These options will suffice for the creation of semi-realistic models in this thesis. The other configurations involving $U(N_a) \times U(N'_a)$ are shown in the figure Fig. 4.9 and in the table 4.1 are preserved for completeness. These configurations do not lead to bi-fundamentals but rather to symmetric and antisymmetric representations of $U(N_a)$ via tensor products. The intersection

Sector	Multiplicity	Representation
$ab + ba + b'a' + a'b'$	$\Pi_a \circ \Pi_b$	$(\square_a, \overline{\square}_b)$
$ab' + b'a + ba' + a'b$	$\Pi_a \circ \Pi'_b$	$(\square_a, \square_b)$
$aa' + a'a$	$\frac{1}{2}\left(\Pi'_a \circ \Pi_a - \Pi_a \circ \Pi_{\mathrm{O6}}\right)$	$\square\!\square_a$
$aa' + a'a$	$\frac{1}{2}\left(\Pi_a \circ \Pi'_a + \Pi_a \circ \Pi_{\mathrm{O6}}\right)$	$\begin{array}{c}\square\\[-4pt] \square\end{array}_a$

Table 4.1: The modified spectrum for open strings in the presence of D6-branes and O_6 planes. The spectrum contains I_{ab} chiral fermions in the representation $(N_a, \overline{N}_b)$, $I_{ab'}$ chiral fermions in the representation (N_a, N_b) and I_{sym} chiral fermions in the symmetric representation plus I_{asym} in the anti-symmetric representation.

number is given by $I_{\mathrm{asym/sym}} \equiv \frac{1}{2}\left(\Pi_a \circ \Pi'_a \pm \Pi_a \circ \Pi_{\mathrm{O6}}\right)$, where the upper positiv sign is used for the antisymmetric representation, while the lower negative sign is used for the symmetric representation.

4.4 Quantum Anomalies

String theory claims and attempts to unify quantum theory and gravity. For this reason, it is necessary that string theory is exempt from quantum anomalies. In general, a quantum anomaly indicates the breakdown or failure of a classical symmetry at the quantum level. According to this, one has to carefully differentiate between anomalies in regard to *local* and *global* symmetries [140, 141].

Anomalies that occur in global symmetries are usually harmless and do not pose any problems for the theory, since they are simply a statement that the symmetry is not exact. A prime example of such an anomaly can be found, for example, in the parity violation of the standard model and can be observed in nature, such as in the process of pion decay $\pi^0 \to \gamma + \gamma$, which would be classically forbidden [142].

In contrast, anomalies in the context of local or gauge symmetries are dangerous and problematic. Gauge symmetries are particularly important to cancel unphysical degrees of freedom. In the event of cancelling such unphysical degrees of freedom, such as for example the polarisation of the photon in the time direction, further new constrains appear on the theory. To put it briefly, one can thus say that anomalies lead to inconsistencies and break the renormalisability and unitarity of the theory. It is a natural and important step in the construction of such effective field theories within string theory to examine anomalies in order to check the consistency of the low energy theory [141–143].

One way to understand and treat local anomalies is through what is known as the *Adler-Bell-Jackiw anomaly triangle*. In these one loop diagrams, a chiral fermion runs into a loop between three external gauge bosons [144]. It is a well-known fact, that these one-loop diagrams have to vanish to provide an anomaly free quantum field theory [141, 142]. This concept can be extended to any dimensions and in the case of a ten-dimensional string theory this anomaly corresponds to a hexagon diagram in spacetime [88]. By introducing Dp-branes as building blocks and a six-dimensional compact space, it is sufficient to examine the Adler-Bell-Jackiw diagrams in four-dimensions for the effective field theory [54, 63].

In the next sections, we will calculate these quantum chiral anomalies of the effective field theory explicitly in the context of intersecting D-branes. On this basis we will consider every possible occurring cases, which is the cancellation of cubic non-Abelian, Abelian, and mixed

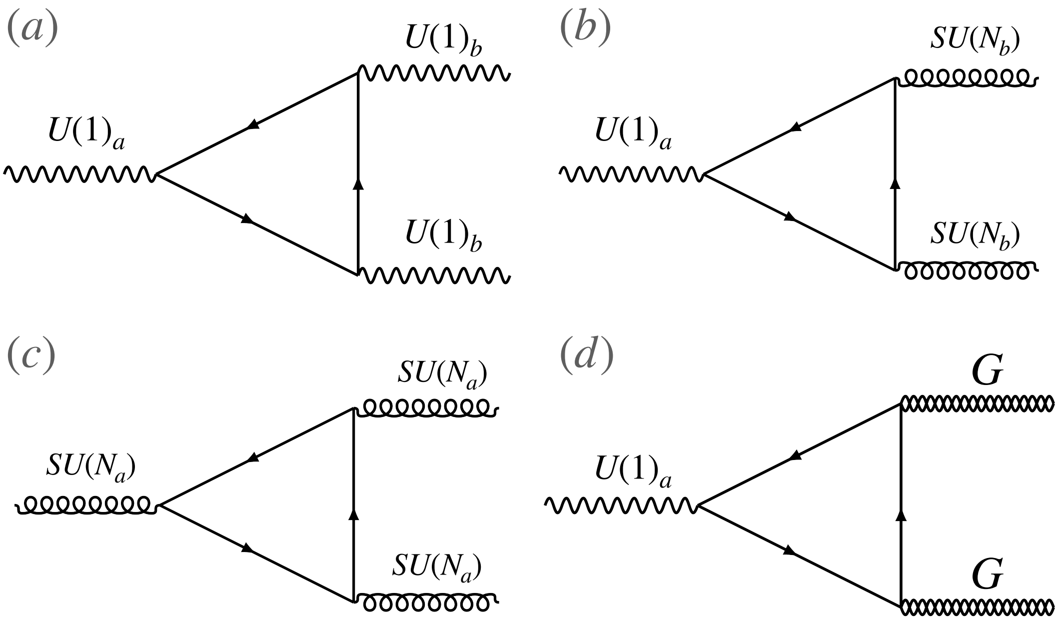

Figure 4.10: Adler-Bell-Jackiw anomaly triangle diagrams for the cubic non-Abelian anomaly (a), the mixed Abelian-non-Abelian anomaly (b), the cubic Abelian anomaly (c) and the mixed Abelian-gravitational anomaly (d). The external legs of these diagrams correspond to gauge bosons, while chiral fermion runs in the loop.

chiral anomalies, and mixed gravitational anomalies.

4.4.1 Cubic Non-Abelian Anomaly

The first case of interest is the non-Abelian gauge anomaly. This occurs when chiral fermions couple to non-Abelian gauge groups such as the $SU(N)$. All possible Adler-Bell-Jackiw anomaly diagrams are depicted in Fig. 4.10. The anomaly is essentially given by [54]

$$\mathrm{tr}_R\left(\{T^a,T^b\}\,T^c\right) = A(R)\ \mathrm{tr}_\square\left(\{T^a,T^b\}\,T^c\right)\ , \tag{4.40}$$

where T^k are the generators of the gauge group $SU(N_a)$ and $A(R)$ denotes the *cubic Casimir* or *anomaly coefficient*, which can be found in the Tab. 4.2. In Eq. (4.40) we refashioned the trace over the generators in a representation R into the trace over the generators in the fundamental

	$\square$	$\overline{\square}$	$\square\square$	$\overline{\square\square}$	$\begin{smallmatrix}\square\\\square\end{smallmatrix}$	$\overline{\begin{smallmatrix}\square\\\square\end{smallmatrix}}$
$\boldsymbol{D(R)}$	N	N	$\frac{N(N+1)}{2}$	$\frac{N(N+1)}{2}$	$\frac{N(N-1)}{2}$	$\frac{N(N-1)}{2}$
$\boldsymbol{Q(R)}$	$+1$	-1	$+2$	-2	$+2$	-2
$\boldsymbol{C(R)}$	$\frac{1}{2}$	$\frac{1}{2}$	$\frac{N+2}{2}$	$\frac{N+2}{2}$	$\frac{N-2}{2}$	$\frac{N-2}{2}$
$\boldsymbol{A(R)}$	$+1$	-1	$N+4$	$-(N+4)$	$N-4$	$-(N-4)$

Table 4.2: Anomaly coefficients for different representations R of $SU(N)$. Indicated are the relevant coefficients for the fundamental, symmetric and antisymmetric representation, which are expressed in form of Young tableaux. The dimension of the representation is given by $D(R)$. The $Q(R)$ is designated to the $U(1)$ charge under de decomposition $U(N) \sim SU(N) \times U(1)$ [17].

representation of the corresponding gauge group. As a consequence, the cubic non-Abelian anomaly is proportional to [145, 146]

$$\mathcal{A}^{aaa}_{\mathrm{SU}(N_a)^3} \sim \sum_R A(R) \; . \tag{4.41}$$

Using the multiplicity of the chiral matter for intersecting D6-brane models, which we derived in section 4.3 and presented in Tab. 4.1, we sum over all fermions and obtain

$$\begin{aligned}
\mathcal{A}^{aaa}_{\mathrm{SU}(N_a)^3} \sim\; & A(\Box_a)\left(\sum_b N_b\, \Pi_a \circ \Pi_b + \sum_{b\neq a} N_b\, \Pi_a \circ \Pi_b'\right) + \frac{A(\begin{smallmatrix}\Box\\\Box\end{smallmatrix}_a)}{2}\left(\Pi_a \circ \Pi_a' + \Pi_a \circ \Pi_{O6}\right) \\
& + \frac{A(\Box\Box_a)}{2}\left(\Pi_a \circ \Pi_a' - \Pi_a \circ \Pi_{O6}\right) = \sum_b N_b\, \Pi_a \circ \Pi_b + \sum_{b\neq a} N_b\, \Pi_a \circ \Pi_b' \\
& + \frac{N_a - 4}{2}\left(\Pi_a \circ \Pi_a' + \Pi_a \circ \Pi_{O6}\right) + \frac{N_a + 4}{2}\left(\Pi_a \circ \Pi_a' - \Pi_a \circ \Pi_{O6}\right) \\
& = \Pi_a \circ \left(\sum_b N_b \left[\Pi_b + \Pi_b'\right] - 4\Pi_{\mathrm{O6}}\right) \overset{\mathrm{T.C.}}{=} 0 \; .
\end{aligned} \tag{4.42}$$

In order to get to the last line we used the fact, that $N_b = N_b'$ and the relations $\Pi_a \circ \Pi_a = 0$, $\Pi_a' \circ \Pi_b = \Pi_b' \circ \Pi_a = -\Pi_a \circ \Pi_b'$ and $\Pi_a \circ \Pi_b = -\Pi_a' \circ \Pi_b'$.

Fortunately, we can conclude that the cubic non-Abelian anomaly vanishes identically by using the tadpole condition from Eq. (4.33), where its application is from now on denoted by the abbreviation T.C. Here we come across a typical property of Type II string theory compactification. The RR tadpole cancellation implies cancellation of anomalies in the effective field theory.

4.4.2 Mixed Abelian – Non-Abelian Anomaly

As in the previous non-Abelian case, the mixed anomalies can be represented again by using triangular diagrams. One gauge boson now belongs to an Abelian $U(1)_a$ while the others correspond to two non-Abelian gauge groups $SU(N_a)$. The mixed–non-Abelian anomaly is proportional to [145, 147]

$$\mathcal{A}^{abb}_{U(1)_a - SU(N_b)^2} \sim \sum_R Q_a(R)\, C_b(R) \; . \tag{4.43}$$

The coefficient $C(R)$ denotes the *quadratic Casimir* and $Q(R)$ is the $U(1)$ charge. For this mixed anomaly we distinguish two cases. For the first case in which the stacks $a \neq b$, only the bi-fundamental fields contribute in the loop and therefore the anomaly in Eq. (4.43) immediately results into

$$\mathcal{A}^{abb}_{U(1)_a - SU(N_b)^2} \sim \frac{N_a}{2}\, \Pi_a \circ \left(\Pi_b + \Pi_b'\right) \; . \tag{4.44}$$

For the second case, where $a = b$ we must consider and sum over all states, because symmetric and anti-symmetric representations are possible [7]. Using Tab. 4.1 again, we obtain

$$\begin{aligned}
\mathcal{A}^{aaa}_{U(1)_a - SU(N_a)^2} \sim\; & \frac{(N_a - 2)}{2}\left(\Pi_a \circ \Pi_a' + \Pi_a \circ \Pi_{\mathrm{O6}}\right) + \frac{(N_a + 2)}{2}\left(\Pi_a \circ \Pi_a' - \Pi_a \circ \Pi_{\mathrm{O6}}\right) \\
& + \frac{1}{2}\sum_b N_b\, \Pi_a \circ \Pi_b + \sum_{b\neq a} N_b\, \Pi_a \circ \Pi_b' \overset{\mathrm{T.C.}}{=} \frac{1}{2} N_a\, \Pi_a \circ \Pi_a' \; ,
\end{aligned} \tag{4.45}$$

which agrees with Eq. (4.44) if $b \to a$. However, in contrast to the previous non-Abelian case, the following is noticeable: The anomaly does *not* vanish after satisfying the tadpole condition. We will deal with this problem and its solution in the next section.

[7] By using symmetric and anti-symmetric representations we can produce chiral matter content by using a single stack of D-branes. This is only mentioned here, since we will exclude these representations when we explicitly construct semi-realistic models.

4.4.3 Cubic Abelian Anomaly

Before we address the apparent problem of the non-disappearing anomalies we turn to the cubic $U(1)$ anomaly. The external legs of the triangular Feynman diagram in that case correspond to three different Abelian gauge groups, say $U(1)_a, U(1)_b$ and $U(1)_c$. Since open strings only have two ends, chiral fields in the framework of intersecting branes are only charged under two different $U(1)$'s. The anomaly in that case is given by [145]

$$\mathcal{A}^{abb}_{U(1)_a - U(1)_b^2} \sim \sum_R Q_a(R)\, Q_b^2(R) \dim(R) \ . \tag{4.46}$$

For the case $a \neq b$ we find analogously to the previous discussed anomaly that

$$\mathcal{A}^{abb}_{U(1)_a - U(1)_b^2} \sim N_a N_b\, \Pi_a \circ \left(\Pi_b + \Pi'_b\right) \ . \tag{4.47}$$

If on the other hand $a = b$, Eq. (4.46) yields

$$\mathcal{A}^{aaa}_{U(1)_a^3} \sim \frac{1}{3} \cdot 3\, N_a^2\, \Pi_a \circ \Pi'_a \ . \tag{4.48}$$

For this case an additional factor of $\frac{1}{3}$ occurs due to the extra symmetry of the triangular diagram [54, 145]. Over and above that, a potential anomaly occurs here again.

4.4.4 Mixed Abelian – Gravitational Anomaly

So far we have dealt with gauge symmetries and their anomaly computation. However, if we consider our effective field theory on a curved spacetime, we must also include mixed gauge–gravitational anomalies. The relevant case we consider is the one in which two gravitons couple with one $U(1)$.

The anomaly in this case is given by [145]

$$\mathcal{A}^{agg}_{U(1)_a - G^2} \sim \sum_R Q_a(R) \dim(R) \ . \tag{4.49}$$

Summing up all states and using Tab. 4.2 and Tab. 4.1 the above expression finally results in

$$\begin{aligned}\mathcal{A}^{agg}_{\mathrm{U(1)}_a - G^2} \sim N_a \left(\sum_b N_b\, \Pi_a \circ \Pi_b + \sum_{b \neq a} N_b\, \Pi_a \circ \Pi'_b \right) + \frac{N_a(N_a - 1)}{2} \left(\Pi_a \circ \Pi'_a + \Pi_{O6} \circ \Pi_a\right) \\ + \frac{N_a(N_a + 1)}{2} \left(\Pi_a \circ \Pi'_a - \Pi_{O6} \circ \Pi_a\right) \overset{\text{T.C.}}{=} 3\, N_a\, \Pi_a \circ \Pi_{O6} \ .\end{aligned} \tag{4.50}$$

Along these lines, we have seen that all anomalies - except for the non-Abelian anomaly, which vanishes identically by imposing the tadpole condition - are a potential danger for our theory. However, these anomalies are only apparent anomalies, and we will in the following see how to deal with them in order to obtain an anomaly free theory. For overview, all found anomalies are summarised in Tab. 4.3.

4.5 The Generalised Green–Schwarz Mechanism

While satisfying the homological condition of the tadpole cancellation was sufficient to cancel non-Abelian anomalies, this is no longer the case for mixed Abelian–non-Abelian, Abelian and mixed Abelian–gravitational anomalies. Tadpole conditions only *partially* contribute to getting rid of the lurking dangerous anomalies. Therefore, one could think here that we are dealing with an anomalous theory and indeed, our effective field theory is anomalous in four-dimensions, but the full theory makes all anomalies disappear because it adds further contributions from the Wess-Zumino action, which we expanded in Eq. (4.13).

So let us take a step back and think again how the effective field theory was built. In Eq. (4.15), we only used the leading order term, which was sufficient to derive the tadpole cancellation. However, higher order terms in the expansion of the Wess-Zumino action provide us with further contributions which represent *counterterms* at tree-level. This is not an isolated or unique feature for compactified type IIA string theories, but rather a general feature of string theory and also plays a role for non-compact spaces, such as the cancellation of gravitational anomalies in ten-dimensional effective theories arising from type I and heterotic string theories. This mechanism ensuring the cancellation of anomalies goes under the name of *generalised Green-Schwarz mechanism* [15, 145, 147–149], which we have seen represents a milestone in the first superstring revolution in 1984. In the next sections we want to understand this mechanism better and show explicitly how it can be used to resolve the found anomalies.

In order to reduce the effective theory action to a four-dimensional action we first expand the 3-cycle $[\Pi_a]$ and the mirror image 3-cycle $[\Pi'_a]$ into the basis $([\alpha],[\beta])$ of 3-cycles[8] [138, 150–153].

$$[\Pi_a^3] = \sum_I^{h_{2,1}+1} \Big(\nu_a^I\,[\alpha_I] + \mu_a^I\,[\beta_I]\Big)\,, \quad [\Pi_a^{3\prime}] = \sum_I^{h_{2,1}+1} \Big(\nu_a^{I\prime}\,[\alpha_I] + \mu_a^{I\prime}\,[\beta_I]\Big)\ . \tag{4.51}$$

It should be emphasised that we do not factorise the 3-cycle and decompose it in 1-cycles and their basis but make the following analysis more general [9]. Since this mechanism is *not* coupled to the choice of the topological space of the internal compact dimensions, we will again generally denote it by $\mathcal{X}_6$. This has the consequence that our orientifold projection remains just as general without a concrete transformation description. The wrapping numbers (ν,μ) and their image wrapping numbers (ν',μ') which were not independent in the toroidal case are now independent in general [54].

The RR forms C_3 and C_5 of Eq. (4.13) are related by $dC_5 \sim \star dC_3$ [54]. Further, we can define a four-dimensional scalar Φ_I (resp. the dual $\widetilde{\Phi}_I$) – or axion as it is referred to in literature – and a four-dimensional 2-form B_I^2 (resp. $\widetilde{B}_i$) according to [54, 63, 138, 150–153]

$$\Phi_I \equiv \ell_s^{-3}\int_{[\alpha_I]} C_3, \quad \text{and} \quad B_I^2 \equiv \ell_s^{-5}\int_{[\beta_I]} C_5\ . \tag{4.52}$$

Analogously, this can be done with their dual forms.

4.5.1 The Axion Action

In the following we consider the Wess-Zumino action for D6-branes, which we derived in section 4.2. In our expansions we will also look at the higher terms and redefine them according to [151]

$$\mathcal{S}_{\mathrm{WZ}}[C_6] = T_6\int_{\mathcal{W}_7} N_a\,C_7 + \mathcal{S}_{BF}^{D6_a} + \mathcal{S}_{ax}^{D6_a} + \ldots \tag{4.53}$$

Redefining the last term in the second line of Eq. (4.13) as $\mathcal{S}_{ax}^{D6_a}$ yields

$$\begin{aligned}\mathcal{S}_{ax}^{D6_a} \equiv{}& \frac{4\pi^3\alpha'^2}{\ell_s^5}\sum_a\int_{\mathbb{R}^{3,1}\times\Pi_a} C_3\wedge\left[\mathrm{tr}\,F^a\wedge F^a + \frac{N_a}{48}\left(\mathrm{tr}\,\mathcal{R}_T\wedge\mathcal{R}_T - \mathrm{tr}\,\mathcal{R}_N\wedge\mathcal{R}_N\right)\right]\\ &+\frac{4\pi^3\alpha'^2}{\ell_s^5}\sum_a\int_{\mathbb{R}^{3,1}\times\Pi'_a} C_3\wedge\left[\mathrm{tr}\,F^a\wedge F^a + \frac{N_a}{48}\left(\mathrm{tr}\,\mathcal{R}_T\wedge\mathcal{R}_T - \mathrm{tr}\,\mathcal{R}_N\wedge\mathcal{R}_N\right)\right]\ .\end{aligned} \tag{4.54}$$

[8]Since we want to keep this discussion as general as possible for any CY_3, the index I is different than in the previous section where i indexed the 2-tori.The index I runs from 1 to $h_{2,1}+1$, where $h_{2,1}$ is a specific *Hodge number* resulting from the *Hodge diamond* of the CY_3. Since this is of no consequence, we will not go further into the clarification of these terms.

[9]To avoid confusion, we therefore use Greek letters here.

Further, by using the definition of Eq. (4.51), we obtain

$$\begin{aligned}\mathcal{S}^{D6_a}_{ax} &= \frac{4\pi^3\alpha'^2}{\ell_s^5}\sum_{I,a}\left(\nu_a^I+\nu_a^{I'}\right)\int_{\mathbb{R}^{3,1}\times[\alpha_I]} C_3\wedge\left[N_a f^a\wedge f^a+\mathrm{tr}_{N_a}\mathrm{F}^a\wedge\mathrm{F}^a+\frac{N_a}{48}\mathrm{tr}\,\mathcal{R}\wedge\mathcal{R}\right]\\ &+\frac{4\pi^3\alpha'^2}{\ell_s^5}\sum_{I,a}\left(\mu_a^I+\mu_a^{I'}\right)\int_{\mathbb{R}^{3,1}\times[\beta_I]} C_3\wedge\left[N_a f^a\wedge f^a+\mathrm{tr}_{N_a}\mathrm{F}^a\wedge\mathrm{F}^a+\frac{N_a}{48}\mathrm{tr}\,\mathcal{R}\wedge\mathcal{R}\right] .\end{aligned} \tag{4.55}$$

In the last step we made use of Eq. (D.2). Furthermore, we apply the relation, that $u(N)\sim u(1)\times su(N)$ at the level of the Lie algebra, which enables to split the four-dimensional field strength F into an abelian and a non-abelian part [145].

$$F = f\mathbb{1}+\sum_m \mathrm{F}^m T^m\ . \tag{4.56}$$

The T^m are the antisymmetric representation matrices of the gauge group in the fundamental representation, with the usual properties

$$\mathrm{tr}\left(T^A\right)=0,\quad \mathrm{tr}\left(T^AT^B\right)=\delta^{AB}. \tag{4.57}$$

This action can be finally reduced to a four-dimensional effective action by using Eq. (4.52).

$$\begin{aligned}{}^{4d}\mathcal{S}^{D6_a}_{ax} &= \frac{1}{4\pi}\sum_{I,a}\left(\nu_a^I+\nu_a^{I'}\right)\int_{\mathbb{R}^{3,1}}\Phi_I\left(N_af^a\wedge f^a+\mathrm{tr}_{N_a}\mathrm{F}^a\wedge\mathrm{F}^a+\frac{1}{48}N_a\,\mathrm{tr}\,R\wedge R\right)\\ &+\frac{1}{4\pi}\sum_{I,a}\left(\mu_a^I+\mu_a^{I'}\right)\int_{\mathbb{R}^{3,1}}\widetilde{\Phi}_I\left(N_af^a\wedge f^a+\mathrm{tr}_{N_a}\mathrm{F}^a\wedge\mathrm{F}^a+\frac{1}{48}N_a\,\mathrm{tr}\,R\wedge R\right)\end{aligned} \tag{4.58}$$

Or in a more compact way with the shortcut $A\wedge A\equiv A^2$

$${}^{4d}\mathcal{S}^{\mathrm{D6}_a}_{\mathrm{ax}} = \frac{1}{4\pi}\sum_{I,a}\int_{\mathbb{R}^{3,1}}\left(\Phi_I,\widetilde{\Phi}_I\right)\begin{pmatrix}\nu_a^I+\nu_a^{I'}\\ \mu_a^I+\mu_a^{I'}\end{pmatrix}\left(N_af^{a2}+\mathrm{tr}_{N_a}\mathrm{F}^{a2}+\frac{1}{48}N_a\,\mathrm{tr}\,R^2\right) \tag{4.59}$$

Finally, we must consider the contribution of the Wess-Zumino action coming from the orientifold plane. As we noted earlier, $O_p^{(\epsilon_1,\epsilon_2)}$ -planes also carry a charge, and have their own DBI and WZ action as we were able to find out in chapter 2. The Dirac-Born-Infeld action for the orientifold plane $O_p^{(\epsilon_1,\epsilon_2)}$ with $\epsilon_1,\epsilon_2\in\{+1,-1\}$ reads [40]

$$\mathcal{S}^{\mathrm{Op}^{(\epsilon_1,\epsilon_2)}}_{\mathrm{DBI}} = -\epsilon_1\,2^{p-4}\,T_p\int_{\mathcal{W}_{p+1}} d^{p+1}\xi\ e^{-\Phi}\sqrt{-\det\left(\gamma_{\alpha\beta}\right)}\ . \tag{4.60}$$

In the same way, a purely topological action for the $O_p^{(\epsilon_1,\epsilon_2)}$-plane can be found

$$S^{\mathrm{Op}^{(\epsilon_1,\epsilon_2)}}_{\mathrm{WZ}} = \epsilon_2\,2^{p-4}\,\mu_p\int_{\mathcal{W}_{p+1}}\sqrt{\frac{\mathfrak{L}\left(\pi^2\alpha'\mathcal{R}_T\right)}{\mathfrak{L}\left(\pi^2\alpha'\mathcal{R}_N\right)}}\wedge\bigoplus_q\varphi^*C_q\Big|_{p+1}\ . \tag{4.61}$$

With the definition of the Hirzebruch L-polynomial labelled $\mathfrak{L}$, which can be found in the appendix A, this equation can be brought into the following form

$$\mathcal{S}^{\mathrm{Op}}_{\mathrm{WZ}} = \epsilon_2\,2^{p-4}\,\mu_p\int_{\mathcal{W}_{p+1}} C_{p+1}-\frac{1}{192}\left(2\pi\alpha'\right)^2C_{p-3}\wedge\left(\mathrm{tr}\,\mathcal{R}_T\wedge\mathcal{R}_T-\mathrm{tr}\,\mathcal{R}_N\wedge\mathcal{R}_N\right)+\ldots) \tag{4.62}$$

The homology cycle $[\Pi_{O6}]$ of the orientifold plane on $\mathbb{T}^6$ can be represented in terms of a homology class of 3-cycles $[\Pi_{O6}]=\sum_I(\nu^I_{O6}[\alpha_I]+\mu^I_{O6}[\beta_I])$. If we follow the exact same steps as in the previous cases, we arrive at

$${}^{4d}\mathcal{S}^{\mathrm{O6}}_{\mathrm{ax}} = \frac{1}{96\pi}\sum_I\int_{\mathbb{R}^{3,1}}\left(\Phi_I,\widetilde{\Phi}_I\right)\begin{pmatrix}\nu^I_{\mathrm{O6}}\\ \mu^I_{\mathrm{O6}}\end{pmatrix}\mathrm{tr}\,R\wedge R\ . \tag{4.63}$$

4.5.2 The BF Action

Next, we focus on the second term in the first line of Eq. (4.13). This term, which we will subsequently baptise as the BF-action reads

$$
\begin{aligned}
\mathcal{S}_{\mathrm{BF}}^{D6_a} &= \frac{4\pi^2\alpha'}{\ell_s^5}\int_{\mathbb{R}^{3,1}\times\Pi_a} C_5\wedge \mathrm{tr}F^a + \frac{4\pi^2\alpha'}{\ell_s^5}\int_{\mathbb{R}^{3,1}\times\Pi'_a} C_5\wedge \mathrm{tr}F^a \\
&= \frac{4\pi^2\alpha'}{\ell_s^5}\sum_{I,a} N_a\left(\nu_a^I-\nu_a^{I'}\right)\int_{\mathbb{R}^{3,1}\times[\alpha_I]} C_5\wedge f^a \\
&+ \frac{4\pi^2\alpha'}{\ell_s^5}\sum_{I,a} N_a\left(\mu_a^I-\mu_a^{I'}\right)\int_{\mathbb{R}^{3,1}\times[\beta_I]} C_5\wedge f^a \ .
\end{aligned}
\tag{4.64}
$$

Here again, we use the relations from Eq. (D.2) and Eq. (4.57). We also get an extra relative minus sign between the contribution of the Dp-brane and the image brane, since the $U(1)_a$ gauge field f^a changes sign under $\Omega_{\mathcal{P}}$ [150, 151]. Again, we find a four-dimensional effective action

$$
\begin{aligned}
{}^{4d}\mathcal{S}_{\mathrm{BF}}^{D6_a} &= 4\pi^2\alpha'\sum_{I,a} N_a\left(\left(\nu_a^I-\nu_a^{I'}\right)\int_{\mathbb{R}^{3,1}}\widetilde{B}_I^2\wedge f^a + \left(\mu_a^I-\mu_a^{I'}\right)\int_{\mathbb{R}^{3,1}} B_I^2\wedge f^a\right) \\
&= 4\pi^2\alpha'\sum_{I,a} N_a\int_{\mathbb{R}^{3,1}}\left(B_I^2,\tilde{B}_I^2\right)\begin{pmatrix}\mu_a^I-\mu_a^{I'}\\ \nu_a^I-\nu_a^{I'}\end{pmatrix}\wedge f^a \ .
\end{aligned}
\tag{4.65}
$$

4.5.3 Stückelberg Axions and Massive U(1)'s

Before we continue with the generalised Green Schwarz mechanism, we want to point out a special and remarkable consequence of the BF action and elaborate it with an illustrative and intuitive example. For this purpose, we consider the following Lagrangian [17, 63, 151, 152]

$$
\mathcal{L} = -\frac{1}{2}dB_2\wedge\star dB_2 - \frac{1}{4g^2}F_a\wedge\star F_a + \underbrace{mB_2\wedge F_a}_{\mathrm{BF-term}} \ , \tag{4.66}
$$

where the constants g and m are arbitrary. The $\star$ denotes the usual Hodge star operator, mapping p-forms to $(d-p)$-forms [63]. Further, we will use the convention $|F|^2 \equiv F\wedge\star F$.

This Lagrangian serves as our toy model to shed light on the so-called *Stückelberg mechanism*. Essentially, the Lagrangian consists of kinetic terms for the 2-form B_2 and the $U(1)_a$ gauge filed $F_a = dA_a$. The last term is central since it represents the coupling between these two fields. To *dualise* (for the dual of B_2) the Lagrangian in Eq. (4.66), we will introduce a Lagrangian multiplier. Thereby we will reformulate the Lagrangian in terms of an arbitrary 3-form H_3, which is treated independently from B_2. Furthermore, we enforce the condition that $dH_3 = 0$ (Bianchi identity), which is implemented by the introduction of the Lagrangian multiplier α. The dualised Lagrangian reads

$$
\mathcal{L}' = -\frac{1}{2}H_3\wedge\star H_3 - \frac{1}{4g^2}F_a\wedge\star F_a + mB_2\wedge F_a + \alpha\, dH_3 \ . \tag{4.67}
$$

If we integrate out the Lagrangian multiplier α, we obtain the condition $dH_3 = 0$ or *locally* $H_3 = dB_2$, respectively. This condition clearly yields back Eq. (4.66) which shows that $\mathcal{L}$ in Eq. (4.66) and $\mathcal{L}'$ in Eq. (4.67) are (locally) equivalent to each other. The trick now is to start with Eq. (4.67) and integrate the last two terms by parts. This gives, if we assume that the boundary terms vanish,

$$
\mathcal{L}' = -\frac{1}{2}H_3\wedge\star H_3 - \frac{1}{4g^2}F_a\wedge\star F_a - mH_3\wedge A + H_3\wedge d\alpha \ . \tag{4.68}
$$

Varying the corresponding action with respect to H_3 gives

$$0 = \delta_{H_3}\mathcal{S}' = \int_{\mathbb{R}^{3,2}} \delta H_3 \wedge [- \star H_3 - (mA - d\alpha)] \ , \tag{4.69}$$

which yields the following equation of motion for H_3

$$\star H_3 = -(mA - d\alpha) \ . \tag{4.70}$$

We can now substitute this result[10] into Eq. (4.67) and obtain the *Stückelberg* Lagrangian

$$\mathcal{L}' = -\frac{1}{4g^2} F \wedge *F - \frac{1}{2}\,(m\,A_a - da) \wedge *\,(m\,A_a - d\alpha) = -\frac{1}{4g^2}|F|^2 - \frac{1}{2}\,|m\,A_a - d\alpha|^2 \ . \tag{4.71}$$

It is a well known fact from QFT that due to gauge invariance terms of the form $m^2 A_\mu A^\mu$ are forbidden for $U(1)$ fields and therefore photons, for example, are consequently massless. Theoretically, the Stückelberg Lagrangian is a realisation of a $U(1)$ gauge field which has a mass term. The field α in Eq. (4.71), which is called Stückelberg-field, Stückelberg-ghost or axionic field, can be considered in some sense analogous to the Goldstone-fields which appear in spontaneous symmetry breaking [154].

While terms like $m^2 A_\mu A^\mu$ were not invariant under gauge transformations of the conventional form $A \to A_\mu + \partial_\mu \Lambda(x)$, the Stückelberg Lagrangian in Eq. (4.71) is obviously invariant under $A_a \to A_a + d\Lambda_a$ if we require that the axionic field α shifts according to

$$\alpha \to \alpha + m\Lambda \ . \tag{4.72}$$

The coupling of the four-dimensional RR 2-form B_I^2 and the field strength f^a corresponding to the $U(1)_a$ results in a mass term

$$\sum_I c_I^a \, B_I^2 \wedge f^a \ . \tag{4.73}$$

Typically, a $U(1)$ generator is given by a linear combination according to

$$Q = \sum_a \xi_a Q_a \ . \tag{4.74}$$

Since in the following it is in our interest that exactly one such generator remains massless, we require that

$$\sum_a c_I^a \xi_a = 0 \quad \forall I \ . \tag{4.75}$$

More concrete details will be discussed in chapter 5, where we will analyse such a $U(1)$ generator in much more detail for the case of a toroidal compactification with an orientifold projection.

4.5.4 The Anomaly Cancellation

In the previous section we have seen that the BF term and all $U(1)$ gauge fields A_μ coupling to $B \wedge F$ get massive after "eating" the axion $\alpha(x)$ via the Stückelberg mechanism. However, it should be emphasised, that it does not matter whether the $U(1)$'s are anomalous or not [63].

Recapitulating, the BF term in Eq. (4.65) was proportional to

$$\sum_{I,a} N_a(\mu_a^I - \mu_a^{I\prime})\, B_I^2 \wedge f^a \quad \text{and} \quad \sum_{I,a} N_a(\nu_a^I - \nu_a^{I\prime})\, \widetilde{B}_I^2 \wedge f^a \tag{4.76}$$

[10] Note, that H_3 is a form in four dimensional spacetime. Thus, $\star\star H_3 = H_3$.

	$SU(N_a)^3$	$U(1)_a - SU(N_b)^2$	$U(1)_a - U(1)_b^2$	$U(1)_a - G^2$
$\mathcal{A} \sim$	0	$\frac{N_a}{2}\Pi_a \circ (\Pi_b + \Pi_b')$	$N_a N_b \Pi_a \circ (\Pi_b + \Pi_b')$	$3\, N_a\, \Pi_a \circ \Pi_{O6}$

Table 4.3: All collected anomalies calculated from the triangular diagrams. We considered all possible constellations and exploit the tadpole condition for the cubic non-Abelian anomaly, the mixed Abelian – Non-Abelian anomaly, the cubic Abelian anomaly and the mixed Abelian – Gravitational anomaly.

The anomalies, which we encountered in this section, are due to the anomalous $U(1)_a$ with associated f^a. By the duality we schematically conclude that the BF term in our case is given by[11]

$$S_{\rm BF} \sim \sum_{I,a} N_a \left(\mu_a^I - \mu_{a'}^I\right) \int_{4d} B_I^2 \wedge f^a \to -\frac{1}{2} \sum_{I,a} \int_{4d} d^4x \left(N_a \left(\mu_a^I - \mu_{a'}^I\right) A_a - d\Phi_I\right)^2 \tag{4.77}$$

As we have elaborated, such a BF term is gauge invariant under $U(1)_a$ if the axion Φ shifts. If we compare this term to the one in Eq. (4.66), we can determine the gauge transformation for the axionic field, which was deduced in Eq. (4.72). This yields for the axion [17, 54, 151, 152]

$$\begin{aligned} \Phi_I(x) &\to \Phi_I(x) + N_a(\mu_a^I - \mu_a^{I\prime})\Lambda_a(x) \equiv \Phi(x) + c_a^I\, \Lambda_a(x) \\ \widetilde{\Phi}_I(x) &\to \widetilde{\Phi}_I(x) - N_a(\nu_a^I - \nu_a^{I\prime})\, \Lambda_a(x) \equiv \tilde{\Phi}(x) - \tilde{c}_a^I \Lambda_a(x) \end{aligned} \tag{4.78}$$

While the BF action in Eq. (4.65) is invariant under the gauge transformation of $U(1)_a$, the action regarding the $F \wedge F$ and $R \wedge R$ terms in Eq. (4.59) and Eq. (4.63) are not. Here, a non-invariance arises at tree-level which can be determined if we transform Eq. (4.59) and Eq. (4.63) according to Eq. (4.78). Specifically, we find that

$$\begin{aligned} \delta_{\Lambda_a}\left(\mathcal{S}_{\rm ax}^{\rm D6} + \mathcal{S}_{\rm ax}^{\rm O6}\right)\Big|_{\rm tree} = \frac{1}{4\pi} \int_{\mathbb{R}^{3,1}} \Bigg\{ &\sum_{I,b} \Lambda_a \left(c_a^I, -\tilde{c}_a^I\right) \begin{pmatrix} \nu_b^I + \nu_b^{I\prime} \\ \mu_b^I + \mu_b^{I\prime} \end{pmatrix} N_b\, f^b \wedge f^b \\ &+ \sum_{I,b} \Lambda_a \left(c_a^I, -\tilde{c}_a^I\right) \begin{pmatrix} \nu_b^I + \nu_b^{I\prime} \\ \mu_b^I + \mu_b^{I\prime} \end{pmatrix} {\rm tr}_{N_b}\, F^b \wedge F^b \\ &+ \sum_{I,b} \Lambda_a \left(c_a^I, -\tilde{c}_a^I\right) \begin{pmatrix} \nu_b^I + \nu_b^{I\prime} \\ \mu_b^I + \mu_b^{I\prime} \end{pmatrix} \frac{1}{48} N_b\, {\rm tr}\, R \wedge R \\ &+ \sum_{I} \Lambda_a \left(c_a^I, -\tilde{c}_a^I\right) \begin{pmatrix} \nu_{\rm O6}^I \\ \mu_{\rm O6}^I \end{pmatrix} \frac{1}{24}\, {\rm tr}\, R \wedge R \Bigg\} \end{aligned} \tag{4.79}$$

By inserting the definition of c_a^I and $\tilde{c}_a^I$ this can be brought into the form

$$\begin{aligned} \delta_{\Lambda_a}\left(\mathcal{S}_{\rm ax}^{\rm D6} + \mathcal{S}_{\rm ax}^{\rm O6}\right)\Big|_{\rm tree} = -\frac{1}{2\pi} \int_{\mathbb{R}^{1,3}} \Lambda_a \Big\{ &N_a \Pi_a \circ (\Pi_b + \Pi_b')\ {\rm tr}_{N_b}\, F^b \wedge F^b \\ &+ N_a N_b \Pi_a \circ (\Pi_b + \Pi_b')\ f^b \wedge f^b + 3 N_a \Pi_a \circ \Pi_{\rm O6}\, \frac{1}{24}\, {\rm tr}\, R \wedge R \Big\}\ . \end{aligned} \tag{4.80}$$

Have we lost now? The BF term just gave us a powerful insight on how to get $U(1)_a$'s massive, which constitutes a mechanism to decouple potential extra $U(1)_a$'s in a product of gauge groups. Especially in the standard model, we will see that this is absolutely necessary to rid of the $U(1)_a$'s in $SU(3)_C \times SU(2)_L \times U(1)_Y \times \sum_a U(1)_a$ at low energies. But all at the costly price of those extra terms in Eq. (4.80). But this is where something almost "magically" happens.

[11] By duality we have schematically $B_I^2 \sim -\Phi_I$ and $\widetilde{B}_I^2 \sim \widetilde{\Phi}_I$ [17, 54, 151, 152].

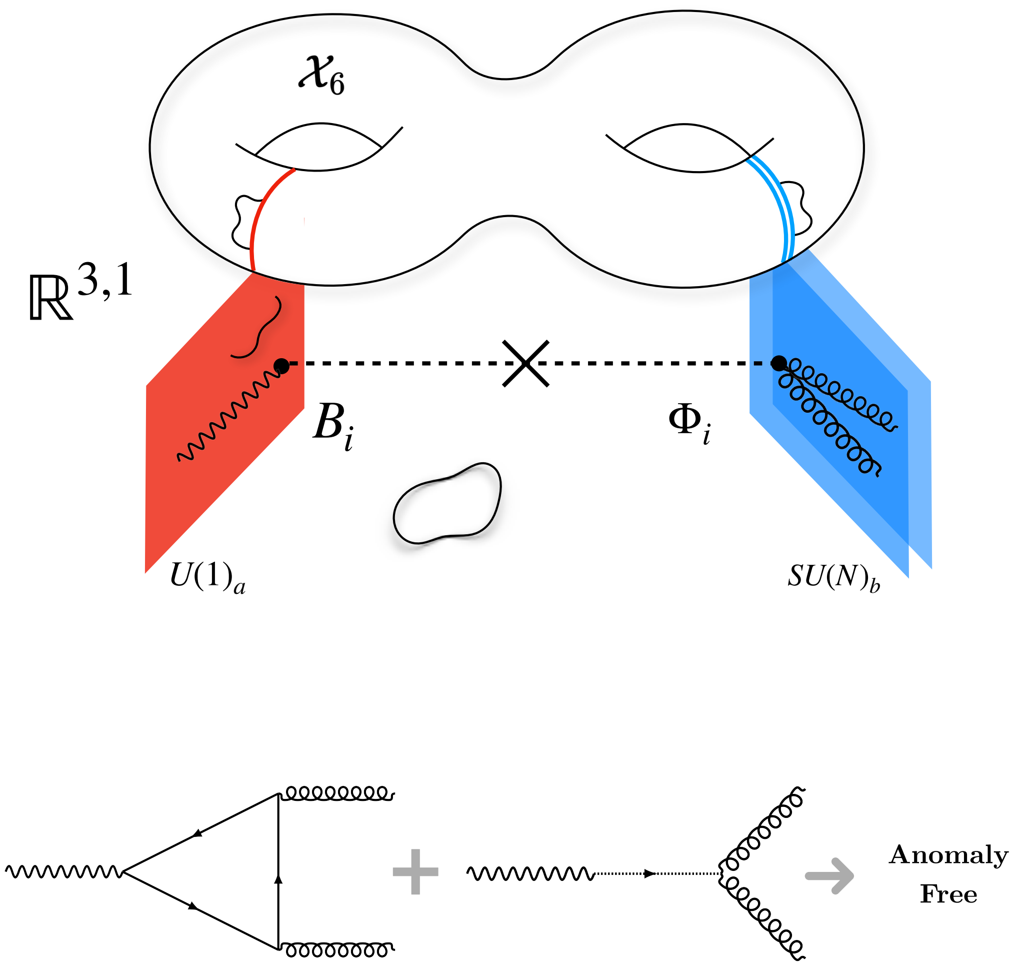

Figure 4.11: While the BF term is gauge invariant due to the axionic shift, the remaining terms are not. If we perform the axiomatic shift in these terms, we see that we get an invariant part and additional terms which destroy the general gauge invariance. These non-invariant terms can lift away exactly those contributions which correspond to the anomalies in the effective theory. These anomalies can be symbolised as one-loop diagrams, while the non-invariant terms are tree-level diagrams that act as counter terms. This is the generalised Green-Schwarz mechanism.

After all, these terms in Eq. (4.80) are exactly the terms that are needed to eliminate the remaining anomalies which we deduced in section 4.4. The critical reader can convince himself by comparing these terms in Eq. (4.80) with those in Tab. 4.3 and agree that they exactly cancel each other out. In terms of Feynman diagrams, these terms represent counter terms which are diagrammatically depicted as tree-level diagrams and are illustrated in Fig. 4.11. In this respect, they are tree-level contributions which correct the loops of quantum anomalies.

In the end it should be said that it seems very unintuitive at first sight that a tree-level diagram cancels a one-loop diagram, compared to the typical counter term cancellation mechanism known from QFT. This unconventional and unreasonable perspective is based and solved if one remembers that this is still an effective four-dimensional field theory, but both diagrams in Fig. 4.11 are due to one-loop diagrams in superstring theory.

Part II

Semi-Realistic SM and Phenomenology

Chapter 5

Towards Semi-Realistic Models of the Standard Model

In this chapter, we will use the framework studied so far to construct semi-realistic standard models with intersecting Dp-branes. We will show in all detail how we can use these intersecting Dp-branes to obtain the chiral spectrum of the standard model with the three generations and the corresponding gauge bosons.

We will start by showing thoroughly how three coincident stacks of Dp-branes introduce nine $U(3)$ gauge fields, one of which decouples and provides the theory with an octet of eight gauge bosons obeying $SU(3)_C$.

Step by step, we will finally construct a minimal standard model, by just using typ IIA string theory, a compact factorizable 6-torus and several intersecting Dp-branes, which, however, gives us exotic chiral additional fermions.

To overcome this problem, we will use the already introduced concept of orientifold projections to construct a non-supersymetric minimal standard model which produces the desired spectrum of the standard model. Furthermore, we will see how the RR 2-forms – created by the generalised Green-Schwarz mechanism – couple to the individual $U(1)$ gauge bosons and endow them with a Stückelberg mass. These $U(1)$'s will disappear from the low-energy limit but remain as global symmetry in the theory. This will be accompanied by two concrete numerical examples.

The standard model of particle physics is mathematically speaking composed by a quantum field theory in four dimensions based on internal gauge symmetry groups. These groups are characterised by the unitary group product

$$\mathcal{G}_{\mathrm{SM}} = SU(3)_C \times G_{\mathrm{GWS}} = SU(3)_C \times SU(2)_L \times U(1)_Y \ . \tag{5.1}$$

The product and the indexing is to be intended in a way that this group acts on different particles in different ways. The standard model is a chiral theory and left-handed and right-handed fermions are in different representations and transform differently under the gauge groups. The group $SU(3)_C$ describes the sector of the strong interaction, which obeys the quantum chromodynamic. The associated fundamental elementary particles are the colour-charged quarks and the gluons which transmit the strong interaction. The electroweak interaction is expressed by the *Glashow-Weinberg-Salam theory* (GWS) and its based on the group $G_{\mathrm{GWS}} = SU(2)_L \times U(1)_Y$, which unifies the weak- and electromagnetic interaction. The chiral $SU(2)_L$ and the hypercharge $U(1)_Y$ describe the gauge bosons $W^{\pm}, W^0$ and B. By *spontaneous symmetry breaking* (SSB) (simply referred as Higgs mechanism) the group is broken down to $U(1)_{em}$ of the electromagnetic interaction. The $SU(3)_C$ and $SU(2)_L$ constitute non-Abelian gauge groups with non-commuting generators. Such theories are also called *Yang-Mills theories* [143, 155–157].

5.1 The Strong Interaction and the Baryonic Brane

Before diving into the world of branes, we would like to point out an inconspicuous but important fact. In quantum chromodynamics the exchange particles of the strong interaction are called gluons g. The representative charge of QCD, in contrast to the electromagnetic interactions, can occur in three different types. Historically, these charge units are called colour charges. A quark particle can thus carry the charge red, green and blue (rgb) or their complementary colours (cym or $\overline{\mathrm{r}}\overline{\mathrm{g}}\overline{\mathrm{b}}$) cyan (anti-red), yellow (anti-green) and magenta (anti-blue). Additionally, the gluons are bi-coloured. The intuitive logic behind this is that a quark can emit a gluon which changes the colour of the quark. This gluon in turn can be absorbed by another quark which leads to another colour change. Before we go on, it is essential to note that quarks are never isolated [141, 143, 158], which goes under the name of *colour confinement*. They can only be found in hadrons, where the colour charges of the quarks must neutralise to the net colour "white". This can be realised by the presence of three quarks with different colour or anti-colour charges. Furthermore, two quarks with complementary colour charge can also form a "white" state. In the former case one speaks of baryons, in the latter one of mesons [159, 160]. The six naive options are therefore:

- A red quark emits a red-antiblue (red-antigreen) gluon, whereby the original red quark turns blue (green) and the blue (green) quark absorbs the gluon which turns it red.
- A blue quark emits a blue-antired (blue-antigreen) gluon, where the original blue quark turns red (green) and the (green) quark turns blue.
- A green quark rmmits a green-antired (green-antiblue) gluon, where the original green quark turns red (blue) and the red (blue) quark turns green.

Now, we could get the wrong idea that these six configurations represent all realistic possibilities and that there must therefore exist six distinct gluons. But this turns out to be wrong and these six combinations are only six of nine combinations of colour and anti-colour. So, what happens to the combinations of gluons like the red-antired, blue-antiblue, green-antigreen gluon? For example, a red quark could emit a red-antired gluon and keep its colour, but no other gluon could absorb it. Here begins a misuse of terminology. The everyday terms like "colour" and the similarity to colour theory is only thought as an analogy to the intuitive comprehensibility of the matter. But it makes no claim to physical reality or a clear correspondence. Mathematically, more rigorously we therefore introduce a colour space. In this space, the colours are basis states and can be understood as coordinate axes in a three-dimensional space. The term "white" or "colour-neutral" can now be translated as those states which are invariant under rotations in this colour space. More precisely, colour-neutral states are singlets under a transformation of the symmetry group $SU(3)_C$. We have seen that we cannot have states with colour-anticolour units, but we can form linear combinations as usual and basically necessary in quantum mechanics [161]. Therefore, we are allowed form the following state

$$g_9 = \frac{1}{\sqrt{3}}\left(|r\bar{r}\rangle + |g\bar{g}\rangle + \left|b\bar{b}\right\rangle\right) \; . \tag{5.2}$$

To this state two linear independent orthogonal states can be formed. They are given by

$$g_7 = \frac{1}{\sqrt{2}}\Big(\,|r\bar{r}\rangle - |g\bar{g}\rangle\Big) \quad \text{and} \quad g_8 = \frac{1}{\sqrt{6}}\Big(\,|r\bar{r}\rangle + |g\bar{g}\rangle - 2\left|b\bar{b}\right\rangle\Big) \; . \tag{5.3}$$

Of all linear combinations of the gluons with all nine colour charges, the one in Eq. (5.2) is the only one that is colour-neutral, which is to be understood in the mathematical sense. For that

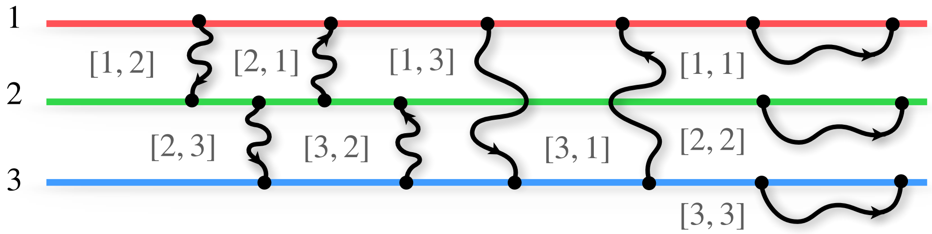

Figure 5.1: The nine open string sectors at a barionic Dp-brane. The open strings are oriented, and their orientation is reflected in the associated Chan-Paton labels. The baryonic brane consists of three coincident Dp-branes, which are illustrated separately for clarity. Strings from the sector $[1,3]$ and sector $[3,1]$ do not pass through the brane between them.

reason, Eq. (5.2) forms a singlet under $SU(3)_C$. The six real coloured gluons together with the linear combinations in Eq. (5.3) constitute a so-called octet [161]

$$\begin{aligned} g_1 &= |r\bar{g}\rangle, \quad g_3 = |r\bar{b}\rangle, \quad g_5 = |b\bar{r}\rangle, \quad g_7 = \tfrac{1}{\sqrt{2}}(|r\bar{r}\rangle - |g\bar{g}\rangle), \\ g_2 &= |g\bar{r}\rangle, \quad g_4 = |b\bar{g}\rangle, \quad g_6 = |g\bar{b}\rangle, \quad g_8 = \tfrac{1}{\sqrt{6}}(|r\bar{r}\rangle + |g\bar{g}\rangle - 2|b\bar{b}\rangle). \end{aligned} \tag{5.4}$$

Of course, this represents a very heuristic argument but it is perfectly founded within the framework of group theory [162–164]. The symmetry group of QCD is $SU(N=3)_C$, which has $N^2 - 1 = 8$ generators (e.g. the *Gell-Mann matrices*). As a side note, there were attempts and efforts in the past to assign a physical reality to this photon-like particle which is transformed here as a colour-neutral singlet [165]. However, in this work we stick to Occam's razor: a hypothetical particle that does not interact with anything – and in the following can not be detected – does not exist [166]. We can now apply this observation to our D-brane scenario.

In chapter 2 we have elaborated that N coincident Dp-branes introduce $U(N)$ gauge fields. These $U(N)$ gauge fields and the corresponding gauge bosons are determined in the low energy regime by a Yang-Mills theory. This relationship between D-brane configurations, the emergence of $U(N)$ gauge bosons, and the gauge groups of the standard model must now be considered more in-depth. To shed more light on this interplay between the standard model of particle physics and the theoretical foundation of the last chapters, a stack of three coincident Dp-branes is introduced. From now on we will call this stack *baryonic brane*. The resulting Chan-Paton indices are denoted by $[rs]$ with $r, s = 1, 2, 3$. As already carefully revealed, a $U(3)$ Yang-Mills theory at low energy arises on the world-volume of these Dp-branes. Exhausting all possibilities how an open string can be stretched in such a configuration, we find that there are nine open string sectors, which are illustrated in Fig. 5.1. Each string state possesses a charge which it carries with respect to the Maxwell fields. In this thesis we use the convention that oriented open strings pick up a positive unit charge at $\sigma = 0$ and in contrast enjoy a negative unit charge at $\sigma = \pi$. For instance, an open string in sector $[13]$ carries the charge $(q_1, q_2, q_3) = (1, 0, -1)$. The charge q_2 is of course zero, since the string neither starts nor ends there. This observation leads to the conclusion that the sum of the individual charges for string sectors that contain two different branes must always be zero. Opposed to that all three partial charges are zero for strings that both initiate and terminate on a single brane, which are of course the strings which start and end on the same brane. Focusing exclusively on the NS sector for simplicity, we can conclude from Eq. (2.32) that the linear combination

$$\sum_{r=1}^{3}\sum_{s=1}^{3}\left(\sum_{i=1}^{p-1}\boldsymbol{A}_i^{rs}\psi^i_{-\frac{1}{2}}\right)|0;\boldsymbol{p};r,s\rangle_{\mathrm{NS}}\ , \tag{5.5}$$

yields 3^2 gauge fields in four dimensions via compactification. Considering the sector that restricts the states living on the same brane, i.e., those states where the Chan-Paton indices are identical to each other and omitting irrelevant momenta and spacetime indices, we conclude with

$$\sum_{r=1}^{3}\boldsymbol{A}^r\psi_{-\frac{1}{2}}\ |0;r,r\rangle_{\mathrm{NS}}\ . \tag{5.6}$$

We already explored in the previous argument that such nine states can be decomposed into a singlet **1** and an octet **8**. Explicitly, this can be seen if we form a linear combination through an orthogonal transformation $\mathrm{T}\in\mathrm{O}(3,\mathbb{R})$, which we insert in the state in Eq. (5.6) via the identity [45]. We obtain

$$\sum_{r,m,n=1}^{3}\overbrace{\boldsymbol{A}^m(\mathrm{T}^t)_{mr}}^{\equiv\widetilde{\boldsymbol{A}}_r}\ \underbrace{\mathrm{T}^{rn}\ \ \psi_{-\frac{1}{2}}|n,n\rangle}_{\equiv|L_r\rangle},\quad\text{with}\quad s=1,2,3. \tag{5.7}$$

From the second part of Eq. (5.7) we find

$$|L_s\rangle=\sum_{r=1}^{3}T^{sr}\ \psi_{-\frac{1}{2}}|r,r\rangle,\quad\text{with}\quad s=1,2,3. \tag{5.8}$$

Moreover by choosing $s=3$ we get explicitly [1] [2]

$$|L_3\rangle=\frac{1}{\sqrt{3}}\left(\psi_{-\frac{1}{2}}|11\rangle+\psi_{-\frac{1}{2}}|22\rangle+\psi_{-\frac{1}{2}}|33\rangle\right),\quad\text{with}\quad\widetilde{q}_3=\frac{1}{\sqrt{3}}\left(q_1+q_2+q_3\right). \tag{5.10}$$

In further consequence, we are able to find the two orthogonal linearly independent states, which join $|L_3\rangle$. Using the explicit form of the matrix T, we find

$$\begin{aligned}|L_1\rangle&=\frac{1}{\sqrt{6}}\Big(\psi_{-\frac{1}{2}}\,|11\rangle+\psi_{-\frac{1}{2}}\,|22\rangle-2\psi_{-\frac{1}{2}-1}\,|33\rangle\Big)\ ,\\|L_2\rangle&=\frac{1}{\sqrt{2}}\Big(-\psi_{-\frac{1}{2}}\,|11\rangle+\psi_{-\frac{1}{2}}\,|22\rangle\Big)\ .\end{aligned} \tag{5.11}$$

If we compare the results just found in Eq. (5.10) and Eq. (5.11) with those in Eq. (5.2) and Eq. (5.3), we can indeed identify these states with those of the gluons from the standard model. Furthermore, as we have observed, that the total charge $\widetilde{g}_3$ disappears when we add up the three individual charges. The nine gauge fields split into two disjoint sets. The first set contains this specific gauge field corresponding to $|L_3\rangle$, while the second set contains the remaining eight fields which interact with each other [45].

At first sight, this observation seems to be rather insignificant, but it has a great importance for the realisation of the standard model. Maxwell gauge fields are described by $U(1)$ theories.

[1] The explicit form of the orthogonal matrix $T\in\mathrm{O}(3,\mathbb{R})$ is given as

$$\mathrm{T}=\begin{pmatrix}\frac{1}{\sqrt{6}}&\frac{1}{\sqrt{6}}&-\frac{2}{\sqrt{6}}\\-\frac{1}{\sqrt{2}}&\frac{1}{\sqrt{2}}&0\\\frac{1}{\sqrt{3}}&\frac{1}{\sqrt{3}}&\frac{1}{\sqrt{3}}\end{pmatrix},\quad\mathrm{T}^t\,\mathrm{T}=\mathrm{T}\,\mathrm{T}^t=\begin{pmatrix}1&0&0\\0&1&0\\0&0&1\end{pmatrix}. \tag{5.9}$$

[2] The $\widetilde{\boldsymbol{A}}_3$ is of course simply given by $\widetilde{\boldsymbol{A}}_3=\frac{1}{\sqrt{3}}\sum_m^3\boldsymbol{A}_m$.

We started with a stack of three coincident Dp-branes whose nine gauge fields are based on a $U(3)$ Yang-Mills theory. By decoupling one of the gauge fields, we obtain two groups where the decoupled field obeys a $U(1)$ theory and the eight remaining interacting fields define a $SU(3)$. This leads to the decomposition[3]

$$U(3) \simeq SU(3) \times U(1) \ . \tag{5.12}$$

The perceptive reader will have already recognised the identification of this configuration with the corresponding gauge group of the standard model. This must now be established decisively.

Let us summarise and establish the connection to the previous Dp-brane configuration. The simple model with a stack of three coincident Dp-branes allows, through the composition $U(3) \simeq SU(3) \times U(1)$ to describe the eight gluons, which represent the transmitters of the strong colour interaction. This was explicitly shown here for the strong interaction section of the standard model. However, this peculiarity of the decomposition is more general. With the help of [45, 63]

$$U(N) \simeq SU(N) \times U(1) \ , \tag{5.13}$$

it is possible to model a minimal semi-realistic standard model. Despite this advantage, however, this very composition will lead to difficulties which have to be addressed and clarified in the following.

5.2 Chiral Matter Content

Before we move on to the construction of a minimal semi-realistic standard model and confront ourselves with its problems, we want to address the matter content by constructing Dp-branes and extending the previous model to clarify the fermionic part of the standard model. Using the baryonic brane, we could identify and relate the resulting gauge bosons with the gluons of the strong interaction. In the standard model, however, there are further elementary particles which are charged under the colour charge and thus have to be affiliated to the baryonic brane in some way. These particles are the quarks.

5.2.1 The Quark Sector

Unlike gluons, quarks carry only one colour charge, they have to be described by oriented open strings which are linked with one end on one of the Dp-branes in the baryonic stack. This means that we get a total of two triplets. One triplet, which combines those states that describe oriented open strings that reach a (r, g, b) brane and a second triplet describing states that are associated with strings leaving a (r, g, b) brane. The (r, g, b) are used here as a labels which can stand for red, green or blue. Furthermore, group theory tells us, that there is a irreducible decomposition given by $8 \oplus 1 = 3 \otimes \bar{3}$, which in words simply says, that the direct product of the colour triplet with the anticolour triplet gives a direct sum consisting of an octet and a singlet [45, 143, 162, 167]. We therefore conclude and choose the convention in such a way that [4]

- a string, which starts from a (r, g, b) brane corresponds to a left-handed (r, g, b) quark $q_{L,\,(r,g,b)}$. These quarks transform under the fundamental representation $\mathbf{3}$ of $SU(3)_C$.
- a string, which ends on a (r, g, b) brane corresponds to a left-handed $(\bar{r}, \bar{g}, \bar{b})$ anti-quark $\overline{q}_{L,\,(\bar{r},\bar{g},\bar{b})}$. These anti-quarks transform under the anti-fundamental representation $\overline{\mathbf{3}}$ of $SU(3)_C$.

[3]Mathematically speaking, we would have to choose a semidirect product here and write it down as $U(3) \simeq SU(3) \rtimes U(1)$. Since this never occurs in literature, however, we want to remain with this small imprecision in order not to lead to any confusion.

[4]In some publications, e.g. [45], the opposite notation is used.

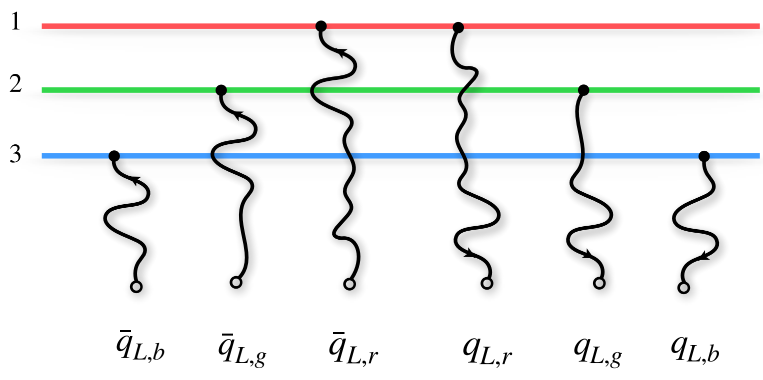

Figure 5.2: According to our convention, left-handed quarks are associated with strings starting from the baryonic brane. They receive a positive unit charge from colour branes. Left-handed antiparticles behave the exact opposite way. They get a negative unit charge by ending on the baryonic brane.

All possibilities that result from this construction are shown in Fig. 5.2. The exact meaning of left-handed in this context will be understood in a moment.

Having clarified the origin of the colour charge of the quarks, the immediate question arises on which D-brane the other end of such a string is located. Quarks do not only obey the strong interaction but are also susceptible to the weak interaction and the associated *quantum flavourdynamic* (QFD) or in the further course by the *electroweak interaction* - after spontaneous symmetry breaking [141, 156].

A crucial point is that the chirality of the standard model comes now into play, since only the left-handed elementary particles transform under this symmetry. The right-handed counterpart is invariant under these transformations and must therefore be represented as singlets under this symmetry group. The symmetry group of the weak interaction is given by the $SU(2)_L$ group whose characteristic charge is the weak isospin I, which can have two possible configurations $I_3 = \pm 1/2$ [45, 63]. In the framework of D-branes we have to ensure, that a left-handed quark is an element charged under both $SU(3)_C$ and $SU(2)_L$. Symbolically, we note, that a left-handed quark is a

$$\underbrace{\text{left-handed}}_{\text{Chirality}} \underbrace{\left\{ \begin{array}{c} \text{(anti)-red} \\ \text{(anti)-green} \\ \text{(anti)-blue} \end{array} \right\}}_{SU(3)_C} \underbrace{\left\{ \begin{array}{c} \text{up} \\ \text{down} \end{array} \right\}}_{SU(2)_L} \text{(anti)-quark} \; . \tag{5.14}$$

To represent a non-abelian $SU(2)_L$, we need therefore a new stack of D-branes with two coincident branes. This can be justified by the fact that we need two new charges which distinguish between an up quark and a down quark. This is realised by two coincident D-branes. These in turn provide a $U(2) \simeq SU(2) \times U(1)$. This D-brane is of course intended to intersect with the baryonic brane, since the strings that provide chiral matter content live close to these intersections as we have explored in chapter 3. We will generically call this new stack the *left* or *weak brane*. Following the convention, a quark

- starting at a (r, g, b) brane and ending on the $I_3 = -1/2$ brane is called a left-handed (r, g, b) up-quark u_L.

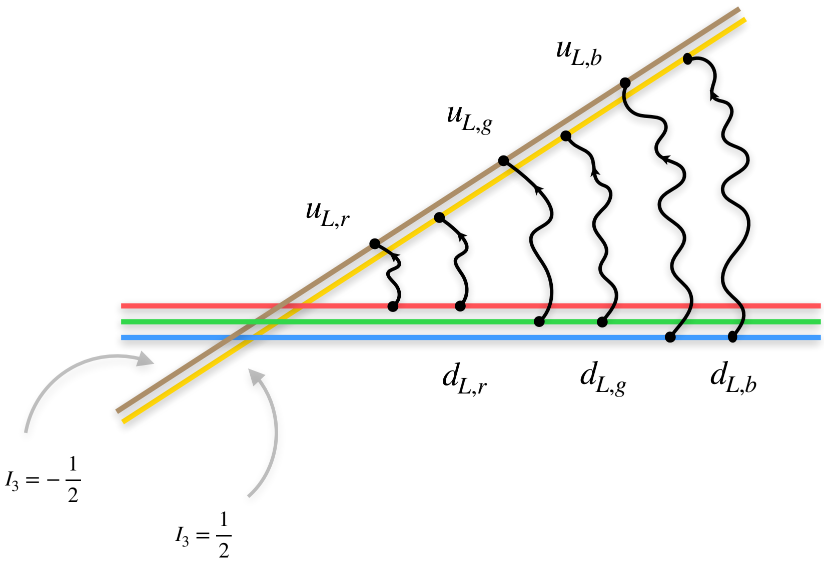

Figure 5.3: Near the intersection of the two stacks of baryonic Dp-branes and left Dp-branes strings are stretched. These open strings transform in the bi-fundamental representation $(N_B, \bar{N}_L)$ of the gauge group $U(N_B) \times U(N_L)$. Roughly speaking, the baryonic Dp-branes supply these strings with their colour charge, while the left Dp-branes provide the weak isospin charge and, again roughly speaking, decide if it is an up or down quark. If the orientation of the strings runs from the baryonic brane to the left brane – as shown in this picture – we get left-handed quarks.

- starting at a (r, g, b) brane and ending on the $I_3 = 1/2$ brane is called a left-handed (r, g, b) down-quark d_L.

The quarks u_L and d_L thus form a doublet under $SU(2)$ whose representation is generally denoted by **2**. These possibilities are displayed in Fig. 5.3.

Such a quark state can now be represented by a (3×2)-matrix, whose two rows can be interpreted as a $SU(3)_C$ doublet, while the three columns are understood as $SU(2)_L$ triplet. Each of the (3×2) states in the representation are charged under the same *hypercharge*. The explicit form of the matrix would be given by[5]

$$Q_L \equiv \begin{pmatrix} u_L \\ d_L \end{pmatrix} \equiv \begin{pmatrix} u_{L\mathrm{r}} & u_{L\mathrm{b}} & u_{L\mathrm{g}} \\ d_{L\mathrm{r}} & d_{L\mathrm{b}} & d_{L\mathrm{g}} \end{pmatrix} . \tag{5.16}$$

Let us summarise the content of the quark sector. In the following, we will occasionally use a notation which is often used in particle physics. Making use of it, the representations are summarised compactly as [162]

$$(\text{Color}, \text{Weak Isospin})_{\text{Hypercharge}} . \tag{5.17}$$

[5]Furthermore, as in the case of the baryonic brane and the gluons, we can also consider those strings which have a left brane as their starting and end point. If we investigate the structure of the left brane more deeply, we can again assign a charge to the branes. A string ending on the left brane has the charge $q_{(i=1,2.)} = -1$ assigned. Starting on such a brane, the charge $q_i = 1$ results. Analogously to the baryonic brane, there is again a decoupling of a $U(1)$, whose charge is

$$\frac{1}{\sqrt{2}}(q_1 + q_2) . \tag{5.15}$$

Thus, within the left brane we get three gauge bosons transforming under $SU(2)_L$ and a decoupled $U(1)$ gauge field. The three fields are of course to be identified with the W^+, W^- and W^0 bosons.

The hypercharge[6] will be denoted with Y.

What did we forget? The left-handed quarks are joined by the right-handed quarks. $SU(2)_L$ is a chiral theory and therefore these right-handed particles do not form doublets with opposite charge to the left-handed particles, as we have seen for the case of $SU(3)_C$, but form singlets under the weak interaction [17,45,63,156]. To realise this, we need an additionally brane. A single so-called *right brane*. In the following, we will not concentrate on the right-handed particles but on the left-handed anti-particles. It is a well-known property of quantum field theory, that we can switch between right-handed particles and left-handed anti-particles by changing their charges. In the language of strings, this is also very intuitive since the orientation of the string changes when we switch from a right-handed representation to a left-handed (anti-) representation. The representation of $SU(2)_L$, which is invariant under $SU(2)_L$, is denoted as $\mathbf{1}$. Therefore, the representations of the quark sector are according to the notation in Eq. (5.17) [7]

$$\begin{pmatrix} u_L \\ d_L \end{pmatrix} \doteq (\mathbf{3},\mathbf{2})_{\frac{1}{6}}, \quad \bar{u}_L \doteq (\bar{\mathbf{3}},\mathbf{1})_{-\frac{2}{3}} \quad \text{and} \quad \bar{d}_L \doteq (\bar{\mathbf{3}},\mathbf{1})_{\frac{1}{3}} \ . \tag{5.20}$$

5.2.2 The Lepton Sector and the Higgs Sector

The same argument applies in the case of the leptons. All leptons form a $\mathbf{1}$ representation under the $SU(3)_C$ and are therefore colour singlets. The left-handed anti-leptons are also singlets under the $SU(2)_L$. The Higgs particle is is a $SU(2)_L$ doublet and a singlet under the $SU(3)_C$. Therefore, we summarise all representations in the leptonic sector as

$$L \equiv \begin{pmatrix} \nu_{eL} \\ e_L \end{pmatrix} \doteq (\mathbf{1},\mathbf{2})_{-\frac{1}{2}}, \quad \bar{e}_L \doteq (\mathbf{1},\mathbf{1})_1, \quad \bar{\nu}_{eL} \doteq (\mathbf{1},\mathbf{1})_0 \quad \text{and} \quad H \equiv \begin{pmatrix} H^- \\ H^0 \end{pmatrix} \doteq (\mathbf{1},\mathbf{2})_{-\frac{1}{2}} \ . \tag{5.21}$$

In the form of an example, we will soon see that the leptonic sector is again realised with a new single brane. The leptonic brane. Especially interesting is the penultimate representation. It reveals that these right-handed neutrinos do not interact with any of these interactions and thus could not be detected until today. Since neutrinos have a mass that is described with the help of different mechanisms, like the *seesaw mechanism*, the existence is strongly postulated [168].

Naively, we might now assume that we could describe the standard model as

$$U(3) \times U(2) \simeq SU(3) \times SU(2) \times U(1) \times U(1)' \ , \tag{5.22}$$

where the decoupled $U(1)$ or $U(1)'$ could eventually provide the hypercharge. But this is not quite true. The hypercharge gets contributions from the decoupled $U(1)$'s in a linear fashion

$$Q_Y = \sum_i c_i \, Q_i \ , \tag{5.23}$$

[6]Another parameter that is important in the particle standard model and serves as a control is of course the electromagnetic charge. Remember: This results from the hypercharge and the third component of the isospin according to

$$Q_{\text{em}} = Y + I_3 \ . \tag{5.18}$$

[7]For completeness we provide the fermionic content also with respect to the right-handed particles. Here, we get

$$3 \times \left[\underbrace{(\bar{\mathbf{3}},\mathbf{2})_{-\frac{1}{6}}}_{\begin{pmatrix} \bar{u}_R \\ \bar{d}_R \end{pmatrix}} + \underbrace{(\mathbf{3},\mathbf{1})_{\frac{2}{3}}}_{u_R} + \underbrace{(\mathbf{3},\mathbf{1})_{-\frac{1}{3}}}_{d_R} + \underbrace{(\mathbf{1},\mathbf{2})_{\frac{1}{2}}}_{\begin{pmatrix} \bar{\nu}_{eR} \\ \bar{e}_R \end{pmatrix}} + \underbrace{(\mathbf{1},\mathbf{1})_{-1}}_{e_R} + \underbrace{(\mathbf{1},\mathbf{1})_0}_{\nu_{eR}} \right] \tag{5.19}$$

Superfields	Bosons	Fermions	$\mathbf{SU(3)_C}$	$\mathbf{SU(2)_L}$	$\mathbf{U(1)_Y}$
Q_L	$(\tilde{u}_L, \tilde{d}_L)$	(u_L, d_L)	$\mathbf{3}$	$\mathbf{2}$	$+\frac{1}{6}$
$\overline{u}_L$	$\tilde{\overline{u}}_L$	$\overline{u}_L$	$\overline{\mathbf{3}}$	$\mathbf{1}$	$-\frac{2}{3}$
$\overline{d}_L$	$\tilde{\overline{d}}_L$	$\overline{d}_L$	$\overline{\mathbf{3}}$	$\mathbf{1}$	$+\frac{1}{3}$
L	$(\tilde{\nu}, \tilde{e}_L)$	(ν, e_L)	$\mathbf{1}$	$\mathbf{2}$	$-\frac{1}{2}$
$\overline{e}_L$	$\tilde{\overline{e}}_L$	$\overline{e}_L$	$\mathbf{1}$	$\mathbf{1}$	$+1$
$\overline{\nu}_{eL}$	$\tilde{\overline{\nu}}_L$	$\overline{\nu}_L$	$\mathbf{1}$	$\mathbf{1}$	0
H_u	(H_u^+, H_u^0)	$(\tilde{H}_u^+, \tilde{H}_u^0)$	$\mathbf{1}$	$\mathbf{2}$	$+\frac{1}{2}$
H_d	(H_d^0, H_d^-)	$(\tilde{H}_d^0, \tilde{H}_d^-)$	$\mathbf{1}$	$\mathbf{2}$	$-\frac{1}{2}$
G	G_μ^a	$\tilde{G}_\mu^a$	$\mathbf{8}$	$\mathbf{1}$	0
W	$W_\mu^\pm, W_\mu^3$	$\tilde{W}_\mu^\pm, \tilde{W}_\mu^3$	$\mathbf{1}$	$\mathbf{3}$	0
B	B_μ	$\tilde{B}_\mu$	$\mathbf{1}$	$\mathbf{1}$	0

Table 5.1: Particle content of the standard model and its supersymmetric extension. The particles as well as their superpartners and their representation under the respective gauge groups are shown.

with Q_i representing the charge of the different $U(1)_i$. We will encounter this in much more detail when we construct the standard model in the next sections.

Finally, it should be mentioned that there are three generations:

- $1^{\mathbf{st}}$ **generation:** In the quark sector we have up-quarks u and down-quarks d. Whereas with the leptons we have electrons e and electron-neutrinos ν_e.
- $2^{\mathbf{nd}}$ **generation:** The quark sector contains charm-quarks c and strange-quarks s. In the leptonic sector we find muons μ and muon-neutrinos ν_μ.
- $3^{\mathbf{th}}$ **generation:** The quark sector concludes with top-quarks t and bottom-quarks b. The τ and tau-neutrino completes the leptonic sector.

These particles agree in their quantum numbers and differ only in their mass, which rises with increasing generation number [169].

In order to extend the standard model and to turn it into a supersymmetric version, the particle multiplets have to be converted into supermultiplets. We thus obtain chiral supermultiplets for the fermionic part and vector supermultiplets for gauge bosons. Furthermore, two Higgs doublet are added to the minimal extended standard model. The content of the standard model and the content of the minimal supersymmetric standard model are summarised in Tab. 5.1.

5.3 Minimal Standard Model on Intersecting D6-Branes

In order to present this machinery of intersecting D-Branrs, we will do this in three steps.

1. We will construct a *minimal standard model with intersecting D-branes*. This is an adaptation of [45]. However, since this source does not contain the various tools, we presented in the first part of this thesis, we will examine it with the help of our previous knowledge. Essentially, we want to lear from this example where it fails and thus find a

N_a	$N_B = 3$	$N_L = 2$	$N_R = 1$	$N_{\widetilde{R}} = 1$	$N_\ell = 1$	$N_{\widetilde{\ell}} = 1$
$(n_a^{(1)}, m_a^{(1)})$	$(1,2)$	$(1,1)$	$(1,1)$	$(1,1)$	$(1,2)$	$(1,2)$
$(n_a^{(2)}, m_a^{(2)})$	$(1,-1)$	$(1,-2)$	$(1,0)$	$(3,-4)$	$(-1,1)$	$(-1,1)$
$(n_a^{(3)}, m_a^{(3)})$	$(1,-2)$	$(-1,5)$	$(-1,5)$	$(1,-5)$	$(1,1)$	$(2,-7)$

Table 5.2: The wrapping numbers of six different stacks of D6 branes wrapped on a factorised 6-torus. These numbers give raise to a minimal standard model. The values are taken from [45].

justification why D6-branes alone are not sufficient.

2. Next, we will construct a *non-supersymmetric standard model using orientifolds.* The example which we analyse belongs to a relatively famous class of models, which can be found, for example, in [17].
3. In the last step, we will take this model based on orientifolds and test it with *two numerical examples.* To do this, we will randomly choose the parameters and analyse the resulting consequences.

Having started to explore how the standard model and its contents can be described by using the framework of D-branes, we want to build a minimal standard model using D6-branes and type IIA superstring theory. For the compactification of the internal dimensions, we use the factorisable $\mathbb{T}^6$. In chapter 4 we established that the generations of the particles can be explained by multiple intersections of the D6-branes wrapped on the internal compact space. We further found in section 5.2 that the colour brane and the left brane produce the left-handed quark sector. These two D-branes should therefore intersect three times on the 6-torus to reproduce the first, second, and third generation of the quark sectors. As we have already elaborated, this is realised with a baryonic stack of $N_\mathrm{B} = 3$ coincident D6-branes and a left stack of $N_\mathrm{L} = 2$ D6-branes. To obtain the three generations in this sector, the corresponding intersection number I_{BL} must necessarily be $+3$. We can check this with the wrapping numbers summarised in Tab. 5.2 by calculating the intersection number. The intersection number between the baryonic and left brane as discussed in Eq. (4.7) results in

$$I_{BL} \equiv \bigotimes_{i=1}^{3} I_{BL}^{i} = \bigotimes_{i=1}^{3} \left(n_B^i m_L^i - m_B^i n_L^i \right) = -1 \cdot (-1) \cdot 3 = 3 \ . \tag{5.24}$$

Thus, we find $|I_{BL}| = 3$ replicas of left-handed fermions near the intersection of the baryonic brane and the left brane transforming in the bi-fundamental representation $(N_B, \overline{N}_L) = (\mathbf{3}, \mathbf{2})$ under the gauge group $SU(N_B = 3) \times SU(N_L = 2)$, where exactly one chiral left-handed fermion is localised (and potentially light scalars) per intersection. According to the convention, if $I_{BL} > 0$, the string leaves the baryonic brane and lands at the left brane creating a left-handed particle [17, 95]. This really corresponds to three generations of left-handed quarks Q_L.

Now, we have to clarify how we get the left-handed anti-quarks.

To realize this, we introduce four more D6-branes wrapping 3-cycles on the six-torus and intersecting schematically as shown in Fig. 5.4. As already indicated, we need a right brane to construct left-handed anti-quarks (resp. right-handed quarks). For this purpose, we introduce a

$N_R = 1$ and a $N_{\widetilde{R}} = 1$ D6-brane. To generate the left-handed antiparticles, the corresponding intersection numbers I_{BR} and $I_{B\widetilde{R}}$ must be negative. Further, the string starts from the right branes and lands on the baryonic brane, yielding the bi-fundamental representation $(\overline{\mathbf{3}}, \mathbf{1})$. Again, we can calculate the intersection number on the $\mathbb{T}^6$ compact space that determines the expected result $I_{BR} = I_{B\widetilde{R}} = -3$. These left-handed anti-quarks correspond to three families of $\overline{u}_L$ and $\overline{d}_L$. These are only distinguishable in their hypercharges. However, this model only offers a heuristic explanation for the calculation of the hypercharge, which we will therefore not consider but will calculated analytically in the next example. At this point we remind that by reversing the strings in the opposite direction we can get the desired representation of the right-handed particles.

To obtain the leptonic sector in all three generations, we introduce two other branes. A $N_\ell = 1$ and a $N_{\widetilde{\ell}} = 1$ leptonic brane. Furthermore, we introduce two $N_\ell = 1$ and $N_{\widetilde{\ell}} = 1$ leptonic branes. With Tab. 5.2 we find the following intersection numbers between the leptonic $N_\ell = 1$ brane and their intersections with the other branes:

$$I_{\ell\widetilde{R}} = 6, \quad I_{L\ell} = 6, \quad I_{R\ell} = -6. \tag{5.25}$$

The first intersection number corresponds to a string running from the leptonic brane to the $N_{\widetilde{R}} = 1$ right brane. According to our convention, these are six copies in a $(\mathbf{1}, \mathbf{1})$ representation. The next intersection number is a string oriented from the leptonic brane to the $N_R = 1$ right brane, since the intersection number is negative. These are six copies in the $(\mathbf{1}, \mathbf{1})$ representation. Finally, through the last intersection number, we have a string that starts at the left brane and ends on the leptonic brane. This can be associated with six copies in a $(\mathbf{1}, \mathbf{2})$ representation. Basically, this is good because we get the leptonic sector except for the hypercharge. But unfortunately we get six families instead of three. The same happens by calculating the intersection numbers $(I_{L\widetilde{\ell}} = 3, I_{R\widetilde{\ell}} = -3, I_{\widetilde{\ell}R'} = 3)$ that contain the other leptonic brane, where we get further additional $(\mathbf{1}, \mathbf{2})$ and $(\mathbf{1}, \mathbf{1})$ representations.

Thus, we find more particles than we wanted and confront a typical problem in models where we have just D6-branes with no further structure. However, this is not surprising and follows from the rule that a set of left-handed states ending at a D6-brane must have the same number of incoming and outgoing states [45]. In other words, there must always be as many strings coming in as strings going out. We can immediately confirm this rule from Fig. 5.4. Considering the left brane, we find that nine quark doublets (three colours and three generations) are arriving on that brane, but there are also three doublets and six doublets from the two leptonic branes leaving the left brane. Thus, according to this rule, we simply cannot get three lepton doublets [45, 63].

Now, this rule seems to come out of nowhere, but we have already seen it in a different form in another place. The RR net charge of the wrapped D6-branes in the compact space must add up to zero which we finally formulated in the tadpole condition as a global consistency condition. The tadpole condition in homology classes was given by

$$[\Pi_{\text{tot}}] \equiv \sum_a N_a \, [\Pi_a] = 0 \ , \tag{5.26}$$

for Dp-branes of type a. Multiplying by $[\Pi_b]$ from the right gives

$$\sum_a N_a \, [\Pi_a] \circ [\Pi_b] = \sum_a N_a I_{ab} = 0 \ , \tag{5.27}$$

where the intersection number $|I_{ab}|$ gives as usual the number of intersections between the a and b brane. If we look carefully at the sum we recognise, that the sum with $I_{ab} > 0$ gives us the number of left-handed states from strings starting at the brane a. However, term with $I_{ab} < 0$ yields minus the number of left-handed states from strings ending at any b brane. Therefore, summing over all a is the number of all outgoing strings minus the number of all incoming strings

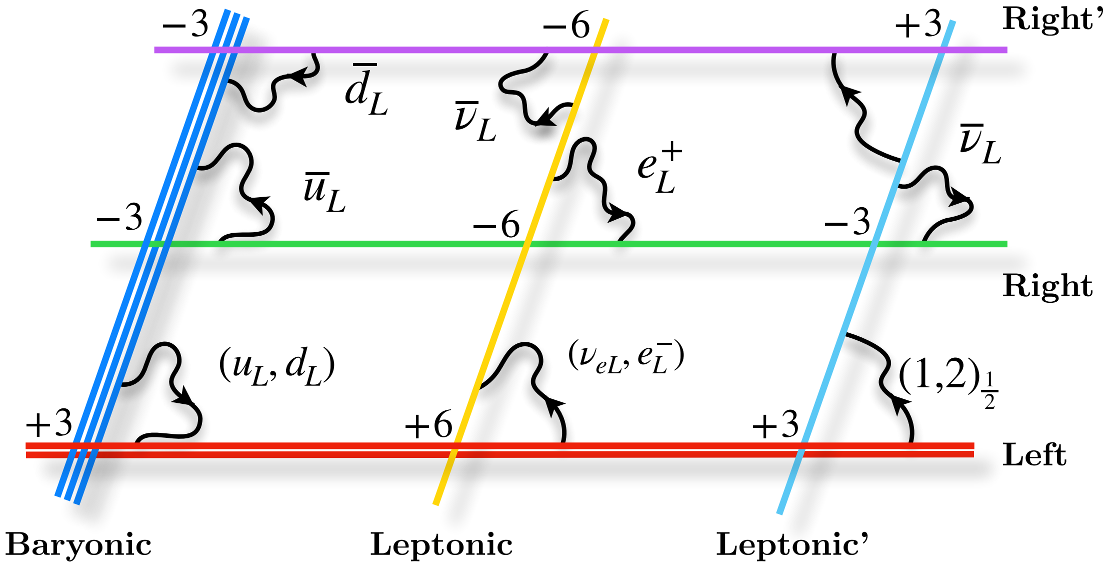

Figure 5.4: Schematic diagram for the construction of a minimal standard model. A $N_B = 3$ baryonic brane and a $N_L = 2$ left brane are used. Furthermore, a $N_R = 1$ right and $N_{R'} = 1$ right brane intersect with two $N_\ell = N_{\ell'} = 1$ leptonic branes. The intersection points are captioned with the related intersection number. The strings are oriented and left-handed particles and left-handed antiparticles are shown. This construction provides the desired spectrum of the standard model, but unlike in the quark sector, we get additional $SU(2)$ doublets to which we cannot assign a physical realisation.

an any a brane. Since the tadpole condition equals zero, these two quantities are equal. [17,63,68]. In Eq. (4.21), we have decomposed the abstract tadpole condition into an integral basis with corresponding wrapping numbers. Thus, it is inherent that we have to follow this rule, since the wrapping numbers have already been chosen to satisfy Eq. (4.21). If we take for example the condition

$$\sum_a N_a m_a^{(1)} m_a^{(2)} m_a^{(3)} = 0 \tag{5.28}$$

putting in our concrete values, we get $\sum_a N_a m_a^{(1)} m_a^{(2)} m_a^{(3)} = N_B - N_L - N_R - N_\ell - 2N_{\tilde{\ell}} + 3N_{\tilde{R}} = 3 - 2 - 1 - 1 - 2 + 3 = 0$.

Nevertheless, this emergence of additional $SU(2)$ doublets and the corresponding exotic chiral matter can be circumvented by introducing orientifolds. This will be the aim of the next section.

5.4 Non-Supersymmetric Standard Model in $\mathbb{T}^6$ Orientifolds

In order to avoid the additional leptonic doublets which we obtained in the previous model, we introduce an orientifold projection. The main idea of orientifolds was introduced in section 4.3. In our general discussion about orientifolds we have discovered that the introduction of such objects alters the spectrum. Therefore, we now have two possible bi-fundamental representations. The representation $(\square_a = N_a, \square_b = N_b)$ and $(\square_a = N_a, \overline{\square}_b = \overline{N}_b)$. On the basis of this new possibility, we want to investigate and construct semi-realistic models.

To construct non-supersymmetric standard model, we will require four different stacks of D-branes. It turns out that these four branes form a minimal set for standard model constructions with D6-branes and an orientifold projection. Besides, we use the nomenclature of the previous model. The intersecting stacks of D6-branes are therefore a $N_B = 3$ baryonic brane which yields $U(3)_{\mathrm{B}} \simeq SU(3)_{\mathrm{C}} \times U(1)_{\mathrm{B}}$, a $N_L = 2$ left brane returning $U(2)_L \simeq SU(2)_{\mathrm{L}} \times U(1)_L$, a $N_R = 1$

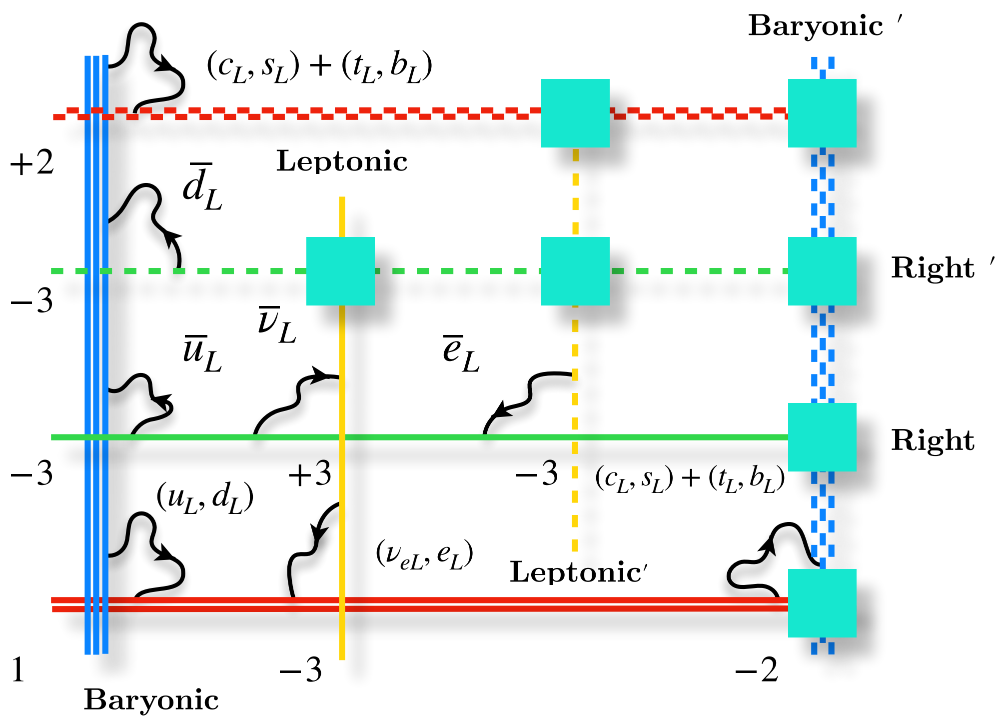

Figure 5.5: Schematic diagram for the construction of a non-supersymmetric standard model with an orientifold projection. For this model, a $N_B = 3$ baryonic brane, a $N_L = 2$ left brane, a $N_R = 1$ right, and a $N_\ell = 1$ leptonic brane intersect. The intersection points are again denoted with the related intersection number. The strings are oriented and left-handed particles and left-handed antiparticles are shown. The orientifold provides the Dp-brane model with their mirror images, which are illustrated in dashed lines. The boxes are indicating that these points are already considered for the spectrum in order to not overcount the matter arising from these intersections. As usual, we show the right-handed particles as left-handed antiparticles.

right brane with $U(1)_R$ and a $N_\ell = 1$ leptonic brane providing $U(1)_\ell$. This results in the gauge group

$$U(3)_B \times U(2)_L \times U(1)_R \times U(1)_\ell \simeq SU(3)_C \times SU(2)_L \times U(1)_B \times U(1)_L \times U(1)_R \times U(1)_\ell \quad (5.29)$$

The construction of this D6-brane model with O6-planes is shown in Fig. 5.5. Here, we introduce dashed lines, which represent the mirrored D6′-branes. Moreover, in such graphical constructions it is also common to frame intersections with a square or a circle if the intersections have already been counted to the spectrum of the matter. Thus, no additional fields are obtained by considering these intersections [45]. We open our discussion by investigating the left-handed quark sector. Looking at Fig. 5.5 shows that the first generation of this doublet is generated in the intersection between the baryonic brane and the left brane. The second and third generations are located in the intersection between the baryonic brane and the image of the left brane. However, these two generations are in the bi-fundamental representation (N_B, N_L) . This choice will eliminate all additional $SU(2)_L$ doublets and exotics we encountered previously [170–174].

Let us analyse this again on the basis of the tadpole condition. The RR tadpole condition in the orientifolded case which we derived in Eq. (4.33) can be manipulated in analogy to Eq. (5.27) and we obtain

$$\begin{aligned}&\left(\sum_a N_a\,[\Pi_a] + \sum_a N_a\,[\Pi'_a] - 4\,[\Pi_{O6}]\right)\circ[\Pi_b] = \\ &\sum_a N_a\,[I_{ab} + I_{ab'}] = \#\left(\square_a, \overline{\square}_b\right) - \#\left(\square_a, \square_b\right) = 0\ ,\end{aligned} \tag{5.30}$$

where we assumed that $I_{\mathrm{O6}_b} = 0$. This means that there should be as many fundamentals as antifundamental representations for any $U(N)$ group. This has a great advantage compared to Eq. (5.27). In order to satisfy this condition, let us apply it again on the left brane.

$$\#\left(\square_a, \overline{\square}_b\right) - \#\left(\square_a, \square_b\right) = 3 + 3 - 6 = 0\ . \tag{5.31}$$

This can also easily be verified by looking at Fig. 5.5. Three quark doublets and three lepton doublets are outgoing at the left brane and six quark doublets are incoming at the same brane.

In this consideration, however, lies a breathtakingly beautiful conclusion. In order for this to work, the number of the generation - which is given by the intersection number - must coincide to that of the number of colours [17, 170–174]. The unsolved generation problem of particle physics gets a concrete answer here

$$\#\text{Colors} = \#\text{Generations}\ . \tag{5.32}$$

The D6-branes wrap 3-cycles in the internal space and as a result there will be some intersections. The occurring intersection numbers must be as follows to give the spectrum of the standard model

$$\begin{array}{llll} I_{BL} = 1, & I_{BL'} = 2\ , & I_{R\ell} = 3, & I_{R\ell'} = -3, \\ I_{BR} = -3, & I_{BR'} = -3\ , & I_{L\ell} = -3, & I_{L\ell'} = 0\ . \end{array} \tag{5.33}$$

The attentive reader will have noticed that not all possible intersection numbers have been listed. This is because they are zero or we postulate them as such. Exotic matter between BB' branes or leptoquarks in $B\ell$ and $B\ell'$ should not exist because they could not be experimentally detected. This a priori postulate will be realised concretely by the choice of the wrapping numbers [17].

The D-brane configuration is shown in Fig. 5.5. Using the intersection numbers, we can check for anomaly cancellation by using Eq. (5.30).

Leaving this fairly general discussion, we now want to make it more explicit by applying it concretely to type IIA superstring theory with D6 branes wrapping factorisable 3-cycles at angles in a $\mathbb{T}^6$ orientifold. We want to construct this model in such a way that we get the standard model with the configurations and quantum numbers of Tab. 5.5. The first step after the choice of the compacted space is therefore the choice of the wrapping numbers. However, we want to choose these as general as possible for the factorised $\mathbb{T}^6 = \mathbb{T}^2 \times \mathbb{T}^2 \times \mathbb{T}^2$. Such a model was considered analytically for the first time in [17].

Before we start, conditions and requirements should be mentioned, which restrict these wrapping numbers. As was pointed out in [17] we have the following restrictions for the wrapping numbers:

1. We have noted in section 4.3 that new representations are possible by introducing orientifolds. However, in order to preserve the standard model, we want to only choose the representations which provide us with the correct spectrum. We therefore exclude symmetric and antisymmetric representations, which would yield matter content with exotic quantum numbers. This requires that we do not allow intersections with D6-branes and their mirror images. The direct consequence of that can be put into the condition

$$\prod_{i=1}^{3} m_a^{(i)} = 0 \quad \forall a = B, L, R, \ell. \tag{5.34}$$

This choice brings an important consequence. We will see that the product in Eq. (5.34) is a coefficient in the BF coupling introduced in chapter 4, which means that in the effective four-dimensional field theory at most three RR fields B_i couple to the Abelian group. Consequently, the upper bound of massive $U(1)$'s is given by three. However, since we want a massless $U(1)$ for the hypercharge, we may only use a maximum of four stacks of D6-branes. Any further choice would lead to additional massive $U(1)$'s and extend the spectrum of the standard model [17,171–173].

2. To get the intersection numbers from Eq. (5.33), we have to lay out the baryonic and leptonic brane parallelly to each other in at least one of the three 2-tori. Likewise, the right and left brane should be parallel to each other. Finally, to get the intersection numbers $I_{BL} = 1$ and $I_{BL'}$ we have to tilt one of the three tori. By default, we choose the third torus here [17,63,171–173].

   The tilted torus is described in Appendix E.2. In a nutshell, the wrapping numbers for the rectangular 2-tori are denoted as (n_a^i, m_a^i), while the image wrapping numbers are $(n_a^i, -m_a^i)$. The image wrapping numbers for tilted 2-tori look different. These are given by $(n_a^i, -n_a^i - m_a^i)$. By a redefinition $\tilde{m}_a = m_a + bn_a$ with $b = 0, 1/2$, we get

$$\begin{array}{ccc} \mathrm{D6}_a - \text{brane} & \mapsto & \mathrm{D6}_{a'} - \text{brane} \\ \left(n_a^i, \tilde{m}_a^i\right) & & \left(n_a^i, -\tilde{m}_a^i\right) \end{array} \tag{5.35}$$

   Note, that we will omit the tilde from the wrapping numbers in sequence when it is clear from the context.

This number of conditions limits the choice of wrapping numbers in a rather complicated way. The most general choice of these wrapping numbers is given in Tab. 5.3 [17].

The phase $\epsilon, \tilde{\epsilon} = \pm 1$ and the parameter $\rho = 1, 1/3$ have two possible settings. The parameter $\beta^i = 1 - b^i$ depends on the modulus of the torus. Since only the third torus is tilted, our configuration inhabits the choice $\beta^{i=1,2} = 1$ and $\beta^3 = 1/2$. The choice of $(n_B^2, n_L^1, n_R^1, n_\ell^2)$ is arbitrary as long as they are elements of $\mathbb{Z}$. The spectrum remains unchanged regardless of which parameters are chosen. We will test this as a theoretical experiment in the last part of this chapter.

However, we have to add the most prominent condition: The tadpole conditions from section 4.3.

3. The tadpole conditions in the presence of an orientifold projection from Eq. (4.38) must be fulfilled by our choice in Tab. 5.3. However, these conditions are fulfilled automatically except for the first one in Eq. (4.38), which becomes

$$\sum_a N_a n_1^a n_2^a n_3^a = \frac{N_a n_B^{(2)}}{\rho \beta^1} + \frac{N_L n_L^{(1)}}{\beta^2} + N_\ell \frac{n_\ell^{(2)}}{\beta^1} = 16 \ . \tag{5.36}$$

   In order to fulfil this condition, we can choose n_a in such a way that Eq. (5.36) is satisfied. A different and more general possibility is the introduction of a *hidden sectors*. Hidden branes are the branes that have no intersection with the branes of the standard model. The easiest way to get such a hidden sector is to place the hidden D6-branes parallel to the orientifold planes. This results in wrapping numbers of the form

$$N_h \, (1/\beta_1, 0) \, (1/\beta_2, 0) \, (2, 0) \ . \tag{5.37}$$

   Introducing such a hidden brane in every torus with the wrapping numbers given as above, the Eq. (5.36) can be rewritten as

$$\frac{3n_B^{(2)}}{\rho \beta^1} + \frac{2n_L^{(1)}}{\beta^{(2)}} + \frac{n_\ell^{(2)}}{\beta^1} + 2N_h n_h^1 n_h^2 = 16 \ . \tag{5.38}$$

N_a	N_B	N_L	N_R	N_ℓ
$(\tilde{n}_a^{(1)}, \tilde{m}_a^{(1)})$	$(1/\beta^1, 0)$	$(n_L^{(1)}, -\epsilon\tilde{\epsilon}\beta^1)$	$(n_R^{(1)}, 3\rho\epsilon\beta^1)$	$(1/\beta^1, 0)$
$(\tilde{n}_a^{(2)}, \tilde{m}_a^{(2)})$	$(n_B^{(2)}, \epsilon\beta^2)$	$(1/\beta^2, 0)$	$(1/\beta^2, 0)$	$(n_\ell^{(2)}, \epsilon\beta^2/\rho)$
$(\tilde{n}_a^{(3)}, \tilde{m}_a^{(3)})$	$(1/\rho, \tilde{\epsilon}/2)$	$(1, 3\rho\tilde{\epsilon}/2)$	$(0, 1)$	$(1, -3\rho\tilde{\epsilon}/2)$

Table 5.3: In order to satisfy the various conditions, the wrapping numbers in the case of D6 branes wrapped on a factorised 6-torus must have the following form with $(n_B^2, n_L^1, n_R^1, n_\ell^2) \in \mathbb{Z}$. The phase $\epsilon, \tilde{\epsilon} = \pm 1$, while the parameter $\rho = 1, 1/3$. The parameter for the rectangular torus is given by $\beta = 1$ and for the tilted torus by $\beta = 1/2$.

5.4.1 Hypercharge and the Story of Massive $U(1)$'s

As already elaborated in subsection 4.5.3 , $U(1)$'s get massive by coupling to a corresponding BF term. Furthermore, the different $D6$-branes were chosen in such a way that there can be at most three RR-fields B_i with $i = 1, 2, 3$. We have explored how the BF terms are generated in general and how they give mass to the $U(1)$ fields via the Stückelberg mechanism. In Eq. (4.51), we expressed the 3-cycles in a homology basis. In this section we therefore have to decompose the 3-cycles into a 1-cycle basis on the factorisable $\mathbb{T}^6$ torus. This basis decomposes according to

$$\alpha_I = \begin{cases} a_1 \times a_2 \times a_3 \\ a_1 \times b_2 \times b_3 \\ b_1 \times b_2 \times a_3 \\ b_1 \times a_2 \times b_3 \end{cases} \quad \text{and} \quad \beta_I = \begin{cases} b_1 \times b_2 \times b_3 \\ a_1 \times b_2 \times a_3 \\ b_1 \times a_2 \times a_3 \\ a_1 \times a_2 \times b_3 \end{cases} \tag{5.39}$$

The 3-cycle can be expressed in terms of 1-cycles

$$[\Pi_a] = \bigotimes_{i=1}^{3} \left(n_a^{(i)} [a_{(i)}] + m_a^{(i)} [b_{(i)}] \right) . \tag{5.40}$$

The same has to be done for the mirror image of the 3-cycle. Since the wrapping numbers n, n' and m, m' are no longer independent of each other, we get according to section 4.3

$$[\Pi_a'] = \bigotimes_{i=1}^{3} \left(n_a^{(i)\prime} [a_{(i)}] + m_a^{(i)\prime} [b_{(i)}] \right) = \bigotimes_{i=1}^{3} \left(n_a^{(i)} [a_{(i)}] - m_a^{(i)} [b_{(i)}] \right) . \tag{5.41}$$

We recall that the coefficients of the BF term where given by

$$c_I^a = \sum_{I,a} N_a \left(\nu_a^I - \nu_a^{I\prime} \right) \quad \text{and} \quad \tilde{c}_I^a = \sum_{I,a} N_a \left(\mu_a^I - \mu_a^{I\prime} \right) . \tag{5.42}$$

The first term in Eq. (5.42) is completely in the basis α. If we write out the product in Eq. (5.40) and Eq. (5.41) and subtract all terms corresponding to the basis given in Eq. (5.39), these terms cancel. This yields $c_a^I = 0$. Following the same train of thought, we thus obtain for the second coefficient in Eq. (5.42) terms proportional to $n^{(2)}n^{(3)}m^{(1)}, n^{(1)}n^{(3)}m^{(2)}, n^{(1)}n^{(2)}m^{(3)}$ and $m^{(1)}m^{(2)}m^{(3)}$. The last term vanishes according to Eq. (5.34). Therefore, we get the following

BF terms:

$$\begin{aligned} i=1: &\quad \textstyle\sum_a N_a n_a^{(2)} n_a^{(3)} m_a^{(1)} \int B_1 \operatorname{tr}(F_a) \ . \\ i=2: &\quad \textstyle\sum_a N_a n_a^{(1)} n_a^{(3)} m_a^{(2)} \int B_2 \operatorname{tr}(F_a) \ . \\ i=3: &\quad \textstyle\sum_a N_a n_a^{(1)} n_a^{(2)} m_a^{(3)} \int B_3 \operatorname{tr}(F_a) \ . \end{aligned} \tag{5.43}$$

Inserting the corresponding values for the wrapping numbers from Tab. 5.3, we obtain

$$\begin{aligned} i=1: &\quad -2\tfrac{\epsilon\tilde{\epsilon}\beta^1}{\beta^2} \int B_1 \wedge \operatorname{tr}(F_L) \ . \\ i=2: &\quad \tfrac{\epsilon\beta^2}{\rho\beta^1} \int B_2 \operatorname{tr}(3F_B + F_\ell) \ . \\ i=3: &\quad \tfrac{\tilde{\epsilon}}{2\beta^1\beta^2} \int B_3 \operatorname{tr}\left(3\beta^2 n_a^{(2)} F_B + 6\rho\beta^1 n_b^{(1)} F_L + \tfrac{2}{\tilde{\epsilon}}\beta^1 n_c^{(1)} F_R - 3\rho\beta^2 n_d^{(2)} F_\ell\right) \ . \end{aligned} \tag{5.44}$$

Recapitulating subsection 4.5.3, the generator of a generic $U(1)$ is given as the linear combination

$$Q_Y = \sum_a \xi_a Q_a \ . \tag{5.45}$$

The condition to obtain a linear combination that can be associated with a massless $U(1)$ was given by

$$\sum_a c_i^a \xi_a = 0 \quad \forall i \ , \tag{5.46}$$

or simply in matrix notation as $\mathbf{C} \cdot \vec{\xi}$ with the matrix $(\mathbf{C})_{ia} = c_i^a$. The rows of this matrix are labelled with i and are thus related to the RR 2-forms B_i. The columns are labelled with a and correspond to the $U(1)_a$ of the respective configuration [17].

The matrix can thus be read off from Eq. (5.44) and is given as

$$(\mathbf{C})_{ia} = \begin{pmatrix} 0 & -\frac{2\epsilon\tilde{\epsilon}\beta^1}{\beta^2} & 0 & 0 \\ \frac{3\epsilon\beta^2}{\beta^1\rho} & 0 & 0 & \frac{\epsilon\beta^2}{\beta^1\rho} \\ \frac{3n_B\tilde{\epsilon}}{2\beta^1} & \frac{3n_L\tilde{\epsilon}\rho}{\beta^2} & \frac{n_R}{\beta^2} & -\frac{3n_\ell\tilde{\epsilon}\rho}{2\beta^1} \end{pmatrix} \tag{5.47}$$

According to Eq. (5.46), the associated vector space of massless $U(1)$'s is given by the nullspace given by Ker($\mathbf{C}$). The number of massive $U(1)$ is given by the Rank($\mathbf{C}$). Computing the kernel of the matrix in Eq. (5.47), we obtain

$$\operatorname{Ker}(\mathbf{C}) = \left\{ \left(-\tfrac{\zeta}{3}, \quad 0, \quad \left(\tfrac{n_B\beta^2 + 3n_\ell\beta^2\rho}{2n_R\tilde{\epsilon}\beta^1}\right)\zeta, \quad \zeta \right) \quad : \zeta \in \mathbb{R} \right\} \tag{5.48}$$

This results in the generator Q_Y for a massless $U(1)$

$$Q_Y = \frac{1}{6}Q_B - \frac{\kappa}{2}Q_R - \frac{1}{2}Q_\ell \quad \text{with} \quad \kappa = \frac{\tilde{\epsilon}\beta^2}{2n_R^{(1)}\beta^1}\left(n_B^{(2)} + 3\rho n_\ell^{(2)}\right) \ . \tag{5.49}$$

To get the appropriate hypercharge, we require that $\kappa = 1$. This finally imposes the fourth and final constraint on our choice of wrapping numbers. Written out, it is

$$n_R^{(1)} = \frac{\tilde{\epsilon}\beta^2}{2\beta^1}\left(n_B^{(2)} + 3\rho n_\ell^{(2)}\right) \ . \tag{5.50}$$

If we look more closely at the four $U(1)$ generators, we see that they are related to quantities that we can give physical meaning to. Q_B is three times the Baryon number $Q_B = 3B$ and

$Q_\ell = L$ is the lepton number. This also clarifies the origin of the names for these respective branes. Q_R we can interpret as twice the third component of the right-handed weak isospin $Q_R = 2I_R$. The last $U(1)$ charge Q_L is associated with mixed $SU(3)$ anomalies and belongs to the so-called *Peccei-Quinn* symmetry. This is a remarkable conclusion drawn here. These global symmetries which are attributed to the standard model - but postulated a posteriori - find a foundation in Dp-brane models. These global symmetries are indeed unbroken gauge symmetries. At this point, we resume and emphasise the fact that the symmetries of the massive gauge bosons are preserved as artefacts of a global symmetry in the low energy limit [17, 170–174].

While the linear combinations $Q_B - 3Q_\ell = 3(B - L)$ and $Q_R = 2I_R$ are free of anomalies, the orthogonal combinations $3Q_B + Q_\ell$ and Q_L are not. These, however, are fixed by the Green-Schwarz mechanism as discussed in subsection 4.5.4, become massive and decoupling in the low energy regime of the theory. We have also noted that the BF term is responsible for whether a $U(1)$ gets massive or not. *Not* the fact whether there is an anomaly or not.

By a clever choice of the intersection angles, it can be further ensured that the spectrum remains tachyon free. However, these tachyons can also be of physical interest, for example by interpreting the bosons in the BR and $BR^{'}$ sector as Higgs gauge bosons [17, 65].

5.4.2 Numerical Examples

To conclude, we will illustrate the found results through a numerical example. As we have seen, the parameters for the wrapping numbers are freely selectable and should lead to the same result regarding the intersection number by construction. We now want to test this and choose the parameters as we please. To ensure this, we let the parameters be randomly generated with a small Mathematica code. The resulting parameters are then selected for the respective model.

Model A

The following code determines the parameters.

In[1]:= parameters = {RandomChoice[{1, −1}, 1],
RandomChoice[{1, −1}, 1],
RandomChoice[{3, 1/3}], RandomInteger[{−3, 3}, 3]};

In[2]:= auxil = parameters [[2]][[1]]/2(parameters [[4]][[1]]
+ 3 parameters[[3]] parameters [[4]][[4]]);

In[3]:= {**StringForm**["ϵ = ", parameters [[1]][[1]]],
StringForm["$\widetilde{\epsilon}$, = ", parameters[[2]][[1]]],
StringForm["ρ = ", parameters[[3]]],
StringForm["$n_B^{(2)}$ = ", parameters[[4]][[1]]],
StringForm["$n_L^{(1)}$ = ", parameters[[4]][[2]]],
StringForm["$n_R^{(1)}$ = ", auxil],
StringForm["$n_\ell^{(2)}$ = ", parameters[[4]][[3]]]}

Out[3]= $\{\epsilon{=}1,\ \widetilde{\epsilon}{=}{-1},\ \rho = \frac{1}{3},\ n_B^{(2)} = 1,\ n_L^{(1)} = 1,\ n_R^{(1)} = -1,\ n_\ell^{(2)} = 1\}$

Out[4]= $\{\epsilon{=}1,\ \widetilde{\epsilon}{=}1,\ \rho = 3,\ n_B^{(2)} = 0,\ n_L^{(1)} = 7,\ n_R^{(1)} = 9,\ n_\ell^{(2)} = 2\}$

N_a	N_B	N_L	N_R	N_ℓ
$(n_a^{(1)}, m_a^{(1)})$	$(1,0)$	$(1,1)$	$(-1,1)$	$(1,0)$
$(n_a^{(2)}, m_a^{(2)})$	$(1,1)$	$(1,0)$	$(1,0)$	$(1,3)$
$(n_a^{(3)}, m_a^{(3)})$	$(3,-\frac{1}{2})$	$(1,-\frac{1}{2})$	$(0,1)$	$(1,-\frac{1}{2})$

Table 5.4: The wrapping numbers for the model A resulting from four stacks of D6-branes. The wrapping numbers are given in such a way, that the first two 2-tori are considered to be rectangular, while the last 2-torus is tilted.

Accordingly to this output, we set $\beta^1 = 1, \beta^2 = 1, \rho = \frac{1}{3}, \epsilon = 1, \tilde{\epsilon} = -1, n_B^{(2)} = 1, n_L^{(1)} = 1, n_R^{(1)} = -1$ and $n_\ell^{(2)} = 1$. The resulting values for the wrapping numbers are listed in Tab. 5.4. With the concrete choice of the wrapping numbers the intersection numbers can now be calculated easily, and we get

$$\begin{aligned}
I_{BL} &= +1 \quad \rightarrow \quad 1\,(\mathbf{3}, \mathbf{2}), \quad I_{BL'} = +2 \quad \rightarrow \quad 2\,(\mathbf{3}, \mathbf{2}) \\
I_{BR} &= -3 \quad \rightarrow \quad 3\,(\overline{\mathbf{3}}, \mathbf{1}), \quad I_{BR'} = -3 \quad \rightarrow \quad 3\,(\overline{\mathbf{3}}, \mathbf{1}) \\
I_{L\ell} &= -3 \quad \rightarrow \quad 3\,(\mathbf{1}, \mathbf{2}), \quad I_{L\ell'} = 0 \\
I_{R\ell} &= +3 \quad \rightarrow \quad 3\,(\overline{\mathbf{1}}, \mathbf{1}), \quad I_{R\ell^*} = -3 \quad \rightarrow \quad 3\,(\overline{\mathbf{1}}, \mathbf{1})
\end{aligned} \tag{5.51}$$

At this point, we have also listed the corresponding representations. One could already guess what kind of particles we might be dealing with here. However, this can only be properly assigned by means of the hypercharge. In fact, we also get the desired intersection numbers from Eq. (5.33), which supports the claim, that arbitrary parameters within their parameter space lead to the same intersection number. It is straightforward to check our choice of wrapping numbers on the various conditions we listed in Eq. (4.38). The tadpole condition in Eq. (5.38) now results in

$$\frac{3n_B^{(2)}}{\rho\beta^1} + \frac{2n_L^{(1)}}{\beta^2} + \frac{n_\ell^{(2)}}{\beta^1} + 2N_h n_h^{(1)} n_h^{(2)} = 9 + 2 + 1 + 2N_h n_h^{(1)} n_h^{(2)} = 16 \tag{5.52}$$

Here is a novelty coming our way. This equation is satisfied by introducing $N_h = 2$ parallel hidden branes running along the orientifold with $n_h^{(1)} = 1, = n_h^{(2)} = 1, n_h^{(3)} = 2$ and $m_h^{(i)} = 0$, where we used Eq. 7.33. Such a hidden brane basically gives another further $U(2)_h$ gauge group which in turn can be thought as a $SU(2)_h \times U(1)_h$. Such hidden branes are generally not connected to the standard model by construction, as in this case. In general, however, such a hidden sector can also be used to extend the gauge group of the standard model. String between standard model branes and such hidden sectors constitute “bridges” or “messenger particles” to some extent.

Next, we need to calculate the hypercharge for this model. For this we need to look at the BF couplings. The BF couplings of the $U(1)$'s to the RR fields in this numerical example are [8]:

$$\begin{aligned} i=1: &\qquad 2\int B_1 \wedge \mathrm{tr}\,(F_L)\ . \\ i=2: &\qquad 3\int B_2 \wedge \mathrm{tr}\,(3F_B + F_\ell)\ . \\ i=3: &\qquad \int B_3 \wedge \mathrm{tr}\left(-\frac{3}{2}F_B - F_L - F_R + \frac{1}{2}F_\ell\right)\ . \end{aligned} \tag{5.53}$$

From this three terms we can read off the coefficients and form the matric $\mathbf{C}$. We thus find

$$(\mathbf{C})_{i\alpha} = \begin{pmatrix} 0 & 2 & 0 & 0 \\ 9 & 0 & 0 & 3 \\ -\frac{3}{2} & -1 & -1 & \frac{1}{2} \end{pmatrix}. \tag{5.54}$$

Computing the kernel of $\mathbf{C}$ yields

$$\mathrm{Ker}(\mathbf{C}) = \left\{ \begin{pmatrix} -\frac{\zeta}{3}, & 0, & \zeta, & \zeta \end{pmatrix} \ :\ \zeta \in \mathbb{R} \right\}\ . \tag{5.55}$$

This kernel indeed leads to the right hypercharge generator

$$Q_Y = \frac{1}{6}Q_B - \frac{1}{2}Q_R - \frac{1}{2}Q_\ell\ , \tag{5.56}$$

We now want to test if we can obtain the desired standard model spectrum using this hypercharge formula. For example, we take the string that runs between the baryonic brane and the left brane. The intersection number is $I_{BL} = 1$ and thus positive. The string is oriented and runs from the baryonic brane to the left brane. Therefore, this represents a state in a bi-fundamental representation $(\mathbf{3}, \mathbf{1})$. Furthermore, through $U(3)_B \simeq SU(3)_c \times U(3)_B$ and through $U(2)_L \simeq SU(2)_L \times U(2)_L$ we have two $U(1)$'s under which the string is charged. The string starts on the baryonic brane and, by convention, receives a positive sign, obtaining $Q_B = 1$. On the left brane it receives a negative charge $Q_L = -1$. If we put this into the formula for the hypercharge in Eq. (5.62), we get $Q_Y = \frac{1}{6}$. This corresponds - comparing to Eq. (5.57)- to $1 \times (\mathbf{3}, \mathbf{2})_{\frac{1}{6}}$ and can be associated with a single family of left-handed quarks Q_L.

We can now also show the same for the string that leaves the baryonic brane and reaches the mirror image of the left brane through the orientifold projection. The O6-plane reverses the direction of the string. The intersection number $I_{BL'}$ is positive and provides two families. Furthermore, by convention, the string receives a positive charge $Q_B = 1$ and another positive charge $Q_L = 1$, which has its origin, of course, in the reorientation of the string. The hypercharge is $Q_Y = \frac{1}{6}$ and this state finally corresponds to $2 \times (\mathbf{3}, \mathbf{2})_{\frac{1}{6}}$. These are therefore two families of left-handed quarks. With this we have determined the entire quark sector. This can now be done for all strings in non-vanishing intersections, which reproduces the right quantum numbers and spectrum of the standard model that are collected in Tab. 5.5.

Model B

For this model, we again choose the parameters based on pseudo-randomness. The parameters for this models are in accordance with the code $\beta^1 = 1, \beta^2 = 1, \rho = 3, \epsilon = 1, \tilde{\epsilon} = 1, n_B^{(1)} = 0, n_L^{(1)} = 7, n_R^{(1)} = 9$ and $n_\ell^{(2)} = 2$. The wrapping numbers resulting from these parameters are listed in Tab. 5.6.

[8] Since the hidden brane lies along the O6-plane, its $U(1)$ group must of course not be taken into account.

Fields	**Intersections**	**Representation**	$\mathbf{Q_B}$	$\mathbf{Q_L}$	$\mathbf{Q_R}$	$\mathbf{Q_\ell}$	**Y**
Q_L	(BL)	$(\mathbf{3},\mathbf{2})$	1	-1	0	0	1/6
L_L	(BL')	$2(\mathbf{3},\mathbf{2})$	1	1	0	0	1/6
$\overline{u}_L$	(BR)	$3(\bar{\mathbf{3}},\mathbf{1})$	-1	0	1	0	$-2/3$
$\overline{d}_L$	(BR')	$3(\bar{\mathbf{3}},\mathbf{1})$	-1	0	-1	0	1/3
L	$(L\ell)$	$3(\mathbf{1},\mathbf{2})$	0	-1	0	1	$-1/2$
$\overline{\nu}_L$	$(R\ell)$	$3(\mathbf{1},\mathbf{1})$	0	0	1	-1	0
$\overline{e}_L$	$(R\ell')$	$3(\mathbf{1},\mathbf{1})$	0	0	-1	-1	1

Table 5.5: The content of the standard model and its representation. Furthermore, the intersection in which the open strings are located is specified. The charges of the individual $U(1)$ generators, as well as the hypercharge are listed.

N_a	N_B	N_L	N_R	N_ℓ
$(n_a^{(1)}, m_a^{(1)})$	$(1,0)$	$(7,-1)$	$(9,9)$	$(1,0)$
$(n_a^{(2)}, m_a^{(2)})$	$(0,1)$	$(1,0)$	$(1,0)$	$(2,\frac{1}{3})$
$(n_a^{(3)}, m_a^{(3)})$	$(\frac{1}{3},\frac{1}{2})$	$(1,\frac{9}{2})$	$(0,1)$	$(1,-\frac{9}{2})$

Table 5.6: The wrapping numbers for the model A resulting from four stacks of D6-branes. The wrapping numbers are given in such a way, that the first two 2-tori are considered to be rectangular, while the last 2-torus is tilted.

Once more we can calculate the intersection numbers, which are given by

$$
\begin{aligned}
I_{BL} &= +1 \quad \rightarrow \quad 1\,(\mathbf{3},\mathbf{2}), \quad I_{BL'} = +2 \quad \rightarrow \quad 2\,(\mathbf{3},\mathbf{2}) \\
I_{BR} &= -3 \quad \rightarrow \quad 3\,(\overline{\mathbf{3}},\mathbf{1}), \quad I_{BR'} = -3 \quad \rightarrow \quad 3\,(\overline{\mathbf{3}},\mathbf{1}) \\
I_{L\ell} &= -3 \quad \rightarrow \quad 3\,(\mathbf{1},\mathbf{2}), \quad I_{L\ell'} = 0 \\
I_{R\ell} &= +3 \quad \rightarrow \quad 3\,(\overline{\mathbf{1}},\mathbf{1}), \quad I_{R\ell^*} = -3 \quad \rightarrow \quad 3\,(\overline{\mathbf{1}},\mathbf{1})
\end{aligned}
\tag{5.57}
$$

As previous, we have also listed the corresponding representations. If we compare these intersection numbers with those of model a, they agree as expected. The tadpole condition in Eq. (5.38) for Model B results in

$$
\frac{3n_B^{(2)}}{\rho\beta^1} + \frac{2n_L^{(1)}}{\beta^2} + \frac{n_\ell^{(2)}}{\beta^1} + 2N_h n_h^{(1)} n_h^{(2)} = 0 + 14 + 2 + 2N_h n_h^{(1)} n_h^{(2)} \stackrel{!}{=} 16 \tag{5.58}
$$

This is a difference from the previous model A. The tadpole condition is satisfied without having to introduce a hidden brane. In such a model there is therefore no hidden sector along the orientifold projection. If follows that $N_h = 0$.

The BF couplings of the $U(1)$'s to the RR fields of model B are:

$$
\begin{aligned}
i = 1: &\qquad -2\int B_1 \wedge \mathrm{tr}\,(F_L) \ . \\
i = 2: &\qquad \frac{1}{3}\int B_2 \wedge \mathrm{tr}\,(3F_B + F_\ell) \ . \\
i = 3: &\qquad \int B_3 \wedge \mathrm{tr}\,(63F_L + 9F_R - 9F_\ell) \ .
\end{aligned}
\tag{5.59}
$$

From this three terms we can read off the coefficients and form the matric $\mathbf{C}$. We thus find

$$
(\mathbf{C})_{i\alpha} = \begin{pmatrix} 0 & -2 & 0 & 0 \\ 1 & 0 & 0 & \frac{1}{3} \\ 0 & 63 & 9 & -9 \end{pmatrix} . \tag{5.60}
$$

Computing the kernel of $\mathbf{C}$ yields

$$
\mathrm{Ker}(\mathbf{C}) = \left\{ \left(-\tfrac{\zeta}{3}, \quad 0, \quad \zeta, \quad \zeta \right) \ : \zeta \in \mathbb{R} \right\} . \tag{5.61}
$$

This kernel indeed leads to the right hypercharge generator

$$
Q_Y = \frac{1}{6}Q_B - \frac{1}{2}Q_R - \frac{1}{2}Q_\ell \ . \tag{5.62}
$$

This analysis naturally leads to the content in Tab. (5.5). We have seen that regardless of the choice of parameters, the same standard model spectrum is generated using the orientifold projections. However, they differ in detail. On the one hand, of course, the wrapping numbers run differently on the 2-tori and, on the other hand, hidden sectors have to be introduced most of the time. In these models, however, these always run along an O6-plane by construction. This concept of hidden branches, i.e., branes that are decoupled from the standard model but still interact with it via open strings, will be briefly addressed again at the very end of the thesis.

Chapter 6

Towards Supersymmetric Standard Models and Beyond

In this chapter, we will super-symmetrically fine-tune the concepts from the previous chapter. Before introducing a $\mathcal{N}=1$ supersymmetric MSSM-like spectrum by using a D6-brane setup, we want to introduce an alternative route to a non-supersymmetric standard model, which will be helpful in the further proceedings.

This model will give us another way to prevent the theory from generating extra $SU(2)$ doublets. To make this possible, we will use the isomorphism $USp(2) \simeq SU(2)$. Although we can generate the spectrum of the SM with such a model, it is not RR tadpole free.

To create a $\mathcal{N}=1$ supersymmetric standard model we need an orbifold in addition to the orientifold projection, which ensures that all RR contributions of the $D6$-branes are cancelled. We will investigate such a model using a $\mathbb{T}^6/(\mathbb{Z}_2 \times \mathbb{Z}_2)$ orbifold. We will keep the original idea of the non-supersymmetric model and extend it accordingly. Finally, we will see that by means of brane recombination, we can obtain a Pati-Salam model - and thus a minimal supersymmetric standard model. This is particularly interesting as it goes beyond the supersymmetric spectrum of a minimal supersymmetric standard model and attempts to create a grand unified theory.

6.1 An Alternative Route to a non-supersymmetric Standard Model

Looking back at chapter 4, we recall that an orientifold projection on the homology of $\mathbb{T}^6$ yields us pairs $(\Pi_a, \Pi_a^{'})$. $\mathcal{R}$ again denotes the $\mathbb{Z}_2$ involution on the internal manifold. In the previous chapter 5, we exploited the fact that we obtain a string charged $U(N_a)$ gauge group through N_a D6-branes on Π_a if $\mathcal{R}(\Pi_a) \neq \Pi_a$. In general, however, $\mathcal{R}(\Pi_a) = \Pi_a$ can hold and thus the induced gauge group is the $SO(2N_a)$ or the symplectic $USp(2N_a)$, which we discussed in more detail in section 4.3 [17,63]. In the further development we want to benefit from this possibility to generate an MSSM-like spectrum. By the isomorphism $USp(2) \simeq SU(2)$ [175] we can generate in our setup the weak interaction sector of $SU(2)_L$ thus with just one left brane, which is fixed under the action of $\mathcal{R}$.

Under these conditions, we will construct the non-supersymmetric standard model which we already considered in the previous chapter 5. For this purpose, we need four different stacks of D6-branes. A $N_B = 3$ baryonic brane, a $N_L = 1$ $USp(2)$ left brane, a $N_R = 1$ right brane and a

N_a	N_B	N_L	N_R	N_ℓ
$(n_a^{(1)}, m_a^{(1)})$	$(1,0)$	$(0,1)$	$(0,1)$	$(1,0)$
$(n_a^{(2)}, m_a^{(2)})$	$(\frac{1}{\rho}, 3\rho)$	$(1,0)$	$(0,-1)$	$(\frac{1}{\rho}, 3\rho)$
$(n_a^{(3)}, m_a^{(3)})$	$(\frac{1}{\rho}, -3\rho)$	$(0,-1)$	$(1,0)$	$(\frac{1}{\rho}, -3\rho)$

Table 6.1: The wrapping numbers for the model A resulting from four stacks of D6-branes. The wrapping numbers are given in such a way, that the first two 2-tori are considered to be rectangular, while the last 2-torus is tilted.

$N_\ell = 1$ leptonic brane. Hence, we find the gauge group[1]

$$U(3)_B \times USp(2)_L \times U(1)_R \times U(1)_\ell \simeq SU(3)_c \times U(1)_B \times SU(2)_L \times U(1)_R \times U(1)_\ell \ . \tag{6.1}$$

The wrapping numbers for this particular setup are selected according to Tab. 6.1 [63, 171–174]. This ensures that the left bane is positioned in such a way that it is overlapping with its image brane on all three 2-tori. The D6-brane setup is depicted in Fig. 6.1. We will again use our developed scheme to analyse such D-brane constructions. According to the wrapping numbers in Tab. 6.1, the desired intersection numbers are given by

$$\begin{array}{lllll} I_{BL} = 3; & I_{BL'} = 3; & I_{BR} = -3; & I_{BR'} = -3; & I_{LR} = 1; \\ I_{\ell L} = 3; & I_{\ell L'} = 3; & I_{\ell R} = -3; & I_{\ell R'} = -3 & I_{LR'} = 1; . \end{array} \tag{6.2}$$

In this model, there are three $U(1)$'s, i.e. a $U(1)_B$, a $U(1)_R$ and a $U(1)_\ell$. Analysing the BF terms, we get only one contribution for the linear combination $3Q_B + Q_\ell$, independent of the choice of ρ. In full, these two terms are given by

$$3 \int B_2 \wedge \mathrm{tr}\,(3F_B + F_\ell) \quad \text{and} \quad -3 \int B_3 \wedge \mathrm{tr}\,(3F_B + F_\ell) \ . \tag{6.3}$$

According to the Green-Schwarz mechanism, this anomalous $U(1)$[2] gets a Stückelberg mass and decouples from the low energy spectrum. The remaining $U(1)$'s get no mass and correspond to massless gauge bosons. For the light $U(1)$'s we identify $3Q_B - Q_\ell$ with $B - L$ and Q_R with the 3$^{\text{rd}}$ component of the weak isospin. The hypercharge is again given by the kernel of the matrix C, which we introduced in section 5.4.1. This can be conveniently calculated, and we get

$$\mathrm{Ker}(\mathbf{C}) = \left\{ \begin{pmatrix} -\zeta, & \eta, & 3\zeta \end{pmatrix} \ : \zeta, \eta \in \mathbb{R} \right\} . \tag{6.4}$$

The hypercharge is consequently given by

$$Q_Y = \frac{1}{6} Q_B - \frac{1}{2} Q_R - \frac{1}{2} Q_\ell \ . \tag{6.5}$$

Thus, the gauge group resulting from this setup is [3]

$$SU(3)_C \times SU(2)_L \times U(1)_{B-L} \times U(1)_R \ . \tag{6.6}$$

[1] We emphasise, that in this case we get no $U(1)_L$.

[2] The rank of the matrix C is rank(C) = 1.

[3] This group is now different from our previous one in the non-supersymmetric model, since there is another massless $U(1)$. However, as we know, also non-anomalous $U(1)$'s can get a Stückelberg mass. This depends only on the choice of our homology cycles Π_a with $a = B, L, R, \ell$. Since we are interested in the Grand Unification Theory here, this aspect will not concern us further.

Fields	Intersections	Representation	$\mathbf{Q_B}$	$\mathbf{Q_R}$	$\mathbf{Q_\ell}$	$\mathbf{Y}$
Q_L	(BL)	$3(\mathbf{3},\mathbf{2})$	1	0	0	1/6
$\overline{u}_L$	(BR)	$3(\bar{\mathbf{3}},\mathbf{1})$	−1	1	0	−2/3
$\overline{d}_L$	(BR')	$3(\bar{\mathbf{3}},\mathbf{1})$	−1	−1	0	1/3
L	(ℓL)	$3(\mathbf{1},\mathbf{2})$	0	0	1	−1/2
$\overline{\nu}_L$	(ℓR)	$3(\mathbf{1},\mathbf{1})$	0	1	−1	0
$\overline{e}_L$	$(\ell R')$	$3(\mathbf{1},\mathbf{1})$	0	−1	−1	1
H	(LR)	$(\mathbf{1},\mathbf{2})$	0	−1	0	1/2
$\overline{H}$	(LR')	$(\mathbf{1},\mathbf{2})$	0	1	0	−1/2

Table 6.2: Content of the standard model, which emerges through the intersections of a baryonic, left, right, and leptonic brane. The left brane is thereby incorporated in such a way that it induces a $USp(2)$ gauge group. In this model, we obtain three $U(1)$ generators.

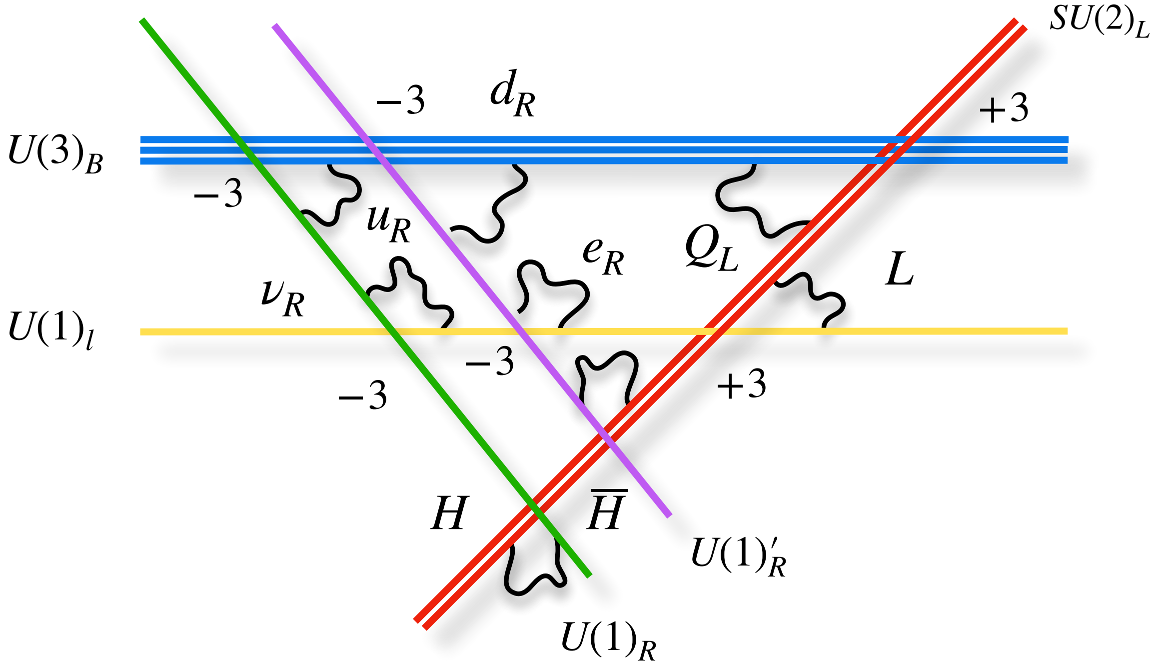

Figure 6.1: Schematic diagram for the construction of a minimal non-supersymmetric standard model. A $N_B = 3$ baryonic brane, a $N_R = 1$ right, and $N_\ell = 1$ leptonic branes are used. Further, we have a stack of left branes, which overlap with their images, yielding $USp(2) \equiv SU(2)$. To make the illustration clearer, we only depicted the relevant branes.

Since we have found a hypercharge in Eq. (6.5) we can determine the spectrum. We also note that this model has intersections between the left and right brane. As previously pointed out, near such intersection strings associated to the Higgs particle are located.

However, as pointed out in [63] and [17], such setups are not RR tadpole free and in the following unstable and thus need additional branes to satisfy these conditions.

With this said, we have provided an alternative to the previous construction, since we avoided unnecessary $SU(2)_L$ doublets - but it gets even better, as we can modify this model to a Pati-Salam-like model of the form

$$SU(4)_C \times USp(2)_L \times USp(2)_R \ . \tag{6.7}$$

6.2 Minimal Supersymmetric Standard Model in $\mathbb{T}^6/(\mathbb{Z}_2 \times \mathbb{Z}_2)$ Orbifolds with Orientifold Projection

6.2.1 The $\mathbb{T}^6/(\mathbb{Z}_2 \times \mathbb{Z}_2)$ Orbifold

It turns out that in general it is not possible to obtain a semi-realistic $\mathcal{N}=1$ supersymmetric standard model spectrum using D6-branes in type IIA string theory with O6-planes on a $\mathbb{T}^6$ compactification. We have already indicated this problem in chapter 4. One can understand this also from the point of view of the tadpole conditions. Most of the conditions in Eq. (4.38) tell us that there are D6-brane contributions to Ramond-Ramond charges that do not have an O6-plane contribution. This means that there must be an inherent brane-antibrane relation [17] in order to obtain these models free of any tadpoles. This obviously destroys supersymmetry. Nevertheless, in this section we want to give a quick idea of how this can be circumvented and a semi-realistic MSSM spectrum can be constructed.

The focus hereby is not on deriving the first supersymmetric model, as this has already been done many times in the past. The goal is to understand this particular model in our context and why it allows for a supersymmetric spectrum compared to the previous models. Furthermore, there is no complete source[4] for this model where this model is analysed in more detail, e.g., the computation for the right hypercharge. Therefore, we want to analyse it again strictly according to our scheme. Before we dive into this topic, we want to clarify some technical details were we mainly follow [63].

In order to obtain a four-dimensional $\mathcal{N}=1$ supersymmetric chiral spectrum, we will introduce the concept of orbifolds. Roughly speaking, we have to solve the problem just discussed and make sure that there are enough O6-planes. For simplicity, we will refer to a particular orientifold of toroidal orbifolds. The particular model we choose is given by

$$\frac{\mathbb{T}^6}{\mathbb{Z}_2 \times \mathbb{Z}_2 \times \Omega_{\mathcal{P}}\mathcal{R}(-)^{\mathcal{F}_L}} \ . \tag{6.8}$$

In such an $\mathbb{T}^6/(\mathbb{Z}_2 \times \mathbb{Z}_2)$ orientifold we have two new generators which we denote by θ and ω. These generators we associate with the two twist or shift vectors $\vec{v} = (\frac{1}{2}, -\frac{1}{2}, 0)$ and $\vec{w} = (0, \frac{1}{2}, -\frac{1}{2})$ [63].

We can explicitly state the action of these generators on our factorisable $\mathbb{T}^6$ space as

$$\begin{aligned} \theta &: (z_1, z_2, z_3) \to (-z_1, -z_2, z_3) \ , \\ \omega &: (z_1, z_2, z_3) \to (z_1, -z_2, -z_3) \ , \end{aligned} \tag{6.9}$$

where we use complex coordinates z_i on the torus as usual. However, since we still have an orientifold projection in addition, this model is also modded out under the action $\Omega\mathcal{R}(-)^{\mathcal{F}_L}$

[4]At least the author of this thesis is not aware of it.

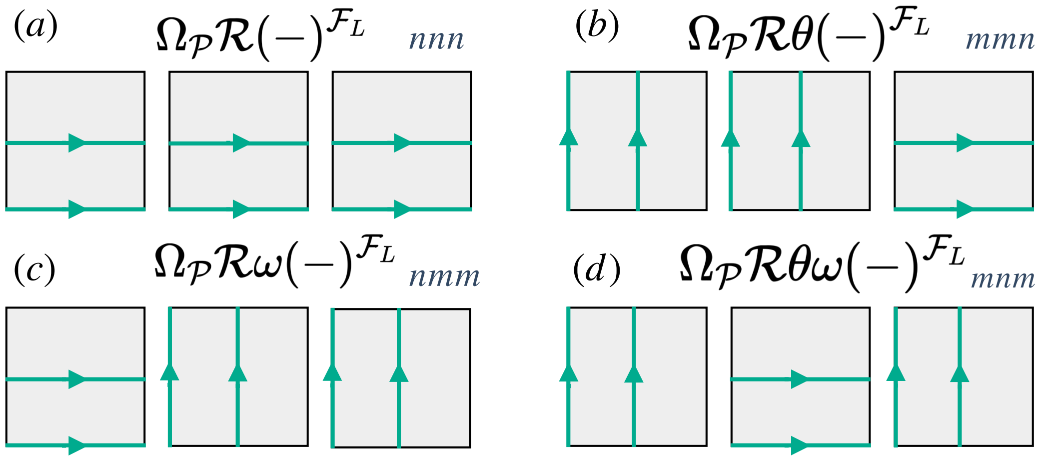

Figure 6.2: In (a), the original orientifold planes, which we have already discussed for the case without orbifolds, are drawn in the factorisable $\mathbb{T}^6 = \mathbb{T}^2 \times \mathbb{T}^2 \times \mathbb{T}^2$. In (b), (c) and (d), however, we obtain further orientifold planes which arise via the θ and ω action.

according to

$$\mathcal{R} : (z_1, z_2, z_3) \rightarrow (\bar{z}_1, \bar{z}_2, \bar{z}_3) \ . \tag{6.10}$$

In summary, there are four different types of O6-planes in this model under these actions. The actions under which they appear are

$$\begin{array}{cc} \Omega_{\mathcal{P}}\mathcal{R}\theta(-)^{\mathcal{F}_L}\,, & \Omega_{\mathcal{P}}\mathcal{R}\omega(-)^{\mathcal{F}_L}, \\ \Omega_{\mathcal{P}}\mathcal{R}\theta\omega(-)^{\mathcal{F}_L}\,, & \Omega_{\mathcal{P}}\mathcal{R}(-)^{\mathcal{F}_L}\ . \end{array} \tag{6.11}$$

These additional O6-planes, originating from the orbifolding, are illustrated in Fig. 6.2. The eight O6-planes of each type wrap 3-cycles in the 6-torus with the wrapping numbers

$$\begin{array}{rl} (1,0)\times(1,0)\times(1,0); & (0,1)\times(0,-1)\times(1,0), \\ (1,0)\times(0,1)\times(0,-1); & (0,-1)\times(1,0)\times(0,1)\ . \end{array} \tag{6.12}$$

Further, we agree that the D6-branes must pass through fix-points of the orbifold projection. Thus, we make sure that they match their orbifold images, but not those of the orientifold projection. For rectangular tori we also obtain the modified tadpole conditions

$$\begin{array}{ll} \sum_a N_a n_a^1 n_a^2 n_a^3 - 16 = 0, & \sum_a N_a n_a^1 m_a^2 m_a^3 + 16 = 0\ , \\ \sum_a N_a m_a^1 n_a^2 m_a^3 + 16 = 0, & \sum_a N_a m_a^1 m_a^2 n_a^3 + 16 = 0\ . \end{array} \tag{6.13}$$

We can conclude that all D6-brane contributions to Ramond-Ramond charges have an O6-plane contribution. The particle content arising from the D6-brane intersections is the same as in the orientifold case, but in the $\mathrm{D}_a\mathrm{D}_a$ sector we obtain a $U(N_a/2)$ vector multiplets plus 3 adjoint chiral multiplets [63].

6.2.2 Going Beyond the SM - The Pati-Salam Model

The standard model is most likely not a final theory and leaves generations of physicists with unsolved questions. Among these questions, there is a particularly fundamental one, asking, why the local gauge interaction with three families of quarks and leptons has exactly the structure $SU(3)_c \times SU(2)_L \times U(1)_Y$. These SM gauge interactions are determined by their gauge charges, whose origin of the charge quantisation is however unexplained. This would give us means to explain why there are no fractionally charged hadrons. Another big problem in particle physics is the unexplained origin of the *hierarchy of family masses* and the quark and leptonic mixing angles. These answers would help to find the origin of the *CP violation*, the *cosmological matter-antimatter symmetry*, and would also provide an explanation for the observable *dark energy* and *dark matter*. Moreover, the SM is not complete, and 19 parameters must be included in the theory by hand. These parameters contain the three gauge couplings g_c, g_L and g_Y. Nine parameters are associated with fermion masses, four with the mixing angles in the CKM[5] matrix. Furthermore, there is the QCD parameter θ and three parameters in connection with the Higgs *vacuum expectation value* (VEV) and quartic coupling. Last but not least, the SM per se fails to provide an explanation for the mass of neutrinos [176, 177].

Those unsolved problems but also the human striving for an aesthetic and simplified final truth have triggered the cry for a grand unified theory.

These GUT's raise the claim that in a very early epoch of the universe and thus at very high energies[6] the fundamental interactions unify into a single force. Howard Georgi and Sheldon Glashow were pioneers in this field and in 1974, they presented the first GUT based on the simple Lie group $SU(5)$ which clearly contains the SM[7].

In this thesis, however, we focus on a semi-simple solution proposed by Abdus Salam and Jogesh Pati [179]. The so-called Pati-Salam model (PSM), which is based on the group product

$$\mathcal{G}_{PS} = SU(4)_C \times SU(2)_L \times SU(2)_R \; . \tag{6.14}$$

This model follows the assumption that leptons and quarks are two faces of the same coin. Therefore, the $SU(3)_C$ is extended to a $SU(3+1)_C$ by adding another colour charge which originally was called *lilac* but is called *violet* today. We identify these violet quarks with the leptons. Furthermore, this model is left-right symmetric and can be embedded into the $SO(10)$ model [180–182].

The fermions in the PSM are embedded as follows:

$$\text{SM}: \qquad \underbrace{(\mathbf{3},\mathbf{2})_{1/6} + (\mathbf{1},\mathbf{2})_{-1/2}}_{\text{PSM} \to (\mathbf{4},\mathbf{2},\mathbf{1})} + \underbrace{(\overline{\mathbf{3}},\mathbf{1})_{1/3} + (\overline{\mathbf{3}},\mathbf{1})_{-2/3} + (\mathbf{1},\mathbf{1})_1 + (\mathbf{1},\mathbf{1})_0}_{\text{PSM} \to (\overline{\mathbf{4}},\mathbf{1},\mathbf{2})} \tag{6.15}$$

The $SU(2)_L$ quarks and fermion doublets are combined into a $(\mathbf{4},\mathbf{2},\mathbf{1})$ representation, denoted as F_L [8].

$$F_L = \begin{pmatrix} u_L^r & u_L^g & u_L^b & u_L^v = \nu_L \\ d_L^r & d_L^g & d_L^b & d_L^v = e_L \end{pmatrix} \; . \tag{6.17}$$

Analogously, the right-handed part is combined into F_R according to

$$F_R = \begin{pmatrix} u_R^r & u_R^g & u_R^b & u_R^v = \nu_R \\ d_R^r & d_R^g & d_R^b & d_R^v = e_R \end{pmatrix} \; . \tag{6.18}$$

We now focus on the concrete realisation of a semi-realistic standard model based on D6-branes wrapping on a 6-torus orbifold with an orientifold projection. Moreover, we will use it to construct

[5] Cabibbo–Kobayashi–Maskawa.

[6] The GUT scale is $\sim 10^{16}$ GEV and thus only a few orders of magnitude below the Planck scale.

[7] Historically, a few hours earlier Georgi found an unification based on the $SO(10)$ group, which is even more complete because $SO(10) \supset SU(5)$ [178].

[8] In order to reduce the number of individual gauge couplings, this group is often extended with an additional $\mathbb{Z}_2$ symmetry, reading

$$SU(3)_c \times SU(2)_L \times U(1)_{B-L} \times U(1)_R \times \mathbb{Z}_2 \; . \tag{6.16}$$

Thus, the multiplets can be considered as a single reducible representation $F_L \oplus F_R$. We will neglect this detail here.

N_a	$(n_a^{(1)}, m_a^{(1)})$	$(n_a^{(2)}, m_a^{(2)})$	$(n_a^{(3)}, m_a^{(3)})$
$N_B = 6$	$(1, 0)$	$(3, 1)$	$(3, -1)$
$N_L = 2$	$(0, 1)$	$(1, 0)$	$(0, -1)$
$N_R = 2$	$(0, 1)$	$(0, -1)$	$(1, 0)$
$N_\ell = 2$	$(1, 0)$	$(3, 1)$	$(3, -1)$

Table 6.3: Modified D6-brane wrapping numbers form Tab. 6.1 giving rise to a chiral spectrum of the standard model. The particular value of ρ is chosen to be $\frac{1}{3}$

a Pati-Salam model. Here, we combine the already found results of the model in section 7.1 and assume, however, that we additionally have an orbifold structure.

We choose the wrapping numbers according to Tab. 6.3 which we already used in the non-supersymmetric model.

To ensure $\mathcal{N} = 1$ supersymmetry, the D6-branes must be related to the O6-planes via a $SU(3)$ rotation. The general condition, which we deduced in section 3.3, was given by

$$\sum_{i=1}^{3} \theta_i = 0 \ . \tag{6.19}$$

Using the tangent and the trigonometric identity

$$\tan(\alpha + \beta) = \frac{\tan\alpha + \tan\beta}{1 - \tan\alpha \tan\beta} \tag{6.20}$$

we get

$$\tan\theta_1 + \tan\theta_2 + \tan\theta_3 - \tan\theta_1 \tan\theta_2 \tan\theta_3 = 0 \tag{6.21}$$

In Eq. (4.11) we have established a relationship between the relative angles of the Dp-branes and the wrapping numbers. The tangent can thus be described by

$$\tan\theta_i = \frac{m^{(i)} R_2^{(i)}}{n^{(i)} R_1^{(i)}} = \frac{m^{(i)}}{n^{(i)}} j^{(i)} \tag{6.22}$$

with $j^{(i)} = \left(\frac{R_2}{R_1}\right)^{(i)}$. This becomes a requirement for the wrapping numbers which reads

$$m_1 m_2 m_3 - m_1 j_2 n_2 j_3 n_3 - m_2 j_3 n_3 j_1 n_1 - m_3 j_1 n_1 j_2 n_2 = 0 \tag{6.23}$$

[9] By just inserting the values from Tab. 6.3 into Eq. (6.22), we come to the conclusion that $j^{(2)} = j^{(3)}$.

[9]There are further discrete constraint coming from K-theory which states

$$\sum_a m_1^a m_2^a m_3^a \equiv \sum_a m_1^a n_2^a n_3^a \equiv \sum_a n_1^a m_2^a n_3^a \equiv \sum_a n_1^a n_2^a m_3^a \equiv 0 (\text{mod} 2) \tag{6.24}$$

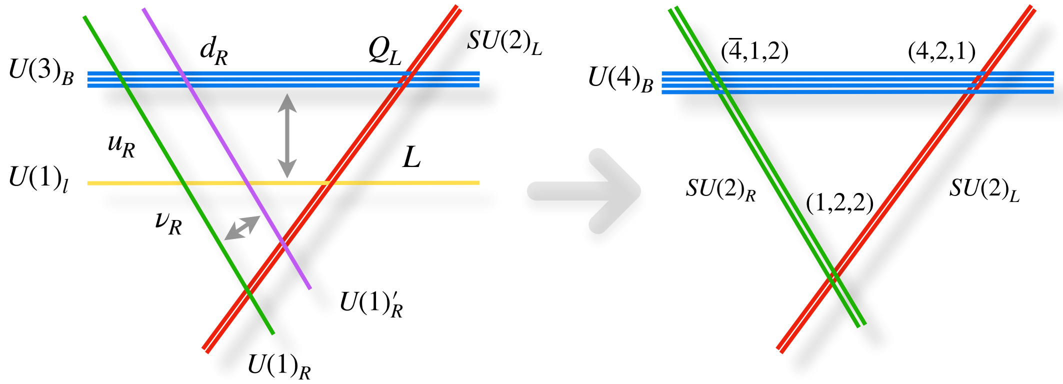

Figure 6.3: Illustration of D6-brane recombination. The leptonic brane and the baryonic brane recombine to form the $U(4)_C$, while the overlapping of the right brane with its image brane results in $SU(2)_R$. The result is a gauge group consisting of $SU(4)_C \times SU(2)_L \times SU(2)_R$.

But how do we get from the gauge group in Eq. (6.6) to the requested Pati-Salam model? To see that

$$SU(4)_C \times SU(2)_L \times SU(2)_R \rightsquigarrow SU(3)_C \times SU(2)_L \times U(1)_R \times \times U(1)_{B-L} \;, \tag{6.25}$$

consider the possibility that we can choose the 3-cycle $\Pi_R = \Pi_R'$ in our configuration. This gives us $U(1)_R \to USp(2)_R \simeq SU(2)_R$, as we have already seen for the left brane. This creates a left-right symmetric model. Moreover, we can also choose $\Pi_B = \Pi_\ell$. If these branes are on top of each other, we get $SU(3)_C \times U(1)_{B-L} \to SU(4)_C$. This results in the gauge group $SU(4)_C \times SU(2)_L \times SU(2)_R$, where the $U(1)_{B-L}$ sits now inside the $SU(4)_C$ [17]. Thus, we get a Pati-Salam spectrum which is broken down (spontaneously) to the standard model by means of brane separation. The Brane recombination and the D6-brane construction of the Pati-Salam model is depicted schematically in Fig. 6.3. The intersection numbers are easily calculated by using the wrapping numbers from Tab. 6.4 and given by

$$I_{BL} = 3, \quad I_{BR} = -3, \quad I_{LR} = 0 \; . \tag{6.26}$$

Someone may now wonder why there is a Higgs sector between the left and right brane despite the diminishing intersection number. This is a more subtle issue and would require T-duality, which we have dispensed in this thesis. However, it can be explained in such a way that there are indeed intersections between these branes. Specifically, in the latter two 2-tori. More can be found, e.g in [63].

However, this $\mathcal{N} = 1$ $\mathbb{Z}_2 \times \mathbb{Z}_2$ type IIA orientifold setup is not RR tadpole free and thus needs additional branes to satisfy the tadpole conditions in Eq. (6.13). In order to satisfy these equations, we have to add two additional D6-branes which we denote as $N_{h_1} = 2$, $N_{h_2} = 2$ and the filler brane $N_F = 40$. It is very easy to see that these extra branes are needed to satisfy the tadpole conditions. As an example, we show it for the first condition in Eq. (6.13).

The first tadpole conditions reads

$$\begin{aligned} \sum_a N_a n_a^1 n_a^2 n_a^3 &= (N_B = 8) \times 3 - (N_{h_1} = 2) \times 24 - (N_{h_2} = 2) \times 24 + (N_f = 40) \\ &= 72 - 96 + 40 = 16, \end{aligned} \tag{6.27}$$

which is exactly the desired result. Analogously, this can be shown for all other three conditions.

N_a	$(n_a^{(1)}, m_a^{(1)})$	$(n_a^{(2)}, m_a^{(2)})$	$(n_a^{(3)}, m_a^{(3)})$
$N_B = 6+2$	$(1,0)$	$(3,1)$	$(3,-1)$
$N_L = 2$	$(0,1)$	$(1,0)$	$(0,-1)$
$N_R = 2$	$(0,1)$	$(0,-1)$	$(1,0)$
$N_{h_1} = 2$	$(-2,1)$	$(-3,1)$	$(-4,1)$
$N_{h_2} = 2$	$(-2,1)$	$(-4,1)$	$(-3,1)$
$N_f = 40$	$(1,0)$	$(1,0)$	$(1,0)$

Table 6.4: The D6-brane wrapping numbers for the concrete realisation of the Pati-Salam model. The lower part corresponds to the wrapping numbers for the additional D6-branes needed to ensure global consistency.

Finally, to determine the hypercharge of this model, we turn to the BF terms. These terms for this model read

$$\begin{aligned} i = 1 &: 24 \int B_2^1 \wedge \mathrm{tr}\,(F_{h_1} + F_{h_2}) \\ i = 2 &: 4 \int B_2^2 \wedge \mathrm{tr}\,(6F_B + 4F_{h_1} + 3F_{h_2}) \\ i = 3 &: 4 \int B_2^3 \wedge \mathrm{tr}\,(6F_B + 3F_{h_1} + 4F_{h_2}) \end{aligned} \tag{6.28}$$

From these three equations, we can read off the coefficients and form the matrix $\mathbf{C}$. We thus find

$$(\mathbf{C})_{i\alpha} = \begin{pmatrix} 0 & 24 & 24 \\ 24 & 16 & 12 \\ -24 & 12 & 16 \end{pmatrix} \tag{6.29}$$

Computing the kernel of $\mathbf{C}$

$$\mathrm{Ker}(\mathbf{C}) = \left\{ \begin{pmatrix} \zeta, & -6\zeta, & 6\zeta, & \zeta \end{pmatrix} \ : \zeta \in \mathbb{R} \right\} . \tag{6.30}$$

This indeed leads to the right hypercharge generator [63]

$$Q_Y = \frac{1}{3} Q_B - 2\,(Q_{h_1} - Q_{h_2}) \ . \tag{6.31}$$

From here it is easy to determine the spectrum of the model. The content created by all these D6-branes is listed in the Tab. 6.6 [63]. Hence, we have found that our considerations lead to a four-dimensional $\mathcal{N} = 1$ supersymmetric Pati-Salam-like spectrum. In order to fulfil the RR tadpole conditions, we had to postulate an additional hidden sector. Moreover, the idea of recombination can be thought further and also applied to the hidden sector [183]. By recombining the branes $h_1, h_2^{'}$ and f, it can be shown [63] that the spectrum can be simplified even more. We list the result in Tab. 6.5 [63]. We thus actually obtain the spectrum corresponding to a

Matter	**Sector**	$\mathbf{SU(4)} \times \mathbf{SU(2)} \times \mathbf{SU(2)} \times [\mathbf{USp(40)}]$
F_L	(BL)	$3(4,2,1)$
F_R	(BR)	$3(\bar{4},1,2)$
H	(LR)	$(1,2,2)$
	(Lh)	$2(\bar{1},2,1)$
	(Rh)	$2(1,1,2)$

Table 6.5: The chiral four-dimensional an $\mathcal{N} = 1$ supersymmetric spectrum, which we obtain by recombination of the hidden D-branes.

left-right MSSM with a single Higgs particle. Unfortunately, we also get exotic leptonic matter. Nevertheless, it is remarkable how close one can get with such a simple D-brane configuration. Of course, one can try to get rid of the extra matter by considering somewhat more complicated orbifolds such as a $\mathbb{Z}_6$ orbifold, e.g., [184]. However, this model represents a toy model, which already allows to calculate and study phenomenological aspects of particle physics [185, 186].

Matter	Sector	$\mathbf{SU(4)} \times \mathbf{SU(2)} \times \mathbf{SU(2)} \times [\mathbf{USp(40)}]$	$\mathbf{Q_B}$	$\mathbf{Q_{h_1}}$	$\mathbf{Q_{h_2}}$	$\mathbf{Q_Y}$
F_L	(BL)	$3(4,2,1)$	1	0	0	1/3
F_R	(BR)	$3(\bar{4},1,2)$	-1	0	0	$-1/3$
H	(LR)	$(1,2,2)$	0	0	0	0
	(Bh_1^*)	$6(\bar{4},1,1)$	-1	1	0	5/3
	(Bh_2)	$6(4,1,1)$	1	0	1	$-5/3$
	(Lh_1)	$8(1,2,1)$	0	1	0	2
	(Lh_2)	$6(1,2,1)$	0	0	1	-2
	(Rh_1)	$6(1,1,2)$	0	1	0	2
	(Rh_2)	$8(1,1,2)$	0	0	1	-2
	$(h_1h_1^*)$	$46(111)$	0	2	0	4
	$(h_2h_2^*)$	$46(111)$	0	0	2	-4
	$(h_1h_2^*)$	$196(111)$	0	1	1	0
	(fh_1)	$(1,1,1) \times [40]$	0	-1	0	2
	(fh_2)	$(1,1,1) \times [40]$	0	0	-1	-2

Table 6.6: The chiral four-dimensional an $\mathcal{N}=1$ supersymmetric spectrum, which we obtain from the Pati-Salam model construction. [63]

Chapter 7

Light Stringy States and their Lifetime - A Quest for Dark Matter

In this chapter, we finally turn our attention to string phenomenology. Intersecting D-brane worlds allow a string scale M_s smaller than the Planck scale M_P. We will explicitly notice that in type IIA superstring theory the string scale depends on the volume of the compactified internal space. This potentially allows a string scale that could already show up signatures at some TeV in future collider experiments.

Concretely, we will focus phenomenologically on a not yet well explored topic: The lifetime of light stringy states raising from higher string state excitations near the intersections of the D-branes. On that account, we will determine the light stringy states at the intersections of three different stacks of D-branes enclosing a triangular area. Therefore, this will allow us to calculate the Yukawa couplings. Considering a certain Yukawa interaction between two fermions and a Higgs field, we will establish a connection between this Yukawa coupling and those of a twisted scalar field, which corresponds to a more massive copy of the Higgs particle and two fermions.

This will allow us to explore and study the decay rate and consequently the lifetime of the twisted Higgs field. Moreover, we will find that the lifetime of such a light stringy state depends on the relative angle between the D-branes. Choosing these angles small enough, the lifetime can be tuned into the order of the age of the universe. This eventually establishes a massive and very weak interacting field with a huge lifetime as a potential candidate for dark matter.

7.1 String Phenomenology and the String Scale

Having demonstrated that intersecting brane world scenarios provide a very powerful and rich framework to engineer semi-realistic constructions of the standard model and beyond, we will now turn to a phenomenological aspect that arises directly from such a model.

Phenomenological studies on such models are of particular interest, since D-branes – covering the Minkowski space $\mathbb{R}^{3,1}$ and wrapping cycles in a six-dimensional compact Calabi-Yau space – exhibit an exciting phenomenological advantage. They allow to adjust the string scale in such a way that so-called stringy resonances are already possible in the range of a few TeV [40, 54, 68].

To investigate this, we consider the ten-dimensional effective spacetime action for the type IIA superstring theory, which is roughly given by

$$\mathcal{S}_{\text{IIA}}^{(10d)} \supset \frac{M_s^8}{(2\pi)^7 g_s^2} \int_{\mathbb{R}^{3,1}\times\mathcal{X}^6} \mathcal{R}_{10d} \; + \; \frac{M_s^{p-3}}{(2\pi)^{p-2} g_s} \sum_a \int_{\mathbb{R}^{3,1}\times\Pi_a} \frac{1}{4} F_{ab}F^{ab} + \dots \tag{7.1}$$

The first part resembles an *Einstein-Hilbert type of action* and denotes the gravitational part, while the second part is a kinetic gauge term for the Dp-brane, which emerges from the expansion of the DBI action in Eq. (2.35). As usual, $\mathbb{R}^{3,1}$ is the physical four dimensional spacetime and $\mathbb{X}^6$ denotes the compactified Calabi-Yau manifold. In such a compactified space, the Dp-brane wraps a $(p-3)$-cycle, which we denote with Π_a. The constant g_s is the string coupling and the scale of the theory is given by the string mass M_s. Upon dimensional reduction, we obtain

$$\mathcal{S}_{\text{IIA}}^{(4d)} \supset \frac{M_s^8}{(2\pi)^7 g_s^2}\mathcal{V}_{\mathcal{X}^6}\int_{\mathbb{R}^{3,1}}\mathcal{R}_{4d} \;+\; \frac{M_s^{p-3}}{(2\pi)^{p-2}g_s}\,\mathcal{V}_{\Pi_a}\int_{\mathbb{R}^{3,1}}\frac{1}{4}F_{\mu\nu}F^{\mu\nu} + \dots \;, \tag{7.2}$$

where $\mathcal{V}_{\mathcal{X}^6}$ is the volume of the compact six-dimensional manifold $\mathcal{X}^6$ and $\mathcal{V}_{\Pi_a}$ is the volume wrapped by the $(p-3)$-cycle. The four dimensional Planck mass M_P is defined as

$$M_P^2 \equiv \frac{8\pi}{\kappa^2} \;, \tag{7.3}$$

where κ^2 is the Einstein gravitational constant. Comparing the coefficients of the first term in Eq. (7.2) with the canonical definition of the Einstein-Hilbert action, we find that the Planck mass is given by

$$M_P^2 = \frac{8M_s^8\mathcal{V}_{\mathcal{X}}}{(2\pi)^6 g_s^2} = \frac{8M_s^2 v_{\mathcal{X}}}{g_s^2} \tag{7.4}$$

In the last step of Eq. (7.4), we defined a dimensionless volume $v_{\mathcal{X}} \equiv \mathcal{V}_{\mathcal{X}}/\ell_s^6$ for the internal space in strings units via $\ell_s = 2\pi/M_s$. By looking at the second term in Eq. (7.2), we can read off the four dimensional Yang-Mills gauge coupling and find that

$$\frac{1}{g_{YM}^2} = \frac{M_s^{p-3}}{g_s(2\pi)^{p-2}}\mathcal{V}_{\Pi_a} = \frac{v_{\Pi_a}}{2\pi g_s} \;, \tag{7.5}$$

where we again defined $v_{\Pi_a} \equiv \mathcal{V}_{\Pi_a}/\ell_s^{p-3}$. Using the Planck mass and the gauge coupling, we can form a quantity which is independent of the string coupling scale obtaining

$$M_{\text{P}} g_{\text{YM}}^2 = \sqrt{32\pi^2} M_s \frac{\sqrt{v_{\mathcal{X}^6}}}{v_{\Pi_a}} \tag{7.6}$$

This already reveals the first compelling difference to heterotic string theory. In heterotic string theory, we – simply speaking – have no volumes on the right side of Eq. (7.6), which means that the string scale is within close range to the Planck scale. On top of that, we are able to examine the found expression in Eq. (7.6) more closely, since the right-hand side is experimentally accessible. The scale on which quantum gravity takes a predominant role is given by $M_{\text{P}} \simeq 1.22 \times 10^{19}$ GeV. Further, we take the Yang-Mills coupling g_{YM}^2 as well as the string coupling g_s^2 of order $\mathcal{O}(1)$ for perturbative reasons. Thus, in order to have $M_s \ll M_{\text{P}}$, we have to ensure that $\sqrt{v_{\mathcal{X}^6}}/v_{\Pi_a} \gg 1$. Moreover, Eq. (7.5) spoils that $v_{\Pi_a} \simeq \mathcal{O}(1)$, which results in $v_{\mathcal{X}^6} \gg 1$ [1]. This is also the reason why intersecting brane worlds are often called large extra dimension worlds [2]. This now allows to adjust the string scale for appropriate compactifications. Interesting possibilities arise, such as $M_s = M_{\text{GUT}}$, where the string scale coincides with the gauge coupling unification scale. The possibility of a string scale which already contains stringy resonances at some TeV is particularly interesting. This would allow experimental string physics

[1] However, there is a caveat. If we use D6-branes in a toroidal background, v_{Π_a} is of the same order as $\sqrt{v_{\mathcal{X}^6}}$, yielding $M_s \sim M_P$ [40].

[2] This is of course no contradiction with our physical perception. The inhabitants of Edwin A. Abbott's **Flatland** [187] would also be left open-mouthed by realising that a huge extra dimension is not accessible to them. Namely, the one that completes our three dimensional space. What the inhabitants can notice, however, are two-dimensional shadows in their two-dimensional world. In this sense, string phenomenology is to some extent the study of such artifacts in our four dimensional world.

and signature detection in future colliders. In order to approximate the string scale to the electroweak scale M_{EW} we also need at least two extra large dimensions in the compact space. To obtain such a scale, such dimensions should be in the size of millimetres [63]. Nevertheless, the extra dimensions cannot have arbitrary sizes, otherwise we would for example explore deviations from Newton's law. Such deviations could not be fount until today. Researchers like those in the Eöt-Wash Group around Eric Adelberger have taken up the challenge of testing Newton's law at sub-millimetre scales. Recent experimental research has found no deviations at a distance of 52 µm. They conclude that the toroidal radius should therefore be less than 30 µm, which corresponds to $M_s > 7\,\text{TeV}$ [188]. Of course, there are also other bounds on the extra dimensions, such as astrophysical ones, which set M_s even higher [63].

Therefore, a wide variety of phenomenological studies have been carried out in such models in recent years. This research includes anomalous Z' physics [189–203], stringy signatures [204–219], Kaluza-Klein states [220–226] and, of course, light stringy states, which we already mentioned in section 3.5.5.

The remainder of this chapter refers to the recent paper *"Lifetimes of light stringy states"* by Pascal Anastasopoulos and my humble self [41]. The most important investigations and results are to be presented here again.

7.2 Local Configuration and Light Stringy States

Recapitulating, we have observed that open strings are localised near the intersections of two stacks of D-branes. Those open strings transform in the bi-fundamental representation $(N, \overline{M})$ of the gauge group $U(N) \times U(M)$, producing massless chiral fields. Moreover, we not only obtain the massless content of the standard model, but a whole tower of additional states, which are exact copies of the state in terms of quantum numbers but differ in mass. The mass of such states is thereby proportional to the relative intersection angle according to [41]

$$M^2 \sim \theta M_s^2 \tag{7.7}$$

To perform explicit calculations, we will determine the configuration of the D-branes. In the following setup, the D-branes fill the Minkowski space as usual, while they wrap 3-cycles in the compactified internal space. Again, we choose this space as a factorisable 6-torus $\mathbb{T}^6 = \mathbb{T}^2 \times \mathbb{T}^2 \times \mathbb{T}^2$, which allows us to determine the vertex operators corresponding to the states. Furthermore, we consider three different stacks of D-branes. We refer to these as D$_a$-brane, D$_b$-brane, and D$_c$-brane. The D$_a$-brane is constituted by a stack of $N_a = 2$ coincident D-branes that provide the weak isospin charge and can be identified in sequence with the left branes discussed in the previous sections. The D$_b$-brane corresponds to a $N_b = 1$ right brane while the D$_c$-brane is a stack of $N_c = 3$ coincident branes, serving as a baryonic brane. These branes are arranged in each 2-torus so that they enclose a "triangle". A schematic sketch of this configuration is given in Fig. (7.1). In such a configuration, we get particles charged under $SU(3)_C$, $SU(2)_L$ and $U(1)_R$. More precisely, we have the following wrapping numbers in the first 2-torus

$$(n_a^1, m_a^1) = (0,1), \quad (n_c^1, m_c^1) = (3,1), \quad (n_b^1, m_b^1) = (1,0)\ . \tag{7.8}$$

The associated intersection numbers can be easily calculated and are $I_{ba} = 1$, $I_{ca} = 3$, $I_{cb} = -1$. Further, the hypercharge for this configuration reads

$$Q_Y = \frac{1}{6} Q_c + \frac{1}{2} Q_b\ . \tag{7.9}$$

A string running from the D$_c$-brane to the D$_a$-brane thus yields the representation $3 \times (\mathbf{3}, \mathbf{2})_{\frac{1}{6}}$, which can be associated to three generations of left-handed quarks Q_L. From the D$_b$-brane

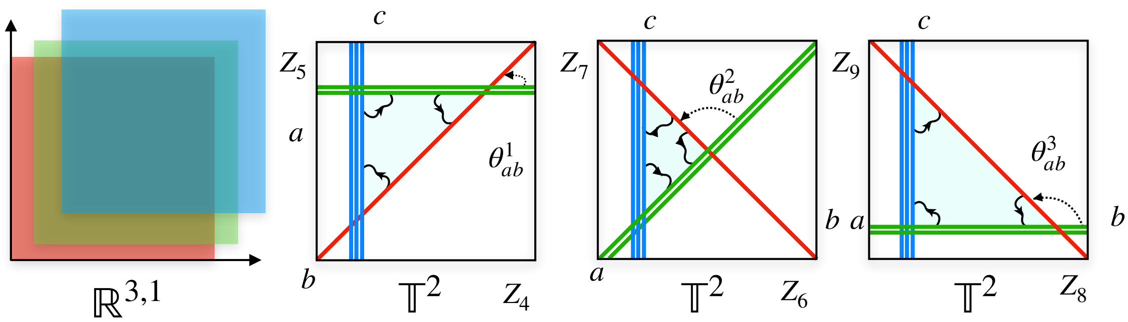

Figure 7.1: A depiction of our configuration: While the D-branes envelop the Minkowski space $\mathbb{R}^{3,1}$, they encircle 3-cycles within the six-dimensional internal compact space $\mathbb{T}^6$, decomposable into three 2-tori $\mathbb{T}^2$. The D-branes within these 2-tori can be portrayed by 1-cycles intersecting at non-trivial angles.

to the D$_a$-brane arises a $(\mathbf{1},\mathbf{2})_{\frac{1}{2}}$ representation, which has the right quantum numbers for a Higgs particle H [3]. Due to the negative intersection number, we finally find the representation $(\overline{\mathbf{3}},\mathbf{1})_{\frac{1}{3}}$ in the cb-sector. This represents a $\overline{d}_L$, or by switching the string orientation, a d_R in the representation $(\mathbf{3},\mathbf{1})_{-\frac{1}{3}}$.

The non-trivial intersection angles are choose in accordance with

$$a^1_{ab}>0,\qquad a^2_{ab}>0,\qquad a^3_{ab}<0,\qquad \sum a^i_{ab}=0\ . \tag{7.10}$$

$$a^1_{bc}>0,\qquad a^2_{bc}>0,\qquad a^3_{bc}<0,\qquad \sum a^i_{bc}=0\ . \tag{7.11}$$

$$a^1_{ca}<0,\qquad a^2_{ca}<0,\qquad a^3_{ca}<0,\qquad \sum a^i_{ca}=-2\ . \tag{7.12}$$

with the usual definition $a_i\equiv\frac{\theta}{\pi}$. Furthermore, we require our system to guarantee $\mathcal{N}=1$ supersymmetry, which translates into the requirement

$$a^1_{ab}+a^1_{bc}+a^1_{ca}=0\quad,\qquad a^2_{ab}+a^2_{bc}+a^2_{ca}=0\quad,\qquad a^3_{ab}+a^3_{bc}+a^3_{ca}=-2\quad. \tag{7.13}$$

The construction of the vertex operators in such a setup were discussed in detail in chapter 3. There, the ground-states of the NS and the R sector were explicitly determined, the mass squared operator was calculated, and the vertex operator was derived. For technical subtleties and details, we therefore refer to chapter 3.

7.2.1 The NS Sector for Light Stringy States

Starting in the NS sector and only focusing on the intersection between the D$_a$-brane and D$_b$-brane, we want to specify the ground state again for completeness. The zero state in the NS sector and the corresponding mass squared reads

$$\Phi(k):\quad \psi_{-\frac{1}{2}-a^3_{ab}}\left|a^1_{ab},a^2_{ab},a^3_{ab}\right\rangle_{\mathrm{NS}},\qquad \text{with}\qquad M^2=\frac{M_s^2}{2}\sum_i^3 a^i_{ab}=0\ , \tag{7.14}$$

where the mass turned out to vanish for a $\mathcal{N}=1$ supersymmetrical configuration. We further recall that we received the following vertex operator

$$V^{(-1)}_{\Phi}=g_{\Phi}\,[\Lambda_{ab}]^{\alpha_1}_{\beta_1}\,\Phi(x)e^{-\phi}\prod_{I=1}^{2}\sigma^+_{a^I_{ab}}\,e^{ia^I_{ab}H^I}\sigma^+_{1+a^3_{ab}}\,e^{i\left(1+a^3_{ab}\right)H^3}e^{ikX}\ . \tag{7.15}$$

[3] It is important to note that in supersymmetric models there generally are two Higgs particles H_u and H_d. In this discussion, we choose one of the two Higgs particles $H\equiv H_u$, since all considerations can be transferred to H_d.

Using BRST symmetry and the physical state condition (3.52), we could show that this corresponds to a massless scalar field. This procedure can now be generalised analogously to the so-called excitations. The first states in the tower which open in the NS sector are given by the pair

$$\widetilde{\Phi}_1(k) \;:\quad a_{a^1_{ab}}\psi_{-\frac{1}{2}-a^3_{ab}}|a^1_{ab},a^2_{ab},a^3_{ab}\rangle_{\rm NS}, \qquad \text{with} \qquad M^2 = M_s^2 a^1_{ab}\;, \tag{7.16}$$

$$\widetilde{\Phi}_2(k) \;:\quad \psi_{-\frac{1}{2}+a^2_{ab}}|a^1_{ab},a^2_{ab},a^3_{ab}\rangle_{\rm NS}, \qquad \text{with} \qquad M^2 = M_s^2 a^1_{ab}\;, \tag{7.17}$$

where we used Eq. (3.32) and the assumption, that the angle a^1_{ab} is smaller than the others.

Using Table (3.1), we can easily find out the corresponding vertex operators, obtaining

$$V^{(-1)}_{\widetilde{\Phi}_1} = g_\Phi[\Lambda_{ab}]^{\alpha_1}_{\beta_1}\,\widetilde{\Phi}_1(x)\,e^{-\phi}\;\tau_{a^1_{ab}}\;e^{ia^1_{ab}H_1}\;\sigma_{a^2_{ab}}\;e^{ia^2_{ab}H_2}\;\sigma_{1+a^3_{ab}}\;e^{i\left(1+a^3_{ab}\right)H_3}\;e^{ipX}\;, \tag{7.18}$$

$$V^{(-1)}_{\widetilde{\Phi}_2} = g_\Phi[\Lambda_{ab}]^{\alpha_1}_{\beta_1}\,\widetilde{\Phi}_2(x)\,e^{-\phi}\;\sigma_{a^1_{ab}}\;e^{ia^1_{ab}H_1}\;\sigma_{a^2_{ab}}\;e^{-i\left(1-a^2_{ab}\right)H_2}\;\sigma_{1+a^3_{ab}}\;e^{ia^3_{ab}H_3}\;e^{ipX}\;. \tag{7.19}$$

Applying the physical state condition (3.52) again, we find a double pole which vanishes for $p^2 + a^1_{ab}M_s^2 = 0$. This leads to the fact that these *first excited* states are physical bosonic fields, which form a massive complex scalar.

7.2.2 The R Sector for Light Stringy States

We will now repeat all the steps for the R sector. In section 3.5, we have discovered that the ground state in a *ab*-sector is given by

$$\Psi^\alpha(k): \quad \left|a^1_{ab},a^2_{ab},a^3_{ab}\right\rangle_{\rm R}, \qquad \text{with} \qquad M^2 = 0\;. \tag{7.20}$$

The mass squared operator vanishes independently of the choice of angles. Further, we obtained the vertex operator

$$V^{(-1/2)}_\psi = g_\psi\,[\Lambda_{ab}]^{\alpha_1}_{\beta_1}\,e^{-\varphi/2}v^\alpha S_\alpha \prod_{I=1}^{2}\sigma_{\theta^I_{ab}}e^{i\left(\theta^I_{ab}-\frac{1}{2}\right)H_I}\sigma_{1+\theta^3_{ab}}e^{i\left(\theta^3_{ab}+\frac{1}{2}\right)H_3}e^{ikX}\;. \tag{7.21}$$

The existence of a simple pole required us to demand the equation of motion of a massless Weyl fermion $k^\mu\bar\sigma^{\dot\alpha\alpha}_\mu v_\alpha(k)=0$. Consequently, the first light stringy states are given by

$$\widetilde{\Psi}^1_1: \quad \psi_{-a^1_{ab}}\,|a^1_{ab},a^2_{ab},-a^3_{ab}\rangle_{\rm R}\,, \qquad \text{with} \qquad M^2 = M_s^2 a^1_{ab}\;, \tag{7.22}$$

$$\widetilde{\Psi}^1_2: \quad \alpha^1_{-a_{ab}}\,|a^1_{ab},a^2_{ab},-a^3_{ab}\rangle_{\rm R}\,, \qquad \text{with} \qquad M^2 = M_s^2 a^1_{ab}\;. \tag{7.23}$$

Table 3.2 yields the associated vertex operators, which are given by

$$\begin{aligned}
V^{(-1/2)}_{\tilde\psi_1} &= g_\psi\,[\Lambda_{ab}]^\beta_\alpha\,\tilde v^\alpha_\psi e^{-\phi/2}S_\alpha\tau_{a^1_{ab}}e^{ia^1_{ab}-\frac{1}{2}H_1}\sigma_{a^2_{ab}}e^{ia^2_{ab}-\frac{1}{2}H_2}\sigma_{1+a^3_{ab}}e^{ia^3_{ab}+\frac{1}{2}H_3}e^{ikX}\;,\\
V^{(-1/2)}_{\tilde\psi_2} &= g_\psi\,[\Lambda_{ab}]^\beta_\alpha\,\overline{\tilde u}^{\dot\alpha}_\psi e^{-\phi/2}C_{\dot\alpha}\sigma_{a^1_{ab}}e^{ia^1_{ab}+\frac{1}{2}H_1}\sigma_{a^2_{ab}}e^{ia^2_{ab}-\frac{1}{2}H_2}\sigma_{1+a^3_{ab}}e^{ia^3_{ab}+\frac{1}{2}H_3}e^{ikX}\;.
\end{aligned} \tag{7.24}$$

Apart from the usual double pole, which vanishes for $p^2 = M_s^2 a^1_{ab}$, we get a single pole that vanishes if we combine the two vertex operators according to $V^{(-1/2)}_{\tilde\psi} = V^{(-1/2)}_{\tilde\psi_1} + V^{(-1/2)}_{\tilde\psi_2}$. From that, we obtain a Dirac equation in terms of a left and right-handed Weyl component.

$$\tilde v_\alpha\sqrt{\alpha'}k^\mu\sigma^{\alpha\dot\alpha}_\mu + \sqrt{\theta^1_{ab}}\overline{\tilde u}_{\dot\alpha} = 0 \quad , \quad \overline{\tilde u}_{\dot\alpha}\sqrt{\alpha'}k_\mu\bar\sigma^{\dot\alpha\alpha}_\mu + \sqrt{\theta^1_{ab}}\tilde v_\alpha = 0\;. \tag{7.25}$$

for the case under consideration, we will not need higher excitations, but the ground states for the *bc* and *ca* sectors. The ground-states are simply

$$\psi(k): \quad \left|a^1_{bc},a^2_{bc},a^3_{bc}\right\rangle_{\rm R} \qquad \text{and} \qquad \chi(k): \quad \left|a^1_{ca},a^2_{ca},a^3_{ca}\right\rangle_{\rm R}\;, \tag{7.26}$$

with the vertex operators

$$\begin{aligned} V_{\psi}^{(-\frac{1}{2})} =& g_{\psi}\, [\Lambda_{bc}]^{\beta}_{\gamma}\, \psi_i^{\alpha} e^{-\phi/2} S_{\alpha} \sigma_{a^1_{bc}} e^{i\left(a^1_{bc}-\frac{1}{2}\right)H_1} \sigma_{a^2_{bc}} e^{i\left(a^2_{bc}-\frac{1}{2}\right)H_2} \sigma_{1+a^3_{bc}} e^{i\left(a^3_{bc}+\frac{1}{2}\right)H_3} e^{ikX} , \\ V_{\chi}^{(-\frac{1}{2})} =& g_{\chi}\, [\Lambda_{ca}]^{\alpha}_{\beta}\, \chi_i^{\alpha} e^{-\phi/2} S_{\alpha} \sigma_{1+a^1_{ca}} e^{i\left(a^1_{ca}+\frac{1}{2}\right)H_1} \sigma_{1+a^2_{ca}} e^{i\left(a^2_{ca}+\frac{1}{2}\right)H_2} \sigma_{1+a^3_{ca}} e^{i\left(a^3_{ca}+\frac{1}{2}\right)H_3} e^{ikX} . \end{aligned} \tag{7.27}$$

7.3 The Twisted and Untwisted Yukawa Couplings

Yukawa couplings are an essential part of the standard model and describe the coupling of the Higgs field to the quarks and leptons. Via the breaking of spontaneous symmetry these fermions gain a mass proportional to the vacuum's expectation value of the Higgs field. It is crucial for a standard model realisation by D-branes to describe such Yukawa couplings and great effort has been done in the past to make this possible. In the following, we are interested in the scenario where two massless fermions couple to a massless scalar or in other words, in a Yukawa coupling corresponding to $Q_L d_R H$ given by our configuration. This has been calculated in detail, which is beyond the scope of this thesis, so we refer to the relevant literature for further detail [227–229]. Further, we will refer to the fields associated with the ground states as untwisted fields, while the light stringy states will be baptised twisted fields.

The Yukawa coupling for the *untwisted* fields – according to our configuration – , which can be computed from the vertex operators in the previous section 7.2, is given by

$$|Y_{\Phi\,\psi\,\chi}| = g_{\rm op}(2\pi)^{-\frac{3}{4}} \left[\Gamma_{1-a^1_{ab},1-a^1_{bc},-a^1_{ca}} \Gamma_{1-a^2_{ab},1-a^2_{bc},-a^2_{ca}} \Gamma_{-a^3_{ab},-a^3_{bc},-a^3_{ca}}\right]^{\frac{1}{4}} \prod_{i=1}^{3} e^{-\frac{A^{(i)}_{\phi\psi\chi}}{2\pi\alpha'}} , \tag{7.28}$$

where we used that

$$\Gamma_{a,b,c} \equiv \frac{\Gamma(a)\Gamma(b)\Gamma(c)}{\Gamma(1-a)\Gamma(1-b)\Gamma(1-c)} . \tag{7.29}$$

The symbol $A^{(i)}_{\phi\psi\chi}$ represents a triangular area, determined by the points $f_{\psi,i}$, $f_{\chi,i}$, and $f_{\phi,i}$ within the $i^{\rm th}$ 2-torus. The computation of these three points in the $i^{\rm th}$ 2-torus follows the formula:

$$f_{\psi\chi,i} = g^i - f^i_I + n_i \widetilde{L}^i_c . \tag{7.30}$$

The points of intersection between the D_a-brane and the D_c-brane within the corresponding $\mathbb{T}^i$ are denoted by g^i. Similarly, the intersection points between the D_b-brane and the D_c-brane are characterized by f^i_I. Lastly, the length $\widetilde{L}^i_c$ is defined[4] by

$$\widetilde{L}^i_c = \frac{|I_{ab}|}{\gcd\left(|I_{ab}|, |I_{bc}|, |I_{ac}|\right)} L^i_c , \tag{7.31}$$

All together, we get a closed expression for the triangle area, described by

$$A^{(i)}_{\phi\psi\chi} = \frac{1}{2} \left| \frac{\sin \pi a^i_{bc} \sin \pi a^i_{ca}}{\sin \pi a^i_{ab}} \right| |f_{\chi\psi,i}|^2 , \tag{7.32}$$

To illustrate these rather intricate definitions, we accompany them with an illustrative depiction. Figure (7.2) reveals the first 2-torus with the three intersecting D-branes wrapping 1-cycles. The fundamental domain $\mathcal{P}_{\rm rect}$ of the rectangular 2-torus is represented by the horizontal line $2\pi R_1$ and the vertical line $2\pi R_2$.

In the intersection between the a- and b-brane lives the scalar tower with Φ and the first light stringy state $\widetilde{\Phi}$. At the points f_1, f_2, f_3 in the ca sector the three generations χ_1, χ_2, χ_3 and

[4] In our specified configuration, we deduce that $\widetilde{L}^i_c = L^i_c$ holds for all three 2-tori.

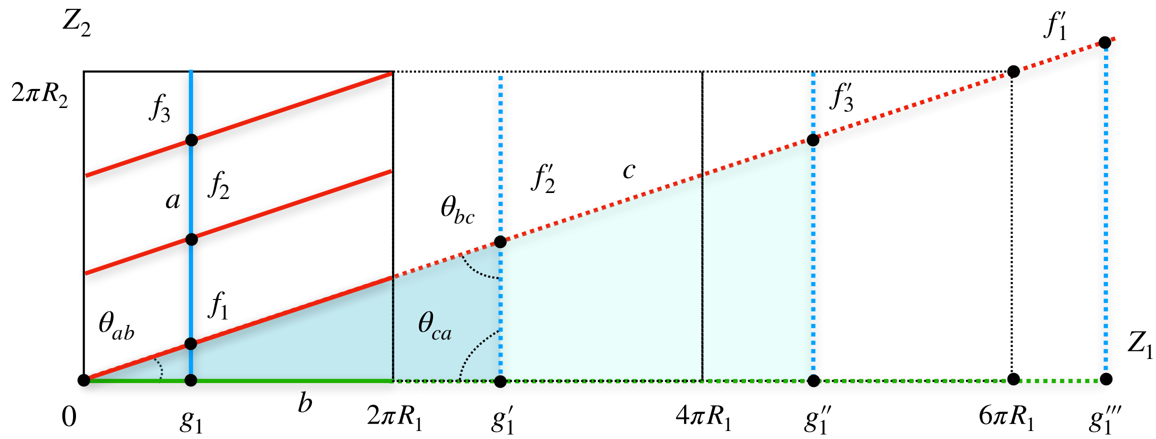

Figure 7.2: A pictorial representation of three intersecting stacks of D-branes on the first 2-torus. The branes wrap the cycles $(n_a^1, m_a^1) = (0,1), (n_b^1, m_b^1) = (1,0)$ and $(n_c^1, m_c^1) = (3,1)$.

their potential twisted tower appear. The D_b-brane and the D_c-branes give rise to an intersection, where the ψ fermions and their light massive states are located.

Subsequently, we want to determine the *twisted* Yukawa coupling between two massless fermions ψ and χ and the twisted field $\widetilde{\Phi}$. In recent works [230–232] it could be shown that the Yukawa coupling for such a condition is directly related to the untwisted Yukawa coupling. Therefore, we can conclude that the Yukawa coupling with twisted states is given by

$$\left|Y_{\widetilde{\Phi}_1\psi\chi}\right| = \frac{|Y_{\Phi\psi\chi}|}{\sqrt{a^1_{ab}}} \left[\Gamma_{1-a^1_{ab},1-a^1_{bc},-a^1_{ca}}\right]^{1/2} \sqrt{\frac{2A^{(1)}_{\phi\psi\chi}}{\pi\alpha'}} \ . \tag{7.33}$$

The physical interpretation is that the twisted scalar field corresponds to an excited Higgs field which decays into untwisted standard model fields. In the next section we will find that this decay rate depends on the angle of the intersection.

7.4 The Lifetime of Twisted Scalars

Since there are no other decay channels at this order for the decay of the twisted scalar into two massless fermions, we can calculate the decay rate $\Gamma_{\widetilde{\Phi}_1}$ and consequently the lifetime $\tau_{\widetilde{\Phi}_1} = \Gamma^{-1}_{\widetilde{\Phi}_1}$ of the twisted scalar $\widetilde{\Phi}_1$ at rest, which is given by

$$\tau_{\widetilde{\Phi}_1} = \frac{1}{\Gamma_{\widetilde{\Phi}_1}} = \frac{8\pi}{m_{\widetilde{\Phi}_1}\sum_{ij}|Y_{\widetilde{\Phi}_1\psi_i\chi_j}|^2} = \tau_{\widetilde{\Phi}_1} = \frac{4\pi^2}{m_{\widetilde{\Phi}_1}} \frac{a^1_{ab}}{|Y_{\Phi\psi\chi}|^2} \left[\Gamma_{a^1_{ab},a^1_{bc},1+a^1_{ca}}\right] \frac{\alpha'}{A^{(1)}_{\Phi\psi\chi}} \ , \tag{7.34}$$

where the sum runs over all flavours and colours and where we used Eq. (7.33) in the last step. Hence, the lifetime for the untwisted scalar Φ_1 at rest is given by

$$\tau_{\Phi_1} = \frac{8\pi}{m_{\Phi_1}\sum_{ij}|Y_{\Phi_1\psi_i\chi_j}|^2} \ . \tag{7.35}$$

Taking the ration between the lifetimes of the twisted and untwisted field, we find

$$\frac{\tau_{\tilde{\Phi}_1}}{\tau_{\Phi_1}} = \frac{\pi\alpha' a^1_{ab}}{|f_{\psi\chi,1}|^2} \frac{m_{\Phi_1}}{m_{\tilde{\Phi}_1}} \left[\Gamma_{a^1_{ab},a^1_{bc},1+a^1_{ca}}\right] \left|\frac{\sin\pi a^1_{ab}}{\sin\pi a^1_{bc}\sin\pi(1+a^1_{ac})}\right| \ . \tag{7.36}$$

Further, we can simplify Eq. (7.36) to

$$\tau_{\tilde{\Phi}_1} \sim \frac{1}{4\pi a^1_{ab}} \frac{m_{\Phi_1}}{m_{\tilde{\Phi}_1}} \left[\Gamma_{a^1_{ab}, a^1_{bc}, 1+a^1_{ca}}\right] \left| \frac{\sin \pi a^1_{ab}}{\sin \pi a^1_{bc} \sin \pi \left(1 + a^1_{ac}\right)} \right| \tau_{\Phi_1} \ , \tag{7.37}$$

where we assumed, that the distance $f_{\psi\chi,1} \sim a^1_{ab} R$. Moreover, we assume, that the radius R of the torus is of order of the string length $R \sim \ell_s = 2\pi\sqrt{\alpha'}$.

In order to analyse this lifetime $\tau_{\widetilde{\Phi}_1}$ of the twisted Higgs more precisely, we will perform an approximation for small angles. For that, we require $a^1_{ab} < \varepsilon_1$, $a^1_{bc} < \varepsilon_2$ and $a^1_{ca} < \varepsilon_3$ with $\varepsilon_i \ll 1$. Thus, we can expand the Gamma function $\Gamma(z)$ around $z = 0$

$$\Gamma(z) = \frac{1}{z}(1 - \gamma z) + \frac{1}{12}\left(6\gamma^2 + \pi^2\right) + \mathcal{O}(z) \ . \tag{7.38}$$

The constant $\gamma \sim 0.577$ is the *Euler–Mascheroni* constant. This simplifies Eq. (7.37) and we obtain

$$\tau_{\tilde{\Phi}_1} \sim \frac{1}{4\pi} \frac{m_{\Phi_1}}{m_{\tilde{\Phi}_1}} \left[\frac{1}{a^1_{ab} \left(a^1_{bc}\right)^2} + \frac{2\gamma a^1_{ca}}{a^1_{ab} \left(a^1_{bc}\right)^2} + \frac{4\gamma^2}{a^1_{bc}} \right] \tau_{\Phi_1} \tag{7.39}$$

If we assume that $a^1_{ab}, a^1_{bc}, a^1_{bc} \sim \varepsilon$ with $\varepsilon \to 0$, we find

$$\tau_{\tilde{\Phi}_1} \sim \frac{1}{4\pi} \frac{m_{\Phi_1}}{m_{\tilde{\Phi}_1}} \left[\frac{1}{\varepsilon^3} + \frac{2\gamma}{\varepsilon^2} + \frac{4\gamma^2}{\varepsilon} \right] \tau_{\Phi_1} \ . \tag{7.40}$$

From that equation, it is rather obvious that we can adjust and tune the lifetime $\tau_{\tilde{\Phi}_1}$ of the excited Higgs to get a very long lifetime. This is basically given by very small angles a^1_{ab} and a^1_{bc}, which in turn corresponds to almost parallel D-branes.

The careful reader may have noticed that we have not designated the mass of the twisted Higgs $m_{\widetilde{\Phi}_1}$ with the same symbol as in the construction of the states $M_{\widetilde{\Phi}_1}$. The reason is that the mass of the twisted Higgs is constituted by two components [233]. On the one hand by the excited vibration of the strings, which is reflected in the mass squared operator, on the other hand by a potential related to the vacuum expectation value and spontaneous symmetry breaking.

To estimate the size of the angles numerically, we choose the empirically measured value of the Higgs mass $m_\Phi \simeq 125\,\text{GeV}$ and its lifetime $\tau_\Phi \simeq 1 \times 10^{22}\,\text{s}$. We also assume that the string scale is around a few TeV and that $m_{\widetilde{\Phi}} \geq m_\Phi$. Furthermore, we require that the lifetime of the twisted Higgs is around $10^{17}\,\text{s}$ [234–237]. This corresponds to the estimated age of universe according to *Hubble's Law*. Thus, we obtain an angle in the order of 10^{-14}.

Essentially, this allows to postulate such a massive and long-lived scalar particle to a serious candidate for dark matter. However, other aspects such as early matter domination, entropy injection, etc. have to be considered and analysed in more detail [238].

Chapter 8

Conclusion and State of the Art

In this thesis we have shed light on the most important technical tools and conceptual foundations needed to build semi-realistic standard models of particle physics utilising intersecting Dp-brane world scenarios. More specifically, we have performed this in the framework of typ IIA superstring theory adopting the bottom-up philosophy. Such semi-realistic models are characterised by four key features:

- We have made manifest, that oriented open superstrings whose respective ends are tied to a stack of N coincident Dp-branes lead to a $U(N)$ gauge theory and, consequently, to a $U(N) \simeq SU(N) \times U(1)$ Yang-Mills theory on the world-volume of the stack of Dp-branes. This supplies us with the gauge group of the standard model

$$\mathcal{G}_{\text{SM}} = SU(2)_C \times SU(2)_L \times U(1)_Y \times \sum_i U(1)_i \; . \tag{8.1}$$

  with possible extra $U(1)_i$'s, which are decoupled at low energy and preserved as mere global symmetry.

- We revealed, that open oriented superstrings can be stretched between two different stacks of N and M Dp-branes that intersect and constitute a relative angle to each other. Via the corresponding vertex operators, we could show that such strings yield massless and chiral fermions at lowest energy, which transform in a bi-fundamental representation $(\mathrm{N}, \overline{\mathrm{M}})$ of $SU(N) \times SU(M)$. This gives a description of the matter content of the standard model. Much more, near such intersections we could identify a whole tower of further potentially massive fermions and their superpartners, whose mass squared operator is a function of the relative angle and phenomenologically go under the name of light stringy states.

- We observed, that in order to obtain a four-dimensional effective field theory, we need to introduce the concept of compactification. The Dp-branes in such a compact spaces can be described via cycles of a homology class. In the concrete case of factorisable 6-torus compactification, we could illuminate, that D6-branes wrap cycles on the internal space giving raise to multiple intersections, which is reflected in the so-called intersection number. This quantity based on topology determines the chirality and the number of copies of the states in such intersections, which introduces the concept of generations or families of particles.

- We could deduce that the relative angles provide a criterion for the preservation of $\mathcal{N} = 1$ supersymmetry.

In order to formulate a four-dimensional field theory of a semi-realistic standard model at low energies consistently, it was inspected for potential quantum anomalies. Moreover, the compactification must ensure that the RR-charges coming from the Dp-branes are net zero, which led us to the famous tadpole condition which we explicitly derived. Further, we were able to demonstrate in detail within our purely topological framework how a generalised Green-Schwarz mechanism resolves quantum anomalies and thwarts potential dangers. In connection with that mechanism, some $U(1)'s$ obtain a Stückelberg mass and decouple from the low energy limit.

In order to ensure that the RR charges are cancelled out in such a model - without introducing anti-branes which destroy the $\mathcal{N} = 1$ supersymmetry - another concept must be introduced: An orientifold projection and the corresponding O_6-planes for the toroidal case. Based on that, we discussed a configuration based on a toroidal orientifold model. We explicitly chose random parameters and used them to analyse this model and the concepts introduced so far and finally were able to determine the content and spectrum of a semi-realistic standard model.

However, such a toroidal model based on orientifold is not supersymmetrical, which is why we have presented a possible generalisation of the model, which in the past has already been able to deliver a supersymmetrical spectrum. We introduced this model and examined and calculated it according to our formal method. In the end we managed to agree that such a model, in addition to the fact that it represents a minimal supersymmetric extension of the standard model (modulo exotic matter fields), also describes and constitutes a grand unified theory. A so-called Pati-Salam model.

In the last part of this thesis, we left the theoretical modelling of semi-realistic standard models and turned to one of many possible phenomenological implications, which result from intersecting brane worlds. By compacting the internal space, the string scale can be set at the TeV scale, which empower empirical possibilities to detect stingy resonances in the future. For this reason, we have designed a minimal brane world scenario which is given by three Dp-branes intersecting each other. This allows to compute the Yukawa couplings for states arising from such a configuration, i.e. the interaction $\sim \bar{Q}_L d_R H$. Stepping away from the lowest energy states this could also be done for a Yukawa coupling where one of the states corresponding to the Higgs particle is excited and thus leads to a twisted Yukawa coupling, i.e. $\sim \bar{Q}_L d_R \widetilde{H}$, and to relate it to the so-called untwisted Yukawa coupling.

Further we accomplished, by means of these Yukawa couplings, to estimate the lifetime of such a twisted scalar field from its decay rate by making reasonable assumptions. We were capable to explicitly illuminate, that the lifetime of this excited Higgs particle is a function of the relative angles of the D-branes and the fine-tuned string scale. Moreover, in such a configuration the lifetime of such a particle can be fairly huge, achieved by two nearly parallel D-branes. A particle associated with such a long-living and approximately stable weak interacting scalar field could be a potentially promising candidate for dark matter. Thus, it is worth investigating this model further in the future.

In recent years, a number of different semi-realistic constructions have been investigated. There has been a great effort in the study of type IIA toroidal orientifolds with $\mathbb{Z}_2 \times \mathbb{Z}_2$, $\mathbb{Z}_6$ or $\mathbb{Z}_6'$ orbifolds [239, 240]. Furthermore, there have been promising investigations in type IIB superstring theory where, although the intuition is no longer explicitly geometric, calculations are simplified and various other Dp-branes, such as D3- [241], D5- [242] and D7-branes [243] can be used. Furthermore, there were attempts to generalize the underlying geometry and to find more abstract backgrounds which are somewhere between Calabi-Yau manifolds and toroidal compactification. Most notable realisations have been investigated with the so-called *Gepner orientifold models* [244–246] or by using non-perturbative generalisations of the so-called *F-theory* [247]. In particular, one aim for the future is to look for statistical methods to systematise the large number of possible models and to sort out possible candidates. This was done a few months ago for example for the toroidal $\mathbb{Z}_2 \times \mathbb{Z}_2$ orbifold with D6-branes. The scientists Gregory J. Loges and Gary Shiu were able to find $\mathcal{O}(10^6)$ consistent models assisted by modern

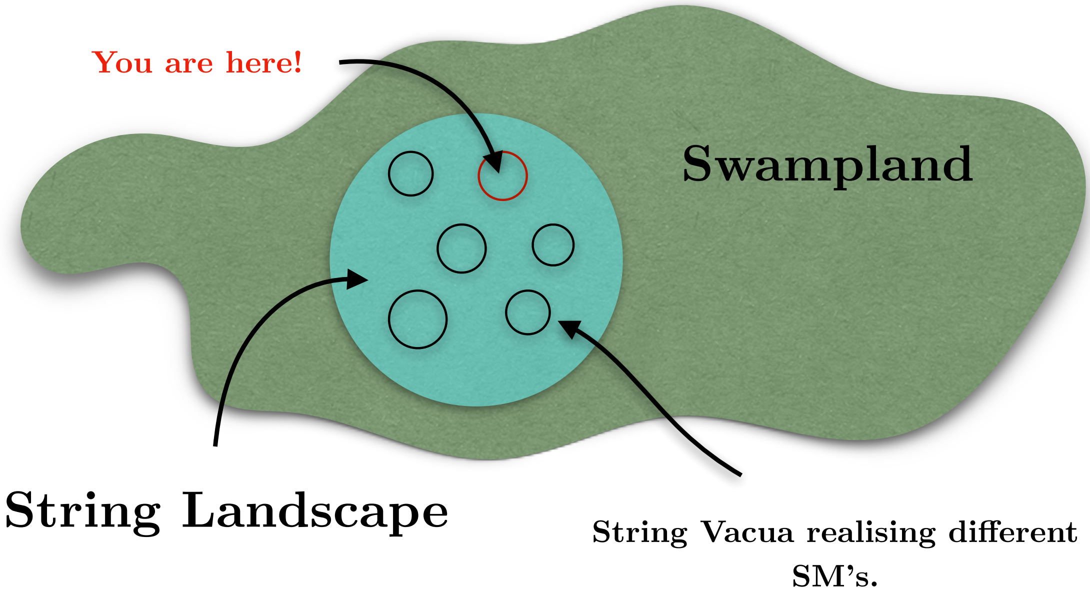

Figure 8.1: The string theory landscape in a theory space contains all the consistent of effective quantum field theory compatible with quantum gravity. One such String vacua corresponds to the standard model of our universe. However, not all consistent effective quantum field theories that are possible in principle can result from string theory [250]. These form the so-called string theory swampland.

computational tools like *machine learning* [248]. Nevertheless, there is still no model that has the most important features of the standard model at the same time. Here, we mean in particular the cancellation of anomalies, the correct Yukawa couplings, the unification of gauge couplings, supersymmetry breaking, the Higgs mechanism, Neutrino oscillations and much more.

Despite that, we have seen in this work that we can already do phenomenology using a semi-realistic model. Furthermore, during this thesis the author had the opportunity and honour to work with Pascal Anastasopoulos and Elias Kiritsis on an aspect of the *holographic principle*, which is in some sense more general than string theory. In such a theory, the underlying action is $\mathcal{S} = \mathcal{S}_{\text{SM}} + \mathcal{S}_{\text{Messenger}} + \mathcal{S}_{Hidden}$, where the hidden sector contains all the physics we do not know, and can be described via hidden branes, while the standard model is constructed with a possible intersecting brane scenario. Recently, it has been shown in their publication [249], that messenger particles (part of $\mathcal{S}_{\text{Messenger}}$) connecting standard model branes and hidden branes can be identified with right-handed neutrinos, putting the seewsaw mechanism in a new perspective.

However, there are also problems on the “stringy” side. Probably the most challenging and head-scratching one was the issue of *moduli stabilisation*. The compactification with Calabi-Yau manifolds brings a variety of moduli. Let us think of a simpler example like the Kaluza-Klein compactification with a circle S^1 and radius R. This radius is associated with an unfixed parameter in the modulo space. In string theory, the background needs to be dynamical. The Calabi-Yau manifold thus dynamically change its moduli. From the point of view of the non-compact four dimensions, such a fluctuation corresponds to a massless or light scalar field. To date, such particles have remained undetected in all experiments and thus these moduli must be stabilised [63]. About ten years ago, a mechanism came along that could stabilise such moduli through the introduction of *flux compactification* [251–253]. This is not the place to talk about such a far-reaching field, but in a nutshell, we can stabilise these moduli so that these fluctuations in the low energy regime remain very small. In physics jargon, such a stabilised background is referred as a *string vacuum*.

Here begins an adventure, or one could almost call it a journey, into an unknown land, or better in this case, unknown universe(s). Intersecting brane world scenarios have a myriad of different possible moduli, compactification backgrounds, choices for the fluxes, D-branes configurations and much more. According to the best estimations, there are between 10^{500} and 10^{272000} inequivalent string vacua, where each of these vacua eventually has a consistent effective QFT, differing from the one in our universe [250, 254, 255]. The task is to find the - hopefully - unique solution that realises our universe in this so-called *string vacua landscape* (see Fig. 8.1). A top-down approach is not possible in this case, as string theory does not explain why compactification proceeds in this way [256, 257]. This has led to heated arguments and intellectual correspondences [255]. If string theory has such a multitude of solutions, doesn't it loose its strength of explainability and prediction? Is such a theory of *multiverses* still falsifiable in a Popperian sense [1] [255]? Should string theory fall into a depression, because to find such a solution seems to be impossible or should it look forward to this task with hope, because with such a quantity of string vacua there must be one that describes our universe? This question remains open. For physicists, a theory with many different solutions is not a problem. In fact, the *Einstein equations* have a large number of solutions that are not realised in our universe. But here is the point. General Relativity does not claim to be an ultimate theory. We know that the general theory of relativity is, in a certain sense, only an effective theory and not an absolutely fundamental theory. But string theory makes a different claim and aspires to the holy grail of being a theory of everything. From that perspective it is fairly unusual to get a vast of solutions.

What remains to be said? As we have seen, the history of string theory is still a very young one. The theory has not yet exhausted all its possibilities and its true nature is still unknown. Criticism of such theories is always necessary. Physics without experiments are not more than ideas and philosophical debates should gain more value again. But in the end, string theory already has its first success to celebrate. It has achieved what most of the most ingenious and brilliant minds in the past thought was impossible. It showed us that quantum field theory and general relativity do indeed fit together. Regardless of whether it ends up being string theory or not.

The very intrinsic *essentia* and innate truth of a puzzle - and presumably the reason why we are so mysteriously attracted and irresistible drawn to it - is that it must have a path to its solution. Otherwise, it would not be a puzzle.

Vienna, February 2024
Elias Niederwieser

[1] At least this seems to explain the *naturalness* of the fundamental constants, i.e. our fundamental constants are such because we live in this very universe in which they just have these values.

Appendix A

Characteristic Classes

Characteristic classes appear over and over again in modern mathematics and theoretical physics. Intuitively speaking, they provide a "measure", which indicates how nontrivial vector bundles are [258]. Probably one of the most famous characteristic classes are the *Stiefel-Whitney* classes, which reveal whether a manifold has a spin structure or not [1] [260]. These topological invariants also play a crucial role in important theorems (e.g., *Riemann-Roch theorem* or the *Atiyah-Singer index theorem*) [261]. In this appendix, some basic concepts should be briefly highlighted in order to lead to a better understanding and comprehensibility at certain points in the main part of this thesis. More details are provided e.g., in [111].

We propose, that $E \xrightarrow{\pi} X$ is a complex vector bundle, with E being the total space and X the base space. The bundle projection π is a continuous surjection with fiber $\mathbb{C}^k$. Further, $G \subset \mathrm{GL}(k, \mathbb{C})$ furnishes the structure group. The field strength $\mathcal{F}$ is Lie algebra-valued [111, 262]. The **total Chern class** is then defined by

$$c(\mathcal{F}) \equiv \det\left(I + \frac{i\mathcal{F}}{2\pi}\right) = \bigoplus_{n=0}^{\infty} c_n(\mathcal{F}) \ . \tag{A.1}$$

In other words, the total Chern class is the direct sum of forms $c_n(\mathcal{F}) \in \Omega^{2n}(X)$ of even degree, which are called the $\mathbf{n^{th}}$ **Chern class**.

For a suitable $g \in \mathrm{GL}(k, \mathbb{C})$ the field strength $\mathcal{F}$ can be diagonalised [111]. This results in $g^{-1}(i\frac{F}{2\pi})g = \mathrm{diag}(\lambda_1, ...\lambda_k) \equiv D$, with λ_i being 2-forms, where in the last step we defined the diagonal matrix D. It can be easily verified that

$$\begin{aligned}
\det(I + D) &= \det\left(I + \frac{ig^{-1}\mathcal{F}g}{2\pi}\right) = \det\left[\mathrm{diag}\left(1 + \lambda_1, \ldots, 1 + \lambda_k\right)\right] = \prod_{n=1}^{k}\left(1 + \lambda_n\right) \\
&= 1 + (\lambda_1 + \ldots + \lambda_k) + (\lambda_1\lambda_2 + \ldots + \lambda_{k-1}\lambda_k) + \ldots + (\lambda_1\lambda_2 \ldots \lambda_k) \\
&= 1 + \sum_{n=1}^{k} \lambda_n + \sum_{m<n} \lambda_m\lambda_n + \ldots + \prod_{n=1}^{k} \lambda_n \\
&= 1 + \mathrm{tr}\, D + \frac{1}{2}\left\{(\mathrm{tr}\, D)^2 - \mathrm{tr}\, D^2\right\} + \ldots + \det D \ .
\end{aligned} \tag{A.2}$$

Without proving, which can be found in [111] or [263] , we state that $\mathcal{P}(\mathcal{F}) \equiv det(I + \frac{i\mathcal{F}}{2\pi})$ is an Γ-invariant polynomial $\mathcal{P}(\gamma\mathcal{F}) = \mathcal{P}(\mathcal{F})$, where Γ is a Lie or algebraic group and $\gamma \in \Gamma$. For the

[1] To be more precise, a spin structure on an oriented Riemannian manifold exists if the second Stiefel-Whitney class of the same manifold vanishes [259].

special case $\gamma\mathcal{F} \equiv g\mathcal{F}g^{-1}$ with $g \in \mathrm{GL}(k,\mathbb{C})$, it yields $\mathcal{P}(\mathcal{F}) = \mathcal{P}(g\mathcal{F}g^{-1}) = -\mathcal{P}(2\pi D)$. Using Eq. (A.1) and comparing it to the coefficients of E. (A.2) leads to the following Chern classes.

$$
\begin{aligned}
c_0(\mathcal{F}) &= 1 \ . \\
c_1(\mathcal{F}) &= \mathrm{tr}\, D = \mathrm{tr}\left(g\frac{\mathrm{i}\mathcal{F}}{2\pi}g^{-1}\right) = \frac{\mathrm{i}}{2\pi}\,\mathrm{tr}\,\mathcal{F} \ . \\
c_2(\mathcal{F}) &= \frac{1}{2}\left[(\mathrm{tr}D)^2 - \mathrm{tr}D^2\right] = \frac{1}{2}(\mathrm{i}/2\pi)^2[\mathrm{sp}\mathcal{F}\wedge\mathrm{tr}\,\mathcal{F} - \mathrm{tr}(\mathcal{F}\wedge\mathcal{F})] \ . \\
&\ \vdots \\
c_k(\mathcal{F}) &= \det D = (\mathrm{i}/2\pi)^k \det\mathcal{F} \ .
\end{aligned}
\tag{A.3}
$$

The **total Chern characteristic** in representation R is defined by

$$
\mathrm{Ch}_{\mathrm{R}}(\mathcal{F}) \equiv \mathrm{tr}_{\mathrm{R}} \exp\left(\frac{i\mathcal{F}}{2\pi}\right) = \sum_{n=1}^{\infty}\frac{1}{n!}\,\mathrm{tr}_{\mathrm{R}}\left(\frac{i\mathcal{F}}{2\pi}\right)^n \tag{A.4}
$$

The $\boldsymbol{n}^{\mathbf{th}}$ **Chern characteristic** $\mathrm{Ch}_{\mathrm{R},n}(\mathcal{F})$ is given by

$$
\mathrm{Ch}_{\mathrm{R},n}(\mathcal{F}) \equiv \frac{1}{n!}\,\mathrm{tr}_{\mathrm{R}}\left(\frac{\mathrm{i}\mathcal{F}}{2\pi}\right)^n \tag{A.5}
$$

The Chern character can be re-expressed by diagonalising $\mathcal{F}$. This yields the well-known relation

$$
\mathrm{tr}_{\mathrm{R}}[\exp(D)] = \sum_{n=1}^{k}\exp(\lambda_n) \tag{A.6}
$$

By expanding the exponential, we further find

$$
\begin{aligned}
\sum_{n=1}^{k}\exp(\lambda_n) &= \sum_{n=1}^{k}\left(1+\lambda_n+\frac{1}{2!}\lambda_n^2+\frac{1}{3!}\lambda_n^3+\cdots\right) \\
&= k + \sum_{n=1}^{k}\lambda_n + \frac{1}{2!}\left[(\sum_{n=1}^{k}\lambda_n)^2 - 2\sum_{m<n}\lambda_m\lambda_n\right] + \ldots
\end{aligned}
\tag{A.7}
$$

Looking back at the second line in Eq. A.2, we find that the Chern character can be expressed in terms of the Chern classes. To be explicit, the first three Chern classes are given by

$$
\begin{aligned}
\mathrm{Ch}_{\mathrm{R},0}(\mathcal{F}) &= k \\
\mathrm{Ch}_{\mathrm{R},1}(\mathcal{F}) &= c_1(\mathcal{F}) \\
\mathrm{Ch}_{\mathrm{R},2}(\mathcal{F}) &= \tfrac{1}{2}\left[c_1(\mathcal{F})^2 - 2c_2(\mathcal{F})\right]
\end{aligned}
\tag{A.8}
$$

The Chern character also satisfies the following properties (The proof is straightforward and can be found in [111])

$$
\begin{aligned}
\mathrm{Ch}_{\mathrm{R}}(E\otimes F) &= \mathrm{Ch}_{\mathrm{R}}(E)\wedge\mathrm{Ch}_{\mathrm{R}}(F) \\
\mathrm{Ch}_{\mathrm{R}}(E\oplus F) &= \mathrm{Ch}_{\mathrm{R}}(E)+\mathrm{Ch}_{\mathrm{R}}(F)
\end{aligned}
\tag{A.9}
$$

Of course, Chern classes are only one example among a great variety of characteristic classes. Apart from other characteristic classes defined for complex vector bundles, such as the *Todd* class, we can also define characteristic classes for real vector bundles. Without going into detail, we present the **Pontryagin class**, which is given by [111]

$$
\begin{aligned}
p_1(\mathcal{F}) =& -\frac{1}{2}\left(\frac{1}{2\pi}\right)^2 \operatorname{tr}\mathcal{F}^2. \\
p_2(\mathcal{F}) =& \frac{1}{8}\left(\frac{1}{2\pi}\right)^4 \left[\left(\operatorname{tr}\mathcal{F}^2\right)^2 - 2\operatorname{tr}\mathcal{F}^4\right]. \\
p_3(\mathcal{F}) =& \frac{1}{48}\left(\frac{1}{2\pi}\right)^6 \left[-\left(\operatorname{tr}\mathcal{F}^2\right)^3 + 6\operatorname{tr}\mathcal{F}^2\operatorname{tr}\mathcal{F}^4 - 8\operatorname{tr}\mathcal{F}^6\right]. \\
&\vdots \\
p_{[k/2]}(\mathcal{F}) =& \left(\frac{1}{2\pi}\right)^k \det\mathcal{F}.
\end{aligned}
\tag{A.10}
$$

Moreover, in this thesis we use the **A-roof** or **Dirac genus**, which is defined by

$$
\hat{A}(\mathcal{F}) = \prod_{n=1}^{k} \frac{\lambda_n/2}{\sinh(\lambda_n/2)} \tag{A.11}
$$

where $\mathcal{F}$ is again diagonalised. An A-roof genus can be rewritten in a compact fashion by using the Pontrjagin classes $p_n(\mathcal{F})$ [111]

$$
\begin{aligned}
\hat{A}(\mathcal{F}) =& 1 - \frac{1}{24}p_1 + \frac{1}{5760}\left(7p_1^2 - 4p_2\right) \\
&+ \frac{1}{967680}\left(-31p_1^3 + 44p_1p_2 - 16p_3\right) + \cdots
\end{aligned}
\tag{A.12}
$$

Last but not least, **the Hirzebruch *L*-polynomial** can be expanded into the same classes and is thus defined by [111]

$$
L(\mathcal{F}) = \prod_{i=1}^{k} \frac{\lambda_i}{\tanh(\lambda_i)} = 1 + \frac{1}{3}p_1 + \frac{1}{45}\left(-p_1^2 + 7p_2\right) + \cdots \tag{A.13}
$$

Appendix B

Commutator for Twisted Modes

In Eq. (3.28) we observed, that inverting the mode expansion for the world-sheet bosons in Eq. (3.27) gives an equation for the modes in terms of a contour integral. This integral reads

$$\alpha^k_{n\pm\epsilon_k} = i\sqrt{\frac{2}{\alpha'}}\oint \frac{dz}{2\pi i}\; z^{n\pm\epsilon_k}\,\partial Z^k(z)\;. \tag{B.1}$$

With this representation of the modes for the internal space, we can calculate the commutator

$$\left[\alpha^I_{m\pm\epsilon_k}, \tilde{\alpha}^J_{n\mp\epsilon_k}\right]\,. \tag{B.2}$$

We start by inserting the integral representation of Eq. B.1 into the commutator of Eq. B.2. We obtain

$$\begin{aligned}\left[\alpha^I_{m\pm\epsilon_k}, \tilde{\alpha}^J_{n\mp\epsilon_k}\right] = &-\frac{2}{\alpha'}\oint_{C_0}\frac{\mathrm{d}z}{2\pi i}\; z^{m\pm\epsilon_k}\,\partial Z^I(z)\oint_{C_0}\frac{\mathrm{d}w}{2\pi i}\; w^{n\mp\epsilon_k}\,\partial Z^J(w)\\ &+\frac{2}{\alpha'}\oint_{C_0}\frac{\mathrm{d}w}{2\pi i}\; w^{n\mp\epsilon_k}\,\partial Z^J(w)\oint_{C_0}\frac{\mathrm{d}z}{2\pi i}\; z^{m\pm\epsilon_k}\,\partial Z^I(z)\;.\end{aligned} \tag{B.3}$$

The contour C_0 symbolises a closed contour around $z = 0$. Next now look at the right handside of Eq. (B.3), where we will suppress the internal dimension indices for compactness. The right-hand side reads

$$\begin{aligned}&-\frac{2}{\alpha'}\oint_{C_0}\frac{dw}{2\pi i}\left[\oint_{C_0}\frac{dz}{2\pi i}\; z^{m\pm\epsilon_k}w^{n\mp\epsilon_k}\,\partial Z(z)\partial Z(w) - \oint_{C_0}\frac{dz}{2\pi i}\; z^{m\pm\epsilon_k}w^{n\mp\epsilon_k}\,\partial Z(w)\partial Z(z)\right]\\ &= -\frac{2}{\alpha'}\oint_{C_0}\frac{dw}{2\pi i}\Bigg[\oint\limits_{\substack{C_0'\\ |w|\leq|z|}}\frac{dz}{2\pi i} z^{m\pm\epsilon_k}w^{n\mp\epsilon_k}\partial Z(z)\partial Z(w) - \oint\limits_{\substack{C_0''\\ |w|\geq|z|}}\frac{dz}{2\pi i} z^{m\pm\epsilon_k}w^{n\mp\epsilon_k}\partial Z(w)\partial Z(z)\Bigg]\end{aligned} \tag{B.4}$$

In the last line of Eq. (B.4) we used a contour deformation, which is depicted in Fig. B.1 for the integrals in the square bracket. After the contour deformation, suggested in Fig. B.1, we find that $|w| \leq |z|$ and that $|w| \geq |z|$ for all z. Specifically, we have $|C_0'| > |C_0| > |C_0''|$. The operators in Eq. (B.4) are thus radial ordered, which we denote with $\mathcal{R}$ and the deformation is homotopic to Fig. B.1. This simplifies the commutator in Eq. (B.3) to

$$[\alpha_{m\pm\epsilon_k}, \tilde{\alpha}_{n\mp\epsilon_k}] = -\frac{2}{\alpha'}\oint_{C_0}\frac{\mathrm{d}w}{2\pi i}\oint_{C_w}\frac{\mathrm{d}z}{2\pi i}\; z^{m\pm\epsilon_k}w^{n\mp\epsilon_k}\mathcal{R}[\partial Z(z)\partial Z(w)]\;. \tag{B.5}$$

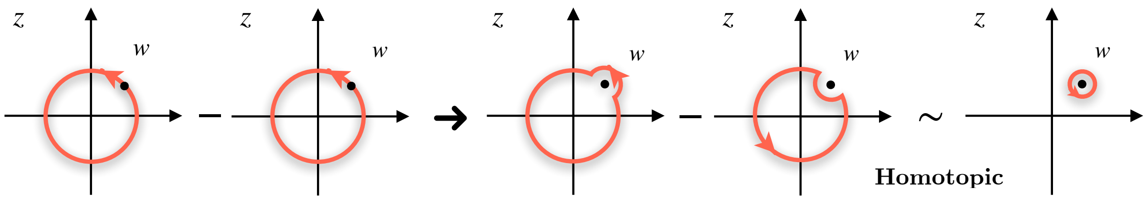

Figure B.1: Deformation of the z-contour while keeping w fixed.

Inserting the known [100] operator product expansion (OPE), we obtain

$$\mathcal{R}[\partial Z(z)\partial Z(w)] = -\frac{\alpha'}{2}\frac{1}{(z-w)^2} + \text{“regular terms”} \ . \tag{B.6}$$

Inserting Eq. (B.6) into Eq. (B.5), we are left with

$$[\alpha_{m\pm\epsilon_k}, \tilde{\alpha}_{n\mp\epsilon_k}] = -\frac{2}{\alpha'}\oint_{C_0}\frac{\mathrm{d}w}{2\pi i}\oint_{C_w}\frac{\mathrm{d}z}{2\pi i}\, z^{m\pm\epsilon_k} w^{n\mp\epsilon_k}\left[-\frac{\alpha'}{2}\frac{1}{(z-w)^2} + \text{“reg. terms”}\right] \ . \tag{B.7}$$

Next we strive to evaluate the z integral in Eq. (B.7). Using the famous *Cauchy's residue theorem* we get

$$\begin{aligned}[\alpha_{m\pm\epsilon_k}, \tilde{\alpha}_{n\mp\epsilon_k}] &= \oint_{C_0}\frac{\mathrm{d}w}{2\pi i}\oint_{C_w}\frac{\mathrm{d}z}{2\pi i} z^{m\pm\epsilon_k} w^{n\mp\epsilon_k}\left[\frac{1}{(z-w)^2}+\dots\right] \\ &= \oint_{C_0}\frac{\mathrm{d}w}{2\pi i}\,\mathrm{Res}_{z=w}\left[z^{m\pm\epsilon_k} w^{n\mp\epsilon_k}\left(\frac{1}{(z-w)^2}+\dots\right)\right] \ ,\end{aligned} \tag{B.8}$$

In order to go on, we expand $z^{m\pm\epsilon_k}$ around w. The expansion of $z^{m\pm\epsilon_k}$ yields

$$z^{m\pm\epsilon_k} = w^{m\pm\epsilon_k} + (m\pm\epsilon_k)\, w^{m\pm\epsilon_k-1}(z-w) + \mathcal{O}\left[(z-w)^2\right] . \tag{B.9}$$

Plugging the expansion of Eq. (B.9) into Eq. (B.8) we find

$$[\alpha_{m\pm\epsilon_k}, \tilde{\alpha}_{n\mp\epsilon_k}] = \oint_{C_0}\frac{\mathrm{d}w}{2\pi i}\ \mathrm{Res}_{z=w}\left[\frac{a_{-2}}{(z-w)^2} + \frac{a_{-1}}{(z-w)} + \dots\right] \ , \tag{B.10}$$

where a_{-1} is the result of the product of the expansion of $z^{m\pm\epsilon_k}$ and the OPE by only keeping terms of $\mathcal{O}\left[(z-w)^{-1}\right]$. By doing so, one gets for the residuum $(m\pm\epsilon)\, w^{m+n-1}$.

Thus, Eq. (B.10) simplifies to

$$[\alpha_{m\pm\epsilon_k}, \tilde{\alpha}_{n\mp\epsilon_k}] = (m\pm\epsilon_k)\oint\frac{\mathrm{d}w}{2\pi i}\, w^{m+n-1} = (m\pm\epsilon_k)\ \delta_{m+n,0} \ , \tag{B.11}$$

which finally yields the only non-zero commutator. Restoring back the internal space indices yields

$$\left[\alpha^I_{m\pm\epsilon_k}, \tilde{\alpha}^J_{n\mp\epsilon_k}\right] = (m\pm\epsilon_k)\ \delta_{m+n,0}\ \delta^{I,J} \ . \tag{B.12}$$

Appendix C

Mass Square Formula

In section (3.4) we found that the mass-squared operator M^2 for an oriented open superstring between intersecting D6-branes at an angle θ is given by Eq. (3.32). To see this in more detail, we have to consider all different "sectors", which are contributing in our mode expansion. Both, for the Minkowski space $\mathcal{M}_4$ in light cone coordinates and the internal complexified space $\mathcal{I}_3$ with the shifted modding in the oscillator modes. Throughout this derivation, we use the notational convention from [45].

Schematically, we expect a Virasoro operator of the following form

$$L_0^{\perp} \sim \sum_{\mathcal{M}} \left(L_{0,\mathrm{NS}}^{\perp} + L_{0,\mathrm{R}}^{\perp} \right) + \sum_{\mathcal{I}} \left(L_{0,\mathrm{NS}}^{\perp} + L_{0,\mathrm{R}}^{\perp} \right) \tag{C.1}$$

where $\mathcal{M}_4$ denotes the summation over the four-dimensional Minkowski spacetime and $\mathcal{I}_3$ the remaining three complex internal coordinates. In the next sections, we will derive the mass-squared operator M^2 and the associated ordering constants. First for the spacetime contribution and then for the internal space. To simplify things, we will restrict ourselves to positive angles and use the definition of the vacuum from Eq. (3.31).

C.1 Virasoro Operator for the R and NS Sector in $\mathcal{M}_4$

First, we compute the Virsoro operator for the Neveu-Schwarz sector for the Minkowski spacetime in light cone coordinates, which reads

$$\begin{aligned}
\sum_{\mathcal{M}} L_{0,\mathrm{NS}}^{\perp} &= \frac{1}{2} \sum_{\mu=1}^{2} \left(\sum_{n\in\mathbb{Z}} \alpha_{-n}^{\mu} \alpha_{n}^{\mu} + \sum_{r\in\mathbb{Z}+\frac{1}{2}} r\ \psi_{-r}^{\mu} \psi_{r}^{\mu} \right) \\
&= \frac{1}{2} \sum_{\mu=1}^{2} \sum_{n=1}^{\infty} \alpha_{-n}^{\mu} \alpha_{n}^{\mu} + \underbrace{\frac{1}{2} \sum_{\mu=1}^{2} \sum_{n=1}^{\infty} \alpha_{n}^{\mu} \alpha_{-n}^{\mu}}_{=:A} \\
&+ \frac{1}{2} \sum_{\mu=1}^{2} \sum_{r\in\mathbb{Z}^{0+}+\frac{1}{2}}^{\infty} r\ \psi_{-r}^{\mu} \psi_{r}^{\mu} + \underbrace{\frac{1}{2} \sum_{\mu=1}^{2} \sum_{r\in\mathbb{Z}^{0+}+\frac{1}{2}}^{\infty} -r\ \psi_{r}^{\mu} \psi_{-r}^{\mu}}_{=:B}
\end{aligned} \tag{C.2}$$

with $\mathbb{Z}^{0+} := \mathbb{Z}^{+} \cup \{0\}$ being the set of non-negative integers. In the second and third line of Eq. (C.2), we see that the first sum on the right-hand side is already normal-ordered. However, the second sum is not normal-ordered. Since normal-ordered operators are very useful because they act in a simple manner on the vacuum state, we have to rewrite the terms A and B in Eq. (C.2) according to

$$
\begin{aligned}
A+B &= \frac{1}{2}\sum_{\mu=1}^{2}\sum_{n=1}^{\infty}\alpha_n^\mu\alpha_{-n}^\mu + \frac{1}{2}\sum_{\mu=1}^{2}\sum_{r\in\mathbb{Z}^{0+}+\frac{1}{2}}^{\infty} -r\ \psi_r^\mu\psi_{-r}^\mu = \frac{1}{2}\sum_{\mu=1}^{2}\sum_{n=1}^{\infty}\left(\alpha_{-n}^\mu\alpha_n^\mu + [\alpha_n^\mu,\alpha_{-n}^\mu]\right)\\
&+\frac{1}{2}\sum_{\mu=1}^{2}\sum_{r\in\mathbb{Z}^{0+}+\frac{1}{2}}^{\infty}\left(r\ \psi_{-r}^\mu\psi_r^\mu - r\ \{\psi_r^\mu,\psi_{-r}^\mu\}\right) = \frac{1}{2}\sum_{\mu=1}^{2}\sum_{n=1}^{\infty}\alpha_{-n}^\mu\alpha_n^\mu + \frac{1}{2}\sum_{\mu=1}^{2}\sum_{n=1}^{\infty} n\eta^{\mu\mu}\\
&+\frac{1}{2}\sum_{\mu=1}^{2}\sum_{r\in\mathbb{Z}^{0+}+\frac{1}{2}}^{\infty} r\ \psi_{-r}^\mu\psi_r^\mu - \frac{1}{2}\sum_{\mu=1}^{2}\sum_{r\in\mathbb{Z}^{0+}}^{\infty}\left(r+\frac{1}{2}\right)\eta^{\mu\mu} = \frac{1}{2}\sum_{\mu=1}^{2}\sum_{n=1}^{\infty}\alpha_{-n}^\mu\alpha_n^\mu + \sum_{n=1}^{\infty} n\\
&+\frac{1}{2}\sum_{\mu=1}^{2}\sum_{r\in\mathbb{Z}^{0+}+\frac{1}{2}}^{\infty} r\ \psi_{-r}^\mu\psi_r^\mu - \sum_{r\in\mathbb{Z}^{0+}}^{\infty}\left(r+\frac{1}{2}\right)\\
&= \frac{1}{2}\sum_{\mu=1}^{2}\sum_{n=1}^{\infty}\alpha_{-n}^\mu\alpha_n^\mu - \frac{1}{12} + \frac{1}{2}\sum_{\mu=1}^{2}\sum_{r\in\mathbb{Z}^{0+}+\frac{1}{2}}^{\infty} r\ \psi_{-r}^\mu\psi_r^\mu - \frac{1}{24}.
\end{aligned}
\tag{C.3}
$$

In the first and second line of Eq. (C.3), we inserted a commutator $[\alpha_m^\mu,\alpha_n^\nu] = m\ \eta^{\mu\nu}\delta_{m+n,0}$ and an anticommutator $\{\psi_r^\mu,\psi_s^\nu\} = \eta^{\mu\nu}\delta_{r+s,0}$, which we found in Eq. (3.29) and Eq. (3.30) for the case that $\theta = 0$, to get the right ordering.

The sums $\sum_{n=1}^{\infty} n$ and $\sum_{r\in\mathbb{Z}^{0+}}^{\infty}\left(r+\frac{1}{2}\right)$ are divergent, but nothing else but the vacuum energy or Casimir energy of the superstring. Hence finite. This follows from the relationship of the Virasoro generator $L_0^\perp$ and the quantum Hamiltonian H [45]. Regularisation and Renormalisation of divergent vacuum energies are standard techniques in QFT and in our case we will use a neat and famous trick via ζ-function regularisation [264].

As a reminder, the Riemann Zeta function $\zeta(s)$ with $s = r + it$ is a meromorphic function in the complex plane with a single pole at $s = 1$ and can be obtained by an analytic continuation of the the series [265]

$$\zeta(s) = \sum_{n=1}^{\infty} n^{-s}. \tag{C.4}$$

For the first divergent sum it follows that

$$\sum_{n=1}^{\infty} n = \zeta(-1) = -\frac{1}{12} \tag{C.5}$$

while the second sum can be regularised to

$$\sum_{r\in\mathbb{Z}^{0+}}^{\infty}\left(r+\frac{1}{2}\right) = \frac{1}{2}\sum_{r\in\mathbb{Z}^{+}_{\text{odd}}}^{\infty} r \tag{C.6}$$

but we know that the sum over all positive integers can be rearranged in the following way

$$\sum_{r=1}^{\infty} r = \sum_{r\in\mathbb{Z}^{+}_{\text{even}}}^{\infty} r + \sum_{r\in\mathbb{Z}^{+}_{\text{odd}}}^{\infty} r = \sum_{r\in\mathbb{Z}^{+}_{\text{odd}}}^{\infty} r + 2\sum_{r=1}^{\infty} r\ . \tag{C.7}$$

Thus, Eq. (C.6) can be massaged into

$$\frac{1}{2}\sum_{r\in\mathbb{Z}^{+}_{\text{odd}}}^{\infty} r = -\frac{1}{2}\sum_{r=1}^{\infty} r = \frac{1}{24}\ . \tag{C.8}$$

Inserting this last results back into Eq. (C.2), we obtain a normal ordered expression with an ordering constant $a_{\mathrm{NS}} = -\frac{1}{8}$. The NS-sector reads

$$\sum_{\mathcal{M}} L_{0,\mathrm{NS}}^{\perp} = \sum_{\mu=1}^{2}\sum_{n=1}^{\infty} :\alpha_{-n}^{\mu}\alpha_{n}^{\mu}: + \sum_{\mu=1}^{2}\sum_{r\in\mathbb{Z}^{0+}+\frac{1}{2}}^{\infty} r\ :\psi_{-r}^{\mu}\psi_{r}^{\mu}: + a_{\mathrm{NS}}\ . \tag{C.9}$$

We can now carry out the same procedure for the Ramond sector.

$$\begin{aligned}\sum_{\mathcal{M}} L_{0,R}^{\perp} &= \frac{1}{2}\sum_{\mu=1}^{2}\left(\sum_{n\in\mathbb{Z}}\alpha_{-n}^{\mu}\alpha_{n}^{\mu} + \sum_{r\in\mathbb{Z}} r\ \psi_{-r}^{\mu}\psi_{r}^{\mu}\right) = \frac{1}{2}\sum_{\mu=1}^{2}\sum_{n=1}^{\infty}\alpha_{-n}^{\mu}\alpha_{n}^{\mu} + \underbrace{\frac{1}{2}\sum_{\mu=1}^{2}\sum_{n=1}^{\infty}\alpha_{n}^{\mu}\alpha_{-n}^{\mu}}_{=:A} \\ &\quad + \frac{1}{2}\sum_{\mu=1}^{2}\sum_{r\in\mathbb{Z}^{0+}}^{\infty} r\ \psi_{-r}^{\mu}\psi_{r}^{\mu} + \underbrace{\frac{1}{2}\sum_{\mu=1}^{2}\sum_{r\in\mathbb{Z}^{0+}}^{\infty} -r\ \psi_{r}^{\mu}\psi_{-r}^{\mu}}_{=:C}\ .\end{aligned} \tag{C.10}$$

The calculation for A in Eq. (C.10) is the same as in (C.3), so all that remains is to calculate the term C.

$$\begin{aligned}C &:= \frac{1}{2}\sum_{\mu=1}^{2}\sum_{r\in\mathbb{Z}^{0+}}^{\infty} -r\ \psi_{r}^{\mu}\psi_{-r}^{\mu} = \frac{1}{2}\sum_{\mu=1}^{2}\sum_{r\in\mathbb{Z}^{0+}}^{\infty}\left(r\ \psi_{-r}^{\mu}\psi_{r}^{\mu} - r\ \{\psi_{r}^{\mu},\psi_{-r}^{\mu}\}\right) \\ &= \frac{1}{2}\sum_{\mu=1}^{2}\sum_{r\in\mathbb{Z}^{0+}}^{\infty} r\ \psi_{-r}^{\mu}\psi_{r}^{\mu} - \frac{1}{2}\sum_{\mu=1}^{2}\sum_{r\in\mathbb{Z}^{0+}}^{\infty} r\eta^{\mu\mu} = \frac{1}{2}\sum_{\mu=1}^{2}\sum_{r\in\mathbb{Z}^{0+}}^{\infty} r\ \psi_{-r}^{\mu}\psi_{r}^{\mu} - \sum_{r\in\mathbb{Z}^{0+}}^{\infty} r \\ &= \frac{1}{2}\sum_{\mu=1}^{2}\sum_{r\in\mathbb{Z}^{0+}}^{\infty} r\ \psi_{-r}^{\mu}\psi_{r}^{\mu} + \frac{1}{12}\ .\end{aligned} \tag{C.11}$$

Plugging this result into the Eq. (C.10), this time we get

$$\sum_{\mathcal{M}} L_{0,R}^{\perp} = \sum_{\mu=1}^{2}\sum_{n=1}^{\infty} :\alpha_{-n}^{\mu}\alpha_{n}^{\mu}: + \sum_{\mu=1}^{2}\sum_{r\in\mathbb{Z}^{+}+\frac{1}{2}}^{\infty} r\ :\psi_{-r}^{\mu}\psi_{r}^{\mu}: + a_{\mathrm{R}} \tag{C.12}$$

with $a_R = 0$.

All together, we can so far summarise

$$\sum_{\mathcal{M}}\left(L_{0,\mathrm{NS}}^{\perp} + L_{0,\mathrm{R}}^{\perp}\right) = \sum_{\mu=1}^{2}\sum_{n=1}^{\infty} :\alpha_{-n}^{\mu}\alpha_{n}^{\mu}: + \sum_{\mu=1}^{2}\sum_{r\in\mathbb{Z}^{0+}}^{\infty}(r+\nu)\ :\psi_{-r}^{\mu}\psi_{r}^{\mu}: - \frac{\nu}{4} \tag{C.13}$$

with $\nu = \begin{cases}\nu = 0, & \mathrm{R} \\ \nu = \frac{1}{2}, & \mathrm{NS}.\end{cases}$

C.2 Virasoro Operator for the R and NS Sector in $\mathcal{I}_3$

In this section, we will repeat the calculation for the internal space. The dependence on the angle θ will make some things slightly more complicated but the main idea stays the same. The R-sector will again give a zero contribution to the ordering constant, thus we will just focus on the NS-sector. The Virasoro operator for that sector is

$$\begin{aligned}
\sum_{\mathcal{I}} L_{0,\mathrm{NS}}^{\perp} &= \frac{1}{2}\sum_{i=1}^{3}\left(\sum_{n\in\mathbb{Z}}\alpha^i_{-n\pm\epsilon_i}\alpha^i_{n\pm\epsilon_i} + \sum_{r\in\mathbb{Z}^{0+}+\frac{1}{2}}\left(r\pm\epsilon_i\right)\ \psi^i_{-r\pm\epsilon_i}\psi^i_{r\pm\epsilon_i}\right) \\
&= \frac{1}{2}\sum_{i=1}^{3}\sum_{n=1}^{\infty}\alpha^i_{-n\pm\epsilon_i}\alpha^i_{n\pm\epsilon_i} + \underbrace{\frac{1}{2}\sum_{i=1}^{3}\sum_{n=1}^{\infty}\alpha^i_{n\pm\epsilon_i}\alpha^i_{-n\pm\epsilon_i}}_{=:D} \\
&+ \frac{1}{2}\sum_{i=1}^{3}\sum_{r\in\mathbb{Z}^{0+}}^{\infty}\left(r\pm\epsilon_i+\frac{1}{2}\right)\ \psi^i_{-r\pm\epsilon_i}\psi^i_{r\pm\epsilon_i} \\
&+ \underbrace{\frac{1}{2}\sum_{i=1}^{3}\sum_{r\in\mathbb{Z}^{0+}}^{\infty} -\left(r\pm\epsilon_i+\frac{1}{2}\right)\ \psi^i_{r\pm\epsilon_i}\psi^i_{-r\pm\epsilon_i}}_{=:E}\ .
\end{aligned} \tag{C.14}$$

We start again with the bosonic part, which can be rewritten to [1]

$$\begin{aligned}
D := \frac{1}{2}\sum_{i=1}^{3}\sum_{n=1}^{\infty}\alpha^i_{n\pm\epsilon_i}\alpha^i_{-n\pm\epsilon_i} &= \frac{1}{2}\sum_{i=1}^{3}\sum_{n=1}^{\infty}\left(\alpha^i_{-n\pm\epsilon_i}\alpha^i_{n\pm\epsilon_i} + \left[\alpha^i_{n\pm\epsilon_i},\alpha^i_{-n\pm\epsilon_i}\right]\right) \\
&= \frac{1}{2}\sum_{i=1}^{3}\sum_{n=1}^{\infty}\alpha^i_{-n\pm\epsilon_i}\alpha^i_{n\pm\epsilon_i} + \sum_{i=1}^{3}\sum_{n=1}^{\infty}\left(n\pm\epsilon_i\right)\delta^{ii} \\
&= \frac{1}{2}\sum_{\mu=1}^{2}\sum_{n=1}^{\infty}\alpha^i_{-n\pm\epsilon_i}\alpha^i_{n\pm\epsilon_i} + \sum_{i=1}^{3}\sum_{n=1}^{\infty}\left(n\pm\epsilon_i\right) \\
&= \frac{1}{2}\sum_{i=1}^{3}\sum_{n=1}^{\infty}\alpha^i_{-n\pm\epsilon_i}\alpha^i_{n\pm\epsilon_i} + \sum_{i=1}^{3}\zeta_H\left(-1,\pm\epsilon_i\right)
\end{aligned} \tag{C.15}$$

where ζ_H is the *Hurwitz-Riemann Zeta function*, a generalisation of the Riemann Zeta function [264]. Formally, this function is defined for complex arguments s with $Re(s) > 1$ and q with $Re(q) > 0$ by

$$\zeta_H(s,q) = \sum_{n=0}^{\infty}\frac{1}{(n+q)^s} \tag{C.16}$$

For $Re(q) > 0$ and $n \in \mathbb{N}$ we have the special expression

$$\zeta_H(-n,a) = -\frac{B_{n+1}(a)}{n+1}. \tag{C.17}$$

where $B_m(x)$ are the *Bernoulli polynomials* [264]

$$B_m(x) = \sum_{n=0}^{m}\frac{1}{n+1}\sum_{k=0}^{n}(-1)^k\begin{pmatrix} n \\ k \end{pmatrix}(x+k)^m. \tag{C.18}$$

Using that for our expression in (C.15), we get

$$\zeta_H\left(-1,\pm\epsilon_i\right) = -\frac{1}{2}B_2(\epsilon_i) = -\frac{1}{2}\left(\epsilon_i^2 \mp \epsilon_i + \frac{1}{6}\right) \tag{C.19}$$

[1] Note that there is no $\frac{1}{2}$ on the second term of Eq. (C.15). This is due to the fact, that we are working with complexified coordinates. Since the physical dimensions have to be real, we have to count the complexified ones twice.

Thus, we obtain

$$D := \frac{1}{2}\sum_{i=1}^{3}\sum_{n=1}^{\infty}\alpha^i_{-n\pm\epsilon_i}\alpha^i_{n\pm\epsilon_i} - \frac{1}{2}\sum_{i=1}^{3}\left(\epsilon_i^2 \mp \epsilon_i + \frac{1}{6}\right) \tag{C.20}$$

The last term in Eq. (C.14) that remains to be considered is E.

$$\begin{aligned}
E &:= \frac{1}{2}\sum_{i=1}^{3}\sum_{r\in\mathbb{Z}^{0+}+\frac{1}{2}}^{\infty} -(r\pm\epsilon_i)\ \psi^i_r\psi^i_{-r} \\
&= \frac{1}{2}\sum_{i=1}^{3}\sum_{r\in\mathbb{Z}^{0+}+\frac{1}{2}}^{\infty}\left[(r\pm\epsilon_i)\ \psi^i_{-r}\psi^i_r - (r\pm\epsilon_i)\ \left\{\psi^i_r,\psi^i_{-r}\right\}\right] \\
&= \frac{1}{2}\sum_{i=1}^{3}\sum_{r\in\mathbb{Z}^{0+}+\frac{1}{2}}^{\infty}(r\pm\epsilon_i)\ \psi^i_{-r}\psi^i_r - \sum_{i=1}^{3}\sum_{r\in\mathbb{Z}^{0+}+\frac{1}{2}}^{\infty}(r\pm\epsilon_i)\,\delta^{ii} \\
&= \frac{1}{2}\sum_{i=1}^{3}\sum_{r\in\mathbb{Z}^{0+}+\frac{1}{2}}^{\infty}(r\pm\epsilon_i)\ \psi^i_{-r}\psi^i_r - \sum_{i=1}^{3}\sum_{r\in\mathbb{Z}^{0+}}^{\infty}\left(r\pm\epsilon_i+\frac{1}{2}\right) \\
&= \frac{1}{2}\sum_{i=1}^{3}\sum_{r\in\mathbb{Z}^{0+}+\frac{1}{2}}^{\infty}(r\pm\epsilon_i)\ \psi^i_{-r}\psi^i_r - \sum_{i=1}^{3}\zeta_H\left(-1,\frac{1}{2}\pm\epsilon_i\right) \\
&= \frac{1}{2}\sum_{i=1}^{3}\sum_{r\in\mathbb{Z}^{0+}+\frac{1}{2}}^{\infty}(r\pm\epsilon_i)\ \psi^i_{-r}\psi^i_r + \frac{1}{2}\sum_{i}^{3}\left[\left(\pm\epsilon_i+\frac{1}{2}\right)^2 \mp \left(\epsilon_i+\frac{1}{2}\right)+\frac{1}{6}\right]\ .
\end{aligned} \tag{C.21}$$

After combining the two ordering constants and simplifying the expression with simple algebra, we are left with

$$\begin{aligned}
\sum_{i=1}^{3} -\frac{1}{2}\left(\epsilon_i^2\mp\epsilon_i+\frac{1}{6}\right)+\frac{1}{2}\left[\left(\frac{1}{2}\pm\epsilon_i\right)^2\mp\epsilon_i-\frac{1}{2}+\frac{1}{6}\right] &= \sum_{i}^{3}\left(\frac{\pm\epsilon_i}{2}-\frac{1}{8}\right) \\
&= -\frac{3}{8}\pm\frac{1}{2}\sum_{i}^{3}\epsilon_i.
\end{aligned} \tag{C.22}$$

All together, the full ordering constant for this system is

$$a_0 = -\frac{1}{8}-\frac{3}{8}\pm\frac{1}{2}\sum_{i}^{3}\epsilon_k = -\frac{1}{2}\pm\frac{1}{2}\sum_{i}^{3}\epsilon_k \tag{C.23}$$

The mass-squared formula M^2 is given by

$$M^2 = \frac{1}{\alpha'}\left(N_\perp - a_0\right) \tag{C.24}$$

which is a direct consequence of the mass shell condition $M^2 = -p^2 = 2p^+p^- - p^ip^i$ [45]. $N_\perp$ is the so-called number operator which in our case is

$$\begin{aligned}
N_\perp = &\sum_{\mu=1}^{2}\left(\sum_{n=1}^{\infty} : a^\mu_{-n}a^\mu_n : + \sum_{r\in\mathbb{Z}^{0+}+\nu} r\ : \psi^\mu_{-r}\psi^\mu_r :\right) \\
&+\sum_{i=1}^{3}\left(\sum_{m=1}^{\infty} : a^i_{-m+\epsilon_i}a^i_{m-\epsilon_i} : + \sum_{r\in\mathbb{Z}^{0+}+\nu}(r-\epsilon_i) : \psi^i_{-r+\epsilon_i}\psi^i_{r-\epsilon_i} :\right)
\end{aligned} \tag{C.25}$$

Finally, we obtain the mass-squared formula

$$
\begin{aligned}
M^2 = &\sum_{\mu=1}^{2}\left(\sum_{n=1}^{\infty} : a^\mu_{-n} a^\mu_n : + \sum_{r\in\mathbb{Z}^{0+}+\nu} r \ : \psi^\mu_{-r}\psi^\mu_r :\right) \\
&+ \sum_{i=1}^{3}\left(\sum_{m=1}^{\infty} : a^i_{-m+\epsilon_i} a^i_{m-\epsilon_i} : + \sum_{r\in\mathbb{Z}^{0+}+\nu} (r-\epsilon_i) : \psi^i_{-r+\epsilon_i}\psi^i_{r-\epsilon_i} :\right) \\
&+ 2\nu a_0
\end{aligned}
\tag{C.26}
$$

with $\nu = \begin{cases} \nu = 0, & \text{R} \\ \nu = \frac{1}{2}, & \text{NS.} \end{cases}$

Appendix D

Homology: A Primer

In this appendix, some common concepts of algebraic topology which the reader may not be familiar with are to be explained briefly and concisely. Although, it is not possible to go into this exciting topic in greater depth here - the ambitious reader can be recommended [63, 111, 266] to find more details.

By adapting the notation from chapter 4, the d-dimensional manifold $\mathcal{M}$ is supposed to be smooth and connected. Furthermore, we define a *r-chain* $\mathcal{C}_r$ as the sum

$$\mathcal{C}_r = \sum_i c_i\, \mho_r^i \ . \tag{D.1}$$

The $\mho_r^i \subset \mathcal{M}$ are r-dimensional oriented submanifolds, while the coefficients $c_i \in \mathbb{F}$ can be either real, complex, or integers. One therefore speaks of real, complex, or integral r-chains [267]. One way to get a better understanding is to interpret r-chains as something which can be integrated over [268].

$$\int_{\sum c_i \mho_i} = \sum_i c_i \int_{\mho_i} \ . \tag{D.2}$$

Moreover, these linear combinations in Eq. (D.1) r-chains introduce a vector space structure on the respective set of submanifolds of $\mathcal{M}$ [63].

Topology allows us to define a boundary operator ∂, which associates the oriented boundary $\partial\mathcal{M}$ to a given manifold $\mathcal{M}$. A special result in topology is that boundaries have no boundary. Thus, the boundary of a boundary is zero.

$$\partial\left(\partial\mathcal{M}\right) \equiv 0. \tag{D.3}$$

By linearity, the boundary operation yields a $(r-1)$-chain

$$\partial\mathcal{C}_r = \sum_i c_i\, \partial\mho_r^i \equiv \mathcal{C}'_{r-1} \ . \tag{D.4}$$

A *r-cycle* is defined to be a r-chain without a boundary and therefore satisfying

$$\partial\mathcal{C}_r = 0 \ . \tag{D.5}$$

A r-chain $\mathcal{C}_r$ is called *trivial* if it is the boundary of a $(r+1)$-chain $\mathcal{C}_r = \partial\mathcal{D}_{r+1}$. Thus, any trivial r-chain is a r-cycle, since $\partial^2 \equiv 0$. However, the reverse is generally not true [1] [266].

Non-trivial cycles can now be characterised by so-called *homology groups*. We define $\mathcal{Z}_r$ to be the set of r-cycles $\mathcal{C}_r \subset \mathcal{M}$ and $\mathcal{B}_r = \{\mathcal{C}_r |\ \mathcal{C}_r = \partial\mathcal{D}_{r+1}\}$ to be the set of r-chains which are boundaries

[1] In the special case that $\mathcal{M}$ can be identified with the $\mathbb{R}^d$, this statement is true in both directions. The reason behind this lies in the so-called *Poincare duality lemma*.

of $(r+1)$-chains and therefore by definition trivial. The *simplicial homology* or r^{th} homology group of $\mathcal{M}$ is then defined as the quotient set

$$H_r(\mathcal{M}, \mathbb{F}) = \frac{\mathcal{Z}_r}{\mathcal{B}_r} \tag{D.6}$$

$H_r(\mathcal{M}, \mathbb{F})$ provides equivalence relations, where two cycles are considered equivalent if they only differ by a boundary or trivial r-chain, respectively. The homology class of a r-cycle is thus

$$H_r(\mathcal{M}, \mathbb{F}) \ni [\,\mathcal{C}_r\,] = \{\mathcal{C}_r \subset \mathcal{M} \,|\, \mathcal{C}_r \sim \mathcal{C}_r + \partial\mathcal{D}_{r+1}\} \ . \tag{D.7}$$

Trivial cycles are in the so-called trivial class $[\emptyset]$. The sets of homology groups are finite-dimensional vector spaces with dimensions

$$b_r(\mathcal{M}) = \dim\left(H_r(\mathcal{M}, \mathbb{F})\right) \ . \tag{D.8}$$

This purely topological number is the famous *Betti number* [63, 269].

D.1 Homology Groups and Betti Number of the 2-Torus

In order to make the previous discussion a little more concrete and to relate it to the present work in chapter 4, we want to give an example by determining the homology groups of the 2-torus $\mathbb{T}^2$.

In the Fig. D.1a, the two cycles Π_1 and Π_1', which have no boundary and are not themselves a boundary, are drawn. These two cycles on the torus are equivalent to each other as they only differ by the boundary U. Looking once more at Fig. D.1b, one can recognise further 1-cycles, e.g., Π_2 and Π_2', which are independent of the first equivalence class. The most general 1-cycle can be thus expressed as the linear combination

$$[\Pi] = m[\Pi_1] + n[\Pi_2]\ , \quad \text{with} \quad m, n \in \mathbb{Z}. \tag{D.9}$$

The 1^{st} homology group of $\mathbb{T}^2$ is therefore equivalent to $H_1(\mathbb{T}^2, \mathbb{Z}) \simeq \mathbb{Z} \oplus \mathbb{Z}$.

Since the surface of the 2-torus is itself boundaryless, it is of course a 2-cycle itself.

Higher dimensional homology groups are not possible due to the dimensionality of the 2-torus itself, but we are able to add another group. Points have no boundary and are therefore 0-cycles. In general, two points always represent a boundary for a curve. If the underlying manifold is connected, the elements of this 0^{th} homology group are equivalent points and ultimately provide a criterion for path connectedness. Summarising all homology groups of the 2-torus yields [2]

$$H_r(\mathbb{T}^2, \mathbb{Z}) \simeq \begin{cases} \mathbb{Z} \oplus \mathbb{Z} & \text{for } r = 1 \\ \mathbb{Z} & \text{for } r = 0, 2 \\ 0 & \text{for } r \geq 3. \end{cases} \tag{D.10}$$

The Betti number can be determined very easily as

$$b_r(\mathbb{T}^2) = \dim\Big(H_r(\mathbb{T}^2, \mathbb{Z})\Big) = \begin{cases} 2 & \text{for } r = 1 \\ 1 & \text{for } r = 0, 2 \\ 0 & \text{for } r \geq 3. \end{cases} \tag{D.11}$$

The Betti number $b_0(\mathbb{T}^2)$ provides the number of paths connected components on $\mathbb{T}^2$. This is exactly one, which does justice to the intuitive assumption one has by thinking of 2-tori. The first Betti number $b_1(\mathbb{T}^2)$ tells us that there have been two 1-dimensional "holes". These are of

[2] The fact that the cases for $r = 1$ and $r = 2$ are identical is of course not a coincidence and has its origin again in the *Poincare duality*, which cannot be discussed here.

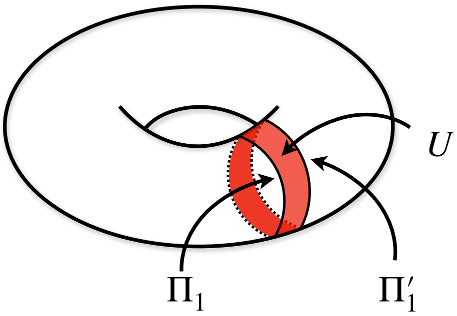

(a) The 1-circles Π_1 and Π_1' are 1-cycles, because they neither have a boundary nor are they boundaries themselves. The cycles are elements of the same equivalence class $H_1(\mathbb{T}^2, \mathbb{Z})$ because they only differ by a boundary U.

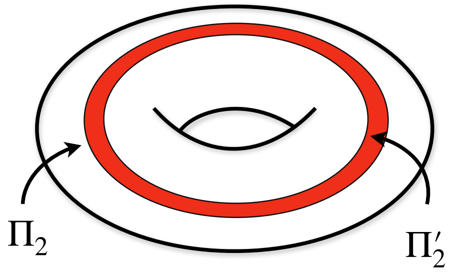

(b) The 1-circles Π_2 and Π_2' are 1-cycles, because they neither have a boundary nor are they boundaries themselves. The cycles are elements of the same equivalence class $H_1(\mathbb{T}^2, \mathbb{Z})$, because they again only differ by a boundary.

Figure D.1: Illustration of an $\mathbb{T}^2$ and linearly independent 1-cycles, which are elements of the homology group $H_1(\mathbb{T}^2, \mathbb{Z})$.

course the equatorial and meridional circular "holes". The last Betti number $b_2(\mathbb{T}^2)$ indicates that there must be a 2-dimensional "hole". This is the cavity that encloses the torus.

Holonomy groups therefore offer a tool to describe a topological feature of a shape that is characterised by the fact that it is "not there". The rank of the r^{th} holonomy group gives the number of r-dimensional "holes". This allows you to define holes and differentiate between different kinds.

Appendix E

Tori and Orientifold Action

In this appendix, we will take a closer look at the orientifold action on rectangular and tilted 2-tori, which we introduced in section 4.3.

E.1 Rectangular Tori

The fundamental domain $\mathcal{P}_{\text{rect}}$ of a rectangular 2-torus can be represented as a planar rectangle in the xy-plane, whose parallel edges can be identified as shown in Fig. E.1a. The orientifold is located along the x-axis. The orientifold projection $\mathcal{R} : (x, y) \mapsto (x, -y)$ reverses the orientation of the string and sends the coordinates (x, y) into $(x, -y)$. This creates a class of equivalence relations, which read

$$(x, y) \sim (x + R_1, y) \quad \text{and} \quad (x, y) \sim (x, y + R_2) \quad \text{with} \quad R_1, R_2 > 0 \; . \tag{E.1}$$

The fundamental domain $\mathcal{P}_{\text{rect}}$ can therefore be defined by those points (x, y) which satisfy $0 \leq x \leq R_1$ and $0 \leq y \leq R_2$. Before we turn to the more interesting case of the tilted torus, we want to show that the orientifold action is a well-defined action and maps equivalent coordinates to corresponding equivalent points, respecting the equivalent relations of Eq. (E.1). This is indeed fulfilled as shown by the simple calculation

$$\begin{aligned} (x, y) &\sim (x + R_1, y) \to (x + R_1, -y) \sim (x, -y), \\ (x, y) &\sim (x, y + R_2) \to (x, -y - R_2) \sim (x, -y). \end{aligned} \tag{E.2}$$

The fixed points under this orientifold action – called $\text{Fix}(\mathcal{R})$ in section 4.3 – are given by

$$(x, y) \sim (x, -y) \; . \tag{E.3}$$

This is trivially fulfilled for $y = 0$. Furthermore, this is satisfied if the coordinates have the form

$$(x, y) = (x, -y + nR_2) \quad \text{with} \quad n \in \mathbb{Z} \; . \tag{E.4}$$

Comparing it to Eq. (E.3) gives us fixed points along the lines $y = \frac{nR_2}{2}$. A simple case distinction must be made here. For the case that n is even, the fixed loci are equivalent to the locus given by $y = 0$ in the sense of the torus identification. In the case where n is odd, the corresponding loci are equivalent to the fixed point line $y = \frac{R_2}{2}$. In sum, we thus get two fixed point loci on the 2-torus.

Let us now consider an arbitrary point (x, y). By a reflection at the orientifold given by $y = \frac{R_2}{2}$, we obtain $(x, y) \mapsto (x, R_2 - y)$. The situation is different for reflections at the orientifold corresponding to $y = 0$, where we have $(x, y) \mapsto (x, -y)$.

By toroidal identification, we find that $(x, -y) \sim (x, R_2 - y)$. The two reflections are thus equivalent to each other

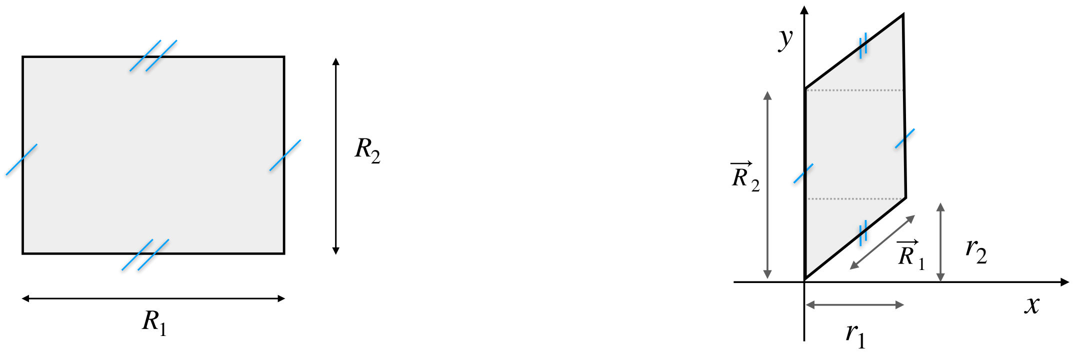

(a) The fundamental domain of a rectangular 2-torus. The vertical lines and horizontal lines are identified with each other. Thus, each vertex corresponds to the same point on the 2-torus.

(b) The fundamental domain of a tilted 2-torus in the xy-plane. Here, $r_2 = s/2$ is chosen.The vertical lines and horizontal lines are again identified with each other.

Figure E.1: The fundamental domain $\mathcal{P}_{\text{rect}}$ of the rectangular 2-torus and the fundamental domain $\mathcal{P}_{\text{tilt}}$ of the tilted 2-torus.

E.2 Tilted Tori

We now turn to the tilted torus. The class of tilted tori is specified by the identifications [45]

$$(x, y) \sim (x + a_1, y + a_2) \quad \text{and} \quad (x, y) \sim (x, y + b) \quad \text{with} \quad a_1, a_2, b > 0 \ . \tag{E.5}$$

The fundamental domain $\mathcal{P}_{\text{tilt}}$ of the tilted torus corresponds to a parallelogram with a vertex at the origin of the coordinate system and sides given by $\vec{R}_1 = (r_1, r_2)$ and $\vec{R}_2 = (0, s)$. For an overview, this is sketched in Fig. E.1b. Concretely, we want to deal with the special case $r_2 = \frac{s}{2}$. Here, too, it is necessary to check whether the orientifold action $(x, y) \mapsto (x, -y)$ is well-defined for the case of tilted tori and where the fixed point lines are to be found. To test the well-definedness of the orientifold action, let us look at the corners of the fundamental domain. It is obvious that $(0, 0) \sim (r_1, r_2)$. Furthermore, the origin at $(0, 0)$ is invariant under $\mathcal{R}$ which yields $(r_1, r_2) \sim (r_1, -r_2)$. This is satisfied if $r_2 = -r_2 + ns$ holds with $n \in \mathbb{Z}$. For us, the relevant case is given by $r_2 = \frac{s}{2}$, which sets $n = 1$. Let us first examine the fact that

$$(x + r_1, -y - r_2) \sim (x + r_1, -y - r_2) - (r_1, r_2) + (0, s) = (x, -y - 2r_2 + s) \ , \tag{E.6}$$

which yields exactly $(x, -y)$ for the case that $r_2 = \frac{s}{2}$. As a consequence,

$$(x, y) \sim (x + r_1, y + r_2) \to (x + r_1, -y - r_2) \sim (x, -y) \ , \tag{E.7}$$

is indeed well-defined under the tilted tori identifications in Eq. (E.5). Again, we have two fixed lines, which we depicted in Fig. E.1b. The first one is defined by the the line along $y = s$, the second one by the line $y = \frac{s}{2}$. Note, that these two fixed lines are one closed line on the tilted torus, which can be seen immediately by keeping in mind that all the corners are identified.

Defining $\vec{R}_1^* \equiv (r_1, -r_2)$ as the image of $\vec{R}_1$ under $\mathcal{R}$ and using $r_2 = \frac{s}{2}$ we find

$$\vec{R}_1^* = (r_1, -r_2) = (r_1, r_2) - (0, 2r_2) = \vec{R}_1 - \vec{R}_2 \ . \tag{E.8}$$

An arbitrary point on $\mathcal{P}_{\text{tilt}}$ can be described a vector $\lambda\vec{R}_1 + \mu\vec{R}_2$, with λ, μ being constant. Acting with $\mathcal{R}$, provides us with

$$\lambda\vec{R}_1 + \mu\vec{R}_2 \to \lambda\vec{R}_1^* - \mu\vec{R}_2 = \lambda(\vec{R}_1 - \vec{R}_2) - \mu\vec{R}_2 = \lambda\vec{R}_1 - (\lambda + \mu)\,\vec{R}_2 \ . \tag{E.9}$$

Recall that we have described closed lines on tori in terms of relatively prime integers - the wrapping numbers. These tuples (n, m) were to be understood in such a way, that we get a line from the origin $(0, 0)$ to a point given by $n\vec{R}_1 + m\vec{R}_2$. In section 4.3, we derived a formula on how we can calculate the intersection number of two such closed lines. Now, one could think that we have implicitly assumed that this revelation is only valid if the compact space is given by a rectangular torus.

In general, the tilted and rectangular tori are similar via a linear invertible mapping given by [45, 63]

$$x \to \frac{1}{r_1}x, \quad y \to -\frac{1}{2r_1}x + \frac{1}{s}y \ . \tag{E.10}$$

This linear map transforms the tilted torus to the unit rectangular torus. This mapping is bijective and the intersection number, which depends on the wrapping numbers, remain preserved under this transformation. This was of course expected, since we derived the intersection number by a purely topological argument and granted it to a completely topological quantity. Consequently, geometric designations and metric related issues should not play a role. The wrapping numbers behave under the orientifold action according to the derived formula in Eq. (E.9), which we explicitly state as

$$(n, m) \mapsto (n, -n - m) \ . \tag{E.11}$$

It is very convenient to express the wrapping numbers by using half integers in the tilted tori basis, which we will denote as the $[\bullet, \bullet]$-basis, in contrast to the $(\bullet, \bullet)$-basis for the rectangular case. The wrapping numbers are related by

$$(n, m) \sim [n, m + \frac{n}{2}] \equiv (\tilde{n}, \tilde{m}) \tag{E.12}$$

Knowing this, we can explicitly write down the intersection number in the $[\bullet, \bullet]$-basis, which we originally computed by using the $(\bullet, \bullet)$-basis. Inverting Eq. (E.12), the intersection number is calculated according to

$$I_{12}^{\text{tilt}} = [n_1 m_2 - m_1 n_2] \sim \left(n_1 \left(m_2 - \frac{n_2}{2}\right) - \left(m_1 - \frac{n_1}{2}\right) n_2\right) = (n_1 m_2 - m_1 n_2) = I_{12}^{\text{rect}} \ . \tag{E.13}$$

Indeed, the intersection number does not depend on wether the tori are rectangular or tilted.

Acknowledgements

First and foremost, I would like to express my genuinely gratitude to Stefan Fredenhagen and Pascal Anastasopoulos. Not only did they enable me to write this thesis under their warm, keen and proficient supervision, but sparked my curiosity for theoretical physics with their contagious and inspiring passion. I am convinced that great brilliance and wisdom are characterised by being able to explain the most difficult and complex things in this universe in a simple, intuitive and honest way. Both have demonstrated this ability and empathy towards their students more than once.

During this thesis I had the pleasure to accompany Pascal Anastasopoulos in his work and was welcomed to participate in his project with Elias Kiritsis. In addition, a dream came true when I was encouraged to publish a paper with him. This trust, which enabled me to grow as a scientist, was unexpected and never took for granted. Thank you Pascal for this adventurous experience and believing in me. I will never forget that.

None of this would have been possible without the support of my great family. Especially my parents Inge Sader and Matthias Niederwieser. And of course, not to forget my sister Viktoria Niederwieser. To follow one's interests and curiosities is still a huge privilege that was only made possible by your love. Thank you for having my back.

During my time in Vienna, far away from home, my flatmates became a second family to me. Thank you Julia Profanter, Lukas Furlan and Mattia Vecchio. You made this time unforgettable for me.

Special thanks are extended to Günther Sader and Hildegard Rainer for igniting the fire within me. Another expression of gratitude goes to Filipp Lausch for the endless hours of engaging physics discussions and becoming one of my dearest friends. Last but certainly not least, appreciation is directed towards Sarah Mair, who consistently reminded me that good can be found in every bad.

This thesis is dedicated to Kreszentia Bacher, Hans Sader and Gabriel Elias Leitner.

The beauty in my life is that this list could go on for a long time. So thank you to everyone who has inspired, supported, challenged and encouraged me.

Bibliography

[1] G. Veneziano, "Construction of a crossing-symmetric, Regge behaved amplitude for linearly rising trajectories," *Nuovo Cimento* **57** (1968) 190–197. https://cds.cern.ch/record/390478.

[2] M. Chalmers, "The roots and fruits of string theory interview with gabriele veneziano," 2018. https://cerncourier.com/a/the-roots-and-fruits-of-string-theory/.

[3] P. D. Vecchia, "The birth of string theory," 2007.

[4] L. Susskind, *The Cosmic Landscape: String Theory and the Illusion of Intelligent Design*. Little, Brown, 2008. https://books.google.at/books?id=yo1cDwAAQBAJ.

[5] L. Susskind, "Harmonic-oscillator analogy for the veneziano model," *Phys. Rev. Lett.* **23** (Sep, 1969) 545–547. https://link.aps.org/doi/10.1103/PhysRevLett.23.545.

[6] L. Susskind, "Structure of hadrons implied by duality," *Phys. Rev. D* **1** (Feb, 1970) 1182–1186. https://link.aps.org/doi/10.1103/PhysRevD.1.1182.

[7] J. H. Schwarz, "String theory: The early years," 2000.

[8] N. Evans, "String theory meets qcd," *Physics World* **16** no. 5, (May, 2003) 35–38. https://eprints.soton.ac.uk/64179/.

[9] D. J. Gross and F. Wilczek, "Ultraviolet behavior of non-abelian gauge theories," *Phys. Rev. Lett.* **30** (Jun, 1973) 1343–1346. https://link.aps.org/doi/10.1103/PhysRevLett.30.1343.

[10] H. D. Politzer, "Reliable perturbative results for strong interactions?," *Phys. Rev. Lett.* **30** (Jun, 1973) 1346–1349. https://link.aps.org/doi/10.1103/PhysRevLett.30.1346.

[11] J. Scherk and J. H. Schwarz, "Dual models for non-hadrons," *Nuclear Physics B* **81** no. 1, (1974) 118–144. https://www.sciencedirect.com/science/article/pii/0550321374900108.

[12] T. Yoneya, "Connection of Dual Models to Electrodynamics and Gravidynamics," *Progress of Theoretical Physics* **51** no. 6, (06, 1974) 1907–1920, https://academic.oup.com/ptp/article-pdf/51/6/1907/5275734/51-6-1907.pdf. https://doi.org/10.1143/PTP.51.1907.

[13] A. Pais, *Subtle is the Lord : The Science and the Life of Albert Einstein: The Science and the Life of Albert Einstein*. Oxford University Press, USA, 1982. https://books.google.at/books?id=KdaiZDaB7TgC.

[14] B. Greene, *The Elegant Universe: Superstrings, Hidden Dimensions, and the Quest for the Ultimate Theory*. Vintage Series. Vintage Books, 2000. https://books.google.at/books?id=8QYs7n3klvYC.

[15] M. B. Green and J. H. Schwarz, "Anomaly cancellations in supersymmetric d = 10 gauge theory and superstring theory," *Physics Letters B* **149** no. 1, (1984) 117–122. https://www.sciencedirect.com/science/article/pii/037026938491565X.

[16] D. J. Gross, J. A. Harvey, E. Martinec, and R. Rohm, "Heterotic string," *Phys. Rev. Lett.* **54** (Feb, 1985) 502–505. https://link.aps.org/doi/10.1103/PhysRevLett.54.502.

[17] F. G. Marchesano Buznego, "Intersecting D-brane models," other thesis, 5, 2003.

[18] P. Candelas, G. T. Horowitz, A. Strominger, and E. Witten, "Vacuum configurations for superstrings," *Nuclear Physics B* **258** (Jan., 1985) 46–74.

[19] M. B. Green and J. H. Schwarz, "Supersymmetrical string theories," *Physics Letters B* **109** no. 6, (1982) 444–448. https://www.sciencedirect.com/science/article/pii/0370269382911108.

[20] E. Witten, "String theory dynamics in various dimensions," *Nuclear Physics B* **443** no. 1-2, (Jun, 1995) 85–126. http://dx.doi.org/10.1016/0550-3213(95)00158-O.

[21] M. J. Duff, "The Theory Formerly Known as Strings," *Scientific American* **278** no. 2, (Feb., 1998) 64–69.

[22] C. Bachas, "A way to break supersymmetry," 1995.

[23] C. Angelantonj, I. Antoniadis, E. Dudas, and A. Sagnotti, "Type-i strings on magnetised orbifolds and brane transmutation," *Physics Letters B* **489** no. 1-2, (Sep, 2000) 223–232. http://dx.doi.org/10.1016/S0370-2693(00)00907-2.

[24] C. Angelantonj and A. Sagnotti, "Type-i vacua and brane transmutation," 2000.

[25] D. Cremades, L. Ibáñez, and F. Marchesano, "Standard model at intersecting d5-branes: lowering the string scale," *Nuclear Physics B* **643** no. 1-3, (Nov, 2002) 93–130. http://dx.doi.org/10.1016/S0550-3213(02)00746-0.

[26] R. Blumenhagen, L. Görlich, B. Körs, and D. Lüst, "Noncommutative compactifications of type i strings on tori with magnetic background flux," *Journal of High Energy Physics* **2000** no. 10, (Oct, 2000) 006–006. http://dx.doi.org/10.1088/1126-6708/2000/10/006.

[27] R. Blumenhagen, L. Goerlich, B. Kors, and D. Lust, "Magnetic flux in toroidal type i compactification," 2000.

[28] R. Blumenhagen, L. Görlich, and B. Körs, "Supersymmetric orientifolds in 6d with d-branes at angles," *Nuclear Physics B* **569** no. 1-3, (Mar, 2000) 209–228. http://dx.doi.org/10.1016/S0550-3213(99)00795-6.

[29] G. Pradisi, "Type i vacua from diagonal -orbifolds," *Nuclear Physics B* **575** no. 1-2, (May, 2000) 134–150. http://dx.doi.org/10.1016/S0550-3213(00)00089-4.

[30] C. Angelantonj and R. Blumenhagen, "Discrete deformations in type i vacua," *Physics Letters B* **473** no. 1-2, (Jan, 2000) 86–93. http://dx.doi.org/10.1016/S0370-2693(99)01480-X.

[31] R. Blumenhagen, L. Görlich, and B. Körs, "Supersymmetric 4d orientifolds of type iia with d6-branes at angles," *Journal of High Energy Physics* **2000** no. 01, (Jan, 2000) 040–040. http://dx.doi.org/10.1088/1126-6708/2000/01/040.

[32] S. Förste, G. Honecker, and R. Schreyer, "Supersymmetric orientifolds in 4d with d-branes at angles," *Nuclear Physics B* **593** no. 1-2, (Jan, 2001) 127–154. http://dx.doi.org/10.1016/S0550-3213(00)00616-7.

[33] R. Blumenhagen, J. P. Conlon, and K. Suruliz, "Type iia orientifolds on general supersymmetric znorbifolds," *Journal of High Energy Physics* **2004** no. 07, (Jul, 2004) 022–022. `http://dx.doi.org/10.1088/1126-6708/2004/07/022`.

[34] G. Aldazabal, S. Franco, L. E. Ibáñez, R. Rabadán, and A. M. Uranga, "Intersecting brane worlds," *Journal of High Energy Physics* **2001** no. 02, (Feb, 2001) 047–047. `http://dx.doi.org/10.1088/1126-6708/2001/02/047`.

[35] G. Aldazabal, S. Franco, L. E. Ibáñez, R. Rabadán, and A. M. Uranga, "D=4 chiral string compactifications from intersecting branes," *Journal of Mathematical Physics* **42** no. 7, (Jul, 2001) 3103–3126. `http://dx.doi.org/10.1063/1.1376157`.

[36] R. Blumenhagen, B. Körs, and D. Lüst, "Type i strings with f- and b-flux," *Journal of High Energy Physics* **2001** no. 02, (Feb, 2001) 030–030. `http://dx.doi.org/10.1088/1126-6708/2001/02/030`.

[37] L. E. I. nez, F. Marchesano, and R. Rabadán, "Getting just the standard model at intersecting branes," *Journal of High Energy Physics* **2001** no. 11, (Nov, 2001) 002–002. `http://dx.doi.org/10.1088/1126-6708/2001/11/002`.

[38] M. Cvetič, G. Shiu, and A. M. Uranga, "Three-family supersymmetric standardlike models from intersecting brane worlds," *Physical Review Letters* **87** no. 20, (Oct, 2001) . `http://dx.doi.org/10.1103/PhysRevLett.87.201801`.

[39] M. Cvetič, G. Shiu, and A. M. Uranga, "Chiral four-dimensional n=1 supersymmetric type iia orientifolds from intersecting d6-branes," *Nuclear Physics B* **615** no. 1-3, (Nov, 2001) 3–32. `http://dx.doi.org/10.1016/S0550-3213(01)00427-8`.

[40] R. Blumenhagen, M. Cvetic, P. Langacker, and G. Shiu, "Toward realistic intersecting D-brane models," *Ann. Rev. Nucl. Part. Sci.* **55** (2005) 71–139, `arXiv:hep-th/0502005`.

[41] P. Anastasopoulos and E. Niederwieser, "Lifetimes of light stringy states," `arXiv:2112.00404 [hep-th]`.

[42] M. Materassi, "Polyakov's string classical mechanics," `arXiv:hep-th/9905028`.

[43] J. Polchinski, *String theory. Vol. 1: An introduction to the bosonic string.* Cambridge Monographs on Mathematical Physics. Cambridge University Press, 12, 2007.

[44] E. Kiritsis, *String theory in a nutshell.* Princeton University Press, USA, 2019.

[45] B. Zwiebach, *A First Course in String Theory.* Cambridge University Press, Cambridge, 2009.

[46] D. Tong, " Lectures on String Theory." Online, 2012. Lecture Notes.

[47] J. Polchinski, "Tasi lectures on D-branes," in *Theoretical Advanced Study Institute in Elementary Particle Physics (TASI 96): Fields, Strings, and Duality.* 11, 1996. `arXiv:hep-th/9611050`.

[48] C. P. Bachas, "Lectures on D-branes," in *A Newton Institute Euroconference on Duality and Supersymmetric Theories.* 6, 1998. `arXiv:hep-th/9806199`.

[49] T. Weigand, "Introduction to String Theory." Online, 2012. Lecture Notes.

[50] E. Castellani, "Reductionism, emergence, and effective field theories," *Studies in History and Philosophy of Science Part B: Studies in History and Philosophy of Modern Physics* **33** no. 2, (2002) 251–267. `https://www.sciencedirect.com/science/article/pii/S1355219802000035`.

[51] R. F. Hauser, “String Theory and M-Theory by Leonard Susskind.” Online, 2019. Lecture Notes.

[52] A. Sen, “Strong - weak coupling duality in four-dimensional string theory,” *Int. J. Mod. Phys. A* **9** (1994) 3707–3750, `arXiv:hep-th/9402002`.

[53] D. C. Dennet, *Darwin’s Dangerous Idea: Evolution and the Meanings of Life.* Simon and Schuster, 1995.

[54] R. Blumenhagen *et al.*, *Basic Concepts of String Theory.* Springer, Berlin Heidelberg, 2012.

[55] Á. Uranga, “Model building in iia : Intersecting brane worlds,” 2012.

[56] V. Bargmann and E. Wigner, “Group Theoretical Discussion of Relativistic Wave Equations,” *Proc Natl Acad Sci U S A.* **43** (1948) 211–223.

[57] A. Duncan, *The Conceptual Framework of Quantum Field Theory.* OUP Oxford, 8, 2012.

[58] A. J. Cain and E. Lehtonen, “Reconstructing young tableaux,” 2021.

[59] C. V. Johnson, *D-Branes.* Cambridge Monographs on Mathematical Physics. Cambridge University Press, 2002.

[60] A. M. Uranga, “Intersecting brane worlds,” *Classical and Quantum Gravity* **22** no. 8, (Mar, 2005) S41–S76. `https://doi.org/10.1088/0264-9381/22/8/002`.

[61] P. Di Vecchia and A. Liccardo, “D Branes in String Theory, I,” *NATO Sci. Ser. C* **556** (2000) 1–60, `arXiv:hep-th/9912161`.

[62] D. Lüst, “Intersecting brane worlds—a path to the standard model?,” *Classical and Quantum Gravity* **21** no. 10, (Apr, 2004) S1399–S1424. `http://dx.doi.org/10.1088/0264-9381/21/10/013`.

[63] L. E. Ibáñez and A. M. Uranga, *String Theory and Particle Physics. An Introduction to String Phenomenology.* Cambridge University Press, Cambridge, 2012.

[64] J. Kim, S. Kim, and K. Lee, “Higgsing towards e-strings,” 2015.

[65] D. Cremades, L. E. Ibánez, and F. Marchesano, “Intersecting brane models of particle physics and the higgs mechanism,” *Journal of High Energy Physics* **2002** no. 07, (Jul, 2002) 022–022. `http://dx.doi.org/10.1088/1126-6708/2002/07/022`.

[66] A. M. Uranga, “TASI lectures on string compactification, model building and fluxes,” tech. rep., CERN, Geneva, 2005. `https://cds.cern.ch/record/933469`.

[67] R. Blumenhagen, B. Körs, D. Lüst, and S. Stieberger, “Four-dimensional string compactifications with d-branes, orientifolds and fluxes,” *Physics Reports* **445** no. 1-6, (Jul, 2007) 1–193. `http://dx.doi.org/10.1016/j.physrep.2007.04.003`.

[68] M. Dine *et al.*, *String Theory and Its Applications: TASI 2010: From meV to the Planck Scale.* World Scientific Publishing Company, Cambridge, 2011.

[69] M. Aganagic, C. Popescu, and J. H. Schwarz, “Gauge invariant and gauge fixed D-brane actions,” *Nucl. Phys. B* **495** (1997) 99–126, `arXiv:hep-th/9612080`.

[70] E. Bergshoeff and P. K. Townsend, “Super D-branes,” *Nucl. Phys. B* **490** (1997) 145–162, `arXiv:hep-th/9611173`.

[71] M. Cederwall, A. von Gussich, B. E. W. Nilsson, P. Sundell, and A. Westerberg, "The Dirichlet super p-branes in ten-dimensional type IIA and IIB supergravity," *Nucl. Phys. B* **490** (1997) 179–201, `arXiv:hep-th/9611159`.

[72] M. Aganagic, C. Popescu, and J. H. Schwarz, "D-brane actions with local kappa symmetry," *Phys. Lett. B* **393** (1997) 311–315, `arXiv:hep-th/9610249`.

[73] J.-H. Park, "A study of a non-abelian generalization of the born-infeld action," *Physics Letters B* **458** no. 4, (Jul, 1999) 471–476. `http://dx.doi.org/10.1016/S0370-2693(99)00592-4`.

[74] A. A. Tseytlin, "On nonAbelian generalization of Born-Infeld action in string theory," *Nucl. Phys. B* **501** (1997) 41–52, `arXiv:hep-th/9701125`.

[75] R. C. Myers, "Dielectric-branes," *Journal of High Energy Physics* **1999** no. 12, (Dec, 1999) 022–022. `http://dx.doi.org/10.1088/1126-6708/1999/12/022`.

[76] W. Chemissany, "On the way of finding the non-Abelian Born-Infeld theory," Master's thesis, Groningen U., 2004.

[77] T. D. Brennan, C. Ferko, and S. Sethi, "A non-abelian analogue of dbi from $t\overline{T}$," *SciPost Physics* **8** no. 4, (Apr, 2020) . `http://dx.doi.org/10.21468/SciPostPhys.8.4.052`.

[78] A. Hashimoto and W. Taylor, "Fluctuation spectra of tilted and intersecting d-branes from the born-infeld action," *Nuclear Physics B* **503** no. 1-2, (Oct, 1997) 193–219. `http://dx.doi.org/10.1016/S0550-3213(97)00399-4`.

[79] W. Taylor IV and M. Van Raamsdonk, "Multiple dp-branes in weak background fields," *Nuclear Physics B* **573** no. 3, (May, 2000) 703–734. `http://dx.doi.org/10.1016/S0550-3213(00)00006-7`.

[80] E. A. Bergshoeff, M. d. Roo, A. Bilal, and A. Sevrin, "Supersymmetric non-abelian born-infeld revisited," *Journal of High Energy Physics* **2001** no. 07, (Jul, 2001) 029–029. `http://dx.doi.org/10.1088/1126-6708/2001/07/029`.

[81] P. Bain, "On the nonAbelian Born-Infeld action," in *NATO Advanced Study Institute: TMR Summer School on Progress in String Theory and M-Theory*. 5, 1999. `arXiv:hep-th/9909154`.

[82] M. Cederwall, A. von Gussich, A. Miković, B. Nilsson, and A. Westerberg, "On the dirac-born-infeld action for d-branes," *Physics Letters B* **390** no. 1-4, (Jan, 1997) 148–152. `http://dx.doi.org/10.1016/S0370-2693(96)01367-6`.

[83] E. S. Fradkin and A. A. Tseytlin, "Nonlinear Electrodynamics from Quantized Strings," *Phys. Lett. B* **163** (1985) 123–130.

[84] C. G. Callan, Jr., E. J. Martinec, M. J. Perry, and D. Friedan, "Strings in Background Fields," *Nucl. Phys. B* **262** (1985) 593–609.

[85] A. Abouelsaood, C. G. Callan, Jr., C. R. Nappi, and S. A. Yost, "Open Strings in Background Gauge Fields," *Nucl. Phys. B* **280** (1987) 599–624.

[86] H. Dorn and H. J. Otto, "Open Bosonic Strings in General Background Fields," *Z. Phys. C* **32** (1986) 599.

[87] M. R. Douglas, "Branes within branes," *NATO Sci. Ser. C* **520** (1999) 267–275, `arXiv:hep-th/9512077`.

[88] M. B. Green, J. A. Harvey, and G. Moore, "I-brane inflow and anomalous couplings on d-branes," *Classical and Quantum Gravity* **14** no. 1, (Jan, 1997) 47–52. http://dx.doi.org/10.1088/0264-9381/14/1/008.

[89] Y.-K. E. Cheung and Z. Yin, "Anomalies, branes, and currents," *Nuclear Physics B* **517** no. 1-3, (Apr, 1998) 69–91. http://dx.doi.org/10.1016/S0550-3213(98)00115-1.

[90] J. F. Morales, C. A. Scrucca, and M. Serone, "Anomalous couplings for d-branes and o-planes," *Nuclear Physics B* **552** no. 1-2, (Jul, 1999) 291–315. http://dx.doi.org/10.1016/S0550-3213(99)00217-5.

[91] M. Billo, B. Craps, and F. Roose, "Ramond-Ramond couplings of nonBPS D-branes," *JHEP* **06** (1999) 033, arXiv:hep-th/9905157.

[92] M. Cvetič and R. Richter, "Proton decay via dimension-six operators in intersecting d6-brane models," *Nuclear Physics B* **762** no. 1-2, (Jan, 2007) 112–147. http://dx.doi.org/10.1016/j.nuclphysb.2006.10.029.

[93] P. Anastasopoulos and M. Bianchi, "Revisiting light stringy states in view of the 750 gev diphoton excess," *Nuclear Physics B* **911** (Oct, 2016) 928–954. http://dx.doi.org/10.1016/j.nuclphysb.2016.08.033.

[94] M. Berkooz, M. R. Douglas, and R. G. Leigh, "Branes intersecting at angles," *Nuclear Physics B* **480** no. 1-2, (Nov, 1996) 265–278. http://dx.doi.org/10.1016/S0550-3213(96)00452-X.

[95] V. Rosenhaus and W. Taylor, "Diversity in the tail of the intersecting brane landscape," *Journal of High Energy Physics* **2009** no. 06, (Jun, 2009) 073–073. http://dx.doi.org/10.1088/1126-6708/2009/06/073.

[96] A. Bilal, "Introduction to supersymmetry," arXiv:hep-th/0101055.

[97] S. P. Martin, "A Supersymmetry primer," *Adv. Ser. Direct. High Energy Phys.* **18** (1998) 1–98, arXiv:hep-ph/9709356.

[98] J. Polchinski, *String theory. Vol. 2: Superstring theory and beyond*. Cambridge Monographs on Mathematical Physics. Cambridge University Press, 12, 2007.

[99] E. Dudas, "Corfu 05 lectures - part II: Orientifolds and model building,". https://doi.org/10.1088/1742-6596/53/1/035.

[100] M. Bertolini, M. Billò, A. Lerda, J. Morales, and R. Russo, "Brane world effective actions for d-branes with fluxes," *Nuclear Physics B* **743** no. 1-2, (May, 2006) 1–40. http://dx.doi.org/10.1016/j.nuclphysb.2006.02.044.

[101] P. Anastasopoulos, M. Bianchi, and R. Richter, "Light stringy states," *Journal of High Energy Physics* **2012** no. 3, (Mar, 2012) . http://dx.doi.org/10.1007/JHEP03(2012)068.

[102] P. Anastasopoulos and R. Richter, "Production of light stringy states," *Journal of High Energy Physics* **2014** no. 12, (Dec, 2014) . http://dx.doi.org/10.1007/JHEP12(2014)059.

[103] M. Cvetic and J. Halverson, "Tasi lectures: Particle physics from perturbative and non-perturbative effects in d-braneworlds," *String Theory and Its Applications* (Nov, 2011) . http://dx.doi.org/10.1142/9789814350525_0005.

[104] P. Anastasopoulos and R. Richter, "Production of light stringy states," *JHEP* **12** (2014) 059, arXiv:1408.4810 [hep-th].

[105] P. Anastasopoulos and R. Richter, "Twisted state production," *PoS* **CORFU2014** (2015) 116.

[106] D. Bailin and A. Love, "KALUZA-KLEIN THEORIES," *Rept. Prog. Phys.* **50** (1987) 1087–1170.

[107] M. Duff, B. Nilsson, and C. Pope, "Kaluza-klein supergravity," *Physics Reports* **130** no. 1, (1986) 1–142. `https://www.sciencedirect.com/science/article/pii/0370157386901638`.

[108] M. J. Duff, "Kaluza-Klein theory in perspective," in *The Oskar Klein Centenary Symposium*. 10, 1994. `arXiv:hep-th/9410046`.

[109] E. Witten, "Search for a realistic kaluza-klein theory," *Nuclear Physics B* **186** no. 3, (1981) 412–428. `https://www.sciencedirect.com/science/article/pii/0550321381900213`.

[110] M. Grana and H. Triendl, "String theory compactifications." Online, 2006. Lecture Notes.

[111] M. Nakahara, *Geometry, topology and physics*. 2003.

[112] T. Hubsch, *Calabi-Yau manifolds: A Bestiary for physicists*. World Scientific, Singapore, 1994.

[113] K. Hori and C. Vafa, "Mirror symmetry," `arXiv:hep-th/0002222`.

[114] M. Kontsevich, "Homological Algebra of Mirror Symmetry," `arXiv:alg-geom/9411018`.

[115] P. S. Aspinwall, B. R. Greene, and D. R. Morrison, "Calabi-yau moduli space, mirror manifolds and spacetime topology change in string theory," *Nuclear Physics B* **416** no. 2, (Mar, 1994) 414–480. `http://dx.doi.org/10.1016/0550-3213(94)90321-2`.

[116] E. Alvarez, L. Alvarez-Gaume, and Y. Lozano, "An Introduction to T duality in string theory," *Nucl. Phys. B Proc. Suppl.* **41** (1995) 1–20, `arXiv:hep-th/9410237`.

[117] A. Strominger, S.-T. Yau, and E. Zaslow, "Mirror symmetry is t-duality," *Nuclear Physics B* **479** no. 1-2, (Nov, 1996) 243–259. `http://dx.doi.org/10.1016/0550-3213(96)00434-8`.

[118] F. Marchesano, "Progress in D-brane model building," *Fortsch.Phys.* **55** (2007) 491–518, `arXiv:hep-th/0702094 [HEP-TH]`.

[119] M. Kaku, *Introduction to Superstrings and M-Theory*. Graduate Texts in Contemporary Physics. Springer, 1999.

[120] P. Anastasopoulos, M. Bianchi, E. Dudas, and E. Kiritsis, "Anomalies, anomalous u(1)'s and generalized chern-simons terms," *Journal of High Energy Physics* **2006** no. 11, (Nov, 2006) 057–057. `http://dx.doi.org/10.1088/1126-6708/2006/11/057`.

[121] W. Taylor, "Tasi lectures on supergravity and string vacua in various dimensions," 2011.

[122] A. Hatcher, *Algebraic topology*. Cambridge University Press, Cambridge, 2002.

[123] G. Aldazabal, S. Franco, L. E. Ibanez, R. Rabadan, and A. M. Uranga, "D = 4 chiral string compactifications from intersecting branes," *J. Math. Phys.* **42** (2001) 3103–3126, `arXiv:hep-th/0011073`.

[124] L. Dixon, J. Harvey, C. Vafa, and E. Witten, "Strings on orbifolds (ii)," *Nuclear Physics B* **274** no. 2, (1986) 285–314. `https://www.sciencedirect.com/science/article/pii/0550321386902877`.

[125] L. Dixon, J. Harvey, C. Vafa, and E. Witten, "Strings on orbifolds," *Nuclear Physics B* **261** (1985) 678–686.
`https://www.sciencedirect.com/science/article/pii/0550321385905930`.

[126] R. Blumenhagen, L. Görlich, and B. Körs, "Supersymmetric orientifolds in 6d with d-branes at angles," *Nuclear Physics B* **569** no. 1-3, (Mar, 2000) 209–228.
`http://dx.doi.org/10.1016/S0550-3213(99)00795-6`.

[127] R. Blumenhagen, L. Görlich, and B. Körs, "Supersymmetric 4d orientifolds of type iia with d6-branes at angles," *Journal of High Energy Physics* **2000** no. 01, (Jan, 2000) 040–040. `http://dx.doi.org/10.1088/1126-6708/2000/01/040`.

[128] R. Blumenhagen, L. Gorlich, and B. Kors, "A New class of supersymmetric orientifolds with D branes at angles," *PoS* **tmr99** (1999) 010, `arXiv:hep-th/0002146`.

[129] A. Dabholkar, "Lectures on orientifolds and duality," in *ICTP Summer School in High-Energy Physics and Cosmology*. 6, 1997. `arXiv:hep-th/9804208`.

[130] R. Blumenhagen, B. Körs, D. Lüst, and S. Stieberger, "Four-dimensional string compactifications with d-branes, orientifolds and fluxes," *Physics Reports* **445** no. 1-6, (Jul, 2007) 1–193. `http://dx.doi.org/10.1016/j.physrep.2007.04.003`.

[131] V. Sanz, S. Abel, J. Santiago, and A. Faraggi, eds., *String phenomenology. Proceedings, 2nd International Conference, Durham, UK, July 29-August 4, 2003*. 2004.

[132] M. Kerstan and T. Weigand, "The effective action of d6-branes in $\mathcal{N} = 1$ type iia orientifolds," *Journal of High Energy Physics* **2011** no. 6, (Jun, 2011) .
`http://dx.doi.org/10.1007/JHEP06(2011)105`.

[133] E. Plauschinn, "The generalized green-schwarz mechanism for type iib orientifolds with d3- and d7-branes," *Journal of High Energy Physics* **2009** no. 05, (May, 2009) 062–062.
`http://dx.doi.org/10.1088/1126-6708/2009/05/062`.

[134] R. Blumenhagen, D. Lüst, and S. Theisen, *Basic Concepts of String Theory*. Springer-Verlag Berlin Heidelberg, Berlin-Heidelberg, 2013.

[135] H. Nieder and Y. Oz, "Supergravity and D-branes wrapping special Lagrangian cycles," *JHEP* **03** (2001) 008, `arXiv:hep-th/0011288`.

[136] N. J. Hitchin, "Lectures on special Lagrangian submanifolds," *AMS/IP Stud. Adv. Math.* **23** (2001) 151–182, `arXiv:math/9907034`.

[137] M. Cvetič, G. Shiu, and A. M. Uranga, "Chiral four-dimensional n=1 supersymmetric type iia orientifolds from intersecting d6-branes," *Nuclear Physics B* **615** no. 1-3, (Nov, 2001) 3–32. `http://dx.doi.org/10.1016/S0550-3213(01)00427-8`.

[138] D. Lust, "Intersecting brane worlds: A Path to the standard model?," *Class. Quant. Grav.* **21** (2004) S1399–1424, `arXiv:hep-th/0401156`.

[139] R. Blumenhagen, L. Görlich, B. Körs, and D. Lüst, "Noncommutative compactifications of type I strings on tori with magnetic background flux," *JHEP* **0010** (2000) 006, `arXiv:hep-th/0007024 [hep-th]`.

[140] S. Weinberg, *The Quantum Theory of Fields, Volume 1: Foundations*. Cambridge University Press, 2005.

[141] M. E. Peskin and D. V. Schroeder, *An Introduction to Quantum Field Theory*. Westview Press, 1995. Reading, USA: Addison-Wesley (1995) 842 p.

[142] R. A. Bertlmann, *Anomalies in Quantum Field Theory*. International Series of Monographs on Physics. Clarendon Press, 2000.

[143] A. Zee, *Quantum field theory in a nutshell*. Princeton University Press, second edition ed., 2010.

[144] S. L. Adler, "Anomalies," arXiv:hep-th/0411038.

[145] E. Plauschinn, "The Generalized Green-Schwarz Mechanism for Type IIB Orientifolds with D3- and D7-Branes," *JHEP* **05** (2009) 062, arXiv:0811.2804 [hep-th].

[146] T. Weigand and F. Xu, "The Green-Schwarz Mechanism and Geometric Anomaly Relations in 2d (0,2) F-theory Vacua," *JHEP* **04** (2018) 107, arXiv:1712.04456 [hep-th].

[147] P. Anastasopoulos, "Anomalies, Chern-Simons terms and the standard model," *J. Phys. Conf. Ser.* **53** (2006) 731–745.

[148] A. Schellekens and N. Warner, "Anomalies, characters and strings," *Nuclear Physics B* **287** (1987) 317–361.
https://www.sciencedirect.com/science/article/pii/0550321387901088.

[149] A. Sagnotti, "A note on the green-schwarz mechanism in open-string theories," *Physics Letters B* **294** no. 2, (Nov, 1992) 196–203.
http://dx.doi.org/10.1016/0370-2693(92)90682-T.

[150] P. Soler Gomis, *Non-perturbative aspects aspects of type II string compactifications*. PhD thesis, Universidad Autónoma de Madrid. Facultad de Ciencias; Universidad Autónoma de Madrid. Departamento de Física Teórica; Instituto de Física Teórica (IFT), 2012.

[151] R. Blumenhagen, B. Körs, D. Lüst, and S. Stieberger, "Four-dimensional string compactifications with d-branes, orientifolds and fluxes," *Physics Reports* **445** no. 1-6, (Jul, 2007) 1–193. http://dx.doi.org/10.1016/j.physrep.2007.04.003.

[152] G. Aldazabal, S. Franco, L. E. Ibáñez, R. Rabadán, and A. M. Uranga, "D=4 chiral string compactifications from intersecting branes," *Journal of Mathematical Physics* **42** no. 7, (Jul, 2001) 3103–3126. http://dx.doi.org/10.1063/1.1376157.

[153] R. Richter, "Perturbative and non-perturbative aspects of orientifold compactifications," 2009.

[154] H. RUEGG and M. RUIZ-ALTABA, "The stueckelberg field," *International Journal of Modern Physics A* **19** no. 20, (Aug, 2004) 3265–3347.
http://dx.doi.org/10.1142/S0217751X04019755.

[155] S. F. Novaes, "Standard model: An Introduction," in *10th Jorge Andre Swieca Summer School: Particle and Fields*, pp. 5–102. 1, 1999. arXiv:hep-ph/0001283.

[156] M. Schwartz, *Quantum Field Theory and the Standard Model*. Quantum Field Theory and the Standard Model. Cambridge University Press, 2014.
https://books.google.at/books?id=HbdEAgAAQBAJ.

[157] T. Cheng and L. Li, *Gauge Theory of Elementary Particle Physics*. Oxford science publications. Clarendon Press, 1984.
https://books.google.at/books?id=lk8GEzVNb10C.

[158] A. Di Giacomo, "Confinement of color: A Review," in *12th International Conference on Selected Problems of Modern Physics (Blokhintsev 03)*. 10, 2003.
arXiv:hep-lat/0310023.

[159] M. Creutz, *Quarks, Gluons and Lattices.* Cambridge Monographs on Mathematical Physics. Cambridge University Press, 1983.
https://books.google.at/books?id=mcCyB3ewyeMC.

[160] F. Halzen, A. Martin, and J. W. . Sons, *Quarks and Leptones: An Introductory Course in Modern Particle Physics.* Wiley, 1984.
https://books.google.at/books?id=zwDvAAAAMAAJ.

[161] D. Griffiths, *Introduction to Elementary Particles.* Physics textbook. Wiley, 2008.
https://books.google.at/books?id=Wb9DYrjcoKAC.

[162] H. Georgi, *Lie Algebras In Particle Physics: from Isospin To Unified Theories.* Frontiers in Physics. Avalon Publishing, 1999. https://books.google.at/books?id=dhY5DgAAQBAJ.

[163] M. Maggiore, *A Modern Introduction to Quantum Field Theory.* EBSCO ebook academic collection. Oxford University Press, 2005.
https://books.google.at/books?id=yykTDAAAQBAJ.

[164] A. Zee, *Group Theory in a Nutshell for Physicists.* In a Nutshell. Princeton University Press, 2016. https://books.google.at/books?id=DmuYDwAAQBAJ.

[165] J. J. Lodder, "On gluon masses, color symmetry, and a possible massive ninth gluon," arXiv:hep-ph/9606317.

[166] J. Baez and J. Bottomley, "Why are there eight gluons and not nine?," 1996.
https://math.ucr.edu/home/baez/physics/ParticleAndNuclear/gluons.html.

[167] B. Hall and B. Hall, *Lie Groups, Lie Algebras, and Representations: An Elementary Introduction.* Graduate Texts in Mathematics. Springer, 2003.
https://books.google.at/books?id=m1VQi8HmEwcC.

[168] S. F. King, "Neutrino mass models," *Reports on Progress in Physics* **67** no. 2, (Dec, 2003) 107–157. http://dx.doi.org/10.1088/0034-4885/67/2/R01.

[169] A. Pich, "The standard model of electroweak interactions," 2012.

[170] R. Blumenhagen, L. Görlich, B. Körs, and D. Lüst, "Noncommutative compactifications of type i strings on tori with magnetic background flux," *Journal of High Energy Physics* **2000** no. 10, (Oct, 2000) 006–006.
http://dx.doi.org/10.1088/1126-6708/2000/10/006.

[171] G. Aldazabal, S. Franco, L. E. Ibáñez, R. Rabadán, and A. M. Uranga, "Intersecting brane worlds," *Journal of High Energy Physics* **2001** no. 02, (Feb, 2001) 047–047.
http://dx.doi.org/10.1088/1126-6708/2001/02/047.

[172] G. Aldazabal, S. Franco, L. E. Ibáñez, R. Rabadán, and A. M. Uranga, "D=4 chiral string compactifications from intersecting branes," *Journal of Mathematical Physics* **42** no. 7, (Jul, 2001) 3103–3126. http://dx.doi.org/10.1063/1.1376157.

[173] L. E. I. nez, F. Marchesano, and R. Rabadán, "Getting just the standard model at intersecting branes," *Journal of High Energy Physics* **2001** no. 11, (Nov, 2001) 002–002.
http://dx.doi.org/10.1088/1126-6708/2001/11/002.

[174] M. Cvetič, G. Shiu, and A. M. Uranga, "Chiral four-dimensional n=1 supersymmetric type iia orientifolds from intersecting d6-branes," *Nuclear Physics B* **615** no. 1-3, (Nov, 2001) 3–32. http://dx.doi.org/10.1016/S0550-3213(01)00427-8.

[175] C. Vafa and B. Zwiebach, "N=1 dualities of SO and USp gauge theories and T duality of string theory," *Nucl. Phys. B* **506** (1997) 143–156, arXiv:hep-th/9701015.

[176] D. Kazakov, "Beyond the standard model' 17," 2018.

[177] R. Alonso and M. West, "On the road(s) to the Standard Model," arXiv:2109.13290 [hep-ph].

[178] W. De Boer, "Grand unified theories and supersymmetry in particle physics and cosmology," *Progress in Particle and Nuclear Physics* **33** (Jan, 1994) 201–301. http://dx.doi.org/10.1016/0146-6410(94)90045-0.

[179] J. C. Pati and A. Salam, "Lepton number as the fourth "color"," *Phys. Rev. D* **10** (Jul, 1974) 275–289. https://link.aps.org/doi/10.1103/PhysRevD.10.275.

[180] D.-S. Li, "A fermions representation in Pati-Salam model," arXiv:2011.14362 [hep-ph].

[181] V. De Romeri, M. Hirsch, and M. Malinský, "Soft masses in supersymmetric so(10) guts with low intermediate scales," *Physical Review D* **84** no. 5, (Sep, 2011) . http://dx.doi.org/10.1103/PhysRevD.84.053012.

[182] G. K. Leontaris and J. Rizos, "A Pati-Salam model from branes," *Phys. Lett. B* **510** (2001) 295–304, arXiv:hep-ph/0012255.

[183] D. Cremades, L. E. Ibánez, and F. Marchesano, "Intersecting brane models of particle physics and the higgs mechanism," *Journal of High Energy Physics* **2002** no. 07, (Jul, 2002) 022–022. http://dx.doi.org/10.1088/1126-6708/2002/07/022.

[184] G. Honecker and T. Ott, "Getting just the supersymmetric standard model at intersecting branes on the Z(6) orientifold," *Phys. Rev. D* **70** (2004) 126010, arXiv:hep-th/0404055. [Erratum: Phys.Rev.D 71, 069902 (2005)].

[185] T. Li, A. Mansha, and R. Sun, "Revisiting the supersymmetric pati-salam models from intersecting d6-branes," 2020.

[186] N. Kitazawa, T. Kobayashi, N. Maru, and N. Okada, "Yukawa coupling structure in intersecting d-brane models," *The European Physical Journal C* **40** no. 4, (Apr, 2005) 579–587. http://dx.doi.org/10.1140/epjc/s2005-02166-4.

[187] E. Abbott, *Flatland: A Romance of Many Dimensions*. Roberts Brothers, 1885. https://books.google.at/books?id=R6E0AAAAMAAJ.

[188] J. Lee, E. Adelberger, T. Cook, S. Fleischer, and B. Heckel, "New test of the gravitational 1/r2 law at separations down to 52 micrometers," *Physical Review Letters* **124** no. 10, (Mar, 2020) . http://dx.doi.org/10.1103/PhysRevLett.124.101101.

[189] E. Kiritsis and P. Anastasopoulos, "The Anomalous magnetic moment of the muon in the D-brane realization of the standard model," *JHEP* **05** (2002) 054, arXiv:hep-ph/0201295.

[190] I. Antoniadis, E. Kiritsis, and J. Rizos, "Anomalous U(1)s in type 1 superstring vacua," *Nucl.Phys.* **B637** (2002) 92–118, arXiv:hep-th/0204153 [hep-th].

[191] D. Ghilencea, L. Ibáñez, N. Irges, and F. Quevedo, "TeV scale Z-prime bosons from D-branes," *JHEP* **0208** (2002) 016, arXiv:hep-ph/0205083 [hep-ph].

[192] P. Anastasopoulos, "4-D anomalous U(1)'s, their masses and their relation to 6-D anomalies," *JHEP* **0308** (2003) 005, arXiv:hep-th/0306042 [hep-th].

[193] P. Anastasopoulos, "Anomalous U(1)s masses in nonsupersymmetric open string vacua," *Phys.Lett.* **B588** (2004) 119–126, arXiv:hep-th/0402105 [hep-th].

[194] P. Burikham, T. Figy, and T. Han, "TeV-scale string resonances at hadron colliders," *Phys.Rev.* **D71** (2005) 016005, `arXiv:hep-ph/0411094 [hep-ph]`.

[195] C. Corianò, N. Irges, and E. Kiritsis, "On the effective theory of low scale orientifold string vacua," *Nucl.Phys.* **B746** (2006) 77–135, `arXiv:hep-ph/0510332 [hep-ph]`.

[196] P. Anastasopoulos, *Orientifolds, anomalies and the standard model.* PhD thesis, Crete U., 2005. `arXiv:hep-th/0503055`.

[197] P. Anastasopoulos, M. Bianchi, E. Dudas, and E. Kiritsis, "Anomalies, anomalous U(1)'s and generalized Chern-Simons terms," *JHEP* **0611** (2006) 057, `arXiv:hep-th/0605225 [hep-th]`.

[198] P. Anastasopoulos, F. Fucito, A. Lionetto, G. Pradisi, A. Racioppi, and Y. Stanev, "Minimal Anomalous U(1)-prime Extension of the MSSM," *Phys.Rev.* **D78** (2008) 085014, `arXiv:0804.1156 [hep-th]`.

[199] R. Armillis, C. Coriano, M. Guzzi, and S. Morelli, "An Anomalous Extra Z Prime from Intersecting Branes with Drell-Yan and Direct Photons at the LHC," *Nucl.Phys.* **B814** (2009) 156–179, `arXiv:0809.3772 [hep-ph]`.

[200] F. Fucito, A. Lionetto, A. Mammarella, and A. Racioppi, "Stueckelino dark matter in anomalous U(1)-prime models," *Eur.Phys.J.* **C69** (2010) 455–465, `arXiv:0811.1953 [hep-ph]`.

[201] L. A. Anchordoqui, H. Goldberg, X. Huang, D. Lüst, and T. R. Taylor, "Stringy origin of Tevatron Wjj anomaly," *Phys.Lett.* **B701** (2011) 224–228, `arXiv:1104.2302 [hep-ph]`.

[202] L. A. Anchordoqui, I. Antoniadis, H. Goldberg, X. Huang, D. Lüst, and T. Taylor, "Z'-gauge Bosons as Harbingers of Low Mass Strings," *Phys.Rev.* **D85** (2012) 086003, `arXiv:1107.4309 [hep-ph]`.

[203] L. A. Anchordoqui, I. Antoniadis, H. Goldberg, X. Huang, D. Lüst, T. Taylor, and B. Vlcek, "LHC Phenomenology and Cosmology of String-Inspired Intersecting D-Brane Models," *Phys.Rev.* **D86** (2012) 066004, `arXiv:1206.2537 [hep-ph]`.

[204] M. Bianchi and A. V. Santini, "String predictions for near future colliders from one-loop scattering amplitudes around D-brane worlds," *JHEP* **0612** (2006) 010, `arXiv:hep-th/0607224 [hep-th]`.

[205] L. A. Anchordoqui, H. Goldberg, S. Nawata, and T. R. Taylor, "Jet signals for low mass strings at the LHC," *Phys.Rev.Lett.* **100** (2008) 171603, `arXiv:0712.0386 [hep-ph]`.

[206] L. A. Anchordoqui, H. Goldberg, S. Nawata, and T. R. Taylor, "Direct photons as probes of low mass strings at the CERN LHC," *Phys.Rev.* **D78** (2008) 016005, `arXiv:0804.2013 [hep-ph]`.

[207] D. Lüst, S. Stieberger, and T. R. Taylor, "The LHC String Hunter's Companion," *Nucl.Phys.* **B808** (2009) 1–52, `arXiv:0807.3333 [hep-th]`.

[208] L. A. Anchordoqui, H. Goldberg, D. Lüst, S. Nawata, S. Stieberger, and T. Taylor, "Dijet signals for low mass strings at the LHC," *Phys.Rev.Lett.* **101** (2008) 241803, `arXiv:0808.0497 [hep-ph]`.

[209] L. A. Anchordoqui, H. Goldberg, D. Lüst, S. Stieberger, and T. R. Taylor, "String Phenomenology at the LHC," *Mod.Phys.Lett.* **A24** (2009) 2481–2490, `arXiv:0909.2216 [hep-ph]`.

[210] D. Lüst, O. Schlotterer, S. Stieberger, and T. Taylor, "The LHC String Hunter's Companion (II): Five-Particle Amplitudes and Universal Properties," *Nucl.Phys.* **B828** (2010) 139–200, `arXiv:0908.0409 [hep-th]`.

[211] L. A. Anchordoqui, H. Goldberg, D. Lüst, S. Nawata, S. Stieberger, and T. Taylor, "LHC Phenomenology for String Hunters," *Nucl.Phys.* **B821** (2009) 181–196, `arXiv:0904.3547 [hep-ph]`.

[212] L. A. Anchordoqui, W.-Z. Feng, H. Goldberg, X. Huang, and T. R. Taylor, "Searching for string resonances in $e^+ e^-$ and $\gamma\gamma$ collisions," *Phys.Rev.* **D83** (2011) 106006, `arXiv:1012.3466 [hep-ph]`.

[213] W.-Z. Feng, D. Lüst, O. Schlotterer, S. Stieberger, and T. R. Taylor, "Direct Production of Lightest Regge Resonances," *Nucl.Phys.* **B843** (2011) 570–601, `arXiv:1007.5254 [hep-th]`.

[214] Z. Dong, T. Han, M.-x. Huang, and G. Shiu, "Top Quarks as a Window to String Resonances," *JHEP* **1009** (2010) 048, `arXiv:1004.5441 [hep-ph]`.

[215] D. Carmi, "TeV Scale Strings and Scattering Amplitudes at the LHC," `arXiv:1109.5161 [hep-th]`.

[216] M. Hashi and N. Kitazawa, "Detectability of the second resonance of low-scale string models at the LHC," *JHEP* **1303** (2013) 127, `arXiv:1212.5372 [hep-ph]`.

[217] L. A. Anchordoqui, I. Antoniadis, D.-C. Dai, W.-Z. Feng, H. Goldberg, *et al.*, "String Resonances at Hadron Colliders," `arXiv:1407.8120 [hep-ph]`.

[218] D. Lüst and T. R. Taylor, "Limits on Stringy Signals at the LHC," `arXiv:1308.1619 [hep-ph]`.

[219] D. Berenstein, "TeV-Scale strings," `arXiv:1401.4491 [hep-th]`.

[220] E. Dudas and J. Mourad, "String theory predictions for future accelerators," *Nucl.Phys.* **B575** (2000) 3–34, `arXiv:hep-th/9911019 [hep-th]`.

[221] E. Accomando, I. Antoniadis, and K. Benakli, "Looking for TeV scale strings and extra dimensions," *Nucl.Phys.* **B579** (2000) 3–16, `arXiv:hep-ph/9912287 [hep-ph]`.

[222] S. Cullen, M. Perelstein, and M. E. Peskin, "TeV strings and collider probes of large extra dimensions," *Phys.Rev.* **D62** (2000) 055012, `arXiv:hep-ph/0001166 [hep-ph]`.

[223] C. Burgess, J. Matias, and F. Quevedo, "MSLED: A Minimal supersymmetric large extra dimensions scenario," *Nucl.Phys.* **B706** (2005) 71–99, `arXiv:hep-ph/0404135 [hep-ph]`.

[224] D. Chialva, R. Iengo, and J. G. Russo, "Cross sections for production of closed superstrings at high energy colliders in brane world models," *Phys.Rev.* **D71** (2005) 106009, `arXiv:hep-ph/0503125 [hep-ph]`.

[225] M. Cicoli, C. Burgess, and F. Quevedo, "Anisotropic Modulus Stabilisation: Strings at LHC Scales with Micron-sized Extra Dimensions," *JHEP* **1110** (2011) 119, `arXiv:1105.2107 [hep-th]`.

[226] D. Chialva, P. B. Dev, and A. Mazumdar, "Multiple dark matter scenarios from ubiquitous stringy throats," *Phys.Rev.* **D87** no. 6, (2013) 063522, `arXiv:1211.0250 [hep-ph]`.

[227] D. Cremades, L. Ibáñez, and F. Marchesano, "Yukawa couplings in intersecting D-brane models," *JHEP* **0307** (2003) 038, `arXiv:hep-th/0302105 [hep-th]`.

[228] M. Cvetič and I. Papadimitriou, "Conformal field theory couplings for intersecting D-branes on orientifolds," *Phys.Rev.* **D68** (2003) 046001, `arXiv:hep-th/0303083 [hep-th]`.

[229] S. Abel and A. Owen, "Interactions in intersecting brane models," *Nucl.Phys.* **B663** (2003) 197–214, `arXiv:hep-th/0303124 [hep-th]`.

[230] P. Anastasopoulos, M. Bianchi, and D. Consoli, "Yukawa's of light stringy states," *Fortsch. Phys.* **65** no. 1, (2017) 1600110, `arXiv:1609.09299 [hep-th]`.

[231] P. Anastasopoulos, M. Bianchi, and D. Consoli, "Yukawa couplings for light stringy states," *PoS* **EPS-HEP2017** (2017) 538.

[232] P. Anastasopoulos, M. Bianchi, and D. Consoli, "Yukawas of light stringy states (at D-brane intersections)," *PoS* **CORFU2017** (2018) 055.

[233] P. Anastasopoulos, E. Kiritsis, and A. Lionetto, "On mass hierarchies in orientifold vacua," *JHEP* **08** (2009) 026, `arXiv:0905.3044 [hep-th]`.

[234] R. Jimenez, A. Cimatti, L. Verde, M. Moresco, and B. Wandelt, "The local and distant universe: stellar ages and h0," *Journal of Cosmology and Astroparticle Physics* **2019** no. 03, (Mar, 2019) 043–043. `http://dx.doi.org/10.1088/1475-7516/2019/03/043`.

[235] R. Wagner-Kaiser, A. Sarajedini, T. von Hippel, D. C. Stenning, D. A. van Dyk, E. Jeffery, E. Robinson, N. Stein, J. Anderson, and W. H. Jefferys, "The acs survey of galactic globular clusters – xiv. bayesian single-population analysis of 69 globular clusters," *Monthly Notices of the Royal Astronomical Society* **468** no. 1, (Mar, 2017) 1038–1055. `http://dx.doi.org/10.1093/mnras/stx544`.

[236] E. M. O'Malley, C. Gilligan, and B. Chaboyer, "Absolute ages and distances of 22 gcs using monte carlo main-sequence fitting," *The Astrophysical Journal* **838** no. 2, (Apr, 2017) 162. `http://dx.doi.org/10.3847/1538-4357/aa6574`.

[237] D. Valcin, R. Jimenez, L. Verde, J. L. Bernal, and B. D. Wandelt, "The age of the universe with globular clusters: reducing systematic uncertainties," *Journal of Cosmology and Astroparticle Physics* **2021** no. 08, (Aug, 2021) 017. `http://dx.doi.org/10.1088/1475-7516/2021/08/017`.

[238] P. Anastasopoulos, Y. Mambrini, and E. Niederwieser, "Twisted Higgs as a Dark Matter candidate," *Work in progress* (2022) .

[239] G. Honecker and J. Vanhoof, "Towards the field theory of the standard model on fractional d6-branes on t6/z6': Yukawa couplings and masses," *Fortschritte der Physik* **60** (09, 2012) .

[240] G. Honecker and W. Staessens, "D6-brane model building and discrete symmetries on t6/z(2)xz(6')xor with discrete torsion,".

[241] H. Verlinde and M. Wijnholt, "Building the standard model on a D3-brane," *JHEP* **01** (2007) 106, `arXiv:hep-th/0508089`.

[242] D. Cremades, L. E. Ibanez, and F. Marchesano, "Standard model at intersecting D5-branes: Lowering the string scale," *Nucl. Phys. B* **643** (2002) 93–130, `arXiv:hep-th/0205074`.

[243] A. P. Braun, "F-theory and the landscape of intersecting d7-branes," 2010.

[244] P. Anastasopoulos, R. Richter, and A. N. Schellekens, "Discrete symmetries from hidden sectors," 2015.

[245] R. Blumenhagen and T. Weigand, "Chiral gepner model orientifolds," 2004.

[246] P. Anastasopoulos, R. Richter, and A. N. Schellekens, "Discrete symmetries from hidden sectors," *JHEP* **06** (2015) 189, `arXiv:1502.02686 [hep-th]`.

[247] T. Weigand, "Lectures on f-theory compactifications and model building," *Classical and Quantum Gravity* **27** no. 21, (Oct, 2010) 214004. `http://dx.doi.org/10.1088/0264-9381/27/21/214004`.

[248] G. J. Loges and G. Shiu, "Breeding realistic d-brane models," 2021.

[249] P. Anastasopoulos and E. Kiritsis, "Emergent neutrinos from heavy messengers," 2022.

[250] T. D. Brennan, F. Carta, and C. Vafa, "The String Landscape, the Swampland, and the Missing Corner," *PoS* **TASI2017** (2017) 015, `arXiv:1711.00864 [hep-th]`.

[251] M. R. Douglas and S. Kachru, "Flux compactification," *Rev. Mod. Phys.* **79** (2007) 733–796, `arXiv:hep-th/0610102`.

[252] M. R. Douglas and S. Kachru, "Flux compactification," *Rev. Mod. Phys.* **79** (2007) 733–796, `arXiv:hep-th/0610102`.

[253] S. Kachru, R. Kallosh, A. Linde, and S. P. Trivedi, "de sitter vacua in string theory," *Physical Review D* **68** no. 4, (Aug, 2003) . `http://dx.doi.org/10.1103/PhysRevD.68.046005`.

[254] W. Taylor and Y.-N. Wang, "The F-theory geometry with most flux vacua," *Journal of High Energy Physics* **2015** (Dec., 2015) 164, `arXiv:1511.03209 [hep-th]`.

[255] J. Read and B. L. Bihan, "The landscape and the multiverse: What's the problem?," 2021. `http://philsci-archive.pitt.edu/18846/`. Forthcoming in Synthese.

[256] R. Brandenberger and C. Vafa, "Superstrings in the early universe," *Nuclear Physics B* **316** no. 2, (1989) 391–410. `https://www.sciencedirect.com/science/article/pii/0550321389900370`.

[257] L. Kofman, A. D. Linde, X. Liu, A. Maloney, L. McAllister, and E. Silverstein, "Beauty is attractive: Moduli trapping at enhanced symmetry points," *JHEP* **05** (2004) 030, `arXiv:hep-th/0403001`.

[258] J. Milnor and J. D. Stasheff, *Characteristic Classes. (AM-76).* Princeton University Press, 2016. `https://doi.org/10.1515/9781400881826`.

[259] L. Fatibene, M. Ferraris, M. Francaviglia, and M. Godina, "A Geometric definition of Lie derivative for spinor fields," in *6th International Conference on Differential Geometry and Applications.* 8, 1996. `arXiv:gr-qc/9608003`.

[260] G. Rudolph and M. Schmidt, *Differential Geometry and Mathematical Physics: Part II. Fibre Bundles, Topology and Gauge Fields.* Theoretical and Mathematical Physics. Springer, 2017.

[261] F. Hanisch and M. Ludewig, "A rigorous construction of the supersymmetric path integral associated to a compact spin manifold," 2021.

[262] R. Bott and L. W. Tu, *Differential Forms in Algebraic Topology.* Graduate Texts in Mathematics. Springer, 1982.

[263] V. Kač, "Invariant Theory." Online, 1994. Lecture Notes.

[264] N. M. Robles, *Zeta Function Regularization.* Master's thesis, Department of Theoretical Physics Imperial College London, 2009.

[265] T. M. Apostol, *Zeta and Related Functions.* Cambridge University Press, Cambridge, 2010.

[266] A. Hatcher, *Algebraic topology.* Cambridge University Press, Cambridge, 2002.

[267] J. R. Blomquist and J. E. Harper, "Integral chains and bousfield-kan completion," 2018.

[268] T. Eguchi, P. B. Gilkey, and A. J. Hanson, "Gravitation, Gauge Theories and Differential Geometry," *Phys. Rept.* **66** (1980) 213.

[269] J. R. Munkres, *Elements of Algebraic Topology.* Addison Wesley Publishing Company, 1984. `http://www.worldcat.org/isbn/0201045869`.